

**MOLECULAR MECHANISMS OF EPITHELIAL TO
MESENCHYMAL TRANSITION (EMT) INDUCED BY SMAD-
INTERACTING PROTEIN 1 (SIP1) IN A SQUAMOUS EPIDERMOID
CARCINOMA CELL LINE**

Thesis submitted for the degree of
Doctor of Philosophy
at the University of Leicester

by

Jakob Mejlvang
Department of
Cancer Studies and Molecular Medicine
University of Leicester

March 2007

UMI Number: U495652

All rights reserved

INFORMATION TO ALL USERS

The quality of this reproduction is dependent upon the quality of the copy submitted.

In the unlikely event that the author did not send a complete manuscript and there are missing pages, these will be noted. Also, if material had to be removed, a note will indicate the deletion.



UMI U495652

Published by ProQuest LLC 2013. Copyright in the Dissertation held by the Author.
Microform Edition © ProQuest LLC.

All rights reserved. This work is protected against
unauthorized copying under Title 17, United States Code.



ProQuest LLC
789 East Eisenhower Parkway
P.O. Box 1346
Ann Arbor, MI 48106-1346

Declaration

The work described in this thesis is entirely my own unless otherwise is stated.

A handwritten signature in black ink, appearing to read 'Jakob Mejlvang', with a stylized flourish at the end.

Jakob Mejlvang

Acknowledgements

I would like to thank my mentor and supervisor, Eugene Tulchinsky, for sharing his knowledge and enthusiasm when both were needed. It is with tears in my eyes that I finish this rewarding and exciting collaboration.

I would sincerely thank Professor K. Mellon for his special support, which was just as important as the daily bread.

In general, I would like to thank students and staff working in Lab 302 for their tolerant and supportive way of being. In particular, I would like to thank Marina Kriajevskaja for everything she has done for me.

Jakob Mejlvang

Bornholm, March 2007

**MOLECULAR MECHANISMS OF EPITHELIAL TO
MESENCHYMAL TRANSITION (EMT) INDUCED BY SMAD-
INTERACTING PROTEIN 1 (SIP1) IN A SQUAMOUS EPIDERMAL
CARCINOMA CELL LINE**

by

Jakob Mejlvang

Department of

Cancer Studies and Molecular Medicine

University of Leicester

Abstract

Programmes of epithelial mesenchymal transition (EMT) are crucial for normal embryonic development and represent a potential oncogenic mechanism aberrantly exploited in oncogenesis. A hallmark of EMT is the inactivation of the E-cadherin adhesive complex, which constitutes the backbone of intercellular adhesion in epithelial tissue. Although, transcriptional repressors of E-cadherin (e.g. SNAIL, SIP1, Slug, ZEB1) has been identified as potent inducers of EMT, little is still known about the EMT-programs they initiate. In this study, we show that ectopic expression of SIP1 in A431 squamous carcinoma cells induces EMT manifested by cell scattering, abrogation of E-cadherin mediated adhesion, loss of apical-basolateral bipolarity, increased invasiveness, down-regulation of epithelial (e.g. E-cadherin, Claudin-4, Keratin 13 and 15) and up-regulation of mesenchymal (e.g. Vimentin) markers. In addition to these classical features of EMT, we show that SIP1 in our model directly represses the cyclin D1 promoter activity and thereby inhibits proliferation through the Rb-pathway. Hence, a fully compromised Rb pathway is likely necessary in order for SIP1 to prosper in oncogenesis. Furthermore, using a SIP1 mutant (SIP1CID^{mt}), incapable of binding the co-repressor CtBP, we found that the intrinsic CtBP-interacting domain (CID) is necessary for the transcriptional repression of E-cadherin. However, expression of SIP1CID^{mt} successfully induces a morphological transformation in A431 cells similar to wild type SIP1 indicating that SIP1-mediated loss of epithelial phenotype is largely independent of the simultaneous down regulation of E-cadherin.

Abbreviations

2D	Two dimensional
3D	Three dimensional
Ab	Antibody
ActD	Actinomycin D
Ala	Alanine
APC	Adenomatosis Polyposis Coli
BMP	Bone Morphogenetic Protein
BrdU	5-bromo-2-deoxyuridine
CAM	Cell Adhesion Molecules
cDNA	complementary DNA
CID	CtBP Interacting Domain
CZF	C-terminal Zinc Finger
DAPI	4,6-diamidino-2-phenylindole
DNA	Deoxyribonucleic acid
DOX	Doxycycline
EC	Extracellular
ECM	Extracellular Matrix
EGF	Epidermal Growth Factor
EGFR	Epidermal Growth Factor Receptor
EMT	Epithelial to Mesenchymal Transition
FACS	Fluorescent-activated Cell Sorting
FGF-1	Fibroblast Growth Factor-1
FGFR	Fibroblast Growth Factor Receptor
G ₀	referrers to the cell cycle phase called G ₀
G ₁	referrers to the cell cycle phase called G ₁
G ₂	referrers to the cell cycle phase called G ₂
GDP	Guanosine Diphosphate
GF	Growth Factor
GFP	Green Fluorescence Protein
GSK-3 β	Glycogen synthase kinase-3 beta
HAV	Histine-Alanine-Valine
HDAC	Histone Deacetylases

HGF	Hepatocyte Growth Factor
His	Histidine
IF	Immunofluorescence
IGFR	Insulin-like Growth Factor Receptor
Ile	Isoleucine
MAPK	Mitogen-activated Protein Kinases
MMP	Matrix Metalloproteinase
mRNA	Messenger Ribonucleic Acid
MTT	3-(4,5-Dimethylthiazol-2-yl)-2,5-diphenyltetrazolium bromide
NAD ⁺	Nicotinamide Adenine Dinucleotide
NADH	Nicotinamide Adenine Dinucleotide (reduced)
N-CAM	Neural Cell Adhesion Molecule
Neg	Negative (controle)
NZF	N-terminal Zinc Finger
PAGE	Polyacrylamide Gel Electrophoresis
PCR	Polymerase Chain Reaction
PI	Propidium iodide
PI3K	Phosphoinositide 3-kinase
PML	Promyelocytic Leukemia Protein
Rb	Retinoblastoma protein
RNA	Ribonucleic Acid
RTK	Receptor Tyrosine Kinase
RT-PCR	Reverse Transcription Polymerase Chain Reaction
SD	Standard deviation
SFK	Src Family Kinases
SID	Smad Interacting Domain
SIP1	Smad Interacting Protein1
siRNA	Small Interfering RNA
TF	Transcription Factor
TGF- α	Transforming growth factor alpha
TGF- β	Transforming growth factor beta
Trp	Tryptophan
UTP	Uridine 5'-triphosphate
Val	Valine

VEGF	Vascular Endothelial Growth Factor
WT	Wild-type
ZF	Zinc Finger

Contents

Declaration	I
Acknowledgements	II
Title and Abstract	III
Abbreviations	IV
Contents	VII
List of figures and tables	XI
Aims of the thesis	1
General introduction	3
<i>Hallmarks of carcinogenesis</i>	3
Introduction	3
Self-sufficiency in growth signals	3
Insensitivity to Anti-growth signals	5
Evading Apoptosis	5
Limitless replicative potential	6
Angiogenesis	6
Invasion and metastasis	7
<i>Epithelial to mesenchymal transition (EMT)</i>	10
Introduction	10
The non-pathological application of EMT	11
The pathological relevance of EMT	11
Inducing EMT	12
Specific introduction	14
<i>The structure and function of E-cadherin</i>	14

Background	14
Structure and extracellular interactions	14
Intracellular interactions	17
Transcriptional regulation of E-cadherin	18
Post-transcriptional regulation of E-cadherin complex	20
Role of E-cadherin in signal transduction	21
<i>SIP1 (Smad-interacting protein1)</i>	25
Introduction	25
The structure and function of SIP1	25
CID and SID	27
Results	30
<i>Part 1; General features of SIP1-mediated epithelial to mesenchymal transition (EMT) in the squamous epidermoid carcinoma cell line, A431</i>	30
<i>Part 2; SIP1 inhibits cell proliferation through direct transcriptional repression of the Cyclin D1 encoding gene CCND1</i>	39
<i>Part 3; SIP1-induced morphological transformation is independent of E-cadherin down regulation</i>	51
Discussion	67
<i>Initial work and the model</i>	67
<i>Proliferation is repressed during SIP1-induced EMT</i>	70
<i>SIP1-mediated morphological transformation</i>	73
<i>Conclusion</i>	77
Materials & Methods	78
<i>Materials</i>	78
Antibody	78
Buffers	79
Chemicals, reagents and equipment	82
Kits	85
Master Mix	86
Primers	86
<i>Methods</i>	90

Adhesion assay	90
Agarose Gel Electrophoresis	91
Cell culture work	91
Cell cycle distribution via FACS	92
Cell lines and clones	92
DNA purification by phenol:chloroform extraction.	93
Immunofluorescence	93
Immunoprecipitation	94
Luciferase reporter assay	94
Matrigel invasion assay (3D)	95
MTT–assay	96
Nuclear run-on	96
PCR	97
Plasmids	98
Preparation of protein samples	101
Purification of eukaryotic genomic DNA	101
Real-time quantitative PCR	102
Reverse transcriptase PCR (RT-PCR)	102
RNA extraction with Trizol	103
SDS-polyacrylamide gel electrophoresis (PAGE)	103
Transfections	104
Western Blotting	104
References	106
Appendix	129

A; (Table)

Table representing genes regulated by SIP1 in A431. These results were obtained by cDNA microarray analysis carried out at the MicroArray Facility of the Flanders Interuniversity, in collaboration with Geert Berx University of Ghent, Belgium 130

B; (Publication)

Andersen H*, Mejlvang J*, Mahmood S, Gromova I, Gromov P, Lukanidin E, Kriaievska M, Mellon JK, Tulchinsky E.; Immediate and delayed effects of E-cadherin inhibition on gene regulation and cell motility in human epidermoid carcinoma cells. **Mol Cell Biol 2005** Vol 25:. (*Shared first-authorship)..... **145**

C; (Publication)

Mejlvang J, Kriaievska M, Berdichevski F, Bronstein I, Lukanidin EM, Pringle JH, Mellon JK, Tulchinsky EM.; Characterization of E-cadherin-dependent and -independent events in a new model of c-Fos-mediated epithelial-mesenchymal transition. **Exp Cell Res. 2007** Jan 15;313(2):380-93 **159**

D; (Publication) (PROOF VERSION)

Mejlvang J, Kriaievska M, Vandewalle C, Chernova T, Sayan AE, Berx G, Mellon JK, Tulchinsky E.; Direct Repression of Cyclin D1 by SIP1 Attenuates Cell Cycle Progression in Cells Undergoing an Epithelial Mesenchymal Transition. **Mol Biol Cell. 2007** Sep 12..... **174**

List of figures and tables

Specific introduction

Figure 1; Schematic representation illustrating the premature E-Cadherin peptide	15
Figure 2; Model illustrating calcium dependent homophilic interactions for E-cadherin.....	16
Figure 3; Human and mouse core promoter sequences of CDH1.....	19
Figure 4; A simplified model of the Wnt signalling pathway.....	22
Figure 5; Schematic illustration of SIP1.....	26

Results Part 1

-General features of SIP1-mediated epithelial to mesenchymal transition (EMT) in the squamous epidermoid carcinoma cell line, A431

Figure 6; Treatment with DOX induces the expression of myc-tagged SIP1 in A431/SIP1 and A431/SIP1ZFmt cells.....	31
Figure 7; Expression of SIP1 induces a morphological transformation in A431 cells.....	32
Figure 8; Expression of SIP1 but not SIP1ZFmt induces expressional changes of key epithelial and mesenchymal markers.....	33
Table 1; Approximately 85% of array data could be verified by RT-PCR.....	34
Figure 9; SIP1 expression represses cell proliferation.....	36
Figure 10; SIP1 expression induces invasion.....	37

Results Part 2

-SIP1 inhibits cell proliferation through direct transcriptional repression of the Cyclin D1 encoding gene CCND1

Figure 11; SIP1 expression represses growth in cell population.....	40
Figure 12; SIP1 expression induces cell cycle arrest in G ₁ /G ₀	41
Figure 13; DOX-induced Ec1WVM expression induces EMT but does not influence proliferation.....	42
Figure 14; Cyclin D1 negatively correlates with hypophosphorylated Rb during SIP1-induced EMT.....	44
Figure 15; Cyclin D1 knockdown is concomitant with Rb hypophosphorylation and G ₁ arrest.....	45
Figure 16; Ectopic Cyclin D1 expression abrogates SIP1-induced Rb hypophosphorylation and G ₁ arrest.....	46

Figure 17; SIP1-induced down regulation of Cyclin D1 is mediated through transcriptional repression.....	48
Figure 18; Functional Z-boxes repress transcription of CCND1 in SIP1 expressing cells.....	50

Results Part 3

-SIP1-induced morphological transformation is independent of E-cadherin down regulation

Figure 19; Exogenous expression of E-cadherin partly restores the epithelial phenotype in MT1TC1/cFos.....	53
Figure 20; Ectopic expression of E-cadherin do not rescue the epithelial phenotype in DOX induced A431/SIP1.....	54
Figure 21; SIP1 regulates gene expression and induces invasion independent of E-Cadherin down regulation.....	56
Figure 22; Expression of SIP1CIDmt in A431 induces cell scattering and loss of bipolarity, but fails to repress <i>CDH1</i> and down-regulate E-cadherin.....	58
Figure 23; The E-cadherin complex disappears from cell-cell contacts during SIP1-mediated EMT.....	60
Figure 24; E-cadherin in SIP1 transformed cells is not distinctly localized.....	61
Figure 25; SIP1-mediated EMT represses the association between E-cadherin and α -catenin.....	62
Figure 26; SIP1-mediated EMT in A431 is coupled with global actin rearrangements and increased formation of focal contacts.....	63
Figure 27; Adhesion to collagen and fibronectin is induced by SIP1.....	64
Figure 28; Src family kinase inhibitor PP2 abrogates SIP1-mediated disruption of cell-cell adhesion.....	65

Aims of the thesis

My collaboration with my supervisor Dr Tulchinsky started at the Danish Cancer Society in Copenhagen where he was supervising my scientific work that would later be used as the foundation of my Master thesis. This work was focused on investigating the role of E-cadherin in c-fos induced Epithelial to Mesenchymal Transition (EMT). At the time I finished my Masters Dr Tulchinsky, now positioned at Leicester University, supported my application for a 1-year scholarship so I could both finish the work originally initiated at the Danish Cancer Society (Mejlvang *et al.*, 2007) and in parallel work on two other projects relating to EMT. One, was based on DOX-inducible expression of dominant negative E-cadherin while the other was based on DOX-inducible expression of Smad Interacting Protein1 (SIP1). Both projects used the human squamous carcinoma cell line A431 as model system. Whereas the project concerning dominant negative E-cadherin was readily developing, the SIP1 project was limited to some preliminary experiments indicating that SIP1 expression induced a EMT-like transformation of the A431 cell line. Encouraged by the virginity of the SIP1 project (until then I had only tried to join well developed projects) as well as the relatively low amount of published work on SIP1 I started a more thorough characterisation of the effects of induced SIP1 expression. As my scholarship came to the end I was offered to continue my studies on SIP1 as a PhD student. My early work on the SIP1 project had not only verified that SIP1-expression induced EMT in A431 but had naturally also led to the opening of several highly relevant scientific questions. Not limited by any modern post-academic doctrines, I continued the work with the general aim to elucidate the mechanisms underlying SIP1-induced EMT in A431 well knowing that three years probably wouldn't be enough. This approach gave me the joy of classic academic work, the trouble of keeping focused but most importantly the possibility

to work as an opportunist by giving most interest to the topics developing fastest. As the end of my PhD approached my goals were narrowed to elucidate two topics; 1) the mechanism of SIP1-mediated repression of the proliferation, 2) the mechanism of SIP1-induced morphological transformation.

The thesis is divided into a *general introduction*, *specific introduction*, *results (Part1-3)* and a *discussion*. The general introduction aims to present the current understanding of carcinogenesis from the perspective of a molecular biologist in addition to an introduction to EMT. The specific introduction aims to give the background on both SIP1 and E-cadherin. The results are divided into three parts. First part (Part 1) covers a broad characterisation of the effects coupled to SIP1 expression in A431. The second part (part 2) contains the results regarding SIP1-mediated repression of proliferation, while part three covers the results obtained during the attempt to elucidate the mechanisms involved in the SIP1 mediated morphological transformation of A431. The discussion serves to bring the presented results into the context of what is known and what is speculated.

General introduction

Hallmarks of carcinogenesis

Introduction

Decades of intensive research have indicated that tumorigenesis is a multi-step process and that these steps reflect genetic and epigenetic alterations causing abnormal regulation of specific genes. Many types of cancers are correlated with age and indicate that four to seven stochastic events are necessary to develop fully malignant cancer. Since more than 200 different types of cancers are known (U.S. National Institutes of Health, 2007), these stochastic steps rather reflect essential alterations in cell physiology that collectively govern tumorigenesis than specific genetic alterations (Hanahan and Weinberg, 2000). These essential alterations or “Hallmarks of Carcinogenesis” is now widely accepted to include gained physiological capabilities in self-sufficiency in growth signals, insensitivity to antigrowth signals, evading apoptosis, limitless replicative potential, angiogenesis and invasion. Although these capabilities often are inter-related, I separately present a brief summary of each capability in the following paragraphs.

Self-sufficiency in growth signals

Cell proliferation is regulated by growth signals. Normally, this regulation occurs in a paracrine manner, where growth signals are transmitted into a cell through transmembrane receptors. These receptors bind exogenous growth factors (GF), such as diffusible growth factors, extracellular matrix (ECM) bound factors and cell-cell adhesion associated factors. Cancer cells show an independency or greatly reduced dependency on exogenous GFs.

Different malignancies exhibit different adaptations responsible for the reduced dependency. The alterations can affect the extracellular GFs, the transmembrane transducers, or the intracellular transduction pathway. Autocrine stimulation has been found in glioblastomas, sarcomas and thyroid carcinoma, where cells have gained the ability to produce GFs (platelet-derived GF and transforming growth factor α (TGF α)) to which they themselves are responsive (Chen *et al.*, 2005; Hanahan and Weinberg, 2000). This auto-stimulation obviously disrupts the dependency on GFs secreted by other cells in the tissue. The transmembrane signal transducers also present a target for successive reduction of GF dependency (Chen *et al.*, 2005). Over-expression of GF-receptors can result in hypersensitivity to GF and thereby a diminished threshold for proliferation. Structural alterations of GF receptors can result in ligand independent activation of the cytoplasmatic domain. For example, mutations in the proto-oncogene *EGFR* (*ERBB1*) (coding for epidermal-GF-receptor) altering the extracellular EGF binding domain can result in an oncoprotein constitutively active even in absence of EGF (Clarke *et al.*, 2001). As the growth signals are transduced into the cell's interior the numbers of interacting players as well as the complexity increases. A central pathway in mitogenic stimulation is the Ras-Raf-MEK-MAPK signalling cascade. Ras is found structurally altered in app 30% of all human tumours with highest abundance in colon and pancreatic carcinomas (Friday and Adjei, 2005). These oncoproteins (Ras mutants) enhance mitogenic signalling downstream of Ras in the absence of stimulation by their upstream regulators. As a result, cells harbouring these Ras mutations are GF-independent. Likewise, the immediate downstream kinase Raf is often mutated in cancer (Dhomen and Marais, 2007). While abundant in carcinoma, up to 70% of melanomas harbour mutations in *BRAF*. The most abundant mutation is the amino acid substitution V600E that increase the kinase activity app 500-fold and constitutively activates the Raf-MEK-MAPK signalling pathway (Emuss *et al.*, 2005; Dhomen and Marais, 2007).

Insensitivity to anti-growth signals

Multiple anti-growth signals operate to maintain cellular quiescence and homeostasis in normal tissue. Like GFs, growth inhibitors are found as soluble, ECM bound and on the surface of cells. The mechanism of signal transduction is similar to growth signals involving specific membrane receptors to transduce the signal over the membrane to a more complex branched signal transduction pathway downstream and eventually regulating transcription. Anti-growth signals inhibit proliferation by reversible and irreversible mechanisms. Cells may be induced to exit the cell cycle and enter the quiescent state (G_0) until extracellular signals induce them to re-enter the cell-cycle. Alternatively, they may be induced to enter an irreversible differentiation program. Cancer cells must counteract these mechanisms in order to obtain immunity to anti-growth signals (Hanahan and Weinberg, 2000). The tumour suppressor Rb (retinoblastoma protein) and its two relatives, p107 and p130, are common targets for anti proliferative signals. In active, hypophosphorylated, state Rb inhibits activity of E2F transcription factors, which controls expression of genes responsible for progression from G_1 to S phase. Transforming growth factor beta ($TGF-\beta$), a soluble anti-growth factor, can prevent the inactivation of Rb and thereby inhibit proliferation (Herrera *et al.*, 1996). A distinguished example of abrogated anti-growth signals is presented by the high abundance of inactivating mutations in both $TGF-\beta$ receptors and transducers located downstream of the $TGF-\beta$ receptor in colon cancer (Grady *et al.*, 1999).

Evading Apoptosis

Since apoptosis is an important process responsible for the elimination of defected and unwanted cells it may also be considered as a process suppressing tumorigenesis. By avoiding apoptosis, cancer cells indirectly increase their mutation and growth rate at the

same time. Proteins acting either as sensors or effectors constitute the apoptotic system. Sensors monitor the intra- and extra-cellular environment and induce apoptosis through effectors, if the pro-apoptotic stimuli exceed a specific threshold. Among many other sensors of apoptosis, the most commonly mutated is probably the tumour suppressor p53, which initiates an apoptotic pathway in response to DNA damage. Inactivation or loss of wild-type p53 occurs in more than 50% of human cancers (Horn and Vousden, 2007).

Limitless replicative potential

Normal cells have limited dividing potential. Early work of Hayflick showed that cells grown in culture are capable of a limited number of divisions followed by the blockage of proliferation (cellular senescence). Recent research has proven that the telomeres are responsible for this division-related clock. During each replication chromosomes lose 50-100 bp of the telomeric ends, which are composed of thousands of G-rich hexanucleotide repeats. This incompleteness in replication is caused by the inability of the DNA-polymerase to synthesize the 3' termini of replicating DNA. Senescence occurs when telomeres reach critical length (reviewed in Hayflick, 2000). In order to acquire limitless replicative potential the telomere length has to be maintained. This maintenance is observed in virtually all types of malignant cancers, and in general (78-100%) achieved through up-regulation of the telomerase, an enzyme, which has the ability to add the hexanucleotide repeats to the 3'-ends of replicating DNA (Shay and Bacchetti, 1997)

Angiogenesis

Since all cells are dependent on oxygen and nutrient supplies, development of new blood vessels (angiogenesis) is essential for normal embryogenesis, organogenesis, wound healing, as well as tumour progression. In normal tissue the initiation of the angiogenic

program is determined by balance between pro- and anti-angiogenic factors. Vascular endothelial growth factor (VEGF), a growth factor selectively stimulating endothelial cells to proliferate, has been found up-regulated in many tumours (Berger *et al.*, 1995). In other malignancies anti-angiogenic factors such as thrombospondin-1 and β -interferon, are down regulated (Ren *et al.*, 2006; Bielenberg *et al.*, 1999).

Invasion and metastasis

In clinical practice, metastases are associated with extremely poor prognosis and metastatic diseases causes app 90% of all cancer deaths (Sporn, 1997). In order to metastasise, tumour cells must detach from their primary site, migrate through extracellular matrix (ECM), traverse specialized tissue borders (e.g. basal lamina), translocate via blood stream or lymphatic pathways and eventually settle in foreign tissue. This process, yet not fully understood, depends on several events including deregulation of cell-cell adhesion molecules, compositional changes of integrins, and activation/secretion of ECM-degradating proteases.

Epithelial cells tightly adhering to each other constitute the epithelial sheet. The integrity of the epithelial sheet is ensured by several specialised adhesive structures mediating either intercellular adhesion or adhesion between cells and the ECM. The majority of these adhesive structures are connected to either intermediate filaments (desmosomes and hemidesmosomes) or to actin filaments (adherens junctions and focal junctions). Cell-cell adhesion molecules (CAMs) are responsible for intercellular adhesion and are divided into two groups according to Ca^{2+} dependency. Cadherins constitute the group of Ca^{2+} -dependent CAMs, which establish their adhesions through homophilic intercellular interactions. The major component of adherens junctions, epithelial cadherin (E-cadherin), is ubiquitously expressed in epithelial cells. As it was revealed in several clinical studies, E-cadherin is lost or deregulated in a large panel of carcinomas, including bladder, prostate,

colorectal, pancreatic, gastric and breast cancer (Bellovin *et al.*, 2005; Byrne *et al.*, 2001; Oka *et al.*, 1993; Weinel *et al.*, 1996; Rao *et al.*, 2006). In addition, loss of E-cadherin expression correlates with higher grade of malignancy, increased invasive potential and poor prognosis (Bellovin *et al.*, 2005; Byrne *et al.*, 2001). Beside the direct involvement in cell-cell adhesion, there is evidence suggesting that E-cadherin is indirectly involved in transduction of anti-growth signals (Croix *et al.*, 1998; Qian *et al.*, 2004). In summary, this has allocated E-cadherin a tumour suppressive role.

Ca²⁺-independent cell-cell adhesion is mediated by CAM's of the immunoglobulin superfamily, another class of adhesion molecules involved in metastasis. In various carcinomas, abnormal expression pattern of neural cell adhesion molecule (N-CAM) isoforms has been observed (Lanza *et al.*, 1993; Todaro *et al.*, 2007). N-CAM's are either down regulated or expression is switched from the highly adhesive isoform (N-CAM120) to less adhesive isoforms. Furthermore, experiments with transgenic mouse indicate that N-CAM120 suppresses metastasis (Perl *et al.* 1999).

Migrating cells will inevitably experience changes in ECM environment through their journey, and must eventually adapt to the environment in which they settle. Changes in ECM associated adhesion are therefore a necessity. Integrins constitute the group of molecules mediating adhesion to ECM. They are heterodimeric transmembrane receptors consisting of one type α and one type β subunit and their adhesion ability depends on the composition of subunit types. In order to facilitate migration, carcinoma cells shift from integrins favouring epithelial attachment to other integrins. More than 20 integrins are known to date; some of them exhibit anti-metastatic abilities whereas expression of others stimulates metastasis (Ramsay *et al.*, 2007).

Serine proteases and metalloproteases are mediators of many important cellular processes such as cell proliferation and differentiation, extracellular matrix modelling, angiogenesis, cell migration and invasion. The underlying working mechanisms of the proteases in these

different processes include the proteolytic cleavage of matrix bound growth factors, receptor cleavage and degradation of ECM itself. As especially remodelling of the ECM is obligatory for tumour progression, both proteases and inhibitors thereof are often found aberrantly utilized in cancer cells.

Epithelial to mesenchymal transition (EMT)

Introduction

Epithelial cells form coherent cell sheets termed epithelium. The integrity of the epithelium is based on specialised cell-cell junctions established between neighbouring epithelial cells, which tightly bind cells together so individual cells are immobilized in context of the epithelial sheet. In addition these specialised junctions, located at the lateral surface, provide the epithelial capability to work as a relative impermeable sheet and separate apical and basal surface. Although the epithelium can consist of both single and multiple sheets, epithelial cells exhibit an apical-basal bipolarity. As the apical and basal surfaces of the cell are differently composed they have different functions and preference for substrates. The organisation of the cytoskeleton in epithelial cell facilitates the intercellular adhesive junctions and ensures rigidity and strength to the epithelial sheet. As a consequence of the epithelial specialisation in intercellular adhesion, most of epithelial markers are components of cell-cell junctions (e.g. E-cadherin, Occludin and Desmoplakin) and cytoskeleton (Cytokeratins). In contrast, mesenchymal cells do not exhibit strong intercellular adhesion and have more elongated morphological structure polarised by a front- and a back- end relying on the direction of locomotion. However, this bipolarity is often lost when mesenchymal cells are grown *in vitro* on 2D substrates (Hay, 2004). Furthermore, mesenchymal cells are highly motile and specialised to reside the extracellular matrix. Classical mesenchymal markers includes Vimentin, MMPs, Fibronectin and N-Cadherin (Lee *et al.*, 2006)

During epithelial to mesenchymal transition (EMT), epithelial cells either reversibly or irreversibly adopt a mesenchymal phenotype. This is manifested by cell scattering, loss of

apical-basal bipolarity, increased motility, increased invasiveness concomitantly with the general up-regulation of mesenchymal and down-regulation of epithelial markers.

The non-pathological applications of EMT

Although, EMT have been observed as a developmental phenomenon for more than 100 years, it was only in the early 1980s that EMT became recognised as a distinct mechanism that epithelial cells (stimulated by the right stimuli in the right context) utilize in order to either transiently or permanently achieve mesenchymal capabilities (Thiery, 2002). EMT has since emerged as a highly conserved mechanism implemented in a variety of vital developmental processes, such as gastrulation, neural crest migration and somitogenesis (Hay, 2004; Nieto, 2001). The earliest developmental event in vertebrates which involves EMT is the gastrulation that takes place at embryonic day 6 and is responsible for the generation of mesoderm and endoderm (Hay, 2004; Lee *et al.*, 2005). During this event epithelial cells situated at an unique place of the epiblast called the primitive streak undergo EMT and thereby generate the first mesenchymal cells. These mesenchymal cells migrate away from the primitive streak and subsequently condense to form the mesoderm (middle layer of the embryo) and the endoderm (inner layer) (Hay, 2004). Of note, the down regulation of E-cadherin has been shown to be crucial for the success of this process (Zohn *et al.*, 2006).

In adult animals, the best-known physiological process involving EMT is the wound-healing process responsible for tissue repair (Lee *et al.*, 2005; Radisky *et al.*, 2007).

The pathological relevance of EMT

The fact that the acquisition of mesenchymal capabilities is clearly pro-metastatic dictates that aberrant stimulation of EMT can facilitate the development of metastatic cancers.

Unfortunately, limitations in studying *in vivo* carcinogenesis in real-time have so far obstructed a clear assessment of how carcinogenic the different programmes of EMT should be considered. However, the fact that mediators of EMT in general enhance tumour formation and/or metastasis have widely recognised EMT as an oncogenic process which stimulate invasiveness via intravasation and extravasation of metastatic cells (Thiery, 2002; Lee *et al.*, 2005; Radisky *et al.*, 2007). Another pathological implementation of the EMT process is evident by the involvement of EMT-generated myofibroblasts in various fibrotic disorders (Radisky *et al.*, 2007). As the complicated interplay between cancer cells and peritumoral fibroblast in tumour associated stroma can influence the fate of the tumour (Desmouliere *et al.*, 2004) EMT might be implicated concomitantly in two independent processes favouring carcinogenesis.

Inducing EMT

The induction of EMT seems to be highly context-dependent as factors inducing EMT in some circumstances have other or no effect elsewhere. Since the first *in vitro* studies of EMT in 1985 reported that conditioned media from embryo lung fibroblasts stimulated a mesenchymal conversion of epithelial MDCK cells (Stocker and Perryman, 1985) various factors have routinely been identified as positive mediators of EMT. So far, growth-factors (e.g. FGF-1, EGF, HGF, TGF- α , TGF- β), receptor tyrosine kinases (e.g. c-Met, FGFR, IGFR and the ERB-family), transcription factors (e.g. Fos, LEF1, Snail, Slug, SIP1) and signal inducing components (e.g., Ras, Rac, Rho, MAPK and PI3K) have been implicated in the induction of EMT *in vitro* (Thiery, 2002; Boyer *et al.*, 2000; Zavadil and Böttinger, 2005). The signalling pathways mediating programmes of EMT still need to be unravelled although there are evidences indicating that different programmes utilize similar downstream pathways.

The transcriptional repression of the E-cadherin gene and consequently diminished expression of E-cadherin based adhesion junctions has emerged to be a central event in all EMT programmes. Three lines of evidence support this. Firstly, most stimuli that induce EMT either concurrently or eventually repress transcription of the E-cadherin gene. Secondly, all known transcriptional repressors of E-cadherin (Snail, Slug, SIP1, ZEB1 and E12/47) can sufficiently by them self induce EMT depending on the context (Comijn *et al.*, 2001; Eger *et al.*, 2005; Vandewalle *et al.*, 2005; Bolos *et al.*, 2003; Peinado *et al.*, 2004b). Finally, blocking E-cadherin function (by either blocking Ab or expression of dominant negative E-cadherin) can effectively stimulate EMT-like morphological transformation (Vestweber and Kemler, 1985; Andersen *et al.*, 2005 (Appendix B)), while reintroduction of E-cadherin into mesenchymal cells often leads to the partial restoration of the epithelial phenotype (Hay, 2004).

Since EMT implements genome-wide changes in gene expression manifested by general and concomitant down-regulation of epithelial markers and up-regulation of mesenchymal markers the EMT-process cannot be simplified to the core disruption of E-cadherin mediated adhesion.

Additional insight in the working mechanisms of transcriptional repressors of E-cadherin, which apparently are the lowest (most downstream) situated mediators of EMT that hold the ability to both repress epithelial markers and stimulate the expression of mesenchymal (Cano *et al.*, 2000; Bindels *et al.*, 2006; Vandewalle *et al.*, 2005), will most likely elucidate the general backbone of EMT-programmes.

Specific introduction

The structure and function of E-cadherin

Background

The cadherin superfamily includes classic cadherins, desmogleins, desmocollins, protocadherins, cadherin related neuronal receptors, fats, seven-pass transmembrane cadherins, and Ret tyrosine kinase. All members of the cadherin superfamily are transmembrane proteins and are characterised by a unique domain called the cadherin motif or the EC domain. These domains are repeated in tandem in the extracellular segment of all cadherins (Yagi and Takaichi, 2000). The most extensively studied cadherins are members of the classic cadherin subgroup, which comprise more than 30 members. The best-studied representatives of this group are epithelial cadherin (E-cadherin), placental cadherin (P-cadherin) and neural cadherin (N-cadherin) all named according to the main tissue in which they are expressed.

Structure and extracellular interactions

E-cadherin plays a major role in the adhesion of epithelial cells through its establishment of calcium dependent homophilic interactions localised to the sites of cell-cell contacts (Beavon, 2000). The human E-cadherin gene (*CDH1*) is located on chromosome 16q22.1 and encodes a 135-kDa precursor protein. This precursor protein is processed in the cytoplasm before it enters the surface, where it plays a key role in the assembly of adherens junctions as mature E-cadherin (120 kDa) (Shapiro *et al.*, 1995). E-cadherin is composed of

a highly conserved N-terminal extracellular domain, a single pass transmembrane domain and a C-terminal cytoplasmatic domain (Figure 1). The extracellular domain is composed of five EC domains (EC I-V). Conserved amino acid residues that are capable of coordina-

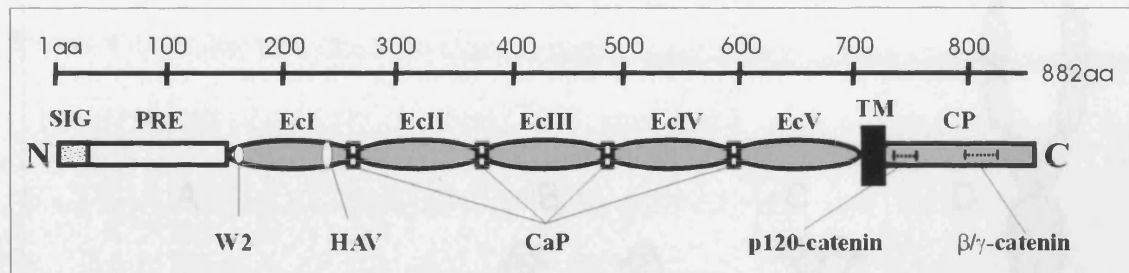


Figure 1. Schematic representation illustrating the premature E-Cadherin peptide. Leader containing a signal sequence (SIG) and a precursor domain (PRE). Extra cellular domain including five (EcI-EcV) EC domains with several Ca^{2+} binding pockets (CaP), a conserved His-Ala-Val sequence (HAV) and a highly conserved Trp (W2). Transmembrane domain (TM) and cytoplasmatic domain (CP) including p120-catenin binding site (p120-catenin) and binding site for β and γ -catenin (β/γ -catenin)

ting Ca^{+2} are present at the end of each domain. Binding of Ca^{+2} to these sites (Ca^{+2} -pockets) provides the structural integrity of the extracellular domain and gives the protein a rigid conformation that allows the mediation of homophilic interactions with E-cadherins located on the surface on adjacent cells. The EcI domain contains highly conserved HAV (His79-Ala80-Val81) and W2 (Trp2) motifs, which have been shown to be essential for the homophilic adhesion (Berx *et al.*, 1996; Chitaev & Troyanovsky, 1998)

Analysis of the crystal structure of E-cadherin has provided some insight into the steric rearrangement underlying calcium dependency of the *cis/trans* dimers. In the absence of Ca^{+2} , the structure is disordered and incapable of any *cis* or *trans* interactions. As concentration of Ca^{+2} increases, the EcI-EcV sub-domains are stabilised by Ca^{+2} in a more rigid structure and are subsequently capable of forming *cis* dimers and eventually *trans* dimers (Figure 2) (Pertz *et al.*, 1999). The Ca^{+2} -pockets between EcII and EcV have the highest affinity and is saturated at app 0,1 mM Ca^{+2} . This probably prevents *cis* interactions before the basic structure has reached some level of rigidity. The pockets between EcI and EcII have a lower affinity for Ca^{+2} which can be saturated at 0,5 mM inducing *cis*

interactions. Although, point mutations have shown that neither the HAV nor the W2 motif is crucial for *cis* interactions (Pertz *et al.*, 1999), they are essential in the formation of *trans*

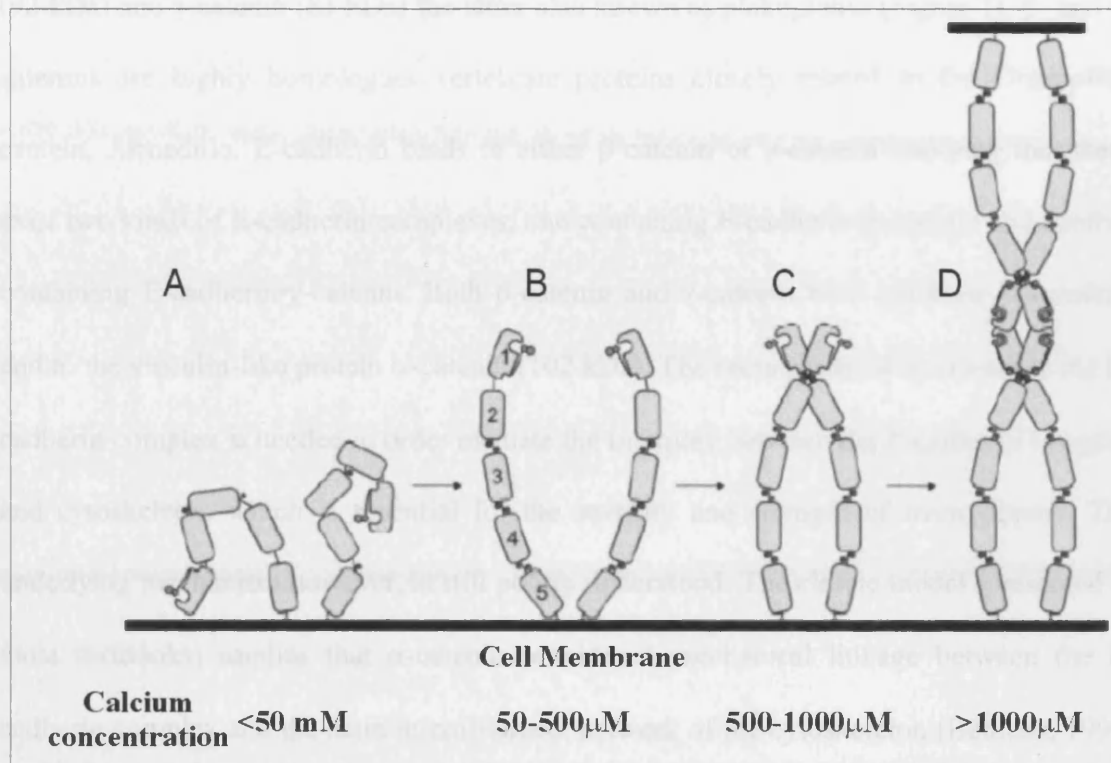


Figure 2. Model illustrating calcium dependent homophilic interactions for E-cadherin; Low Ca^{2+} concentrations stabilise the rod-like structure (A and B), medium and high concentrations result in *cis*-dimerization (C) and W2 docking in its hydrophobic cavity which enables *trans*-interaction (D). EcI to EcV are drawn as gray blocks, with the hydrophobic cavity to which W2 binds in EcI. See text for details (Adapted from Pertz *et al.*, 1999)

dimers. HAV and W2-dependent *trans* interactions occur when E-cadherin molecules are completely saturated (1 mM Ca^{+2}). 1 mM Ca^{+2} concentrations induce conformational changes in the HAV motif allowing W2 to dock into a hydrophobic pocket generated by Ala80. This W2 docking eventually leads to the formation of *trans* dimers functioning as junctions across the intercellular space in a zipper like fashion. The importance of the highly conserved His79 and Val81 is yet unclear while substitution of Ala80 to Ile totally abolishes adhesion (Pertz *et al.*, 1999; Renaud-Young and Gallin, 2002).

Intracellular interactions

The cytoplasmatic tail of E-cadherin interacts with the p120-catenin (120 kDa), β -catenin (92 kDa) and γ -catenin (83 kDa) the latter also known as plakoglobin (Figure 1). β - and γ -catenins are highly homologous vertebrate proteins closely related to the *Drosophila* protein, Armadillo. E-cadherin binds to either β -catenin or γ -catenin implying that there exist two kinds of E-cadherin complexes, one containing E-cadherin• β -catenin and another containing E-cadherin• γ -catenin. Both β -catenin and γ -catenin bind via their N-terminal end to the vinculin-like protein α -catenin (102 kDa). The recruitment of α -catenin to the E-cadherin complex is needed in order to mediate the interplay between the E-cadherin complex and cytoskeleton which is essential for the stability and strength of *trans* dimers. The underlying mechanism however, is still poorly understood. The classic model (presented in most textbooks) implies that α -catenin provides a mechanical linkage between the E-cadherin complex and the actin microfilament network of the cytoskeleton (Behrens, 1999; Watabe-Uchida *et al.*, 1998), a linkage established either by direct interactions with F-actin (Rimm *et al.*, 1995) or mediated through the actin binding proteins Vinculin and α -actinin (Watabe-Uchida *et al.*, 1998). As recent evidence shows that α -catenin associates with E-cadherin and actin in a mutually exclusive manner (Yamada *et al.*, 2005; Drees *et al.*, 2005) this model has been severely compromised. Furthermore, strong evidence suggests that monomeric α -catenin associates with the E-cadherin complex while dimeric α -catenin binds actin filaments and suppresses Arp2/3-mediated branched actin formation (implemented in formation of lamellipodia)(Drees *et al.*, 2005). Especially the latter findings by Drees and colleagues have given rise to an improved and more prudent model; α -catenin concentration is locally increased in the cytoplasm near cell-cell contacts by the recruitment of monomeric α -catenin by the E-cadherin complex. The increase in concentration enables the formation of α -catenin dimers that subsequently bind actin. This

directly inhibits Arp2/3-mediated branched formation of actin and either passively or actively through formins stimulates linearly actin formation finally resulting in a network of actin filaments favouring strong intercellular adhesion (Drees *et al.*, 2005; Gates and Peifer, 2005; Weis and Nelson, 2006).

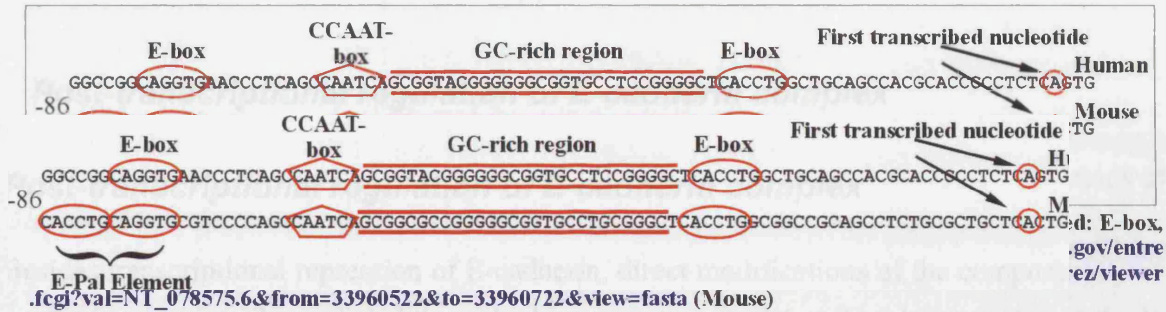
p120-catenin (also known as p120^{ctn} and p120^{cas}) binds to the juxta-membrane part of E-cadherin (Figure 1). Although p120-catenin is an armadillo homologue like β -catenin and γ -catenin, it does not interact with α -catenin.

The formation of the E-cadherin- β -/ γ -catenin complex begins in the cytoplasm, during the translocation of immature newly synthesised cytoplasmatic E-cadherin to the membrane. At the plasma membrane, α -catenin binds to the NH₂-terminal region of β -catenin and eventually stimulates the formation of stable *trans*-interactions (Beavon, 2000; Steinberg and McNutt, 1999).

Transcriptional regulation of E-cadherin

Although somatic mutations of *CDH1*, E-cadherin coding gene, have been identified in diffuse gastric cancer (Becker *et al.*, 1994) and lobular breast cancer (Berx *et al.*, 1995 and 1996) other mechanisms are responsible for the general deregulation of E-cadherin in carcinogenesis (Ji *et al.*, 1997). Analyses of the human and murine *CDH1* promoter have revealed different regulatory sequences responsible for the epithelial-specific expression of E-cadherin. Investigations of the murine *CDH1* promoter have revealed two positive regulatory elements, a CCAAT-box and two AP-2 binding sites imbedded in GC-rich region (Hennig *et al.*, 1995 and 1996). Furthermore, *in vivo* footprinting analysis revealed that a palindromic sequence containing two E-boxes (5'-CANNTG-3') placed in tandem, known as the E-pal element, is involved in transcriptional repression in mesenchymal cells

and in transcriptional activation in epithelial cells (Hennig *et al.*, 1996). However, this E-pal element is not fully conserved in the human *CDH1* promoter and only contains one



E-box (Figure 3). Both promoters contain the CCAAT-box, a GC-rich region as well as an additional E-box situated between the GC-region and the first transcribed nucleotide (Figure 3). An enhancer is located in the first intron of murine *CDH1* (Hennig *et al.*, 1995 and 1996). In humans, the two E-boxes has been found to be involved in repression in fibroblasts and different tumour cell lines (Giroldi *et al.*, 1997). Four Zinc-finger proteins, Snail, Slug, ZEB1 and SIP1, in addition to one basic helix-loop-helix (bHLH) protein, E12/47, have been found to repress E-cadherin transcription through direct interactions with the E-boxes. In addition these repressors exhibits an inverse correlation with E-cadherin expression in a panel of different cell-lines indicating an *in vivo* repression (Hajra *et al.*, 2002; Comijn *et al.*, 2001; Cano *et al.*, 2000; Batlle *et al.*, 2000; Perez-Moreno *et al.*, 2001; Eger *et al.*, 2005).

Studies of the methylation status of the *CDH1* promoter in different human carcinomas and fibroblast cell lines revealed a hypermethylation of CpG islands of the *CDH1* promoter exclusively in E-cadherin negative cell lines (Hennig *et al.*, 1995). This correlation suggests a role for promoter DNA methylation in silencing E-cadherin in invasive carcinomas. Alterations in chromatin structure of the *CDH1* promoter were also reported. In E-cadherin-expressing cells chromatin was loosened in contrast to the non-expressing

cells were it was condensed (Hennig *et al.*, 1995). The specific factors that repress E-cadherin most likely vary depending on cell-type and context.

Post-transcriptional regulation of E-cadherin complex

Besides transcriptional repression of E-cadherin, direct modifications of the components of adherens junctions are implicated in EMT and conversion into invasive phenotype. These effects are primarily mediated through changes in tyrosine phosphorylation status of the E-cadherin associated proteins; β -catenin and p120-catenin. It has been reported, that tyrosine phosphorylation stimulates cell scattering, whereas dephosphorylation of membranous proteins contributes to stronger adhesion. Expression of oncogenic *v-src*, a cytoplasmatic tyrosine kinase, leads to decreased cadherin-mediated adhesion concomitantly with tyrosine phosphorylation of several components of adhesive complexes (Behrens *et al.*, 1993; Takeda *et al.*, 1995; Irby *et al.*, 2002). Although tyrosine phosphorylation by *v-src* is responsible for the transformation (Irby *et al.*, 2002) it remains to be elucidated which components are implicated (Takeda *et al.*, 1995). In addition, members of the RTK-family like EGF-R and erbB-2 are also implicated in disassembly of cadherin-mediated cell-cell adhesion via tyrosine phosphorylation of β -catenin (reviewed in Hajra and Fearon, 2002).

Rho-family GTPases have been implicated in multiple steps of cellular transformation, including alterations of the adhesion status of tumour cells. These GTPases cycle between inactive GDP-bound and active GTP-bound forms. When activated, they interact with a variety of effectors to trigger distinct signalling cascades. RhoA, Rac and Cdc42 are known to mediate the E-cadherin dependent adhesion. They are required for the formation of the E-cadherin complex, although evidence suggests a variety of mechanisms for mediating the adhesion. Rac1 and Cdc42 were found to regulate functional complex formation through interactions with IQGAP1 (Fukata *et al.*, 1999). IQGAP1 regulates the E-cadherin complex

by interacting with β -catenin, causing α -catenin to dissociate from the E-cadherin complex and eventually abolishing the linkage to the cytoskeleton. In MDCK cells, activated Rac1 and Cdc42 dissociate IQGAP1• β -catenin complexes promoting formation of adhesive complexes (Fukata and Kaibuchi, 2001). Rho-family GTPases are also known to be key mediators of cytoskeleton dynamic including assembly of actin filaments. Inappropriate regulation of this process would also cause adhesive malfunction.

Role of E-cadherin in signal transduction

In addition to its well-studied role in cell adhesion, E-cadherin is also implicated in signal transduction. Since E-cadherin itself lacks intrinsic catalytic activity, E-cadherin mediated signalling is, probably, mediated through E-cadherin-associated proteins or via its engagement with receptor tyrosine kinases. Evidence suggests that the catenins play individual roles in different signalling pathways. Since the presents of the E-cadherin complexes could regulate the stability and cellular localisation of catenins, expression of E-cadherin might influence catenin-dependent signal transduction pathways.

The key role of β -catenin in Wnt-signalling pathways was originally discovered by mutation assays in *Drosophila*. As it became evident later, this pathway plays an important part in embryonic development in other species, including mammals (Beavon, 2000; Behrens, 1999). In the absence of Wnt-signalling β -catenin is either associated with the E-cadherin complex or is distributed in the cytoplasm as a free cytosolic pool. Cytoplasmatic β -catenin is found in complex with APC (Adenomatous Polyposis Coli), GSK-3 β (Glycogen Synthase Kinase 3 β) and an adaptor protein Axin. In this complex β -catenin is rapidly phosphorylated by GSK-3 β and subsequently degraded by the ubiquitin/proteasom system (Figure 4) (Reviewed in Wijnhoven, 2000).

Wnt signalling is initiated by extracellular Wnt glycoproteins, which bind to the transmembrane receptor Frizzled (Frz), leading to activation of the protein called Dishevelled (Dsh). Activated Dsh counteracts phosphorylation of β -catenin by GSK-3 β .

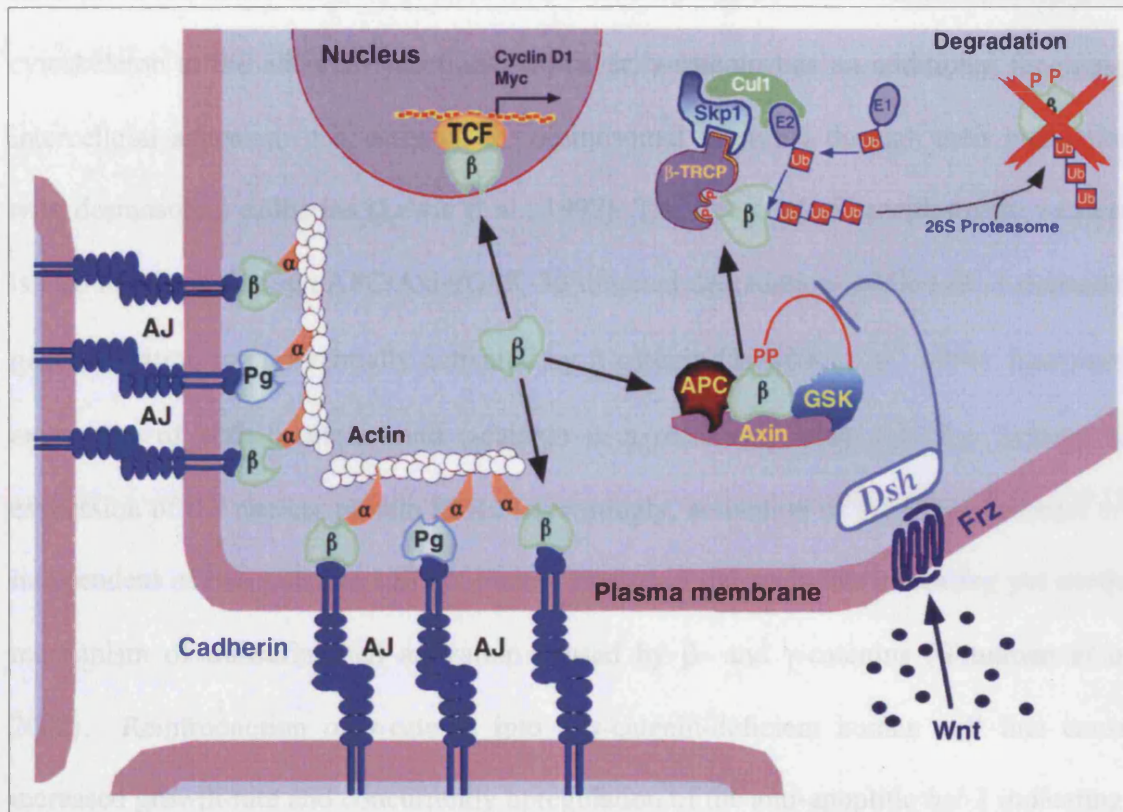


Figure 4. A simplified model of the Wnt signalling pathway; E-cadherin bound β -catenin (β) and γ -catenin/plakoglobin (Pg) links to the actin cytoskeleton via α -catenin (α) to form the adherens junctions (AJ). In absence of Wnt signalling the cytoplasmic pool of β -catenin is degraded by a complex including Glycogen Synthase Kinase 3 β (GSK), Adenomatous Polyposis Coli (APC), and Axin, which phosphorylate β -catenin. This protein complex mediates ubiquitination of β -catenin through the ubiquitination machinery (β -TrCP, Skp1, Cul1, and E1&E2 ubiquitination components), which subsequently directs it to degradation by the 26S proteasome. The binding of Wnt to Frizzled (Frz) receptors activates Wnt signalling, and Dishevelled (Dsh) inhibits β -catenin phosphorylation by GSK. This results in β -catenin accumulation in the nucleus, where it complexes with T cell factor (TCF) and transactivates target genes as *Cyclin D1* and *Myc*. (Scheme adapted from Conacci-Sorrell *et al.*, 2002)

Unphosphorylated β -catenin is not targeted for degradation and thereby accumulates in the cytoplasm. Stabilisation and increased levels of cytosolic β -catenin enables its interactions with the LEF/TCF transcription family members and translocation to the nucleus leading to the activation of target genes. For example, β -catenin•TCF4 complexes promote

transcription of the genes, *c-myc* and *cyclin D1*, relevant to cell cycle progression (Fearon and Dang, 1999; Wijnhoven, 2000; He *et al.*, 1998; Shtutman *et al.*, 1999).

As already mentioned, β -catenin and γ -catenin are very homologous proteins with similar function in cell adhesion. Both of them mediate the linkage between classical cadherins and cytoskeleton at the adherens junctions. However, γ -catenin has an additional function in intercellular adhesion: it is essential for desmosomal assembly through their interactions with desmosomal cadherins (Lewis *et al.*, 1997). The free pool of cytoplasmatic γ -catenin is also regulated through APC/Axin/GSK-3 β directed degradation, while LEF-1-dependent gene activation is preferentially activated by β -catenin (Simcha *et al.*, 1998). Exogenous expression of both β -catenin and γ -catenin in a renal carcinoma cell line induced the expression of the nuclear protein PML. Interestingly, activation of the PML promoter was independent of two putative LEF/TCF sites located in the promoter indicating yet another mechanism of transcriptional activation caused by β - and γ -catenins (Shtutman *et al.*, 2002). Reintroduction of γ -catenin into a γ -catenin-deficient human cell line caused increased growth-rate and concurrently upregulation of the anti-apoptotic *bcl-2* indicating a growth regulatory function for γ -catenin (Hakimelahi *et al.*, 2000).

p120-catenin regulates Rho GTPases by binding/sequestering inactive (GDP-bound) Rho and thereby inhibiting Rho signalling (Hajra and Fearon, 2002). In addition, immunoprecipitation experiments indicate that p120 binds a DNA-binding protein named Kaiso and E-cadherin in mutually exclusive manner (Daniel and Reynolds, 1999). Binding sites for Kaiso has so far been found in the promoter of matrilysin and the methylated S100A4 promoter, indicating that transcription of these two genes might be regulated via a Kaiso-p120-catenin pathway (Daniel *et al.*, 2002).

Besides playing the central role in mediating the interplay between adherens junctions and the cytoskeleton, α -catenin might also play a role in signal transduction. Conditional

knockout of α -catenin in keratinocytes results in enhanced proliferation and sustained activation of Ras-MAPK cascade (Vasioukhin *et al.*, 2001). α -catenin directly interacts with β - and γ -catenin, F-actin, Vinculin, α -actinin, 1-Afadin, ZO-1, Spectrin and Ajuba (Provost and Rimm, 1999; Pokutta *et al.*, 2002; Marie *et al.*, 2003). Whether these interactions affect any signalling remain to be elucidated. However, in addition to catenins, ZO-1 and Ajuba have been found to influence differentiation and proliferation when accumulated in nuclei (Kanungo *et al.*, 2000). α -catenin itself is normally localised in the cell-cell contacts and in the cytoplasm, but nuclear transport of α -catenin has been reported in colon carcinoma cell lines (Giannini *et al.*, 2000). Same studies connected its nuclear localisation with inhibition of the β -catenin/Tcf dependent transcription.

SIP1 (Smad-interacting protein 1)

Introduction

A crucial event in EMT is loss of E-cadherin, a surface receptor which is often mutated or lost in cancer cells and which plays a central role in the formation of adherens junctions (Peinado *et al.*, 2004a). In recent years, several direct transcriptional repressors of the E-cadherin gene (Snail, Slug, E12/E47, ZEB1 and SIP1) have been identified (Battle *et al.*, 2000; Cano *et al.*, 2000; Bolos *et al.*, 2003; Perez-Moreno *et al.*, 2001; Comijn J *et al.*, 2001; Eger *et al.*, 2005). They belong to three different protein families, Snail/Slug, ZEB1/SIP1 and E12/E47. Whereas studies suggest that Snail and Slug function in a number of EMT-initiating signals to down-regulate E-cadherin transcription (De Craene *et al.*, 2005), the role of SIP1 in signalling pathways triggering EMT has not been addressed scrupulously. Several recent reports implicate SIP1 in different fields of embryogenesis (Sheng *et al.*, 2003; van Grunsven *et al.*, 2000) and SIP1 expression has been proven crucial in the development of neuroepithelium, postotic vagal neural crest cells, somites and ocular lens (Maruhashi *et al.*, 2005; Van de Putte *et al.*, 2003; Yoshimoto *et al.*, 2005). Clinical investigations regarding the expression of SIP1 in various cancers are still few and a positive relation between SIP1 and cancer progression is limited to a small set of cancers comprising gastric, hepatocellular, ovarian and breast carcinomas (Rosivatz *et al.*, 2002; Miyoshi *et al.*, 2004; Elloul *et al.*, 2005).

The structure and function of SIP1

The human gene *ZFHX1B* (zinc finger homeobox 1b) is located at 2q22 and encodes the transcriptional repressor SIP1. SIP1 and its close relative ZEB1 (also known as δ EF1) are the only known members belonging to the vertebrate Zfh-1 family of transcription factors.

They are characterised by two-handed ZF clusters and a homeo-domain (Figure 5). The mature SIP1 protein is 1214aa long and comprises 5 distinct protein motifs; the homeo-domain, a Smad interacting domain (SID), CtBP (C-terminal binding protein) interacting domain (CID), and two bipartite clusters of zinc-fingers (ZF) termed N-terminal ZF (NZF) and C-terminal ZF (CZF) domain. The homeo-domain of Zfh-1 (*Drosophila*) comprises

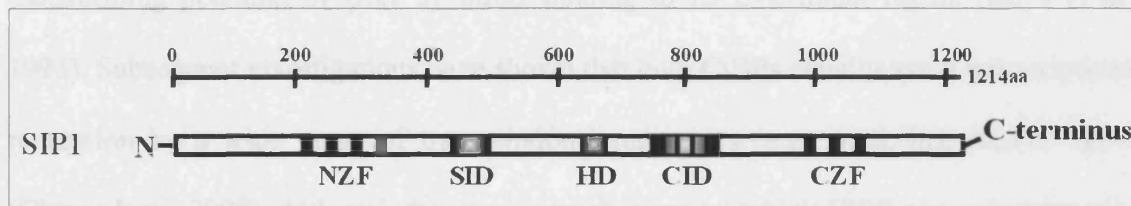


Figure 5; Schematic illustration of SIP1. NZF & CZF, N and C-terminal ZF domain (black boxes represent CCHH type while grey represent CCHC); SID, Smad interacting domain; HD, Homeo domain like domain; CID, CtBP interacting domain.

amino acids in a helix responsible for binding DNA. In contrast to Zfh-1 the responsible elements are not conserved in neither SIP1 nor ZEB1, suggesting that these homeo-like domains have lost their original ability to bind DNA (Verschueren *et al.*, 1999).

In addition to the two clusters of trimeric CCHH-type ZF's found in SIP1 one CCHC-type ZF is located in continuation of the N-terminal cluster. Interestingly, these ZF's are highly (app 90%) homologous with those within ZEB1 indicating that these TF's have overlapping range of target genes. Successful binding to DNA is dependent on binding of both ZF domains to separate E-box elements (CACCT/CACCTG) in the target promoter (Comijn *et al.*, 2001; Remacle *et al.*, 1999). The distance between E-box's and their relative orientation varies between potential target genes e.g. E-Box's in the human E-cadherin promoter are separated by 44bp while the distance is 8bp in the mouse follistatin promoter (Tylzanowski *et al.*, 2001). Of note, *CDH1* is not the only target for direct SIP1-mediated transcriptional repression. SIP1 has recently been found to directly repress a panel of genes (connexin-26, plakophilin-2 and ZO-3) whose products are involved in intercellular junctions (Vandewalle, 2005).

CID and SID

In humans the family of CtBP proteins includes two highly homologous (83% similarity on aa level) members that are encoded by separate genes, *CtBP1* and *CtBP2* (Katsanis and Fisher, 1998). CtBP1 was originally identified as a 45kDa phosphoprotein repressing the transforming potential of E1A by direct binding to its C-terminal region (Boyd *et al.*, 1993). Subsequent investigations have shown that both CtBPs equally assist transcriptional repression by a wide range of transcriptional repressors (e.g. Snail, net, KLF8, Tcf-4) (Chinnadurai, 2002). Although the precise mechanism by which CtBP plays its repressing role remains to be fully elucidated it appears that both direct and indirect mechanisms are involved. Direct transcriptional repression is presented by the recruitment of histone deacetylases (HDAC type I and II) as well as histone methyltransferase (euchromatic histone-lysine N-methyltransferase 2), which in turns repress gene expression by modifying local chromatin structure (Shi *et al.*, 2003; Sundqvist *et al.*, 2001). Indirect repression could be mediated through several adaptor proteins e.g. CtIP (CtBP interacting protein), RIP140 (Chinnadurai, 2002). Additionally, dimeric CtBP also act as a NAD⁺ regulated dehydrogenase through an intrinsic region with high homology to 2-hydroxy acid dehydrogenases (Kumar *et al.*, 2002). The controversial combination of CtBPs co-repression function and its metabolic associated enzymatic activity has recently been explained in a suggested model of Thio *et al.* (2004), where NADH-dependent CtBP homodimerization is suggested to regulate co-repressor function. This is supported by evidence positively correlating nuclear levels of NADH with the repressor potential (Zhang *et al.*, 2002) and thereby allocating CtBP a redox-mediated transcriptional regulatory role. Another mechanism regulating CtBP functional activity implicates phosphorylation of an intrinsic serine residue (Ser158). Phosphorylation of CtBP by Pak1 (p21/Cdc42/Rac1-activated kinase 1) inhibits its NADH-dependent dehydrogenase activity and reduced its

repressing potential of the E-cadherin promoter. Interestingly, in MCF-7 cells, siRNA-mediated knockdown of Pak1 induced a translocation of CtBP from cytoplasm to nuclei indicating that the phosphorylation also controls trafficking (Barnes *et al.*, 2003).

SIP1 contains four consensus CtBP1 binding sequences (PLXL(S/T)) in a 100aa-wide region now designated as the CtBP interacting domain (CID), which is responsible for co-immunoprecipitation with CtBP (Shi *et al.*, 2003; Postigo and Dean, 2000). Although these data clearly implicate CtBP in SIP1-mediated repression, in MDCK cells, SIP1 is thought to repress E-cadherin transcription independently of CtBP (van Grunsven *et al.*, 2003).

Although Verschueren *et al.* reported SIP1 interaction with the MH2 (MAD homology 2) domain of receptor-mediated Smads (R-Smads) *in vitro*, very little is known *pro tempore* about the significance of this interaction. Smads are mediators in the signalling pathways of the TGF- β (Transforming Growth Factor β) superfamily. GF activated transmembrane receptors conduct their signal by phosphorylating R-Smads, which in turn bind Smad4 and translocate to the nucleus where they either repress or activate transcription dependent on coregulators. While Smad 1, 5 and 8 respond to BMP (Bone Morphogenetic Proteins) and GDF (Growth Differentiation Factors) signals, Smad 2 and 3 acts downstream of TGF- β and activin. Smad6 and 7 are known as inhibitory (I-Smads) as they antagonise R-Smads.

Both SIP1 and ZEB1 contain a Smad interacting domain (SID) but seem to have an opposed impact on TGF β 1 and BMP-2 induced pathways. Whereas ZEB1 enhance the up regulation of target genes (e.g. p21, c-jun) possibly through the recruitment of P/CAF and p300, SIP1 (lacking a (P/CAF)/p300 recruitment domain) repress the signal (Postigo, 2003; Postigo *et al.*, 2003). Whether this effect is due to titration or recruitment of CtBP remains to be further investigated.

Although no existing evidence suggests that SIP1 can act as a direct activator of transcription SIP1 expression is correlated with transcriptional up regulation. Recently,

SIP1 dependent up regulation of Foxe3 was found in the formation of the ocular lens. Promoter studies showed that this was independent on the SID domain but greatly enhanced by Smad8 co-expression. Interestingly Smad8 expression by its own did not influence expression (Yoshimoto *et al*, 2005). These results emphasize the complexity and need for further investigations of the relationship between SIP1 and Smads.

Results

Part 1

General features of SIP1-mediated epithelial to mesenchymal transition (EMT) in the squamous epidermoid carcinoma cell line, A431

Ectopic SIP1 expression in the squamous epidermoid carcinoma cell line A431 induces epithelial to mesenchymal transition. The aim of this study is to shed more light on the EMT-inducing potential of the SIP1. To address this issue, we generated clones of squamous epidermoid carcinoma cells (A431) with the DOX-regulated expression of 6xMyc-tagged wild type SIP1 (clone A431/SIP1) and SIP1 with mutated Zn-finger domain (clone A431/SIP1ZFmut). Of note, van Grunsven and colleagues (van Grunsven *et al.*, 2003) showed that SIP1ZFmut is not able to bind the E-cadherin promoter and consequently repress E-cadherin transcription. In our system treatment with DOX resulted in rapid accumulation of SIP1 in ~90% of A431/SIP1 and SIP1ZFmut in A431/SIP1ZFmut cells (Figure 6).

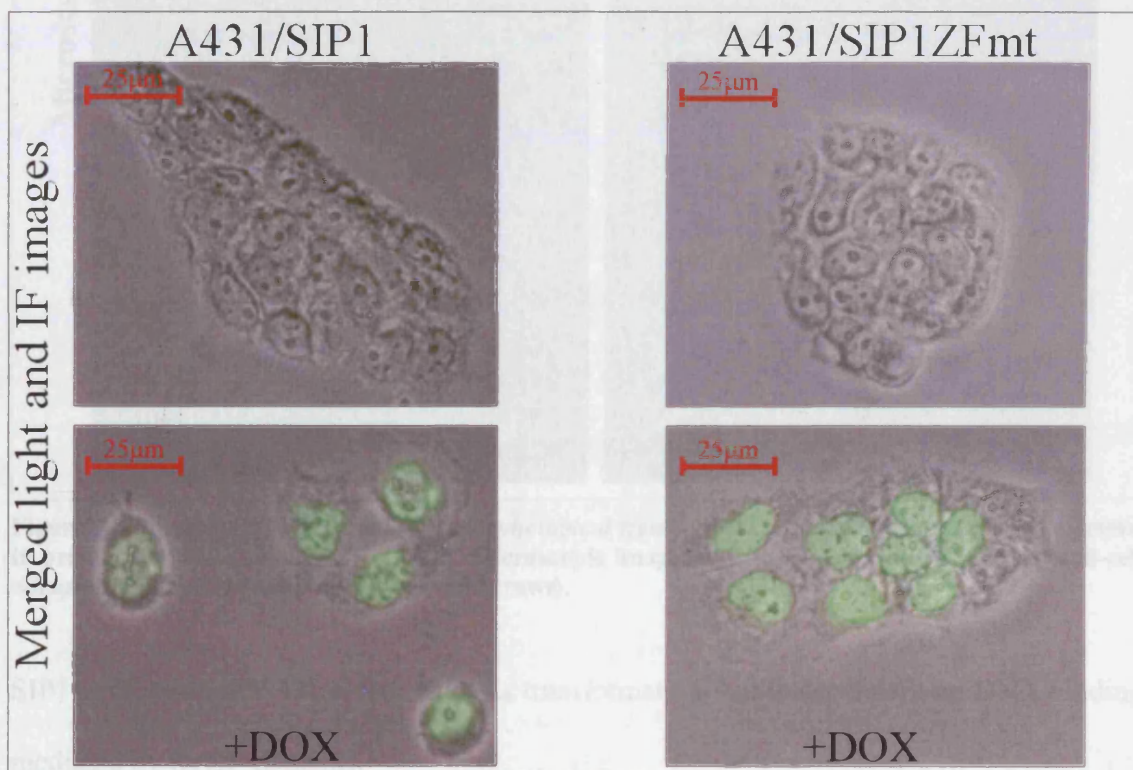


Figure 6. Treatment with DOX induces the expression of myc-tagged SIP1 in A431/SIP1 and A431/SIP1ZFmut cells. Cells were grown in presence or absence of DOX for 48h. Images shows merged fluorescence- and light-microscopy images of acetone-methanol fixed cells stained for myc.

Whereas 48h of DOX treatment in A431/SIP1 cells induced a dramatic morphological conversion towards a fibroblastic phenotype, DOX-induced A431/SIP1ZFmut cells retained the classic epithelial morphology (Figure 7). These results clearly demonstrate that

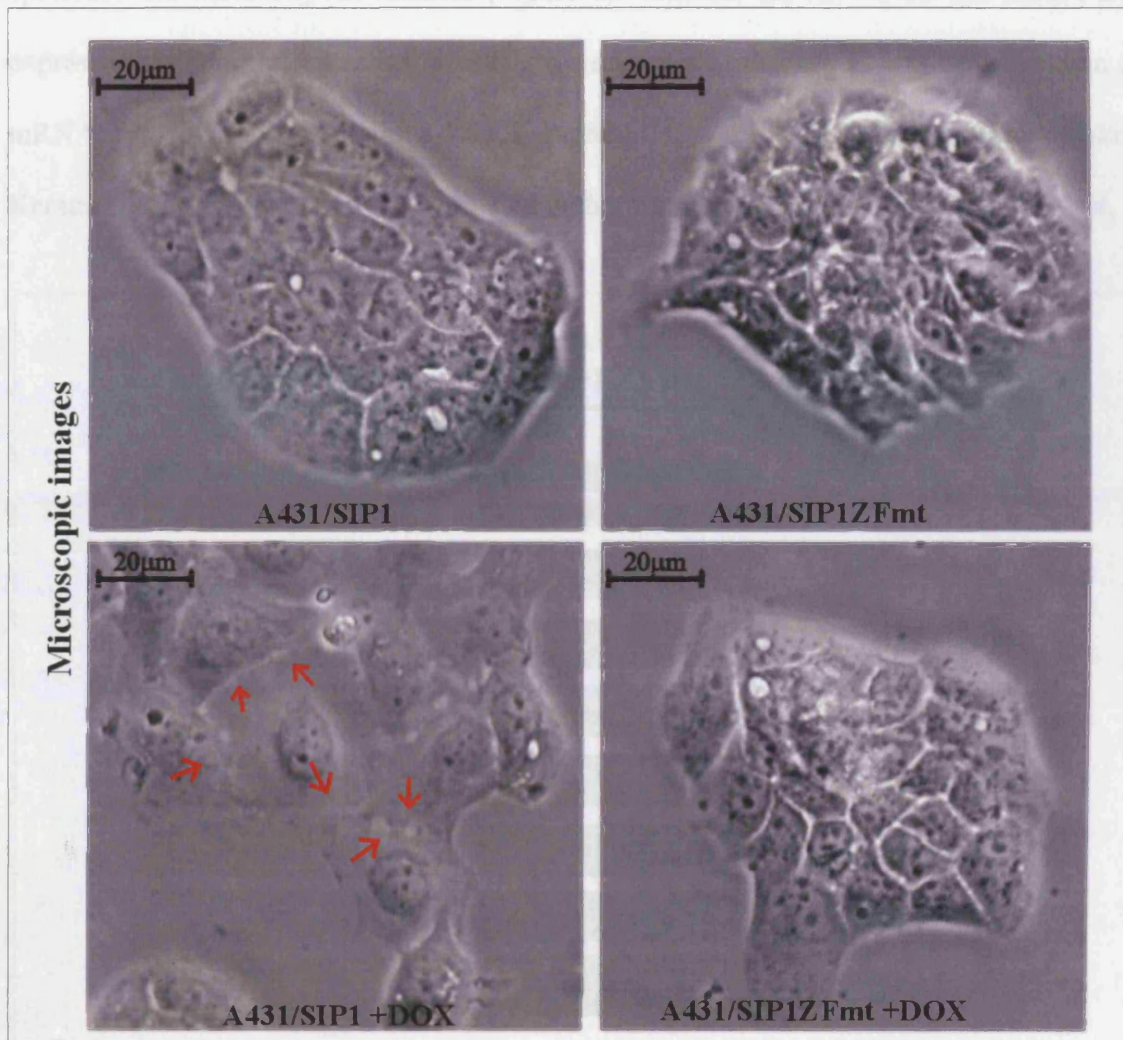


Figure 7. Expression of SIP1 induces a morphological transformation in A431 cells. Cells were grown in presence or absence of DOX for 48h. Microscopic images of cells *in vivo*. Note the loss of cell-cell adhesion and apical-basal bipolarity (red arrows).

SIP1 expression in A431 cells induces a transformation that is dependent on DNA binding mediated by its ZF-domains.

As the SIP1-induced transformation involved several cellular aspects such as, loss of intercellular adhesion, loss of bipolarity (assessed by phase-contrast microscopy) and induced scattering, we speculated that SIP1 induced a coordinated genetic programme

regulating several mesenchymal as well as epithelial genes. mRNA from both DOX-induced and noninduced A431/SIP1 and A431/SIP1ZFmt cells were subjected to semi quantitative RT-PCR analysis in order to check the expressional level of a few key epithelial and mesenchymal markers (Figure 8). Whereas SIP1ZFmt did not induce any expressional changes, expression of SIP1 was negatively correlated with the expression of mRNA encoding the epithelial markers; E-cadherin, Claudin-4, Desmoglein, Desmoplakin, Keratin 15 and 13 but positively correlated with the expression of Vimentin and S100A4.

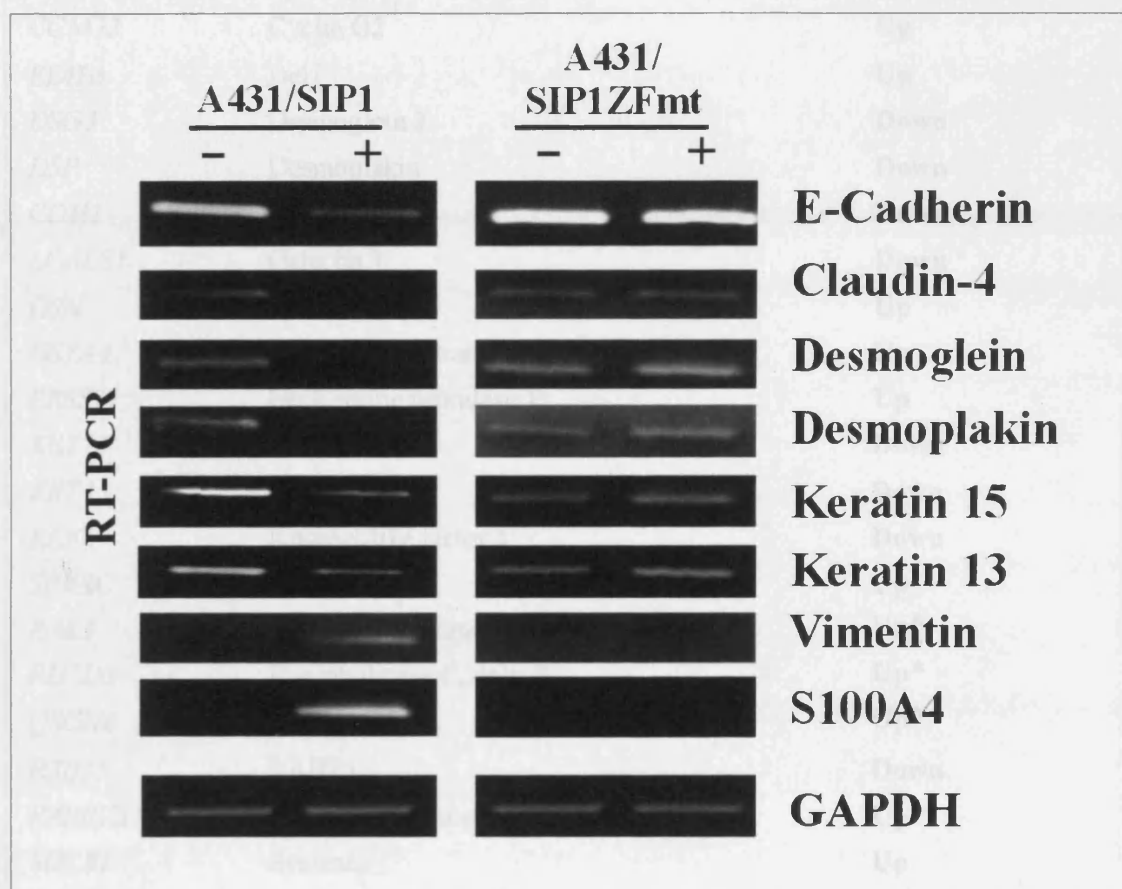


Figure 8. Expression of SIP1 but not SIP1ZFmt induces expressional changes of key epithelial and mesenchymal markers. mRNA was isolated from subconfluent cell cultures and subsequently used to estimate mRNA levels of selected transcripts by RT-PCR.

In collaboration with Dr Berx (University of Ghent, Belgium) a comprehensive analysis of gene expression (cDNA-array) was performed in order to identify specific genes involved in SIP1-mediated transformation and to determine the magnitude of the genetic re-

programming (Array data are presented in Appendix A). We found that SIP1 expression in A431 induced a global (2% of investigated genes were affected >1.8-fold) change in gene expression within 48h. To verify the quality of array data specific genes were subsequently

<u>Gene</u>	<u>Protein</u>	<u>Regulatory effect by SIP1</u>
<i>ATOH8</i>	Atonal homolog 8	Up
<i>CAV2</i>	Caveolin 2	Down
<i>CLDN4</i>	Claudin 4	Down
<i>CFL2</i>	Cofilin 2	Up
<i>CCND1</i>	Cyclin D1	Down
<i>CCNG2</i>	Cyclin G2	Up
<i>EDIL3</i>	Del1	Up
<i>DSG3</i>	Desmoglein 3	Down
<i>DSP</i>	Desmoplakin	Down
<i>CDH1</i>	E-cadherin	Down
<i>LGALS1</i>	Galectin 1	Down
<i>GSN</i>	Gelsolin	Up
<i>GSTA4</i>	Glutathione S-transferase A4	Up
<i>PRSS11</i>	HtrA serine peptidase 1	Up
<i>KRT13</i>	Keratin 13	Down
<i>KRT15</i>	Keratin 15	Down
<i>KLF4</i>	Kruppel-like factor 4	Down
<i>SPARC</i>	Osteonectin	Up
<i>PAK1</i>	p21-activated kinase 1	Up*
<i>PLCD3</i>	Phospholipase C, delta 3	Up*
<i>QSCN6</i>	Quiescin Q6	Up*
<i>RAB25</i>	RAB25	Down
<i>RARRES1</i>	Retinoic acid receptor responder 1	Up
<i>SDCBP</i>	Syntenin	Up
<i>TERT</i>	Telomerase reverse transcriptase	Down
<i>THBS1</i>	Thrombospondin 1	Up
<i>UBN1</i>	Ubinuclein 1	Down*
<i>VEGFC</i>	Vascular endothelial growth factor C	Up
<i>VIM</i>	Vimentin	Up

Table 1. App 85% of array data could be verified by RT-PCR. Indicated genes, originally identified as SIP1 responsive genes by the cDNA array, were investigated by RT-PCR. A discrepancy between the cDNA array and RT-PCR was found in 4 (indicated with *) out of 29 genes analysed.

selected and their expression were evaluated by semi quantitative RT-PCR (Table 1). A discrepancy between array data and RT-PCR was found in app 15% (4/29) of investigated genes, allocating data obtained from the array a relatively high credibility. The majority of regulated genes contain no canonical SIP1-binding elements in their promoters suggesting that their transcription is regulated indirectly. When we grouped SIP1-regulated genes according to their cellular function, a clear pattern emerged. Canonical epithelial markers were down regulated while mesenchymal markers were up regulated upon SIP1 expression. In contrast SIP1ZFmut influenced none of the 29 genes examined by RT-PCR. Interestingly, this indicates that SIP1 does not regulate transcription by titrating proteins through its intrinsic SID and CID (see schematic representation of SIP1 in Figure 1), since these domains are not impaired in SIP1ZFmut. Taken together, SIP1 induces a coordinated transformation of the A431 cell line that we recognise as an epithelial to mesenchymal transition.

SIP1-mediated EMT in A431 is concomitant with repressed proliferation. Working with A431/SIP1-inducible clones, we noticed that cells maintained in the presence of DOX seemed to proliferate more slowly than untreated cells. Cell scattering and morphological transformation that occur during EMT reflect fundamental alterations in cellular physiology and could possibly represent a swap from a proliferative to an invasive phenotype. To test this hypothesis, we examined how SIP1 expression influenced cell cycle progression and cell invasion.

Staining non-induced/induced A431/SIP1 and A431/SIP1ZFmut cells with Propidium iodide and subsequently analysing the stained cells by FACS provided an estimated profile of the cell-cycle distribution of the different cell cultures. The expression of SIP1 clearly induced a shift in PI/FACS profile (Figure 9A) and the proportion of cells residing G₁/G₀ was significantly higher in SIP1-expressing cells than in non-expressing cells (Figure 9B). In

contrary, DOX-induced expression of SIP1ZFmt did not influence the PI/FACS profile in A431/SIP1ZFmt cells and did not change the proportion of cells in G_1/G_0 (Figure 9B).

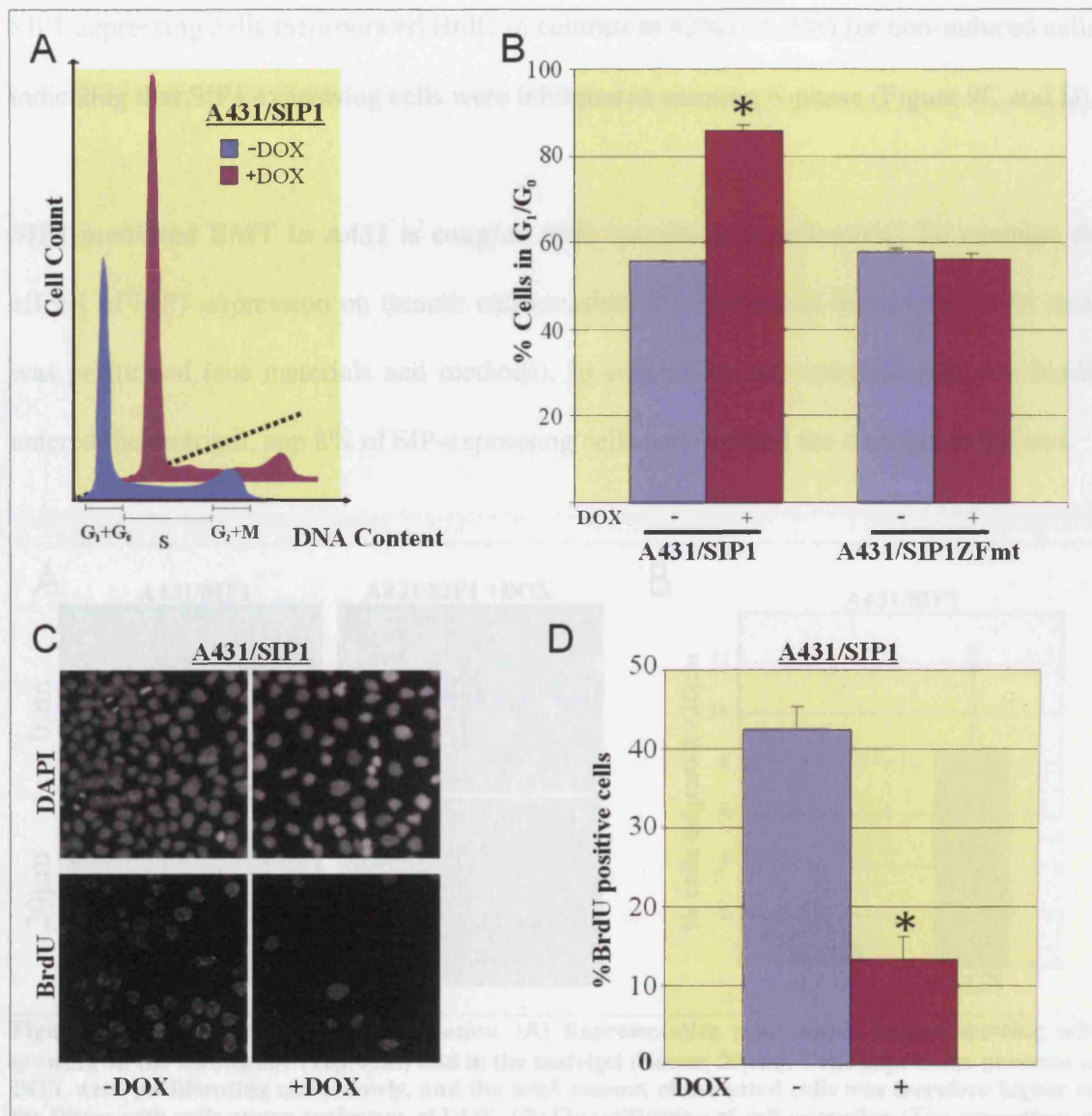


Figure 9. *SIP1* expression represses cell proliferation. (A+B) A431/SIP1 and A431/SIP1ZFmt cells were seeded and maintained either with or without DOX for 48h before the cell-cycle profiles was determined by Propidium iodide/FACS. The experiment was based on triplicates. Similar experiments but with varying conditions (e.g. cell density, time of media change) showed the same trend. (A) Representative examples of cell cycle profiles of non-induced/induced A431/SIP1 cells. (B) Diagram representing the proportion of cell population residing G_1/G_0 in indicated clones with/without DOX treatment. (C+D) A431/SIP1 cells were seeded in 12-well plates and maintained with/without DOX for 48h followed by 40min BrdU pulse labelling. BrdU incorporation was detected by fluorescence microscopy with monoclonal anti-BrdU antibody. (C) Representative microscopic images showing cells in total (Top, DAPI) and cells in S-phase (Lower, BrdU). (D) Proportion of cells incorporating BrdU (Proportion of BrdU-positive cells was quantified in six randomly chosen microscopic fields and presented as mean \pm SD. The experiment was repeated twice with similar results.). * (Students T-test, two-tailed, $p < 0.01$)

In order to assess the influence of SIP1 expression on proliferation by another method we measured the proportion of induced and non-induced A431/SIP1 cells in S-phase by BrdU incorporation. Proliferation was significantly repressed by SIP1. Only 13% (+/- 3%) of SIP1 expressing cells incorporated BrdU in contrast to 42% (+/- 3%) for non-induced cells, indicating that SIP1 expressing cells were inhibited in entering S-phase (Figure 9C and D).

SIP1-mediated EMT in A431 is coupled with increased invasiveness. To examine the effects of SIP1 expression on tumour cell invasion, 3-dimensional *in vitro* invasion assay was performed (see materials and methods). In contrast to non-induced cells that hardly entered the matrigel, app 8% of SIP-expressing cells had invaded the matrigel at the end

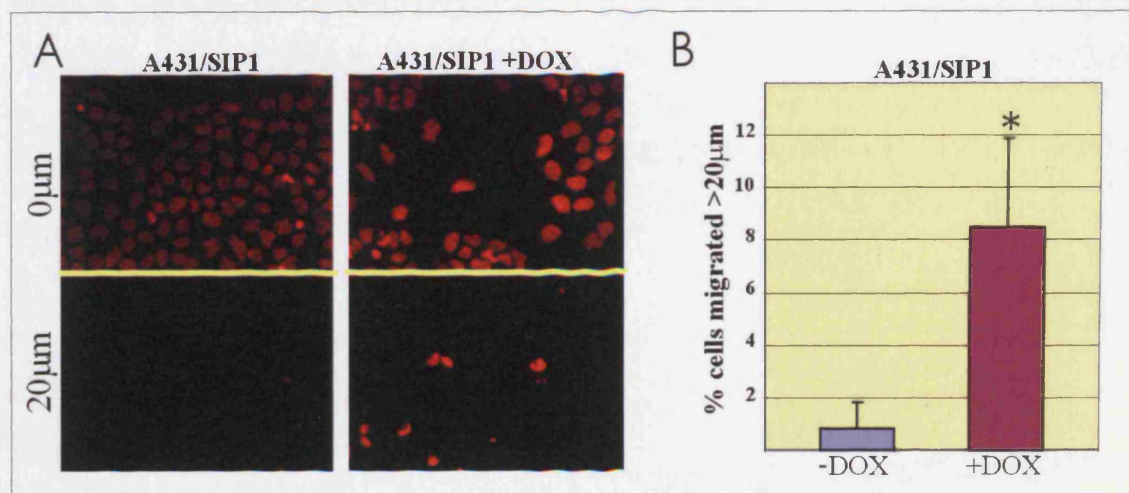


Figure 10. SIP1 expression induces invasion. (A) Representative microscopic images showing cells growing on the membrane (Top, 0µm) and in the matrigel (Lower, 20µm). Cells kept in the presence of DOX were proliferating more slowly, and the total amount of untreated cells was therefore higher on the filters with cells grown in absence of DOX. (B) Quantification of cell migration (The percentage of cells invading matrigel was quantified in twelve microscopic fields. The diagram represents the mean ± SD)* (Students T-test, two-tailed, p<0.01)

of the assay (96h) (Figure 10). Furthermore, SIP1-expressing cells migrated into the matrigel at the distance of more than 50 µm.

Summary. Presented data demonstrate that SIP1 induces EMT in A431 cells. This was manifested by cell scattering, loss of epithelial apical-basal bipolarity, increased invasiveness and a coordinated switch from an epithelial to a mesenchymal pattern of gene expression. In addition to the acknowledged features of EMT, expression of SIP1 in A431 cells inhibited proliferation.

Results

Part 2

SIP1 inhibits cell proliferation through direct transcriptional repression of the Cyclin D1 encoding gene CCND1.

SIP1 expressing cells accumulate in G₁. To further analyse the effects of SIP1 on cell growth, we estimated the cell growth of DOX-treated and non-treated A431/SIP1 cells by the MTT-assay (Figure 11A).

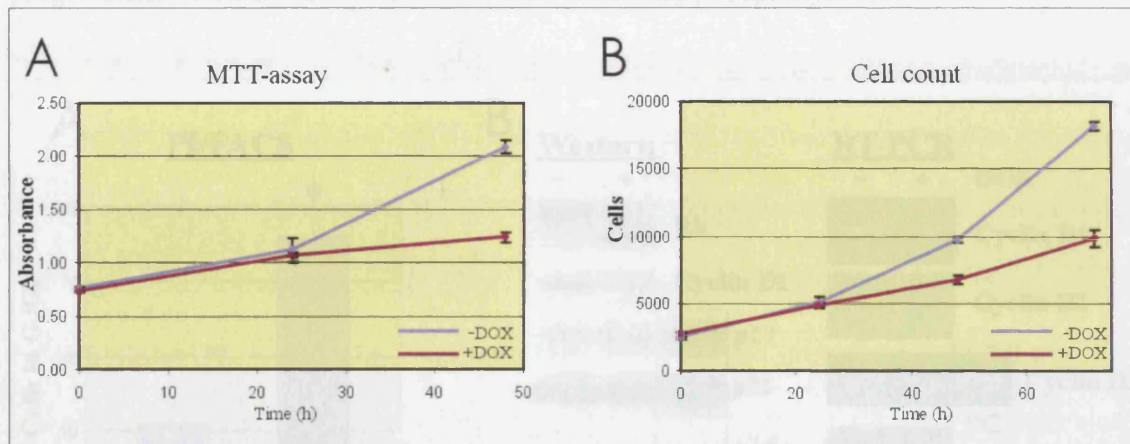


Figure 11. *SIP1 expression represses growth in cell population.* Growth in cell population was estimated by MTT-assay (A) and cell counting (B). Each diagram represent a single experiment based on triplicates for each time point and displays means \pm SD. Both experiments were carried out twice with similar results.

Although net cell growth was independent of DOX during the first 24h, a significant suppression of growth was detected beyond 24h of induction. Since the MTT-assay is only an indirect method for estimating cell growth we decided to apply the traditional but time consuming technique, cell counting. Equal amounts of A431/SIP1 cells were seeded in six dishes, maintained with and without DOX and counted in 24, 48 and 72 hours (Figure 11B). After 24 hours of DOX-treatment, SIP1 strongly decreased the doubling time of A431 cells ($T_2 \approx 24$ hours in non-stimulated and $T_2 \approx 48$ hours in DOX-treated cells) (Figure 11A and B).

As the preliminary PI/FACS analysis of cell cycle distribution indicated that SIP1 induced an accumulation of cells in G₁ (Figure 9) we decided to increase the resolution by carrying out the same experiment, at the same conditions, several times. Once again, the FACS analysis of A431/SIP1 cell cultures maintained with or without DOX for 48 hours demonstrated that SIP1-expressing cells were accumulated in the G₁ phase. The percentage

of cells present in S, G₂ and M-phase was 2 times lower in cells undergoing SIP-mediated EMT (24 +/-4% versus 49 +/-3%). Since G₁/S transition in mammalian cell cycle is regulated by Rb pathway, and phosphorylation of the Rb protein is critical for G₁/S progression, we examined the effect of SIP1 on the Rb phosphorylation.

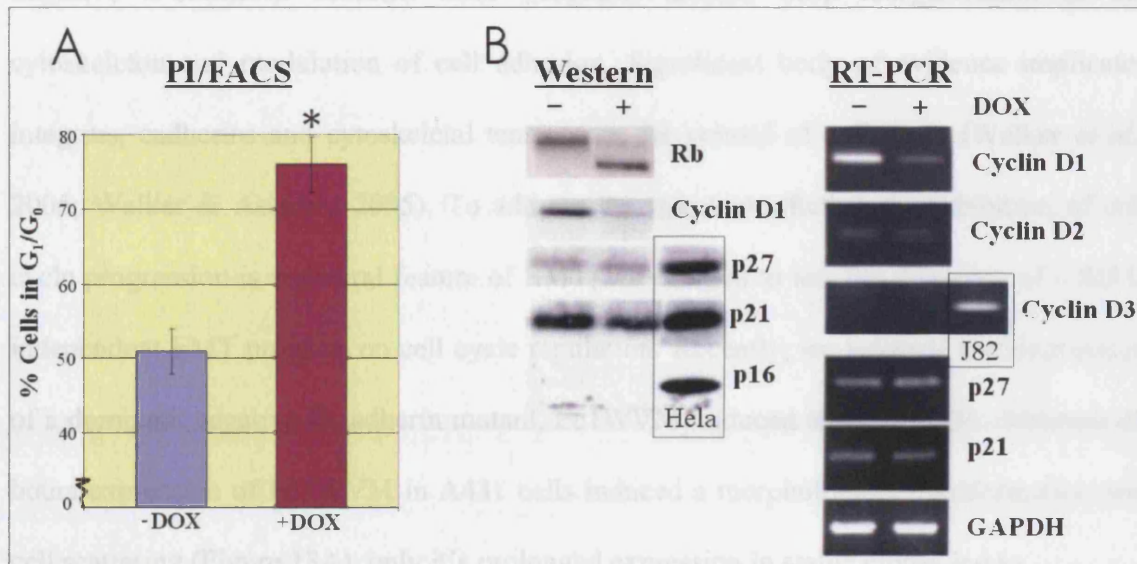


Figure 12. *SIP1* expression induces cell cycle arrest in G₁/G₀. (A) A431/SIP1 cells were seeded and maintained with/without DOX for 48h before they were collected and stained by propidium iodide. Subsequent, cell cycle distribution was estimated by FACS. The diagram represents means \pm SD of 3 separate experiments. (B) Immunoblots and RT-PCR showing relative levels of protein and mRNA of crucial regulators of the G₁/S transition. Total cell lysates from HeLa and RNA purified from J82 were used as positive controls where indicated. * (Students T-test, two-tailed, $p < 0.01$)

We found that in our system, accumulation of cells in G₁ of the cell cycle was concomitant with the hypophosphorylation of Rb (Figure 12B). The previously described microarray analysis (Appendix A) revealed a strong (6.7-fold) down-regulation of the *CCND1* gene, which encodes cyclin D1, a critical regulator of Rb phosphorylation. We confirmed SIP1-mediated repression of cyclin D1 on both, mRNA and protein levels (Figure 12B). Next, we analysed expression of other key proteins regulating Rb phosphorylation and cell cycle progression through G₁ phase. Whereas the levels of cyclin D2, cyclin E and p27^{Kip1} were not altered in A431 cells upon SIP1 induction, expression of cyclin D3 and p16 was not detected in neither non-induced nor induced A431/SIP1 cells (Figure 12B). Unexpectedly,

the expression of p21^{Cip1} was slightly reduced in SIP1-expressing cells on protein but not on the mRNA level.

Transition into S phase of the cell cycle is inhibited by SIP1 but not by a dominant negative E-cadherin mutant. EMT programs involve deep reorganization of the cytoskeleton and modulation of cell adhesion. Significant body of evidence implicates integrins, cadherins and cytoskeletal tensions in the control of cell cycle (Walker *et al.*, 2005; Walker & Assoian, 2005). To address the question whether the inhibition of cell cycle progression is a general feature of EMT, we decided to test the influence of a SIP1-independent EMT program on cell cycle regulation. Recently, we reported that expression of a dominant negative E-cadherin mutant, Ec1WVM, induced EMT in A431. Whereas 48 hours expression of Ec1WVM in A431 cells induced a morphological transformation and cell scattering (Figure 13A), only its prolonged expression in stable clones led to

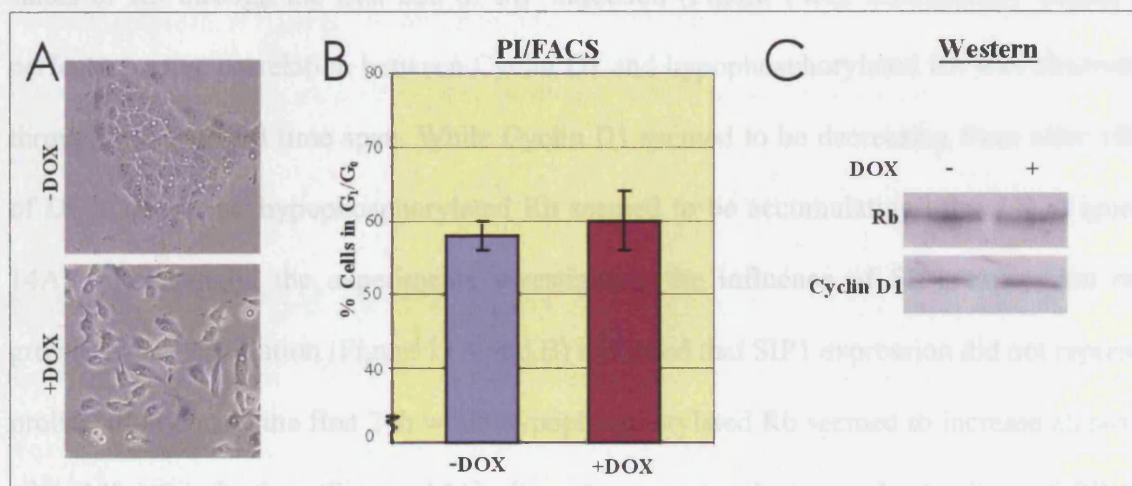


Figure 13. DOX-induced Ec1WVM expression induces EMT but does not influence proliferation. (A) Microscopic images of A431/EcWVM cultured with/without DOX for 48h. (B) Cell cycle distribution was analysed by FACS after 48h of maintenance with/without DOX. Diagram represents the means \pm SD of triplicates. (C) Immunoblot shows expression of indicated proteins.

activation of the mesenchymal marker vimentin (Andersen *et al.*, 2005 (Appendix B)).

Neither long-term (Andersen *et al.*, 2005) nor short-term Ec1WVM expression (Figure 13B) inhibited G₁/S phase transition in A431 cells. In agreement with these data, we

observed no effects on neither Rb phosphorylation nor cyclin D1 expression during EclWVM-induced EMT (Figure 13C). These data show that in different EMT models, the G₁ to S transition depends on the specific nature of the individual EMT-inducing signal.

Cyclin D1 down-regulation is tightly followed by Rb hypophosphorylation in time. As 48h of SIP1 expression was correlated with Cyclin D1 down regulation as well as Rb hypophosphorylation we decided to investigate whether the obvious negative correlation between Cyclin D1 and hypophosphorylated Rb was kept through the transition. A431/SIP1 cells were seeded in 9 small flasks and kept overnight in the CO₂-incubator. The following day media was changed and all except one was added DOX. After 8h, protein samples were prepared from the flasks every 2h, giving lysate-samples from +8h to +22h in addition to the negative control (non-induced cells). This allowed us to assess, by western analysis, the general expression level of Cyclin D1 as well as the phosphorylation status of Rb through the first 22h of SIP induction (Figure 14A). Interestingly almost a perfect negative correlation between Cyclin D1 and hypophosphorylated Rb was observed through the depicted time span. While Cyclin D1 seemed to be decreasing from after 10h of DOX treatment, hypophosphorylated Rb seemed to be accumulating after 14h (Figure 14A). Interestingly, the experiments investigating the influence of SIP1 expression on growth in cell population (Figure 11A and B) indicated that SIP1 expression did not repress proliferation during the first 24h while hypophosphorylated Rb seemed to increase already after 14h of induction (Figure 14A). In order to get a better understanding of SIP1-mediated regulation of proliferation we decided to analyse the cell cycle distribution by PI/FACS after 24h as well as 48h of DOX treatment (Figure 14B). Already at 24h after SIP1-induction a significant higher proportion of SIP1-expressing cells (54% vs. 38%) were residing G₁/G₀ compared to non-induced cells.

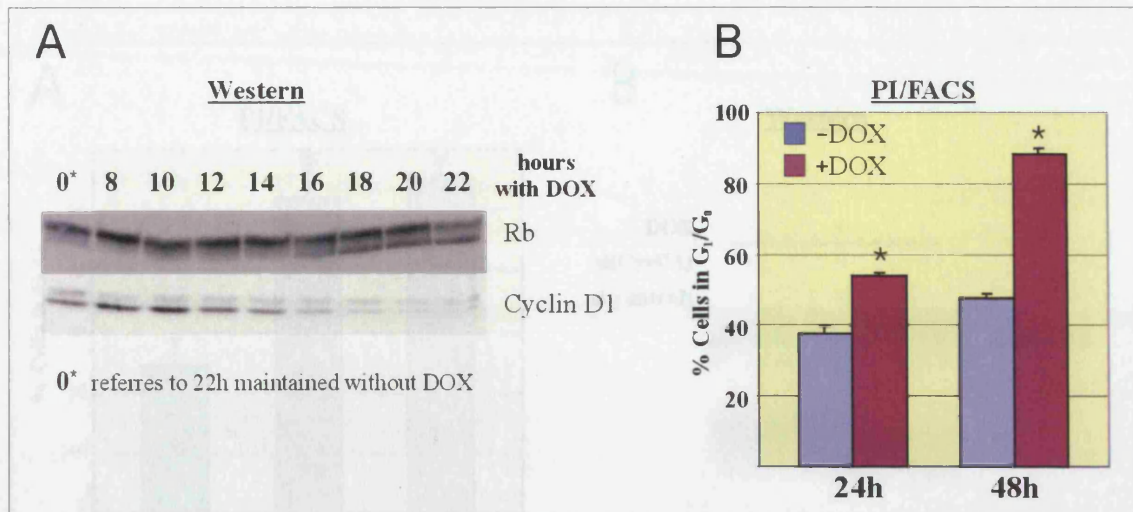


Figure 14. Cyclin D1 negatively correlates with hypophosphorylated Rb during SIP1-induced EMT. (A) Protein lysates was isolated from A431/SIP1 cells maintained in DOX for various durations. Western analysis was performed to assess the expression of indicated proteins at the different time points. (B) Non-induced/induced A431/SIP1 cells were subjected to PI/FACS analysis 24 hours and 48 hours post DOX induction. The diagram presenting means +/-SD is based on triplicates. * (Students T-test, two-tailed, $p < 0.01$)

The difference were further increased at the time point 48h were 88% of SIP1 expressing cells were situated in G₁/G₀ in contrast to 48% for non-induced cells. Taken together, the observed events make it plausible to hypothesize that SIP1 induces directly/indirectly the down regulation of Cyclin D1 which is followed by hypophosphorylation of Rb, restricted G₁ to S transition (accumulation of cells in G₁) which is eventually reflected in repressed proliferation.

Cyclin D1 down-regulation is necessary and sufficient for SIP1-induced cell cycle arrest in G₁. Cyclin D1 down regulation correlated with Rb hypophosphorylation and accumulation of the cells in G₁/G₀ phase of the cell cycle. To analyse whether SIP1 affects cell cycle distribution via Cyclin D1, we used two approaches. Firstly, we suppressed the expression of endogenous Cyclin D1 in A431/SIP1 cells by transfecting cells with siRNA targeting Cyclin D1 messenger. In non-induced A431/SIP1 cells, the siRNA-mediated reduction in Cyclin D1 levels resulted in Rb hypophosphorylation and accumulation of cells in G₁/G₀, resembling the effect of SIP1 expression (Figure 15A and B).

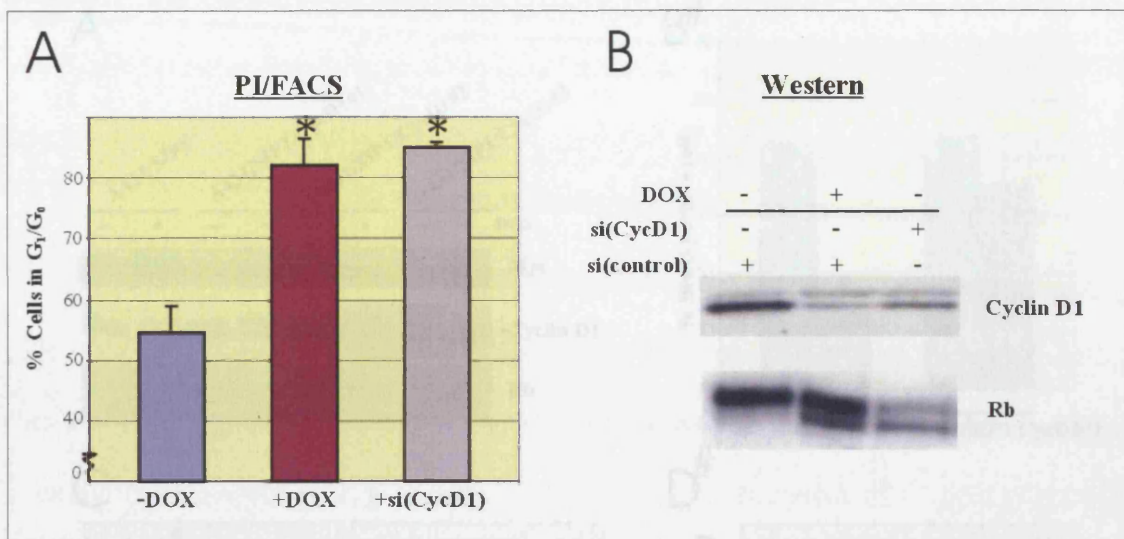


Figure 15. Cyclin D1 knockdown is concomitant with pRb hypophosphorylation and G₁ arrest. A431/SIP1 cells were transfected with either control siRNA or siRNA targeting cyclin D1 mRNA. Cells transfected with control siRNA were divided and cultured with/without DOX. (A) 48h after transfection cell cycle distribution was analysed by PI/FACS (Diagram is based on triplicates). (B) Immunoblot showing protein levels (48h after transfection) of Cyclin D1 and Rb. *(both compared to A431/SIP1 transfected with control siRNA but maintained without DOX, Students T-test, two-tailed, $p < 0.01$)

In parallel, we generated clones of A431/SIP1 cells with simultaneous DOX-regulated expression of SIP1 and Cyclin D1 (A431/SIP1/CycD1#1-3). In A431/SIP1/CycD1#1, concomitant expression of exogenous cyclin D1 and SIP1 resulted in a partial restoration of Cyclin D1 levels (Figure 16A). Interestingly, Rb hypophosphorylation was partly suppressed in this clone, and the proportion of cells retained in G₁ decreased from 85% (A431/SIP1, +DOX) to 62% (A431/SIP1/CycD1#1, +DOX) (Figure 16C). In A431/SIP1/CycD1#2 and A431/SIP1/CycD1#3, DOX-treatment led to a very high expression of Cyclin D1, significantly exceeding levels of endogenous Cyclin D1 in non-induced A431/SIP1 cells. In these clones, over-expression of Cyclin D1 completely blocked Rb hypophosphorylation and abrogated the effect of SIP1 on cell cycle distribution (differences in proportion of cells in G₁/G₀ between non-induced and induced A431/SIP1/CycD1#2 and 3 was not found to be statistically significant by two-tailed Students T-test; $p = 0.26$ for A431/SIP1/CycD1#2 and $p = 0.06$ for A431/SIP1/CycD1#3)

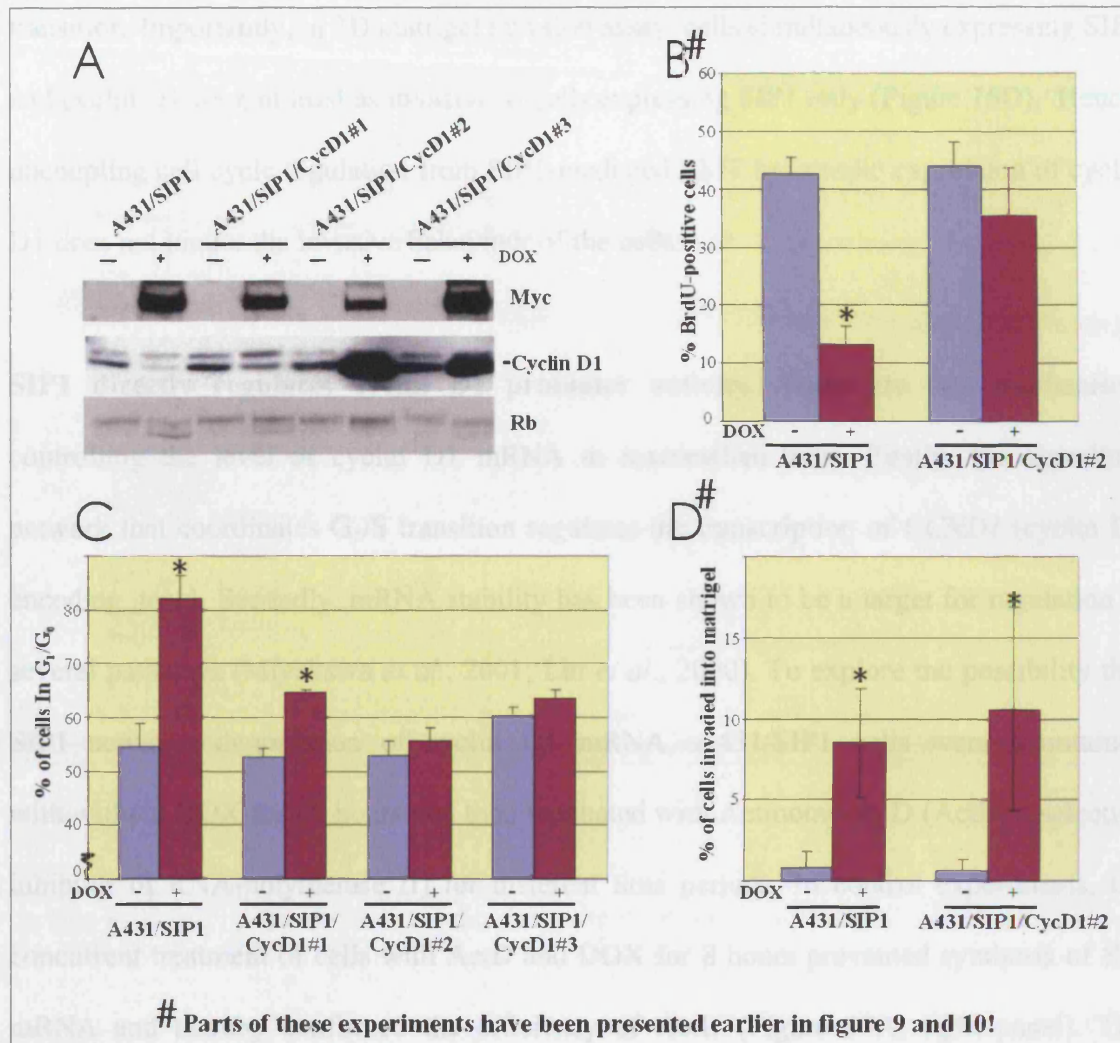


Figure 16. Ectopic Cyclin D1 expression abrogates SIP1-induced Rb hypophosphorylation and G₁ arrest. Clones with simultaneous DOX-regulated expression of SIP1 and Cyclin D1 were generated (A431/SIP1/CycD1#1-3). (A) Immunoblot of A431/SIP1 and A431/SIP1/CycD1 clones cultured with/without DOX for 48h. (B) Analysis of BrdU incorporation in A431/SIP1 and A431/SIP1/CycD1#2 cultured with/without DOX for 48h. Means and SD are based on six samples. (C) Analysis of cell cycle distribution was investigated by PI/FACS analysis of A431/SIP1 and A431/SIP1/CycD1 cells cultured with/without DOX for 48h. The diagram represent means \pm SD based on triplicates. (D) Invasive potential was estimated for induced/noninduced A431/SIP1 and A431/SIP1/CycD1#2 cells by 3D *in vitro* invasion assay. The mean percentage (\pm SD) of cells invading matrigel is based on twelve randomly selected microscopic fields. *(Students T-test, two-tailed, $p < 0.01$)

(Figure 16 A and C). Furthermore, the ectopic expression of cyclin D1 also bypassed the effect of SIP1 on BrdU incorporation (differences in proportion of cells incorporating BrdU between non-induced and induced A431/SIP1/CycD1#2 was not found to be statistically significant by two-tailed Students T-test; $p = 0.21$) (Figure 16B). Taken together, these data indicate that repression of cyclin D1 is indispensable for SIP1-mediated repression of G₁/S

transition. Importantly, in 3D matrigel invasion assay, cells simultaneously expressing SIP1 and cyclin D1 were at least as invasive as cells expressing SIP1 only (Figure 16D). Hence, uncoupling cell cycle regulation from SIP1-mediated EMT by ectopic expression of cyclin D1 does not hinder the invasive behaviour of the cells.

SIP1 directly regulates cyclin D1 promoter activity. There are two mechanisms controlling the level of cyclin D1 mRNA in mammalian cells. Firstly, the signalling network that coordinates G₁/S transition regulates the transcription of *CCND1* (cyclin D1 encoding gene). Secondly, mRNA stability has been shown to be a target for regulation in several pathways (Miyakawa *et al.*, 2001; Lin *et al.*, 2000). To explore the possibility that SIP1 activates degradation of cyclin D1 mRNA, A431/SIP1 cells were maintained with/without DOX for 48 hours and then incubated with Actinomycin D (ActD, a selective inhibitor of RNA-polymerase II) for different time periods. In control experiments, the concurrent treatment of cells with ActD and DOX for 8 hours prevented synthesis of SIP mRNA and thereby confirmed the efficiency of ActD (Figure 17A, right panel). The application of ActD for 4 or 8 hours revealed that cyclin D1 mRNA was very stable in DOX-treated and untreated A431/SIP1 cells as compared to the stability of Fra-1 or SIP1 mRNA (Figure 17A). To determine whether there was any significant difference in cyclin D1 mRNA stability between non-induced and induced cells we quantified the mRNA levels by real time PCR. A reduction in mRNA after 4h of ActD treatment was estimated to 85% in non-induced and 73% in induced cells (Figure 17B). However this difference could not be verified as statistically significant (Students T-test; p=0.3695, n=5). To examine whether SIP1 regulates the transcription rate of cyclin D1, we carried-out nuclear run-on assay with nuclei prepared from DOX-treated or untreated cells. Biotin-labelled UTP was incorporated into nascent transcripts. After the transcriptional reaction was completed,

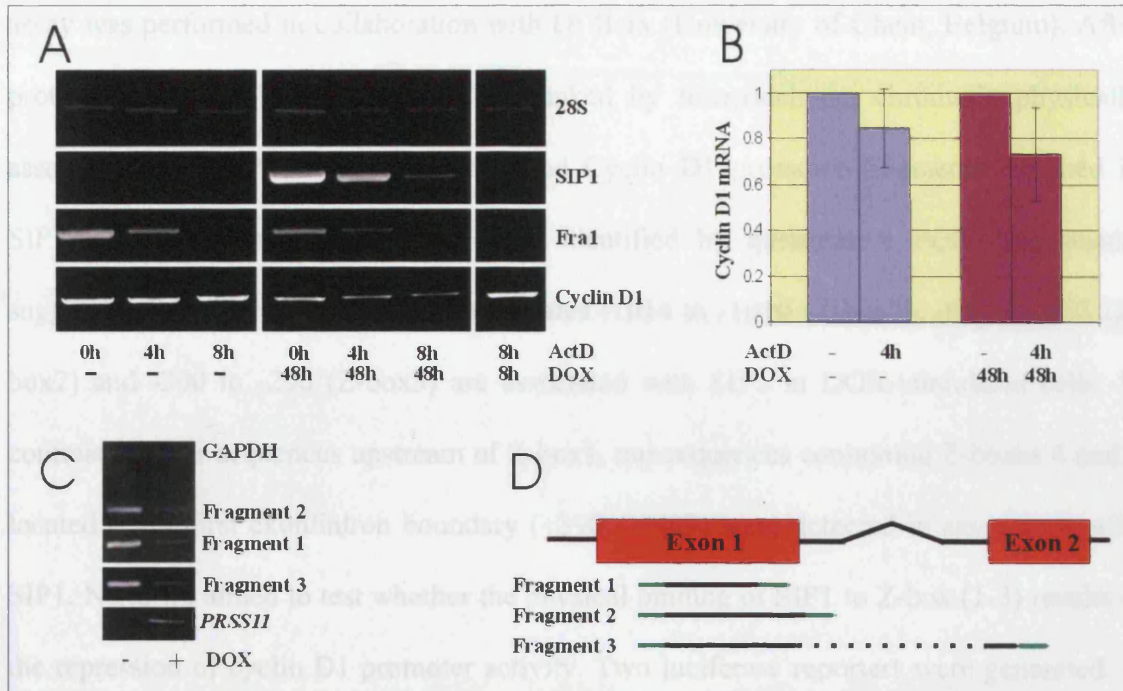


Figure 17. *SIP1*-induced down regulation of *Cyclin D1* is mediated through transcriptional repression. (A) A431/*SIP1* cells were maintained with or without DOX for 48 hours. ActD was added for 4 or 8 hours and expression of *Cyclin D1*, *SIP1* and *fra-1* mRNA was analysed by RT-PCR. 28S rRNA was used as an ActD-insensitive control. As a positive control for ActD, DOX and ActD were added simultaneously for 4h (right panel). The experiment was carried out twice with similar results. (B) Quantification of *Cyclin D1* mRNA levels in A431/*SIP1* cells maintained with or without DOX using real time PCR. Cells were treated with ActD for 8 hours. Diagram is based on triplicates. (C) Nuclei were isolated from A431/*SIP1* cells maintained with or without DOX for 48 hours and subjected to nuclear run-on assay (described in Materials and Methods). Isolated transcripts corresponding to GAPDH, *prss11* and *Cyclin D1* were quantified by RT-PCR. (D) Schematic representation depicting fragments of the *Cyclin D1* mRNA detected by RT-PCR in C.

newly synthesised RNA was affinity-purified and subjected to RT-PCR analysis. With three primer sets (Figure 17D), we demonstrated that *SIP1* significantly inhibited the transcription rate of *CCND1* (Figure 17C). In contrast, the *in vitro* transcription of *prss11* (a gene up-regulated by *SIP1*) was significantly increased upon *SIP1* expression. In all control reactions, in which non-labelled UTP was used, no PCR product was detected (data not shown). From these experiments, we concluded that transcriptional repression of the *Cyclin D1* promoter rather than mRNA destabilisation is responsible for *Cyclin D1* inhibition in course of *SIP1*-mediated EMT.

To assess whether the repression of *CCND1* by *SIP1* is direct, we used chromatin immunoprecipitation (ChIP) assay to analyse the *in vivo* binding of *SIP1* to potential *SIP1*-binding sites (Z-boxes) located in the vicinity of the *cyclin D1* transcription start site. ChIP

assay was performed in collaboration with Dr Berx (University of Ghent, Belgium). After protein-DNA complexes had been crosslinked by formaldehyde, chromatin physically associated with SIP1 was pulled-down and Cyclin D1 promoter fragments enriched in SIP1-containing chromatin fraction were identified by quantitative PCR. The results suggested that three Z-boxes with coordinates -1014 to -1010 (Z-box1), -857 to -853 (Z-box2) and -300 to -290 (Z-box3) are associated with SIP1 in DOX-stimulated cells. In contrast, neither sequences upstream of Z-box1, nor sequences containing Z-boxes 4 and 5 located at the first exon/intron boundary (+390 - +409) were detected in association with SIP1. Next, we aimed to test whether the physical binding of SIP1 to Z-box (1-3) results in the repression of cyclin D1 promoter activity. Two luciferase reporters were generated. A wild type reporter (pCCND1LUC) contained -1025 to +18 of the Cyclin D1 promoter sequence cloned upstream of the firefly luciferase gene. The second reporter (pCCND1 μ LUC) contained the same sequence but with three intrinsic Z-boxes mutated by a single nucleotide substitution (5'-AGGTG to 5'-AGATG) (Figure 18C). This particular substitution has previously been shown to block the binding of SIP1 to *CDH1* promoter DNA (Remacle *et al.*, 1999). All reporters (including control vector, Figure 18A) were more active in DOX-treated cells. However, mutating Z-boxes 1-3 resulted in the significantly greater activation of the reporter by SIP1 (Figure 18B). Taken together with the results of ChIP analysis, these data indicate that SIP1 represses transcription of Cyclin D1 via direct interaction with Z-boxes 1-3 in the cyclin D1 promoter.

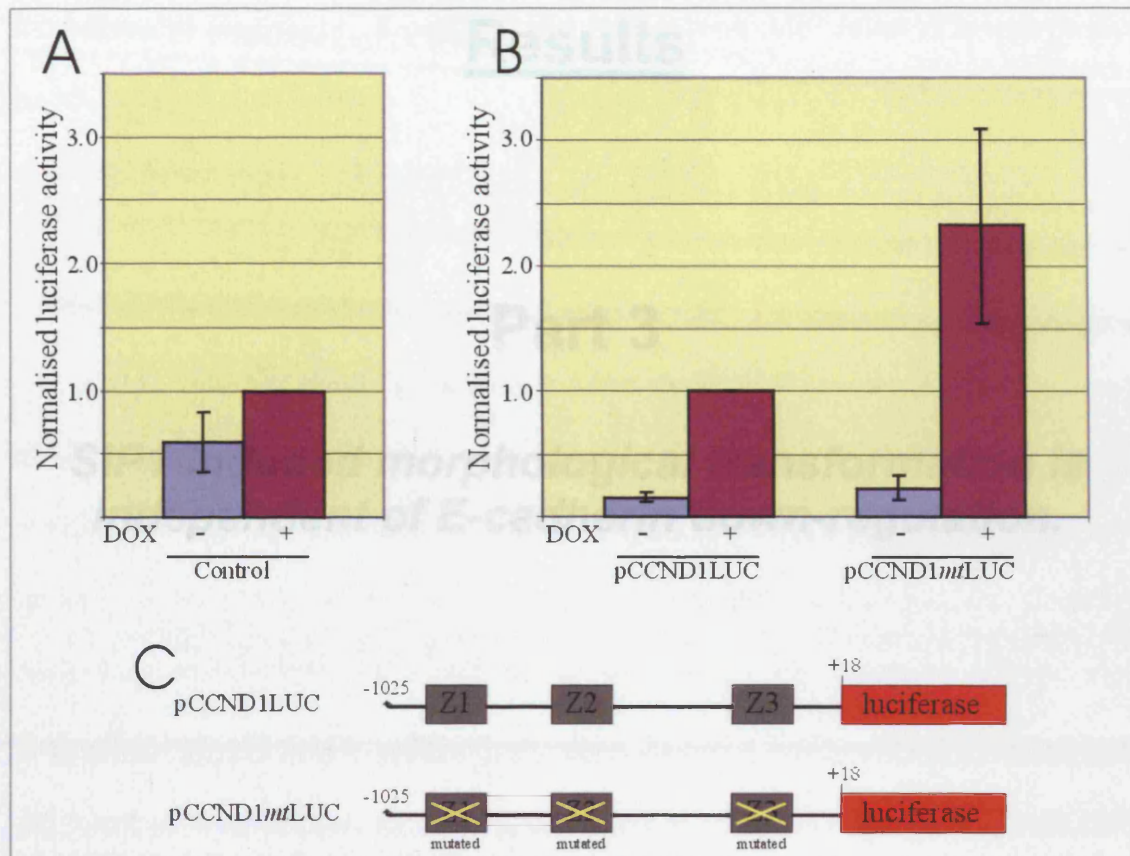


Figure 18. Functional Z-boxes repress transcription of CCND1 in SIP1 expressing cells. Luciferase reporter assay was performed as described in Material and Methods. **(A)** Activity of control vector (pGL3-Basic). **(B)** Activity of pCCND1LUC and pCCND1mutLUC. (Diagrams in **A** and **B** represent means \pm SD of three independent experiments, where each experiment was based on triplicates). **(C)** Schematic representation of luciferase constructs. Z(1-3) correspond to Z-box(1-3).

Summary. In A431 cells, expression of SIP1 repressed proliferation and concomitantly induced accumulation of cells in the G₁-phase of the cell cycle. SIP1 inhibited the expression of Cyclin D1 and induced hypophosphorylation of Rb. As demonstrated by ChIP and luciferase reporter assays, SIP1 binds the Cyclin D1 promoter and directly represses transcription. By expressing exogenous Cyclin D1 and using siRNA-mediated knockdown of Cyclin D1 we demonstrated that SIP1-mediated repression of Cyclin D1 in A431/SIP1 cells was both necessary and sufficient for Rb hypophosphorylation as well as cell cycle arrest in G₁. On the other hand, EMT induced in A431 cells by a dominant negative mutant of E-cadherin had no effect on cell cycle.

Results

Part 3

SIP1-induced morphological transformation is independent of E-cadherin down-regulation.

Expression of Flag-tagged E-cadherin does not repress SIP1 induced morphological transformation. The hallmark of EMT is abrogation of E-cadherin mediated intercellular adhesion. Since EMT programmes involve E-cadherin deregulation on both RNA and protein level, we assumed that SIP1-mediated repression of E-cadherin was directly responsible for the morphological transformation in SIP1-mediated EMT. This assumption was in line with my previous studies on c-Fos-mediated EMT in a mouse mammary carcinoma cell line (MT1TC1). In this model the epithelial cell line MT1TC1 was transfected with retrovirus expressing c-fos generating the cell line MT1TC1/cFos. In contrast to MT1TC1, MT1TC1/cFos had a mesenchymal phenotype and expressed diminished protein-levels of E-cadherin as well as α - and β -catenin (Figure 19B). Interestingly MT1TC1/cFos cells still expressed unaltered levels of mRNA encoding α - and β -catenin while mRNA encoding E-cadherin was immensely decreased (Figure 19B) indicating that E-cadherin could have a stabilising effect on α - and β -catenin proteins. Encouraged by the fact that MT1TC1/cFos cells still expressed α - and β -catenin mRNA we generated several clones of MT1TC1/cFos expressing exogenous myc-tagged E-cadherin, namely MT1TC1/cFos/Ec1#1-3. Not only did the exogenous expression of E-cadherin in MT1TC1/cFos cells restore the protein-levels of α - and β -catenin (Figure 19C) but also the mesenchymal phenotype was partly reverted to an epithelial phenotype (Figure 19A). All in all this approach provided a unique possibility to study the effect of E-cadherin associated elements of EMT. A similar approach was chosen to investigate the direct role of E-cadherin repression in SIP1-mediated EMT in A431 cells. In order to address this question, several A431/SIP1 clones with the stable expression of exogenous E-cadherin (pIRESFlag-Ec1) were generated. Of note, pIRESFlag-Ec1 encodes WT E-cadherin conjugated with the Flag-tag at the C-terminus and includes a 17 amino acid deletion in the cytosolic domain

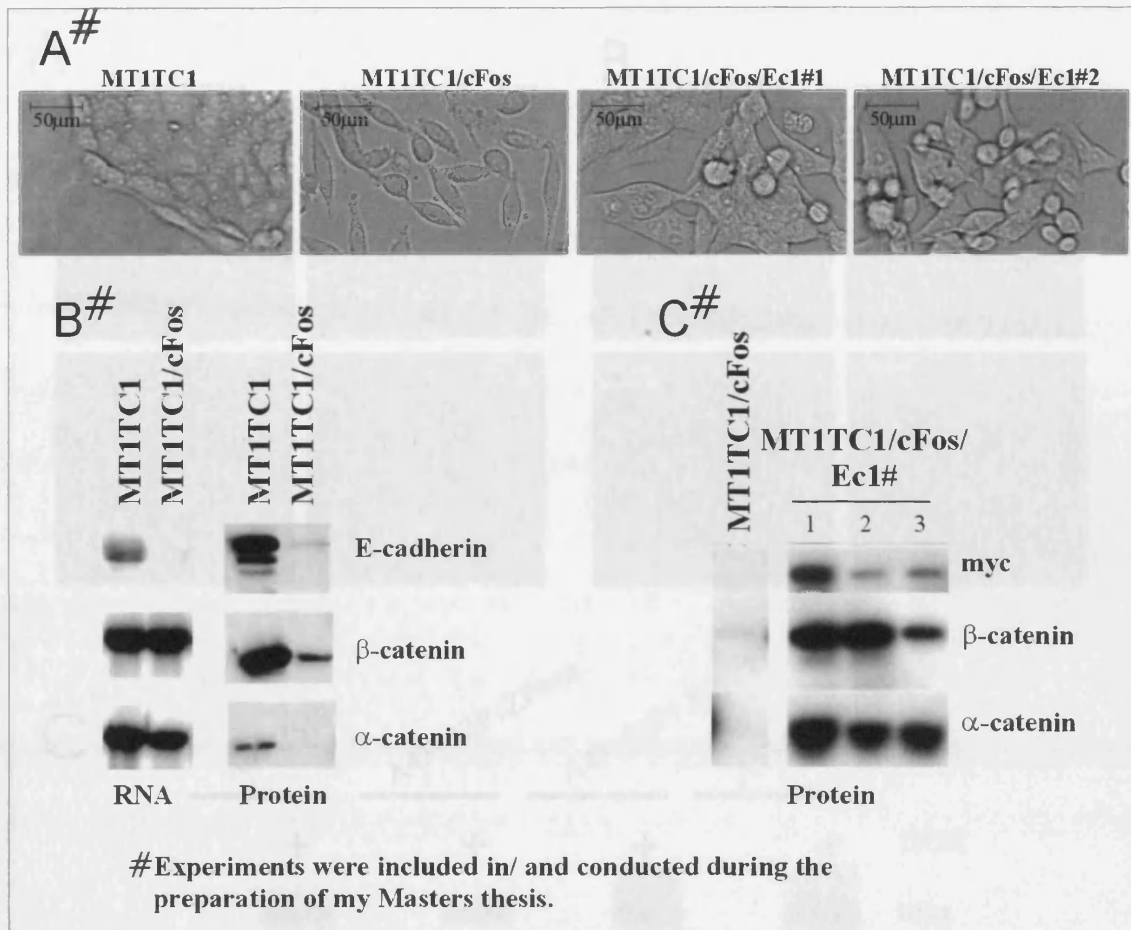


Figure 19. Exogenous expression of E-cadherin partly restores the epithelial phenotype in MT1TC1/cFos. Mesenchymal like MT1TC1/cFos cells were generated by the transfection of retroviral carried cDNA encoding cFos. The MT1TC1/cFos clone was subsequently transfected with wild type myc-tagged E-cadherin generating the clones MT1TC1/cFos/Ec1#1-3. (A) Microscopic images of MT1TC1, MT1TC1/cFos and MT1TC1/cFos/Ec1#1-2. (B) Western and Northern analysis of the components of the E-cadherin complex in MT1TC1 and MT1TC1/cFos. (C) Western analysis of myc-tagged E-cadherin, α - and β -catenin in MT1TC1/cFos and MT1TC1/cFos/Ec1#1-3. Note the restoration of α - and β -catenin.

eliminating the recognition by a commercial anti-E-cadherin antibody (BD Transduction Laboratories, clone C20820). These modifications do not interfere with the functional activity of E-cadherin molecules and allow us to differentiate between exogenous and endogenous E-cadherin in transfected cells, by using anti-Flag and C20820 antibodies (Chitav & Troyanovsky, 1998).

As expected, and previously shown by van Grunsven and colleagues, expression of SIP1ZFmut did not influence the transcription of *CDH1* and was therefore used as a nega-

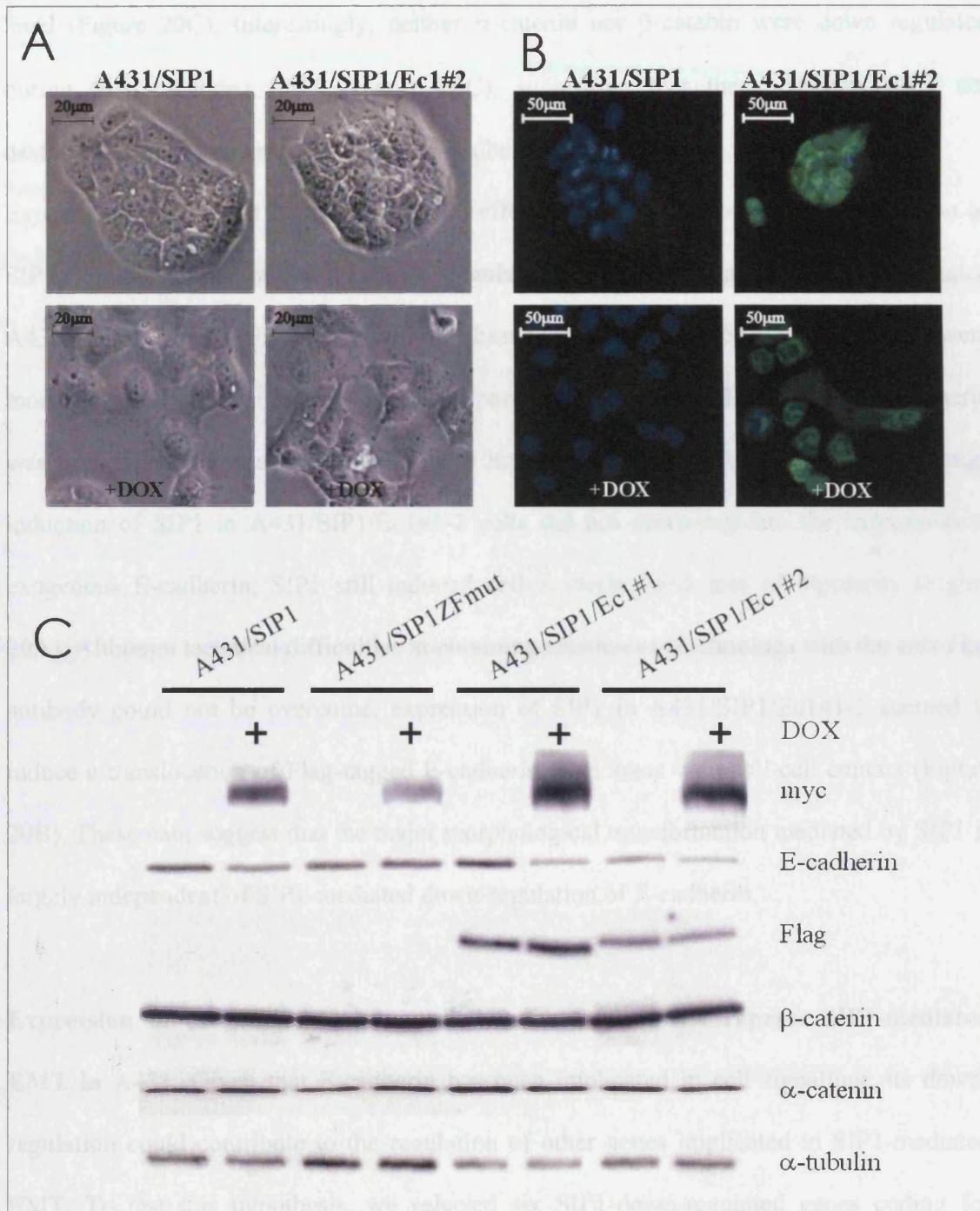


Figure 20. Ectopic expression of E-cadherin do not rescue the epithelial phenotype in DOX induced A431/SIP1. Clones of A431/SIP1 cells constitutively expressing Flag-tagged E-cadherin were generated (A431/SIP1/Ec1#1 and 2). (A+B) Indicated clones were grown in absence/presence of DOX for 48h. Right panel(A) shows representative *in vivo* images of indicated clones while left panel (B) shows DAPI (blue) and Flag(green) IF-staining. (C) Total protein lysates were prepared from indicated clones, grown in absence/presence of DOX for 48h, and later analysed by western blotting.

transcription of these genes was examined in A431/SIP1 and A431/SIP1/Ec1#2 transfected with/without DOX for 48h. Transcription of none of these genes was significantly influenced by exogenous E-cadherin (Figure 21A).

level (Figure 20C). Interestingly, neither α -catenin nor β -catenin were down regulated during SIP1-mediated EMT (Figure 20C), suggesting that these catenins were not destabilised by the down-regulation of E-cadherin.

Exogenous Flag-tagged E-cadherin had no effect on neither DOX-regulated expression of SIP1, nor the ability of SIP1 to down-regulate endogenous E-cadherin in DOX-treated A431/SIP1/Ec1 cells (Figure 20C). In the absence of DOX, A431/SIP1/Ec1#1-2 cells were morphologically indistinguishable from the parental A431 cells and Flag-tagged E-cadherin was predominately localised in areas with intercellular contacts (Figure 20B). Although induction of SIP1 in A431/SIP1/Ec1#1-2 cells did not down-regulate the expression of exogenous E-cadherin, SIP1 still induced cell scattering and loss of bipolarity (Figure 20A). Although technical difficulties in obtaining conclusive IF-stainings with the anti-Flag antibody could not be overcome, expression of SIP1 in A431/SIP1/Ec1#1-2 seemed to induce a translocation of Flag-tagged E-cadherin from areas with cell-cell contact (Figure 20B). These data suggest that the major morphological transformation mediated by SIP1 is largely independent of SIP1-mediated down-regulation of E-cadherin.

Expression of exogenous Flag-tagged E-cadherin does not repress SIP1-mediated EMT in A431. Given that E-cadherin has been implicated in cell signalling, its down-regulation could contribute to the regulation of other genes implicated in SIP1-mediated EMT. To test this hypothesis, we selected six SIP1-down-regulated genes coding for components of epithelial filaments (keratins 13 and 15), tight junction (claudin-4), desmosomes (desmoglein and desmoplakin), cell cycle (cyclin D1) and one SIP1-activated gene encoding mesenchymal marker vimentin. Transcription of these genes was examined by RT-PCR in the A431/SIP1 and A431/SIP1/Ec1#1-2 maintained with/without DOX for 48h. Transcription of none of these genes was significantly influenced by exogenous E-cadherin (Figure 21A).

Although the role of E-cadherin as invasion suppressor is well documented in a number of cell models, the exact underlying mechanisms are less clear. As described previously, SIP1-mediated EMT in A431 cells was coupled with increased invasiveness (Figure 10). To investigate the role of E-cadherin in SIP1 induced invasion, the A431/SIP1 clones expressing exogenous E-cadherin (A431/SIP1/Ec1#1 and 2) were tested in parallel with A431/SIP1 in inverse 3-dimensional *in vitro* invasion assay. As shown in figure 21B, SIP1

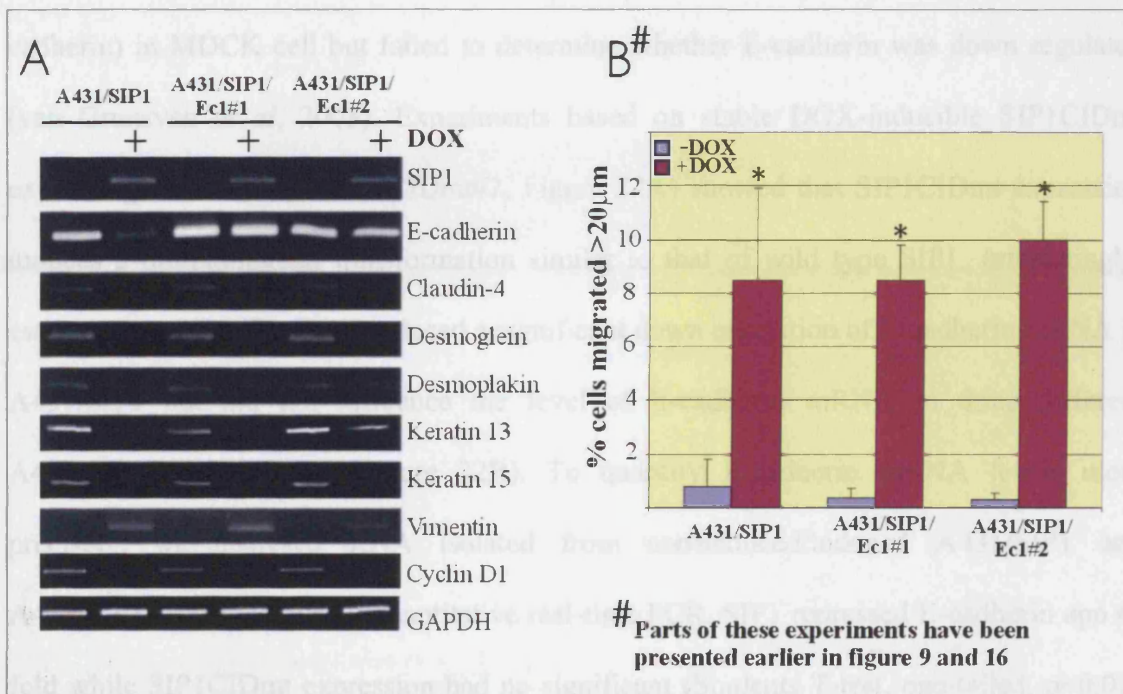


Figure 21. *SIP1* regulates gene expression and induces invasion independent on *E-Cadherin* down regulation. (A) mRNA levels of selected gene transcripts measured by RT-PCR in indicated clones. (B) Migration into matrigel was assessed by the Inverse 3D-Invasion assay. The percentage of cells invading was quantified in twelve microscopic fields. The diagram represents mean \pm SD. *(Students T-test, two-tailed, $p < 0.01$)

expression induced the same level of invasiveness in A431/SIP1/Ec1#1-2 as in A431/SIP1 cells, demonstrating that exogenous E-cadherin does not suppress SIP1-stimulated invasion. These unexpected results, obtained by expressing exogenous E-cadherin in A431/SIP1, suggest that the early stages (<48h) of SIP1-mediated EMT are independent of the down regulation of E-cadherin.

SIP1-CtBP interaction is critical for the repression of *CDH1*, but dispensable for morphological transformation of A431 cells. In order to investigate the role of E-cadherin down-regulation in SIP1-mediated EMT by another approach and to address the disputed question whether CtBP is required for SIP1 to repress E-cadherin, we generated clones of A431 with DOX inducible expression of myc-tagged SIP1CIDmt (mutated SIP1 incapable of binding CtBP). Of note, van Grunsven and colleagues showed that the expression of SIP1CIDmt induced cell scattering (inc. changed staining pattern for E-cadherin) in MDCK cell but failed to determine whether E-cadherin was down regulated (van Grunsven *et al*, 2003). Experiments based on stable DOX-inducible SIP1CIDmt expressing clones (A431/SIP1CIDmt#2, Figure 22A) showed that SIP1CIDmt expression induces a morphological transformation similar to that of wild type SIP1. Interestingly, estimated by RT-PCR, DOX induced a significant down regulation of E-cadherin mRNA in A431/SIP1 but did not influence the level of E-cadherin mRNA in three different A431/SIP1CIDmt clones (Figure 22B). To quantify E-cadherin mRNA levels more precisely, we analysed RNA isolated from non-induced/induced A431/SIP1 and A431/SIP1CIDmt#2 cells by quantitative real-time PCR. SIP1 repressed E-cadherin app 4-fold while SIP1CIDmt expression had no significant (Students T-test, one-tailed, p=0.02) influence on the level of E-cadherin mRNA (Figure 22D), strongly suggesting that SIP1 represses *CDH1* in a CtBP-dependent manner. This pattern was reflected on protein level. In contrast to A431/SIP1, DOX non-induced and induced A431/SIP1CIDmt#2 expressed the same level of E-cadherin protein (Figure 22C). This clearly uncouples E-cadherin down regulation from SIP1 induced cell scattering and loss of bipolarity.

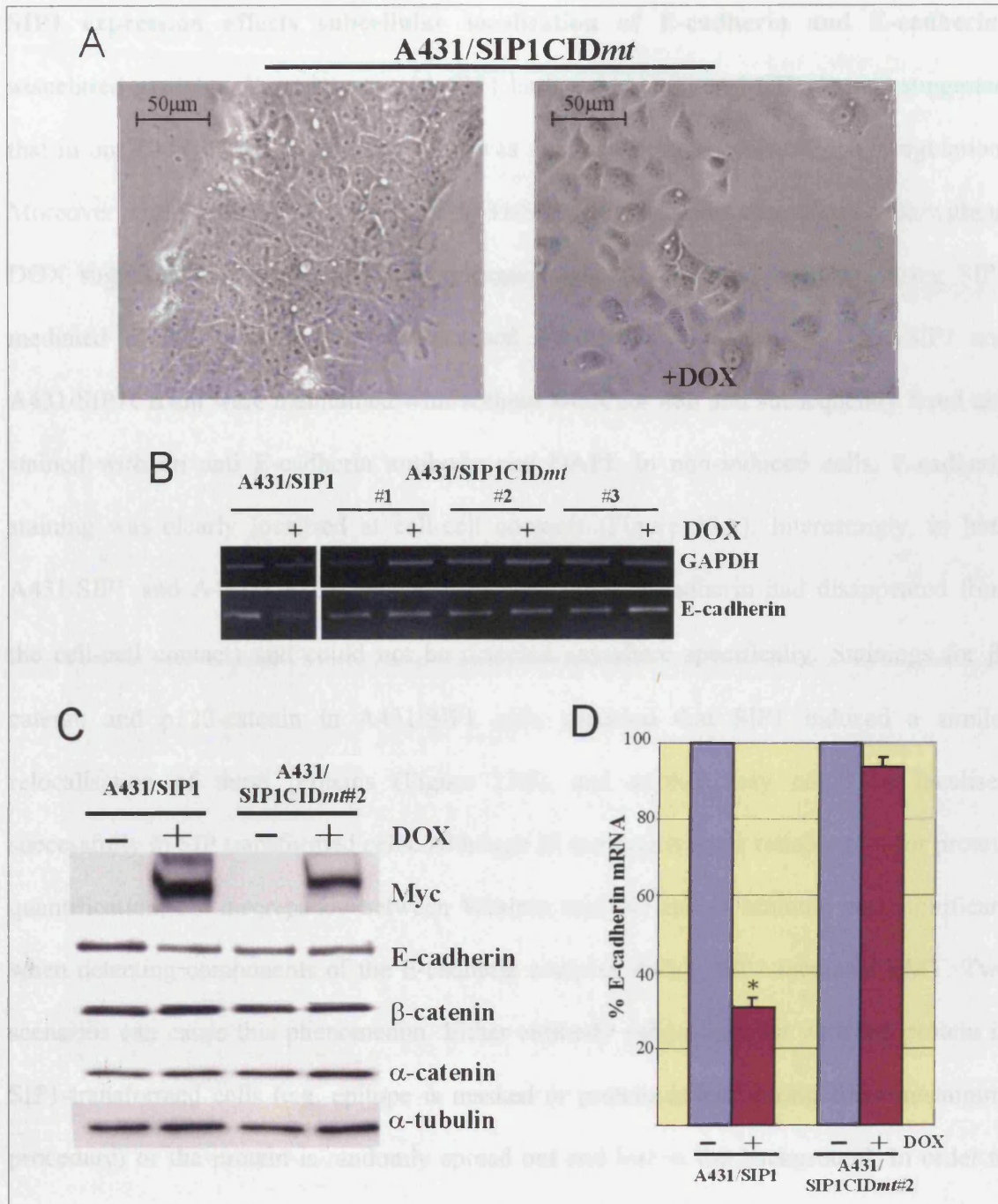


Figure 22. Expression of *SIP1CIDmt* in *A431* induces cell scattering and loss of bipolarity, but fails to repress *CDH1* and down-regulate *E-cadherin*. (A-D) Indicated clones were maintained with/without DOX for 48h prior to investigations. (A) Photographic images of noninduced/induced *A431/SIP1CIDmt#2*. (B) Levels of *E-cadherin* mRNA were estimated by RT-PCR in indicated clones. (C) Total protein lysates were prepared from indicated clones and used to estimate the expression of indicated proteins by western blotting. (D) Expression of *E-cadherin* mRNA was quantified by real time PCR. Diagram represents means and SD of triplicates. * (Students T-test, one-tailed, $p < 0.01$)

SIP1 expression affects subcellular localisation of E-cadherin and E-cadherin-associated proteins. Experiments with SIP1 harbouring a mutated CID domain suggested that in our EMT model, cell dissociation was not caused by E-cadherin down-regulation. Moreover, anti-Flag immunostaining of A431/SIP1/Ec1#1-2 cells maintained with/without DOX suggested that E-cadherin was relocated from the cell-cell contacts during SIP1 mediated EMT. To verify that SIP1 caused E-cadherin relocation, A431/SIP1 and A431/SIP1CIDmt were maintained with/without DOX for 48h and subsequently fixed and stained with an anti E-cadherin antibody and DAPI. In non-induced cells, E-cadherin staining was clearly localised at cell-cell contacts (Figure 23A). Interestingly, in both A431/SIP1 and A431/SIP1CIDmt DOX-induced cells, E-cadherin had disappeared from the cell-cell contacts and could not be detected anywhere specifically. Stainings for β -catenin and p120-catenin in A431/SIP1 cells revealed that SIP1 induced a similar relocation of these proteins (Figure 23B), and neither they could be localised successfully in SIP transformed cells. Although IF staining is not a reliable tool for protein quantification, the discrepancy between Western analysis and IF staining was significant when detecting components of the E-cadherin complex during SIP1-mediated EMT. Two scenarios can cause this phenomenon. Either antibody cannot interact with the protein in SIP1-transformed cells (e.g. epitope is masked or protein is lost during fixation/staining procedure) or the protein is randomly spread out and lost in the background. In order to discriminate between these possibilities, A431/SIP1 cells were transiently transfected with pCMVEGL4-GFP, encoding functional E-cadherin coupled to GFP (Green Fluorescence Protein), and analysed *in vivo* by fluorescence microscopy. By this approach we avoided fixation and staining procedures as well as epitope-masking. In non-induced cells GFP-tagged E-cadherin was detected in similar pattern to endogenous E-cadherin previously

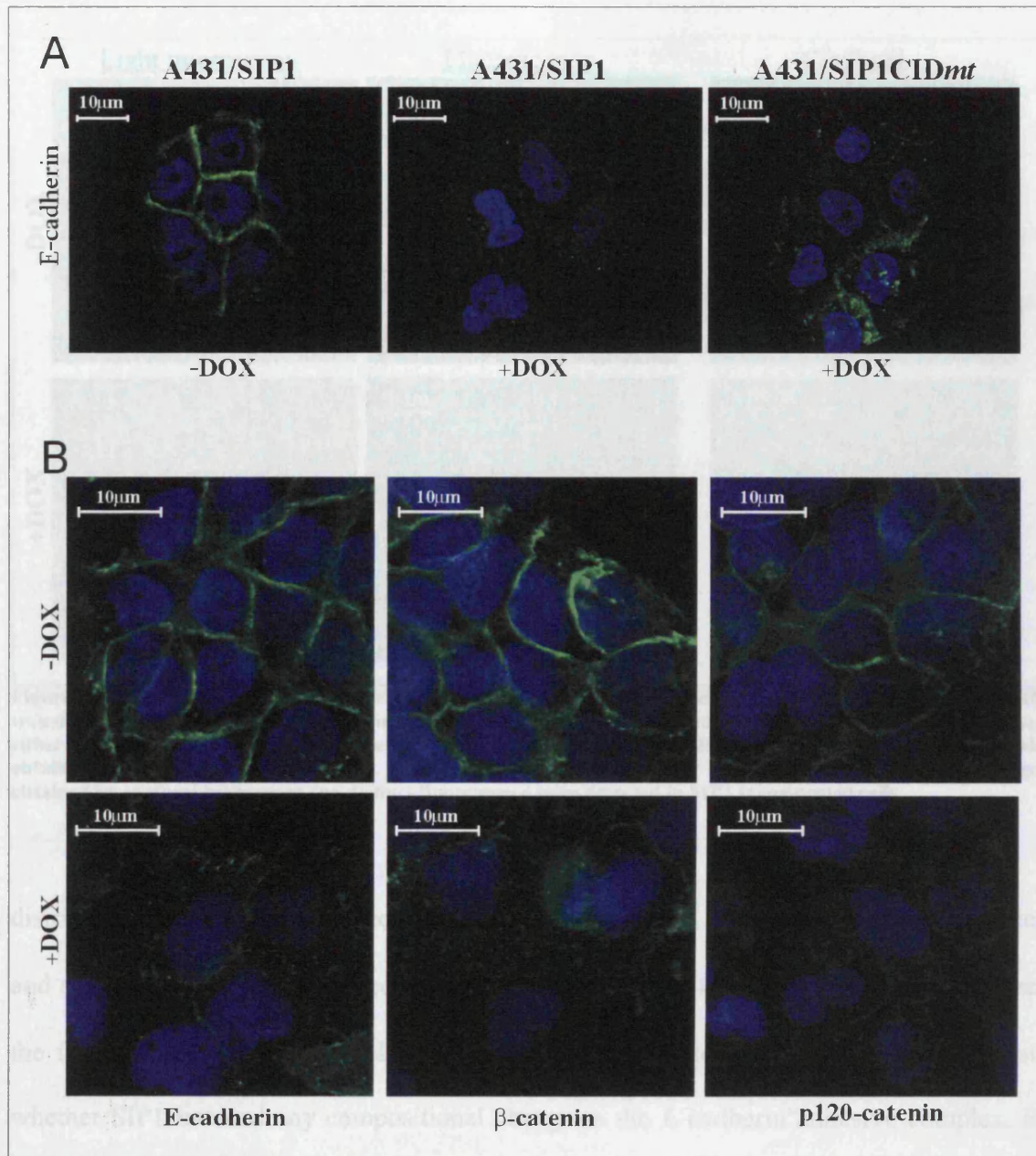


Figure 23. The E-cadherin complex disappears from cell-cell contacts during SIP1-mediated EMT. IF-stainings of A431/SIP1 and A431/SIP1CIDmt cells maintained with/without DOX for 48h. (A) Indicated clones were stained with anti E-cadherin antibody (green) and DAPI (blue). (B) A431/SIP1, +/- DOX, stained with anti E-cadherin, β-catenin and p120-catenin in combination with DAPI (blue).

detected by IF staining (Figure 23B and 24 (top-middle and top-right)), namely at cell-cell contacts. Similarly to endogenous E-cadherin, GFP-tagged E-cadherin disappeared from the cell-cell contacts and could not be specifically localised in SIP1 expressing cells (Figure 24). Since during SIP1-mediated EMT, E-cadherin was not lost, but rather re-

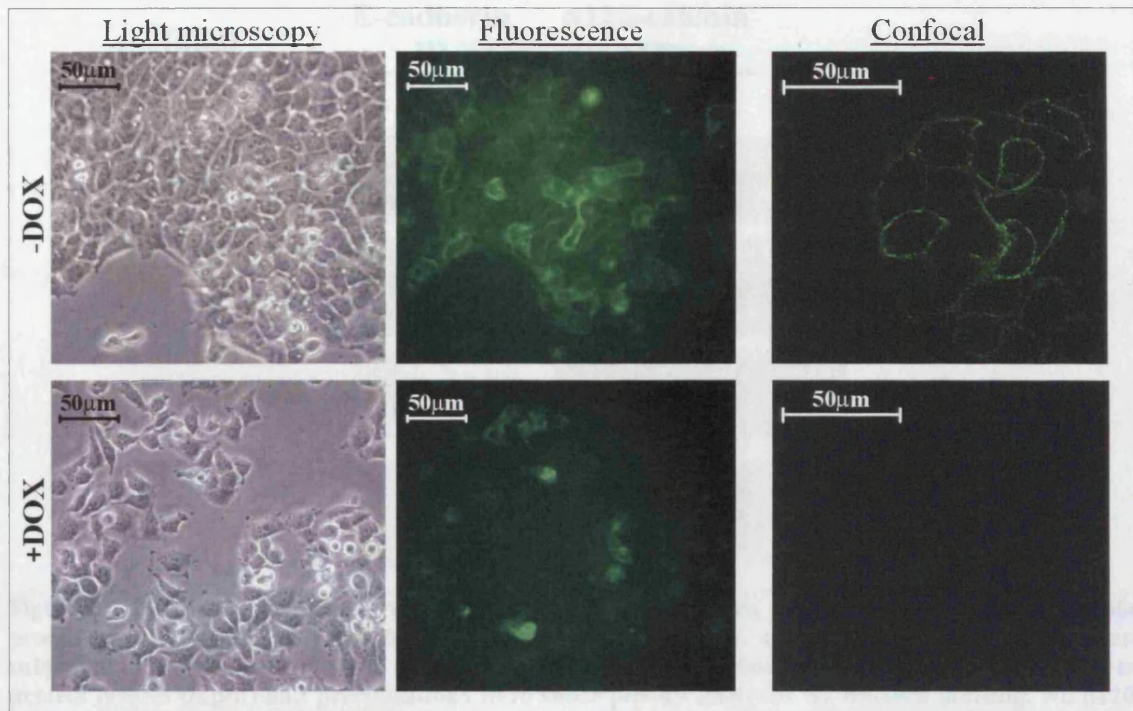


Figure 24. *E-cadherin in SIP1 transformed cells is not distinctly localized.* A431/SIP1 cells were transiently transfected with pCMVEGL4-GFP (encoding GFP-coupled E-cadherin) and subsequently split to be maintained either with or without DOX for 48h. Left and middle images; Light and fluorescence images of the same field obtained by phase contrast microscopy. Intensity of fluorescence can not be compared. Right images; Images obtained by confocal microscopy (no distinct fluorescence were detected in SIP1 transformed cells).

distributed within cells, we speculated that the association between E-cadherin complex and actin filaments was disrupted. As α -catenin is believed to mediate the bridge between the functional E-cadherin complex and the actin cytoskeleton, we decided to investigate whether SIP1 induced any compositional change in the E-cadherin adhesive complex. E-cadherin complexes were immunoprecipitated with anti-E-cadherin or anti-p120-catenin antibodies from lysates prepared from A431/SIP1 cells maintained for 48h in presence/absence of DOX. Immunoprecipitations were subsequently used in western blot analysis to estimate the amounts of E-cadherin, α -catenin, β -catenin and p120-catenin pulled down (Figure 25). Both anti-E-cadherin antibody and anti p120-catenin antibody, pulled down less α -catenin in lysates from SIP1-expressing cells, whereas E-cadherin and β -catenin was pulled down to the same extent. This shows that interactions between E-

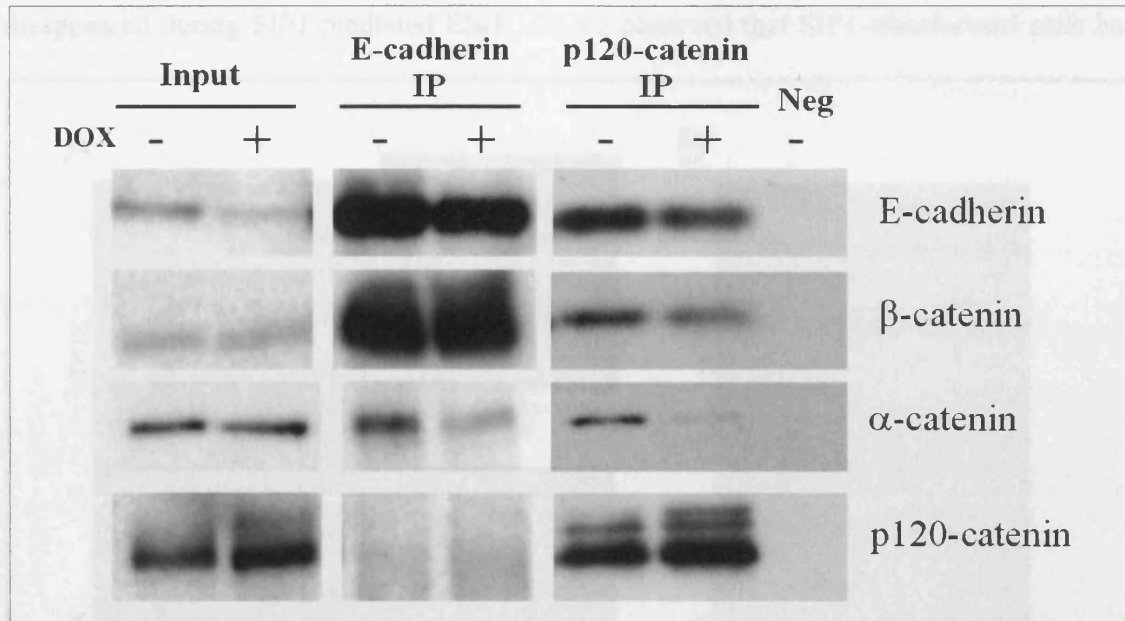


Figure 25. *SIP1*-mediated EMT represses the association between *E-cadherin* and α -catenin. Total protein lysates prepared from A431/*SIP1* cells grown 48h in absence/presence of DOX, were subjected to immunoprecipitation by anti *E-cadherin*, anti p120-catenin and no antibody (Neg). Total protein lysates (input) and precipitations were subsequently analysed by western blotting. No p120-catenin was detected in precipitations by anti *E-cadherin* since p120-catenin and anti *E-cadherin* antibody compete for the same epitope.

Cadherin-containing complexes and α -catenin are significantly weakened during *SIP1*-mediated EMT.

Adhesion to collagen and the formation of focal contacts are stimulated during *SIP1*-mediated EMT. Cortical actin is disrupted. *E-cadherin* mediated intercellular adherens junctions are dependent on the anchorage of *E-cadherin* to the actin filaments. If the interaction between α -catenin and the *E-cadherin* complex's is abrogated, this anchorage would be disabled causing the unzipping of *E-cadherin* mediated cell-cell adhesion and the morphology, we decided to investigate whether we could detect any consequently cell dissociation. As *SIP1* expression in A431 did induce major changes in cellular rearrangements in the pattern of actin filaments. Staining induced/non-induced A431/*SIP1* cells for F-actin (Figure 26A) showed that the cortical actin, in the adhesion belt,

disappeared during SIP1-mediated EMT. As we observed that SIP1-transformed cells had

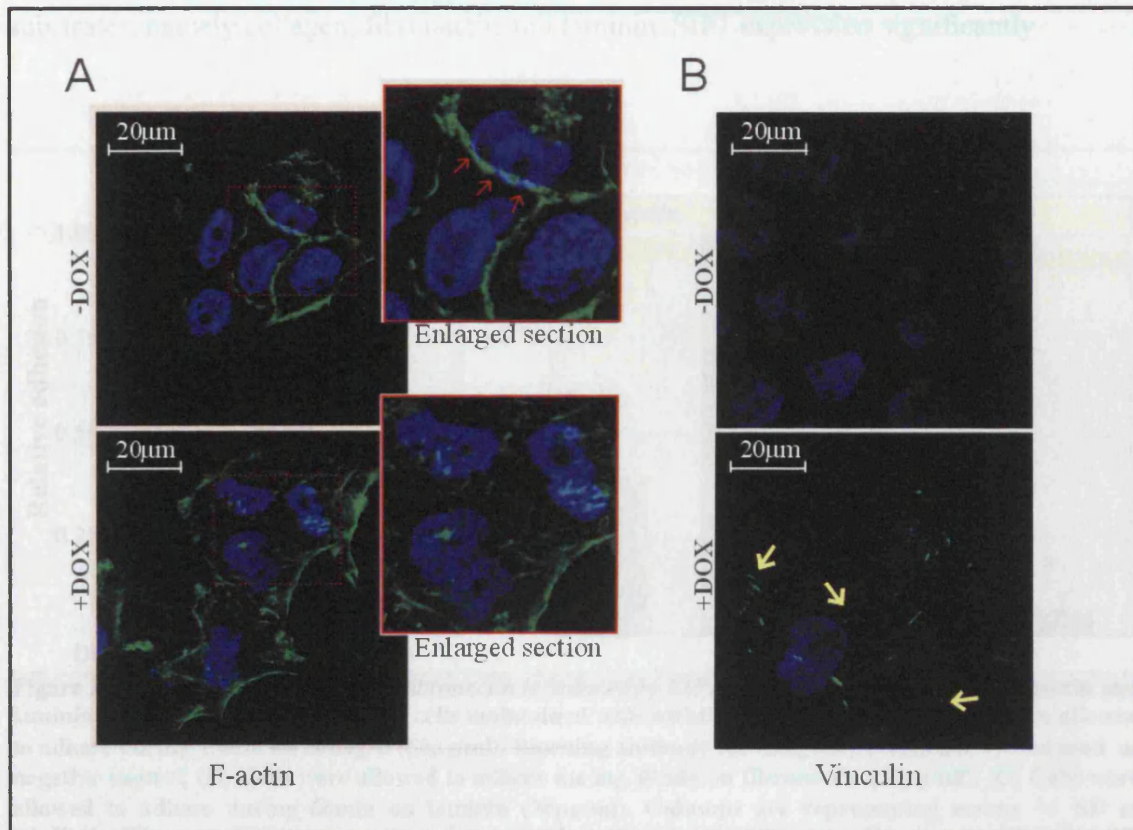


Figure 26. SIP1-mediated EMT in A431 is coupled with global actin rearrangements and increased formation of focal contacts. A431/SIP1 maintained with/without DOX for 48h were stained by phalloidin and anti-Vinculin in combination with DAPI and analysed by confocal microscopy. (A) Cells stained for F-actin (green). Red arrows in enlarged part designate cortical actin. (B) Cells stained for vinculin (green). Yellow arrows designate focal contacts.

lost their characteristic epithelial apical-basal bipolarity concomitant with a global rearrangement of actin filaments, we asked the question as to whether SIP1 activated cell adhesion to the extracellular matrix. We therefore decided to stain non-induced/induced A431/SIP1 cells for vinculin. Microscopy of these stainings (representative images are shown in Figure 26B), showed a significant increase in vinculin-based focal contacts. The concurrent disappearance of cortical actin and increase in focal contacts suggests that a swap in preference from cell-cell adhesion to cell-ECM (extracellular matrix) adhesion is triggered by SIP1 expression in A431. To address this issue, we decided to estimate the

functional status of ECM-interacting receptors by measuring adhesion to different substrates, namely collagen, fibronectin and laminin. SIP1 expression significantly

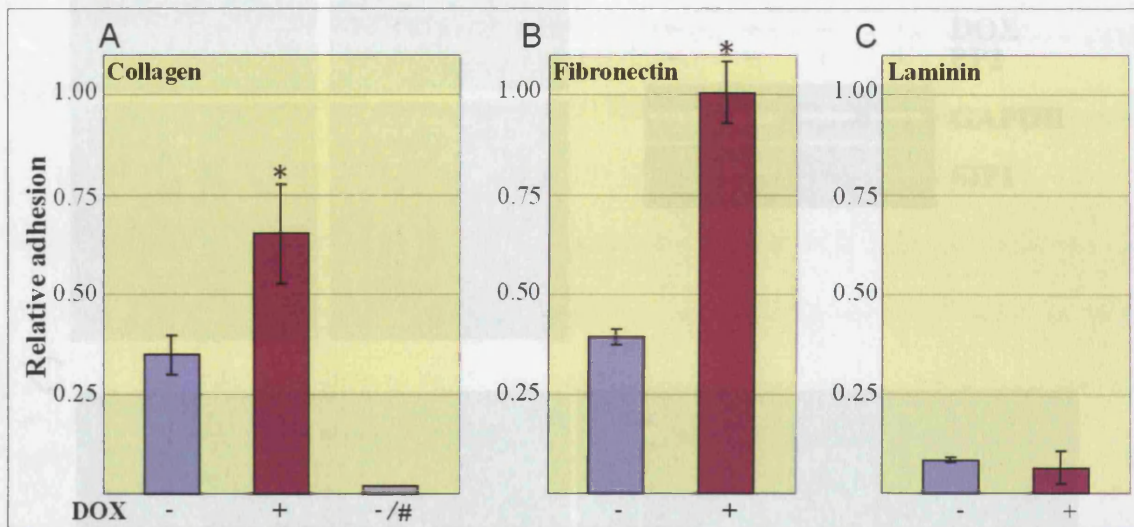


Figure 27. Adhesion to collagen and fibronectin is induced by SIP1. Adhesion to collagen, fibronectin and laminin was measured in A431/SIP1 cells maintained with/without DOX for 48h. (A) Cells were allowed to adhere during 15min on collagen (50 μ g/ml). Blocking antibody for integrin β 1 (marked #) was used as negative control. (B) Cells were allowed to adhere during 30min on fibronectin (50 μ g/ml). (C) Cells were allowed to adhere during 60min on laminin (20 μ g/ml). Columns are representing means \pm SD of triplicates. The experiment was conducted twice with similar results. *(Students T-test, two-tailed, $p < 0.05$)

stimulated adhesion to collagen and fibronectin but had no influence on adhesion to laminin (Figure 27A-C).

As SIP1CIDmt, incapable of repressing E-cadherin, still induced a mesenchymal conversion of A431, we speculated that the essential mechanism responsible for the SIP1-mediated morphological transformation of A431 cells rather involved the regulation of kinase-based signal-transduction pathways than a general down-regulation of epithelial markers. In order to test this hypothesis we applied a “shotgun” approach, analysing the effect of a different kinase inhibitors on the SIP1-mediated morphological transformation of A431. Of several inhibitors investigated (AG490, KN93, LY294002, PP2, Ro318220, SB202190, TBB and UO126) only the Src family kinase (SFK) inhibitor, PP2, had a clear inhibitory effect on the SIP1-mediated morphological transformation. In absence of DOX,

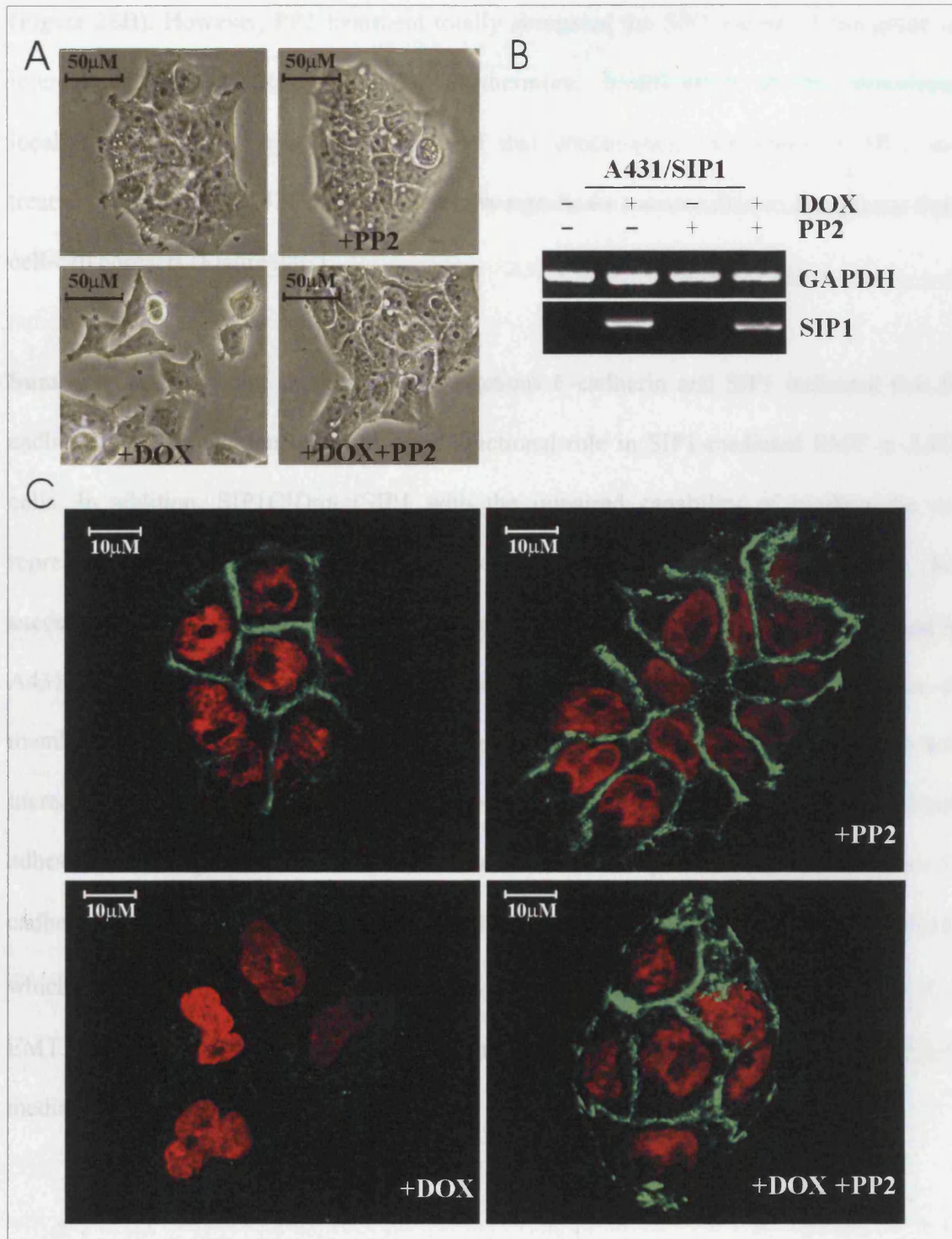


Figure 28. *Src* family kinase inhibitor PP2 abrogates SIP1-mediated disruption of cell-cell adhesion. A431/SIP1 cells were maintained with/without DOX either in presence (1µM) or absence of PP2. (A) Microscopic images of cells *in vivo*. (B) Relative mRNA expression of SIP1 assessed by RT-PCR. (C) Distribution of E-cadherin (green) analysed by IF (red, DAPI stained nuclei).

PP2 had no significant effect on the phenotype of A431 cells (Figure 28A and C). As expected, treatment with PP2 did not suppress the DOX-stimulated expression of SIP1

(Figure 28B). However, PP2 treatment totally abrogated the SIP1-mediated disruption of intercellular adhesion (Figure 28A). Furthermore, investigation of the subcellular localisation of E-cadherin by IF, revealed that concomitant expression of SIP1 and treatment with PP2 in A431 did not induce any significant translocation of E-cadherin from cell-cell contacts (Figure 28C).

Summary. Concomitant expression of exogenous E-cadherin and SIP1 indicated that E-cadherin down regulation did not play a functional role in SIP1-mediated EMT in A431 cells. In addition, SIP1CIDmt (SIP1 with the impaired capability of binding the co-repressor CtBP) failed to repress E-cadherin at both RNA and protein level, but successfully induced a morphological transformation similar to SIP1, when expressed in A431. However, SIP1 and SIP1CIDmt expression did induce the disappearance of membranous E-cadherin concurrently with global rearrangement of the cytoskeleton and increased formation of vinculin-containing focal contacts. In addition, SIP1 stimulated cell adhesion to collagen and fibronectin but not laminin. Compositional analysis of the E-cadherin complex by immunoprecipitations showed that in contrast to p120- and β -catenin which retained in complex with E-cadherin, α -catenin dissociated during SIP1-mediated EMT. Furthermore, the Src-family kinase inhibitor PP2 inhibits the SIP-induced signal mediating morphological conversion of A431.

Discussion

Initial work and the model

Programmes of epithelial mesenchymal transition are crucial for normal embryonic development but also represent a potential oncogenic mechanism aberrantly exploited during cancer progression. A hallmark of EMT is the inactivation of the E-cadherin adhesive complex, which constitutes the backbone of intercellular adhesion in epithelial tissue. Of note, E-cadherin is lost or deregulated in the majority of carcinomas including bladder, prostate, colorectal, pancreatic, gastric, and breast cancer (Bellovin *et al.*, 2005; Byrne *et al.*, 2001; Oka *et al.*, 1993; Weinel *et al.*, 1996; Rao *et al.*, 2006). Several transcriptional repressors of E-cadherin (e.g. SIP1, Snail, Slug, and ZEB1) have been identified as important regulators of EMT; *in vivo* during embryonic development (Yoshimoto *et al.*, 2005; Carver *et al.* 2001) and *in vitro* in several cell models (Eger *et al.*, 2000 and 2005; Grotegut *et al.*, 2006; Savagner *et al.*, 1997). Furthermore, in a number of clinical studies, expression of these proteins has been found to be positively correlated with cancer aggressiveness and poor prognosis, thereby giving them the status as proto-oncogenes. (Elloul *et al.*, 2005; Come *et al.*, 2006; Rosivatz *et al.*, 2002). Interestingly, increasing evidence demonstrates that neither Snail/Slug nor ZEB-1/SIP1 family members are restricted to the repression of *CDH1* but rather regulate a panel of genes. (Ikenouchi *et al.*, 2003; Vandewalle *et al.*, 2005). As they individually have both multiple direct targets and the ability to induce genome-wide expressional changes (Comijn *et al.*, 2001; Eger *et al.*, 2005; Vandewalle *et al.*, 2005; Bolos *et al.*, 2003; Peinado *et al.*, 2004b) these transcription factors, that are central players in TGF β or RTK/Ras (Comijn *et al.*, 2001; Schmidt *et al.*, 2005; Savagner 2001) pathways, most likely mediate EMT via a cascade of regulatory events which constituted can be described as a genetic programme.

In this thesis I presented extensive studies of ectopic expression of SIP1 in the squamous epidermoid cell line A431. As evident from data presented in the Results Part 1, we found that A431 cells expressing SIP1 for 48h underwent a radical conversion from a classical epithelial phenotype to a phenotype largely characterised by mesenchymal-specific features. On the morphological level this became evident as the epithelial cells lost their cellular integrity in a process where cells flattened and scattered (Figure 7). Simultaneously, cells became invasive (capable of invading matrigel, Figure 10) and experienced a general shift in gene expression with down regulation of key epithelial markers and up regulation of mesenchymal markers (Figure 8). In collaboration with Dr Berx (University of Ghent, Belgium) we managed to estimate that expression of approximately 4% of all human genes was altered more than 2-fold after 48h of SIP1 expression. As SIP1 is unlikely to directly mediate the expression of the majority of these genes (most of the promoters do not contain any known SIP1 recognition sites) one should expect that SIP1 initiates a branched cascade of gene-regulatory events. In contrast to the very evident changes SIP1-expression caused, expressing a chimera of SIP1 with impaired Zn-fingers, SIP1ZFmut, had no evident influence on A431. This clearly indicates that SIP1 needs to bind DNA in order to carry out its function. Furthermore, as SIP1ZFmut has both a functional SID- and a functional CID-domain, we must conclude that SIP1 in general does not function by titrating neither SMADs nor CtBP. Of note, this might also indicate that our SIP1-expression in A431 is not coupled to artefacts caused by supraphysiological titration of these proteins. Taken together, we conclude that SIP1 expression does induce an epithelial to mesenchymal transition in A431 and that SIP1 does so by directly regulating the transcription of a panel of SIP1-responsive genes which functions as the first step in a cascade of gene-regulatory events orchestrating the transformation. Interestingly, along with the well-acknowledged features of EMT, SIP1-mediated EMT was coupled with repressed proliferation (Figure 9). Since this is not the first time that repressors of *CDH1*

(E-cadherin encoding gene) have been found to repress proliferation (Vega *et al.*, 2004; Turner *et al.*, 2006) it might turn out to be a common feature for EMT-programmes mediated by this group of proteins.

Before continuing the discussion further a notion about the model has to be made. The majority of my studies were based on the clone A431/SIP1 that expresses SIP1 in the presence of DOX. This gave a unique opportunity to study the immediate effects of SIP1-expression multiple times without clonal artefacts and in different contexts. The quality of inducible systems is mainly determined by expression level, homogeneity of the clone and whether the inducing agent has any side effects. Ideally non-induced cells should not express the exogenous protein while induced cells should express it at a “natural” level. Defining the “natural” level can often be difficult since the endogenous level often is varying between cell types. Furthermore, in cases where we want to express the protein of interest in a cell type where its endogenous expression is not detectable no preference for a “natural” level exists. In our model the clone A431/SIP1 had no relevant leakage, as the clone was indistinguishable from the parental clone A431/tet-on. Whether DOX-treated A431/SIP1 cells expressed a “natural” level of SIP1 is uncertain. SIP1ZFmut expression had no detectable effect on A431 indicating that SIP1-mediated EMT is not caused by an artificial titration of CtBP or SMADs, hence SIP1 expression in A431 is in the sub-supernatural area. The lack of any detectable effect by SIP1ZFmut expression (obtained by DOX treatment) also indicates that DOX has no side effects in our model. On the other hand, the possibility that the effects of DOX counteracts the effects of SIP1ZFmut expression does not allow us to exclude the possibility that DOX actually has a side effect. DOX treated A431 and A431/tet-on cells serve as the best negative controls and it is a lack of scientific responsibility that this approach has not been used to assess the side effects caused by DOX treatment. An even worse influx of artefacts is caused by the heterogeneity of the clone. In our model, 48h of DOX treatment causes the accumulation of SIP1 in the

nucleus of approximately 90% of treated cells. As natural selection also functions in a petri dish the specific selective pressure will determine whether proportion of SIP1-expressing cells will decrease or increase with time. The fact that SIP1 expression in our model represses proliferation dictates that the proportion of SIP1-expressing cells will decrease with time. Hence, if a SIP1-activated cascade of events leads to a certain effect after 4 days the “background” of cells not expressing SIP1 will mask/diminish the effect. This lack of homogeneity clearly limits our model.

In the majority of experiments with A431/SIP1 I used the time point of 48h of DOX treatment, which is, approximately the time it took for SIP1 to induce a complete morphological transformation. Since a cascade of regulatory events causes SIP1-induced EMT, the transition that most probably ends in a stable cell type cannot be understood by experiments based on one time point. This is best illustrated by an example; the fact that increased phosphorylation of Src is not detected after 48h of SIP1-expression does not exclude that Src phosphorylation is playing a crucial part in mediating SIP1-induced EMT. Of note, two weeks of c-Fos expression in a mouse mammary epithelial cell line gradually caused EMT (Eger *et al.*, 2000).

After the overall examination of SIP1-expression in A413 described in Results Part 1 we decided to investigate two features of SIP1-mediated EMT; the mechanism of SIP1-induced repression of the proliferation and the mechanism of SIP1-induced morphological transformation.

Proliferation is repressed during SIP1-induced EMT

Given that normal differentiating cells do not divide, the intriguing question arises as to whether embryonic utilized programmes of EMT, in general, are coupled with restricted proliferation. Interestingly, both Slug- and Snail-mediated EMT have been coupled with repression of the cell cycle (Turner *et al.*, 2006; Vega *et al.*, 2004). Studies by Vega *et al.*,

showed that Snail expression in MDCK cells induce the accumulation of cells in the G₁ phase of the cell cycle. This effect was concomitant with hypophosphorylation of Rb, down regulation of cyclin D1 and D2 and increased expression of p21^(WAF1/CIP1) (Vega *et al.*, 2004). However, the particular roles of these cell cycle regulators were not further addressed in this study. Here, we analysed how the EMT program induced by the expression of SIP1 affected cell cycle progression.

In the Result Part 2 I showed that SIP1-mediated EMT is coupled with a significant down regulation of Cyclin D1 that gradually takes place after 10h of DOX treatment (Figure 14). The down regulation of Cyclin D1 is closely followed in time by a gradual hypophosphorylation of Rb. Assessed by western analysis approximately 50% of Rb is found in the hypophosphorylated form at 20h of DOX treatment (Figure 14). Within the first 24h of DOX treatment A431/SIP1 cells are starting to accumulate in G₁ (Figure 12) while growth in cell population is decreasing after 24h of DOX treatment (Figure 11). The chronological order of these events makes it highly plausible that SIP1 regulates the proliferation through the Cyclin D1/Rb pathway. The experiments showing that Cyclin D1 down regulation by siRNA is sufficient to provoke both hypophosphorylation of Rb and accumulation of cells in G₁ (Figure 15) combined with the experiments showing that concomitant ectopic expression of Cyclin D1 and SIP1 abrogates the SIP1-mediated hypophosphorylation of Rb as well as the SIP1-mediated accumulation of cells in G₁ (Figure 16), strongly supports this hypothesis. Furthermore, the expression of other known regulators of the G₁/S transition checkpoint as Cyclin D2, Cyclin D3, p21 and p27 seems not to be correlated with the SIP1-mediated repression of proliferation (Figure 12). Taken together, these experiments comprise substantial evidence supporting the hypothesis that SIP1 mediates the repression of proliferation in A431 through the Cyclin D1/Rb pathway.

As several Z-boxes (potential SIP1 binding sites) are present in the *CCND1* (Cyclin D1 encoding gene) promoter and decreased levels of Cyclin D1 are observed relatively quickly

after SIP1 expression, we were forced to address the question whether SIP1 directly represses the transcription of Cyclin D1 encoding gene. Firstly, we determined that expression of SIP1 did not significantly influence the stability of Cyclin D1 encoding mRNA (Figure 17). Secondly, we found that the decreased levels of Cyclin D1 encoding transcripts were due to repressed initiation of transcription of *CCND1* (Figure 17). As we found that functional Z-boxes in the *CCND1* promoter have a repressive effect on the transcription of the gene in the presence of SIP1 (Figure 18) and that SIP1 actually binds to the same Z-boxes (shown by ChIP-data obtained by Dr Berx group in Belgium, Mejlvang *et al.*, 2007 (Appendix D)) substantiates that SIP1 directly represses the transcription of *CCND1*. Summarised, the data presented in Result Part 2 indicates that SIP1 directly represses Cyclin D1, affecting the phosphorylation status of Rb that eventually triggers an accumulation of cells in G1 and thereby inhibits the proliferation.

Although SIP1 belongs to a protein family only distantly related to Snail/Slug, its effect on cell cycle distribution in human epidermoid A431 cells is similar to the effects of Snail in MDCK cells and Slug in normal keratinocytes (Vega *et al.*, 2004; Turner *et al.*, 2006). Taken together, these observations indicate that targeting the G₁/S checkpoint in order to repress proliferation is not an unusual feature of different EMT-inducing transcription factors in different cell lines.

The studies on Snail-induced EMT of MDCK cells (Vega *et al.*, 2004) and data presented here suggest that cells undergoing evolutionary conserved programs of EMT acquire a growth disadvantage. Therefore, the functional status of the Rb pathway may determine the configuration of EMT programs aberrantly utilized by cells of growing tumours. In carcinoma cells maintaining partial control over G₁/S restriction point, members of the SIP1 and Snail protein families may induce a transient EMT, which will contribute to metastatic dissemination without stable repression of epithelial markers (e.g. E-cadherin) in primary tumours. One of the events abrogating the Rb pathway is over

expression of cyclin D1 that is frequently associated with carcinomas in humans (in part, as a result of amplification of the cyclin D1 gene) (Knudsen *et al.*, 2006). Concurrent expression of cyclin D1 and SIP1 in A431 cell line generated cells that were capable to proliferate and invade into matrigel at the same time (Figure 12). We suggest that accumulated defects in the Rb pathway *in vivo* would permit a stable EMT resulting in the appearance of most aggressive tumour cell variants.

Interestingly, SIP1 expression in A431 repressed the transcription of *TERT* (Table 1, page 29), the gene encoding the telomerase reverse transcriptase that is known to maintain telomere ends. Similarly, Ozturk and colleagues found that SIP1 controlled the expression of *TERT* in hepatocellular carcinoma derived cells and thereby played an important role in replicative senescence (Ozturk *et al.*, 2006). Taken together, this suggests that SIP1 might have a dual role in repressing proliferation.

In contrast to the SIP1 model, functional inhibition of E-cadherin by a dominant negative E-cadherin mutant induces a gradual EMT in A431 cells without attenuating the cell cycle (Figure 13). Likewise, prolonged inactivation of epithelial adhesion by matrix metalloproteinases secreted by stroma cells or E-cadherin gene mutations may represent a mechanism of a stable EMT in tumour cells retaining partial control over G₁/S transition.

In conclusion, our data indicate that the functional status of the Rb pathway may determine the spectrum of EMT pathways utilized by cancer cells in course of tumour progression.

SIP1-mediated morphological transformation

The disruption of adherens junctions mediated by E-cadherin during EMT is well documented although the underlying mechanisms need to be further investigated. As the broad definition of EMT naturally covers a broad variety of programmes controlling morphological transformation, one should expect that several mechanisms mediate

disruption of cell-cell adhesion. A simple and classical hypothesis covering a consensus of EMT programmes suggests that the disruption of epithelial integrity is directly due to reduced expression of proteins mediating epithelial cell-cell adhesion, including E-cadherin. This hypothesis, based on numerous investigations correlating down regulation of E-cadherin with concomitant disruption of adherens junctions, has also been proposed for SIP1-mediated EMT (Vandevaille *et al.*, 2005).

One approach to test the hypothesis that E-cadherin plays a key role in SIP1-mediated EMT in A431 is to counteract the SIP1-mediated down regulation of endogenous E-cadherin by expressing exogenous E-cadherin on top of SIP1. In the Result Part 3 this approach was applied by generating clones of A431/SIP1 constitutively expressing Flag-tagged E-cadherin. Surprisingly, expression of exogenous Flag-tagged E-cadherin had no distinct effect on SIP1-mediated EMT in A431 (Figure 20 and 21). No clear conclusion can be drawn from this negative result as the experiment is deprived of a positive control, hence the Flag-tagged E-cadherin construct might not successfully substitute down regulated endogenous E-cadherin. Although the functionality of the construct should not be questionable (Chitaev *et al.*, 1998) we could not verify that cellular distribution of Flag-tagged E-cadherin, assessed by IF-staining, was identical with endogenous E-cadherin in neither DOX treated nor nontreated cells. This might be due to a different expression level (Flag-tagged E-cadherin is either sub or super-naturally expressed), the Ab against the Flag-tag is not suitable for IF-staining or that the behaviour/function of Flag-tagged E-cadherin is not identical with endogenous E-cadherin. This uncertainty clearly minimise the conclusive potential of the experiments. Surprisingly, the SIP1 chimera SIP1CIDmt (incapable of binding CtBP) induced an EMT similar to SIP1 in A431 but failed to repress E-cadherin (Figure 22), which clearly shows that SIP1-mediated EMT is permitted even in the absence of E-cadherin down regulation. Taken together, these two independent lines of evidence strongly indicates that down regulation of E-cadherin is dispensable for the SIP1-

mediated EMT and thereby also dispensable for the disruption of both cell-cell adhesion and epithelial basal-apical bipolarity. This is in line with recent investigations of a related EMT programme. In TGF- β 1 mediated EMT of the mouse mammary carcinoma cell line NmuMG, both SIP1 and Snail were rapidly up regulated (<12h). While E-cadherin levels remained constant for up to 3 days, a morphological transformation including disruption of E-cadherin mediated cell-cell adherens junctions was evident already after 24h of induction (Maeda *et al.*, 2005).

Recently, activated internalisation of proteins mediating adherens junctions has been identified as a potent mechanism controlling functional status of adherens junctions (Fujita *et al.*, 2002; Akhtar and Hotchin, 2001). However, in our model, this mechanism seems not to control the fate of E-cadherin as we do not see any accumulations of E-cadherin or its associated catenins in any cytosolic compartment (Figure 23 and 24). Neither did we detect any translocation of E-cadherin from the plasma membrane when analysing membrane/cytoplasm-fractionated lysates from non-induced/induced A431/SIP1 cells (preliminary data, not presentable).

Another potential mechanism controlling E-cadherin mediated cell-cell adhesion is the maintenance of the integrity with its associated catenins. Competition for catenins could be induced through activation of other cadherins, e.g. N-cadherin. However, E-cadherin does not lose its association with neither β -catenin nor p120-catenin during SIP1-mediated EMT in A431 (Figure 25), indicating that there is no such competition. The important finding that α -catenin dissociates from the E-cadherin complex during the transformation (Figure 25) is the best clue for finding the underlying mechanism controlling SIP1-mediated disruption of intercellular adhesion. Several observations indicate that disruption of E-cadherin-mediated adhesion happens as a consequence of α -catenin dissociation from the E-cadherin• β -catenin complex. E.g. IQGAP1, acting downstream of Rho-GTPases cdc42

and Rac1, has been shown to regulate the E-cadherin-mediated adhesion by disrupting the link between β -catenin and α -catenin. (Kuroda *et al.*, 1998). Furthermore, the expression of E-cadherin• α -catenin fusion proteins has been shown to rescue cell-cell adhesion both *in vivo* and *in vitro* (Nagafuchi *et al.*, 1994; Pacquelet *et al.*, 2005). Of note, cells expressing truncated β -catenin (incapable of binding α -catenin) are incapable of establishing E-cadherin mediated cell-cell adhesion (Oyama *et al.*, 1994). Further investigations, such as expressing an E-cadherin• α -catenin fusion protein, are obviously needed in order to determine whether dissociation of α -catenin precedes the collapse of E-cadherin mediated cell-cell adhesion or *vice versa* during SIP1-mediated EMT in A431.

Concomitant with the disruption of adherens junctions, we detect a significant rearrangement of actin filament, increased focal adhesion and increased affinity for substrates as collagen and fibronectin (Figure 26 and 27). As integrin β 1 and β 3, both known to mediate the cellular attachment to collagen and fibronectin, are essential for TGF β -induced EMT in mouse mammary epithelial cells (Bhowmick *et al.*, 2001; Galliher *et al.*, 2006) SIP1 could in a similar fashion mediate a cellular transformation through an integrin-dependent signalling pathway. In support for this hypothesis, SIP1-mediated morphological conversion of A431 was totally abrogated by the Src-family kinase inhibitor PP2 (Figure 28). However, additional experiments are still needed in order to confirm that a signal essential for SIP1-mediated EMT is conducted through a member of the Src kinase family.

In MDCK, the expression of both SIP1 and SIPCIDmt induced EMT (van Grunsven *et al.*, 2003). Based on promoter studies and the fact that both SIP1 and SIPCIDmt induced the dissociation of E-cadherin from the cell-cell contacts, Grunsven and colleagues concluded that SIP1 transcriptionally repressed E-cadherin independent of CtBP recruitment. In a similar way, we find that both SIP1 and SIPCIDmt induced EMT in

A431. But based on our additional findings, that SIP1^{CIDmt}-mediated EMT is not coupled with down regulation of E-cadherin (although it incorporates dissociation of E-cadherin from the cell-cell contacts), we conclude that SIP1 is dependent on CtBP recruitment in order to repress the E-cadherin encoding gene. This is in line with recent studies of SIP1 sumoylation by the polycomb protein Pc2. In these studies sumoylation of SIP1 inhibited its interaction with CtBP and simultaneously relieve the repression of E-cadherin by SIP1 (Long *et al.*, 2005). Furthermore, Shi *et al.* demonstrated that CtBP is required for the constitutive repression of endogenous E-cadherin in U2OS cells (Shi *et al.*, 2003).

Conclusion

Out of the two specific aims stated in the section “Aims of the thesis” I find that one has been successfully accomplished, namely how SIP1 repress proliferation in A431. Summarised, we showed that SIP1 directly repress the transcription of *CCND1* (Cyclin D1) in A431. This down regulation was closely followed in time by an increase in hypophosphorylated Rb, accumulation of cells in G1 and at last evident as decreased net-growth in cell population.

In contrast, our aim to determine the underlying mechanism responsible for SIP1-mediated morphological transformation of A431 has not been met. Nevertheless, I do not consider my effort during the attempt for wasted. Many important observations have been made. One, particularly worth mentioning, is that the morphological transformation initiated by the expression of SIP1 in A431 is independent on E-cadherin down regulation. Certainly further studies have to be made before I dare to present a hypothesis explaining the general mechanism responsible for the SIP1-mediated morphological transformation of A431.

Materials and methods

Materials

Antibody

Primary

myc (clone 9E10)	Santa-Cruz
α -catenin (#610193)	BD Bioscience
α -tubulin (#T5168)	Sigma
β -catenin (#610153)	BD Bioscience
Cyclin D1 (#2922)	Cell signaling
E-cadherin (#610181)	BD Bioscience
Flag (#F3165)	Sigma
Integrin β 1 (#MAB1965)	Chemicon
Phalloidin-Fluorescein Isothiocyanate (#P5282)	Sigma
p120-catenin (#610133/4)	BD Bioscience
p16 (#sc-1207)	Santa-Cruz
p21	Santa-Cruz
p27 (#2552)	Cell signaling
Vinculin	Neomarkers

Secondary

Alexa Flour 488 donkey-anti-mouse	Molecular Probes
Rabbit anti-mouse HRP conjugated Ab	DAKO
Goat anti-rabbit HRP conjugated Ab	DAKO

Buffers

DNA Loading Buffer

40% sucrose

0.1% bromophenol blue

0.1 % xylene cyanol

TAE (50x) (Tris-acetate-EDTA electrophoresis buffer)

2 M Tris-acetate, 50 mM EDTA

For 1000ml

242g Tris-base

57.1ml Acidic acid

100ml of 0.5 M EDTA (pH 8.0)

TBE (5x) (Tris-borate-EDTA electrophoresis buffer)

450 mM Tris-borate, 10mM EDTA

For 1000ml

54g Tris-base

27.5g Boric acid

20ml of 0.5 M EDTA (pH 8.0)

TBS-T (10X)

For 1000ml

90ml 1M Tris-Cl (pH 8.0)

122.5ml 5M NaCl

10ml Tween 20

774.5ml H₂O

Protein Run Buffer (5x)

125 mM Tris

2.5 M Glycine

0.5% SDS (pH 8.5-8.7)

SDS Gel-loading Buffer

50mM Tris-Cl (pH 6.8)

2% SDS

10% Glycerol

Lysis buffer (isolation of genomic DNA)

10 mM Tris-Cl (pH 8.0)

0.1 M EDTA (pH 8.0)

0.5% SDS

RNase 20 µg/ml

NP-40 IP buffer

0.1M NaCl;

50mM TRIS pH8.0;

0.5%NP-40;

1mM DTT;

10mM beta-glycerophosphate;

5mM NaF; 0.1mM Na₃VO₄;

10µg/ml leupeptine;

2 μ g/ml aprotinine;

0.1mM PMSF

Nuclei Lysis Buffer

10mM Tris-Cl (pH 7.4)

3mM MgCl₂

10mM NaCl

150mM Sucrose

0.5% NP40

Nuclei Lysis Buffer (devoid of NP-40)

10mM Tris-Cl (pH 7.4)

3mM MgCl₂

10mM NaCl

150mM Sucrose

Nuclei freezing buffer

40% glycerol

50mM Tris-Hcl (pH 8.5)

5mM MgCl₂

0.1mM EDTA.

Nuclei Transcription Buffer (2x)

4mM of each NTP

200mM KCL

20mM Tris-Cl (ph 8.0)

5mM MgCl₂

4mM DTT

200mM Sucrose

20% Glycerol

Nuclear Run-on Binding Buffer

10mM Tris-Cl pH 7.5

1mM EDTA

2M NaCl

Chemicals, reagents and equipment

Acrylamide (40%)

VWR

Agarose

Invitrogen

Ammonium persulfate

Sigma

Ampicillin

Sigma

Aprotinine

Sigma

β-mercaptoethanol

Sigma

Biotin-16-UTP

Roche

BSA (Bovine serum albumin)

Sigma

Bromophenol Blue

Sigma

Chloroform

Sigma

CaCl₂

Aldrich

Cellcounter (CASY1)

Schaerfe

System

dNTPs

Invitrogen

DAPI (4',6-diamidino-2-phenylindole,dihydrochloride)	Molecular Probes
D-MEM (Dulbeccos Modified Eagles Medium)	Gibco
Dimethyl sulphoxide (DMSO)	Sigma
DNase I	Roche
Doxycycline	Sigma
Dried milk <1% fat (Marvel)	Waitrose
ECL™ Western Blotting Detection Reagents	Amersham
EDTA	Sigma
Ethanol	Sigma
Ethidium bromide	Sigma
Fetal Bovine Serum	Perbio
Filter Paper	Whatman
Formaldehyde (37%)	Sigma
Extensor Hi-Fidelity PCR Master Mix	ABgene
Glycerol	Sigma
Immobilon P	Millipore
KCl	Sigma
Kodak BioMax Light Film	VWR
Lennox L Agar	Invitrogen
Leopeptin	Sigma
Luminomitor tube	Sarstedt
Luminometer (Lumat LB9501)	Berthold
Luria Broth Base	Invitrogen
Methanol	VWR
Microplate reader (GENios)	Tecan

MTT(3-[4,5-dimethylthiazole-2-yl] 2,5,-diphenyl tetrazolium bromide)	Sigma
MgCl ₂	Sigma
NaCl	Fisher
Native Plus <i>Pfu</i> Buffer	Stratagene
NaHCO ₃	Sigma
Na ₂ HPO ₄	Sigma
Non-enzymatic dissociation buffer (PBS-based)	Invitrogen
NP-40	Sigma
Nucleic Acid molecular markers	Bioline
ONPG (o-nitrophenol-b-galactopyranoside)	Sigma
Paraformaldehyde (16%, methanol free)	EMS
PBS tablets	Oxoid
PCR-wax	Applied Biosystems
PCR-tube	Applied Biosystems
PCR machine	Perkin Elmer
Penicillin/Streptomycin	Gibco
Petri dishes	Nunc
<i>Pfu</i> DNA polymerase	Stratagene
PMSF (phenylmethyl sulphonyl fluoride)	Sigma
Ponceau S solution	Sigma
Power supplies	BIO-RAD
Phenol/chloroform	Sigma
Propidium Iodide	Sigma
Protein G Sepharose (beads)	Amersham

Protein Kinase K	Sigma
Protein markers	Biolabs
Reporter Lysis Buffer (5x).	Promega
Rnase A (59 Kunitz units/mg)	Sigma
RNase secure reaction	Ambion
Scalpel	Swann- morton
SDS	Sigma
Semi-dry blotting apparatus	Sigma
SSC (20x)	Eppendorf
SuperScript III Reverse Transcriptase	Invitrogen
T4 DNA ligase	Invitrogen
TEMED	Sigma
Tissue culture incubator (CO ₂ -incubator)	Heraeus
tRNA	Sigma
Tris base	Sigma
Triton X-100	Sigma
Trypsin-EDTA (0.25% Trypsin with EDTA 4Na)	Gibco
Tween 20	Sigma
Waterbath (SUB6)	Grant Instruments Ltd

Kits

BCA protein assay kit	Pierce
Cell Line Nucleofector kit	Amaxa Biosystems

QIAfilter™ Plasmid Maxi Kit

Qiagen

Wizard SV GEL and PCR Clean-Up System

Promega

5-Bromo-2'-deoxy-uridine Labeling and Detection Kit I

Roche

Master Mix

RT-Master Mix

200µl 5X first strand buffer

10µl of 100mM dATP

10µl of 100mM dCTP

10µl of 100mM dTTP

10µl of 100mM dGTP

10µl of 0.1M DTT

445µl H₂O

20µl RNase Secure Reagent

Primers

28S	5' cgactccgaagtcccatct 3' acagcttctcccgctgctg
Atonal homolog 8	5' ctcgcatcttgctgtgcgca 3' agtttggacagcttctgccc
Caveolin 2	5' gttcgcggactcggaccagg 3' gatgtgcagacagctgagggtg
Claudin 4	5' cggcccacaacatcatccaag 3' tggctcagtctctgcccagt
Cofilin 2	5' ggtgatactgtagaggacccc 3' ctccaagtgtcgaacggtcc
CyclinD1	5' ctctgtgctgccaagtgga 3' gccacgaacatgcaagtggc
CyclinD1-	5' ggaacaccagctcctgtgc

Fragment1	3' ggtctcctccgccttcagc
CyclinD1- Fragment2	5' ggaacaccagctcctgtgc 3' ggatccctagaaacaccacgg
CyclinD1- Fragment3	5' ggaacaccagctcctgtgc 3' ggggaagcttctgttcctcgcagacctacgg
CyclinD2	5' cgactccgaagtcccatct 3' acagcttctcccgtgctg
CyclinD3	5' tacctgtcttgcgccccac 3' tcccacttgagcttcctag
Cyclin G2	5' gctgaaagcttgcaactgccg 3' ggtatcgttggcagctcagg
Del1	5' ggtagccgtctggctcttgg 3' GCATGGATTAGGAGTGCAGG
Desmoglein3	5' ggctcttccccagaactacagg 3' ccactccagagattcggtaggtg
Desmoplakin	5' cgcggatcaacactctgggcc 3' ccatttggtcattggcctgggc
E-cadherin	5' tctacgcctgggactccacctac 3' ctcttggccagtgatgctgtag
FRA-1	5' tcacccccagcctggctcttc 3' cccaagctggctctactgtg
Galectin 1	5' gagtgccttcgagtgcgagg 3' ctgcaacacttcaggctgg
Gelsolin	5' caacagcatggtggtggaacac 3' tcaggtagtcacccagctgcac
Glutathione S-transferase A4	5' ggcccaagctccactatccc 3' ccagcagatccagtgctccc
GAPDH	5' tcttccaggagcgagatccc 3' caccaccctggtgctgtagc
HtrA serine peptidase (<i>PRSS11</i>)	5' acgccaacacctacgccaac 3' gcttggtggtcaccacgtgg
Keratin13	5' ggtgctggatgagctcactc

3' ggcgtggaaccattcctcag
Keratin15 5' gtggcatgagggctctgtggc
 3' ggagttgtcgatggtggtgg
Kruppel-like factor 4 5' gtctggcccggcgggaaggg
 3' ggtggcggccactgactccgg
Osteonectin 5' ctttctccttgctggccg
 3' gcacaccttctcaaactcgcc
p21-activated kinase1 5' ggagtcggcagcaaagatgc
 3' cccgtaaactccctgtgac
**Phospholipase C,
delta 3** 5' cgctacctcctcttcaagg
 3' ccagtgtcatcagctcatgctgc
Quiescin Q6 5' ggcgctctattcgccttccg
 3' ctctcagcacagtccaggg
RAB25 5' gatggggaatggaactgagg
 3' ctcttcagccatcgctcc
**Retinoic acid receptor
responder 1** 5' cgtggcttccagcacagagcg
 3' ctcacactagtgagctgtgcc
S100A4 5' gcggtgccctctggagaag
 3' gttttcatttcttctctgggctgc
Syntenin 5' cagaagcttctgctcctatccc
 3' ccattgatctgaagtacttgggtcccc
SIP1 5' ccctaattctgtttcttcttctcctac;
 3' ccacaatctgtagaaccttttgtaacctcac
**Telomerase reverse
transcriptase** 5' ggtgtacggcttcgtgcggg
 3' GGCCAGGATCTCCTCACGC
Thrombospondin 1 5' gggactaggcgtcctgttcc
 3' tcatctgcctcagggatgcc
Ubinuclein 1 5' ccgaggggaaggtaaaaggcc
 3' caccttccttcaacttccgc
**Vascular endothelial
growth factor C** 5' cttcgagtcggactcgacc
 3' gtccttgagttgaggttggcc
Vimentin 5' gccgttgaagctgctaactacc;
 3' gagtgctgcaactgagtgctgc)

(Neighbouring laboratories provided Primers for p21 and p27)

Methods

Adhesion assay

Preparation of substrate covered 96-well plates: 100µl of substrate (Laminin: 20µg/ml diluted in 0.1M NaHCO₃; Fibronectin: 50µg/ml diluted in 0.1M NaHCO₃; Collagen 50µg/ml diluted in 0.02M Acetic acid) was pipetted into each well and incubated 1h in CO₂-incubator (37°C, 5% CO₂). Wells were subsequently washed twice with PBS, once with serum free media containing 0.1% BSA, and then incubated (in CO₂-incubator) 15min in serum free media containing 0.1% BSA.

A431/Sip1 cells grown in absence/presence of DOX (subconfluent 175cm²-flasks) were washed twice with PBS and incubated in 4ml of non-enzymatic dissociation buffer until cells detached from plastic (app 15min). 7ml of PBS were added to the cell suspension and resuspended well by pipetting, precipitated by centrifugation (500g, 5min), washed once with PBS and finally resuspended in a small volume (app 200µl) of PBS. After counting cells (described in “cell culture”), cells were diluted to a concentration of 2.0×10^5 cells/ml in serum free media containing 0.1% BSA. 100 µl of cells suspension were pipetted into wells covered by substrate (experimental plate) and incubated for 15min in CO₂-incubator. In order to control that equal amounts of Sip1 induced/non-induced cells were seeded, 100 µl of cells were seeded in uncoated wells (control plate) and incubated until all cells were properly attached to the plastic (app 3h). After incubation, attached cells were washed 3 times with serum free media containing 0.1% BSA (liquid was removed by gently tapping the plate up side down on tissue paper). Attached cells were fixed and stained for 5min in 100 µl of 0.2% crystal violet in 10% EtOH. Excessive staining solution was diminished by several washes in PBS. After residual PBS had been removed 100µl of solubilisation buffer (50mM NaH₂PO₄ (pH4.5), and 25% EtOH) were added to each well and left for incubation

at RT for 5min while shaking. Finally absorbance at 580nm was measured for each well in a microplate reader.

Agarose Gel Electrophoresis

Gels were run in submarine gel tanks (Merck Eurolab ltd) for horizontal agarose mini-gels. (50-5000bp) DNA samples were run on 1-2% agarose/1x TBE gels (containing app 1µg/ml of ethidium bromide) at app 100V. (>5000bp) DNA samples were run on 0.5-1% agarose/1xTAE gels at app 100V and subsequently stained in 1xTAE buffer containing app 1µg/ml of ethidium bromide.

DNA was monitored on an UV transilluminator and photographed using an UVP digital imaging system (BioDoc-It™ System).

Cell culture work

The human epidermoid carcinoma cell line A431 and clones thereof was maintained in D-MEM (Glucose 4500 mg/L, GlutaMAX™I, Pyrovate) supplemented with 10% Fetal Bovine Serum, Penicillin (45 units/ml) and Streptomycin (45µg/ml). Cells were grown in a tissue culture incubator (CO₂-incubator) at 37°C and 5%CO₂. To induce the expression of rtTa, media was supplemented with 2µg/ml of doxycycline.

Cells (after wash with PBS) were lifted by 5-10 min incubation with Trypsin-EDTA (app 20µl/cm²). In order to passage, cells were resuspended in min. 15 fold D-MEM and replated. For counting and transfections, cells were washed first in 10ml D-MEM then once in 10 ml PBS. Cells were resuspended in an appropriate volume of PBS and 10µl were diluted in 10ml of Isoton and finally counted by CASY1-cellcounter as described by manufacturer.

Cell cycle distribution via FACS

Cells (70% confluent 25cm² tissue culture flask) were harvested with trypsin, washed once in PBS and finally resuspended in 200µl of PBS. To fix cells, 800µl of pre-chilled 70% EtOH/PBS was added while vortexing before they were incubated at 4-6°C for at least 2h. After fixation, cells were precipitated by centrifugation (500g, 5min at 16°C) and resuspended in 800µl PBS. To stain DNA exclusively, 100µl of DNase-free RNase A (10 mg/ml prepared in 10mM Tris-HCl, pH 7.5) and 100µl of PI (500µg/ml) were added and left to incubate at 37°C for 1h. The cellular DNA content was evaluated using FACS flow cytometer.

Cell lines and clones

The A431 cell line was originally isolated from an epidermoid carcinoma of the vulva of a 85 year old female. The cell line has since been used in a variety of studies in cell biology. Besides a high expression level of EGF receptor (Hunts *et al.*, 1985) A431 cells are characterised by mutational inactivation of the tumoursuppressor p53 (Park *et al.*, 1994).

To generate A431 clones with DOX-inducible expression of SIP, SIP1ZFmt and SIP1CIDmt, we used a clone of A431 cells expressing Tet-responsive transcriptional activator rtTA (Andersen *et al.*, 2005 Appendix B)). Cells were transfected either with the pTREmyc-SIP1, pTREmyc-SIP1ZFmt and pTREmyc-SIP1CIDmt along with the pTK-Hyg vector (Clontech: <http://www.clontech.com/images/pt/PT3082-5.pdf>). Selection of stable clones was carried out in the presence of 60 µg/ml of hygromycin B.

A431/SIP1/CycD1#1-3 with concurrent DOX-regulated expression of SIP1 and cyclin D1 were obtained by co-transfecting A431/SIP1 cells with pBIcycD1 and pIRESpuro (Clontech;http://www.clontech.com/images/pt/dis_vectors/PT3198-5.pdf) followed by the selection of puromycin-resistant cells in the presence of 0.5 µg/ml of puromycin.

A431/SIP1/Ec1#1-2 with constitutive expression of Flag-tagged E-cadherin concurrent with DOX-regulated expression of SIP1 was obtained by transfecting A431/SIP1 with pIRESFlag-Ec1 and subsequently selected for puromycin resistance (0.5 µg/ml of puromycin).

The A431 clone with DOX-regulated expression of Ec1WVM (31D6) was originally described in (Andersen et al., 2005)

DNA purification by phenol:chloroform extraction

100µl of DNA was mixed with 2µl EDTA (0.5M), 1µl tRNA, 100µl phenol:chloroform and vortexed on the side for 20 sec. Phases were separated by centrifugation (10.000g, 10 min, 4°C) before supernatant was transferred to a new eppendorf tube. DNA was then precipitated by centrifugation (10.000g, 10min) after adding 5µl NaCl (5M) and 250µl EtOH. Pellet (containing purified DNA) was washed once in 70% EtOH before it finally was dissolved in an appropriate volume of H₂O.

Immunofluorescence (IF)

For immunofluorescent stainings, cells were grown for 2 days in 10-well glass microscope slides (VWR). Cells were washed in PBS and fixed in ice-cold acetone/methanol (1:1) solution for 4 min followed by a 45sec incubation in 0.5% Triton/PBS. After rinsing with PBS, the slides were incubated with primary antibodies diluted in PBS for 1 hour at RT. Excessive primary Ab was removed by 5 washes in PBS. Secondary Ab was diluted in PBS and applied for 1h at RT before 5 washes in PBS were repeated. When nuclear staining by DAPI was desired an addition incubation of 5min with DAPI/PBS (0.25µg/ml) was carried out within the 5 washes. After excessive PBS was removed from the slides an appropriate

amount of Fluoromount was carefully added on top of the fixed cells and finally covered by a coverglass.

Slides/stainings were examined and photographed using a confocal inverted microscope (Zeiss Axiovert 200M).

Immunoprecipitation

Subconfluent cell cultures (175cm² flask) maintained with/without DOX were washed briefly in ice-cold PBS and incubated in ice-cold freshly prepared NP-40 IP buffer for 10 min on ice. Lysates were transferred by pipette to pre-chilled 1.5ml eppendorf tubes, and centrifuged 10min at 20.000g, 4°C. Supernatant was transferred to new tubes and an aliquot was taken to represent “input”. 500µl of supernatant from each sample was incubated 1h with 0.75mg primary antibody, followed by additional 1h incubation with 1.5mg of secondary antibody, and finally incubated O/N with 40µl (50%) pre-cleaned protein G sepharose beads (all incubations were carried out at app 6°C while rotating). Beads were isolated and cleaned by 6 cycles of; precipitation by centrifugation (100g, 30 sec), resuspension in 500µl NP-40 IP buffer and 5min rotation (all at 4-10°C). Beads were finally resuspended in 30µl of 2xSDS buffer inc. 0.1% bromophenol blue and 100mM β-mercaptoethanol and boiled 5min.

Luciferase reporter assay

To determine transcriptional activity of luciferase reporter constructs, cells were transfected with 0.2µg-2µg of reporter constructs. The efficiency of each transfection was assessed by co-transfecting cells with 0.4 µg of β-galactosidase expression vector, pCMVβ-gal (Invitrogen). 2*10⁶ of transfected cells were split in two 5cm dishes and maintained with or without DOX for 48 hours.

After cells had been washed twice in PBS, 500µl of PBS was pipetted into the dishes to prevent dehydration. Cells were scraped with a rubber cell-scraper, transferred by pipette to eppendorf, and precipitated by centrifugation (450g, 5min at 16°C). Supernatant was removed and cells resuspended in 70µl of 1xReporter Lysis Buffer were vortexed (10sec) and left on ice for 15min. Cellular debris was precipitated by centrifugation (10.000g, 1min, 16°C) while lysate was transferred to new eppendorf tubes.

β-galactosidase activity was estimated by its efficiency to hydrolyse the substrate o-nitrophenol-b-galactopyranoside (ONPG). A fresh mastermix of substrate was prepared prior to each assay, containing 2µl of 100x Mg²⁺ solution (0.1M MgCl₂, 4.5M β-mercaptoethanol), 44µl of ONPG (4mg/ml in 0.1 sodium phosphate (pH 7.5) and 134µl of 0.1 sodium phosphate (pH 7.5) per sample mix. 20ml of lysate was mixed with 180 ml of mastermix and left at 37°C until the mix reached a visible faint yellow colour. A background control sample was simultaneously prepared with 1xReporter lysis buffer. Optical density at 405nm was measured by a spectrophotometer, subtracted the background value, and used as a standard for transfection efficiency. Luciferase activity was measured by pipetting 5µl of lysate into a luminometer tube and placing the tube in the luminometer (100 µl substrate were injected, samples were measured for 5sec).

The luciferase activity was finally normalised to the activity of β-galactosidase.

Matrigel invasion assay (3D)

Invasion was analysed in inverse invasion assay as previously described (McGarry et al., 2004) with minor modifications. The matrigel was thawed slowly on ice before it was carefully mixed with 1 volume of PBS and immediately pipetted using pre-chilled pipette-tips into transwells (120µl pr well). The matrigel was allowed to settle during a 2h incubation period at 37°C. Meanwhile, cell suspensions of 5x10⁵ cells/ml were prepared in

serum containing DMEM. 120 μ l of the cell suspension was pipetted onto the convex part of the polycarbonate membrane, placed in an inverted 12-well tissue culture plate, and allowed to adhere in the tissue-culture incubator (37°C, 5%CO₂) for minimum 3 hours. Subsequently, cells were washed twice in DMEM before inserts were replaced in wells containing 1 ml of DMEM with or without DOX. In three days, cells were fixed in methanol and stained for 1 hour in propidium iodide solution (10 μ g/ml of PBS). Optical sections were scanned at 10 μ M intervals using the confocal microscope Zeiss Axiovert 200M. Three independent experiments were performed and representative results are shown. To perform statistical analysis of the invasive potential of A431/SIP1 and A431/SIP1/CycD1 cells, the amount of cells entered matrigel and remaining at the filter were calculated in twelve optical fields. The values are expressed as a percentage of cells penetrated matrigel.

MTT –assay

Cells were plated out 3×10^4 cells/cm² in 96 well plates, one triplicate for each time point, and left O/N. At time point 0h, media was changed and cells were thereafter maintained in media with/without DOX. At each time point, media was discarded from the specific triplicate and replaced with 200 μ l-acclimatised media containing 0.5mg/ml MTT. After a 2h incubation period, cells were washed once with PBS and incubated shaking at RT for 15min in 200 μ l DMSO. Absorbance was measured at 570nm with background subtractions at 650nm.

Nuclear run-on

In large, the Nuclear run-on assay was performed as described in Patrone *et al.*, 2000.

Nuclei preparation: Cells (80% confluent 175cm² Flask) were harvested by trypsination and washed twice in PBS. In order to break the plasma membrane cells were resuspended in 4ml Nuclei Lysis Buffer and incubated on ice for 5min. Nuclei were then recovered by centrifugation (170g, 4C, 5min) and washed in Nuclei lysis buffer (devoid of NP-40). Pellet was resuspended in 100µl Nuclei Freezing Buffer and stored at -80°C until *in vitro* RNA synthesis was carried out.

In vitro RNA synthesis: One volume of nuclei was gently mixed with one volume of Nuclei Transcription Buffer (2x) before 8µl of Biotin labelled UTP (10nmol/µl) was supplied to the solution. A negative control was established devoid of biotin labelled UTP. Synthesis was carried at 29°C and stopped after 30min by the addition of 6µl CaCl₂ (250mM; final conc. 7.5 mM) and 6µl RNase-free DNase I (60 U in total). DNase I was allowed to work for 10min (29°C) before RNA was purified by Trizol.

Isolation of *de novo* transcripts: 50µl of Streptavidin conjugated beads (Dynabeads M-280) was resuspended in Nuclear Run-on Binding Buffer and mixed with an equal volume of RNA. Mixture was incubated 20 min at 42°C followed by 2h at RT. Beads were washed 2 times in 2x SSC containing 15% formamide and 5 times in 2xSSC (A magnetic apparatus supplied by Dynal was used to collect bead-pellet). Pellet was finally resuspended in H₂O and used for semiquantitative RT-PCR.

PCR

2µl of primer mix (0.1nmol of each) was mixed with 4µl of dNTP-mix (100nmol of each), 4µl H₂O, 1.25 ml of 10x Native Plus *Pfu* Buffer and pipetted into a PCR-tube. Gem wax (PCR wax) was added to the tube and melted during 5min incubation at 72°C. The tube was subsequently transferred to ice. When the wax had solidified, 1µl of Template-DNA, 32µl

of H₂O, 3.75µl of 10x Native Plus *Pfu* Buffer and 1µl *Pfu* DNA polymerase was added on top of the wax. PCR-cycles were designed according to primer and template characteristics. Finally, PCR was performed at a GeneAmp PCR System 2400 (Perkin Elmer).

Plasmids

pTREmyc-SIP1 (pUHDmyc-SIP1) was kindly provided by van Roy F (University of Ghent, Belgium) while pTREmyc-SIPZFmt and pTREmyc-SIPCIDmt were provided by K. Verschueren (University of Leuven, Belgium). The SIP1 constructs have previously been described by Comijn *et al.*, 2001 and van Grunsven *et al.*, 2003

pcDNA3-Flag-E-cadherin (described by Chitaev *et al.*, 1998) was kindly provided by S.M. Troyanovsky (Washington University Medical School, St. Louis, USA). Coding sequence for Flag tagged E-cadherin was subcloned into pIRESpuro (Clontech ;http://www.clontech.com/images/pt/dis_vectors/PT3198-5.pdf) to generate pIRESFlag-Ec1.

pCMVEGL4-GFP (GFP-E-cadherin, described in Koyama-Honda *et al.*, 2005) was provided by I. Koyama-Honda (Kyoto University, Japan).

pCCND1LUC, pCCND1mtLUC and pBIcycD1 were personally cloned in the lab. The cloning of pCCND1LUC and pCCND1mtLUC is described in detail in the following paragraph.

pCCND1LUC was created by amplifying the -1025 to +18 (0 refers to the first transcribed nucleotide) fragment of *CCND1* by PCR using genomic DNA purified from A431 as a template and two primers with intrinsic endonuclease restriction sites. The forward primer (5'ggggctagcaaattctaaaggtgaaggacg) harboured a *Nhe*I endonuclease restriction site (underlined) while the reverse (5'ggggaagcttcccctgtagtccgtgtgacg) contained a *Hind*III restriction site. PCR

was carried out with 2x pre-cycles of (30 sec with 92°C , 30 sec with 61°C, 2min with 72°C) followed by 28 cycles of (30 sec with 92°C , 30 sec with 69°C, 2min with 72°C). After synthesis, the PCR product was purified by phenol:chloroform extraction and eventually dissolved in 10µl H₂O. Insert (fragment containing *CCND1* promoter) and pGL3-basic vector (Promega; <http://www.promega.com/tbs/tm033/tm033.pdf>) were double-digested in parallel by the endonucleases NheI and HindIII. Restriction was carried out for 2h at 37°C in 15µl (containing 10µl DNA, 1.5µl NEB Buffer 2, 1.5µl 10xBSA (NEB) , 1µl NheI and 1µl of HindIII) and was followed by a heat inactivation of the nucleases (94°C, 5min). Insert and vector were mixed with 4µl of DNA Loading Buffer, loaded and run on a 1% Agarose/TBE gel. After sufficient electrophoresis bands were visualised by illuminating the gel with 365 nm UV light, cut out with a sterile scalpel and transferred to 1.5 ml eppendorf tubes. DNA was eluded from the gel slices via Wizard SV GEL and PCR Clean-Up System as instructed by the manufacturer. To evaluate the relative concentration of eluded DNA, aliquots were mixed with DNA loading buffer (5:1), run on a 1% Agarose/TBE gel and finally visualised by UV radiation. 1-fold of vector and 4-fold of inserts and was ligated at 16°C O/N (8µl of vector+insert was mixed with 1µl of T4-DNA-ligase-buffer (10x) and 1µl T4-DNA-ligase). To assess vector self-ligation, a ligation reaction containing vector but no insert was carried out in parallel. The following day 1µl of each reaction was carefully mixed with 15µl of newly thawed competent cells (*E.coli*, Invitrogen). Bacteria were transformed by a heat-shock (42°C, 1min), chilled on ice and incubated at 37°C for 1h after the addition of 150µl Luria Broth Media (Luria Broth Base, 25g/L). Finally, cells were plated out on agar plates (Lennox L Agar, 32g/L) containing 100µg/ml ampicillin and left O/N at 37°C to form colonies. Single colonies were picked and inoculated into 250ml of ampicillin containing LB media and left at 37°C O/N with shaking. Plasmid DNA was isolated from the cultures by using QIAfilter™ Plasmid

MAXI-prep kit as instructed by manufacturer. Existence of the desired *CCDN1*-fragment was verified first by cutting the plasmid with *NheI* and *HindIII*, and later by sequencing (performed by PNAOL, Leicester University).

pCCND1mtLUC was designed to deviate from pCCND1LUC by the 4 point mutations G(-1017)A, G(-859)A, C(-300)T and C(-294)T. Three fragments (Frag1(-1030 to -844), Frag2(-874 to -284), Frag3(-317 to +18)) was amplified from 1ng of pCCND1LUC using the following primers; Fragment1(forward5' ggggctagcaaattctaaagAtgaagggacg, reverse5' ccgggagaaacacaTctctgaatggaaagc); Fragment2(forward5' gctttccattcagagAtgtgtttctcccgg, reverse5' gggggtgagAtggagAtggctctgcagtaggg); Fragment3(forward5' cccctactgcagagccaTctccaTctcaccccc, reverse5' ggggaagcttcccctgtagtccgtgtgacg) (mutated nucleotides represented by letters in uppercase). A fusion of fragment 1 and 2 was obtained by PCR amplification using fragment1 and fragment2 as template (diluted 1:100.000) and following primers (forward5' ggggctagcaaattctaaagAtgaagggacg, reverse5' gggggtgagAtggagAtggctctgcagtaggg). In parallel, a fusion of fragment2 and 3 was generated by the use of forward5' gctttccattcagagAtgtgtttctcccgg, reverse5' ggggaagcttcccctgtagtccgtgtgacg.

Finally the desired fragment was amplified by using fragment1+2 and fragment 2+3 as template and the following primers (forward5' ggggctagcaaattctaaagAtgaagggacg, reverse5' ggggaagcttcccctgtagtccgtgtgacg). This insert was cloned into pGL3 basic vector as described for pCCND1LUC.

To generate the DOX-regulated cyclin D1 expression vector (pB1cycD1), cyclin D1 coding sequence was amplified by following primers; (forward5' cagcggccgccccagccatggaacaccagctcc, reverse5' ccgtcgacgcctcagatgtccacgtccc) and cloned into pBI vector (Clontech; <http://www.clontech.com/images/pt/PT3070-5.pdf>) between *NotI* and *Sall*.

Preparation of protein samples

Lysates were prepared from 80% confluent cell cultures (unless specified otherwise). Cells were washed twice in PBS and subsequently lysed in an appropriate volume of 1xSDS gel-loading buffer. Lysate was transferred to 1.5µl eppendorf tubes and immediately boiled for 10min. Protein concentration was measured using BCA protein assay kit as manufacturer recommended and used to equilibrate lysates. Finally lysates were dyed and reduced by adding 0.1% bromophenol blue and 100mM β-mercaptoethanol.

Purification of eukaryotic genomic DNA

Genomic DNA was isolated from a 80% confluent (175cm² flask) culture of A431/Sip1. Cells were washed thrice with ice-cold PBS before lysis was carried out in 10ml of lysis buffer (for isolation of genomic DNA) for 1h at 37°C. Lysate was transferred by pipetting to a 50ml tube where 50µl proteinase K (20mg/ml) was added and incubated in water bath for 3h at 50°C with occasional mixing. After incubation lysate was allowed to cool down before two phenol-extractions (1xVolume of 0.1M Tris-Cl (pH 8.0) equilibrated phenol mixed with lysate by rotation for 15min and separated by centrifugation (15min, 4000g, 16°C)) and one chloroform-extraction was carried out. Purified genomic DNA was then precipitated by centrifugation (5000g for 5min) after addition of 0.2xVol of 10M ammonium acetate and 2xVol of EtOH. Finally the DNA wash washed once in 70% EtOH before it was dissolved in appropriate volume of H₂O.

Real-time quantitative PCR

cDNA was obtained as described for RT-PCR. PCR was performed using SYBR Green PCR Master Mix in the PRISM 7700 Sequence Detection System (Applied Biosystems). Each sample was run in triplicate. The C_T (threshold cycle when fluorescence intensity exceeds 10 times the S.D. of the baseline fluorescence) values for the target amplicon and endogenous control were determined for each sample. Quantification was performed using the comparative C_T method ($\Delta\Delta C_T$).

Reverse transcriptase PCR (RT-PCR)

RT-PCR was performed in two steps; generation of cDNA by reverse transcriptase (using the RNA as a template and random hexamers as primers), which in the later step can be used as a template in PCR amplification with specific primers targeting the mRNA of interest.

Reverse Transcription was carried out with the SuperScript III Reverse Transcriptase. 5ul of RNA/primer mixture containing 1µg RNA and 50u of random hexamers was incubated 3min at 90°C followed by an immediate transfer to ice where 14.3µl RT-master mix was added. Transcription was initiated by the addition of 0.7µl enzyme (RT) and carried out for 10min at 23°C and 45min at 50°C before enzyme was heat inactivated by 5min incubation at 90°C. The newly synthesised first strand cDNA was diluted with H₂O and used as a stock for PCR.

PCR amplification of the cDNA was carried out using Extensor Hi-Fidelity PCR Master Mix. 10µl of H₂O containing an appropriate amount of cDNA and 10µM of forward and reverse primers were mixed with 10ml of master mix to be used in "hot start" PCR.

RNA extraction with Trizol

80% confluent cells cultures were washed 3 times with PBS. Traces of PBS were removed and cells were lysed in 4ml (175cm² Flask) of Trizol. Cell lysate was collected, after scrabing, with a pipette and transferred to 15ml tube. 600µl of Chloroform were added and mixed by vortexing the tube on the side for 20 sec. After incubation on ice for 10min the water phase was separated by centrifugation (20.000g; 10min; 4°C) and transferred to new tube. RNA was precipitated by adding 2.5 fold of ethanol followed by centrifugation (20.000g; 10min; 4°C). RNA pellet was washed once in 70% ethanol and finally dissolved in an appropriate volume of RNase free H₂O. RNA concentration was estimated by measuring the OD at 260nm. (1OD~40µg of RNA)

SDS-polyacrylamide gel electroforesis (PAGE)

The SDS-PAGE was performed on a Vertical mini-gel system (Sigma). Gels contained 4% stacking gel on top of a separating gel of desired polyacrylamide percentage. 10 ml of stacking gel were obtained by mixing 6.8ml H₂O, 1.7ml 30% acrylamide mix, 1.25ml 1M Tris (pH 6.8), 0.1ml 10% SDS, 0.1ml 10% ammonium persulfate and 10ul TEMED. 10 ml of separating gel were made by mixing 7.3ml of appropriate acrylamide/H₂O mix (e.g. 2.0ml 30% acrylamide mix and 5.3ml H₂O for a 6% gel), 2.5ml 1M Tris (pH 8.8), 0.1ml 10% SDS, 0.1ml 10% ammonium persulfate and 4-8 ul TEMED. Polymerised gels were mounted in the electrophoresis unit and buffer-champers were filled with 1x Protein Run Buffer. Protein samples were incubated at 37°C for 5 min just before 5-30µg was loaded into the gel pockets. Gels were run at 100V until appropriate protein separation was reached.

Transfections

Cells for transfection were grown to 70-90% confluence. Cells were incubated in fresh media 2h prior transfection. Simultaneously, aliquots of media were placed in the tissue culture incubator (37°C, 5%CO₂) for acclimatisation. Cells were harvested by trypsin, washed once in PBS and then counted.

For transfection by electroporation, cDNA/siRNA was mixed with 2x10⁶ cells resuspended in 70µl of PBS, transferred to electroporation cuvette and incubated on ice for 15 min. Cells were electroporated with a single pulse of 250V and 250 µFd (using the Gene Pulser Xcell electroporation system) and immediately resuspended in acclimates media and plated. The transfection of 0.5µg of pmaxGFP in A431 cells had an efficiency at app 20%.

Transfection (nucleofection) by the Cell Line Nucleofector kit was carried out as described by manufacturer with minor deviations. cDNA/siRNA was mixed with 2x10⁶ cells resuspended in 100µl Nuclofection buffer V and nucleofected by the T-20 program. Cells were immediately resuspended in acclimates media and plated. The nucleofection of 0.5µg of pmaxGFP in A431 cells had an efficiency at app 90% and no significant toxicity.

Western Blotting

Blotting was performed in a semi-dry blotter. 6cm x 8.5cm Immobilon P membranes were wetted in methanol followed by 1-2 min incubation in 1xBlotting Buffer. Protein was transferred to the membrane by blotting for 1.5h at 4mA/cm². Blotting efficiency was assessed by staining the membrane with ponceau before the membranes were finally dried.

Dried membranes were wetted by methanol and blocked with 10ml of 4% dried milk in 1xTBS-T for 15-30 min at RT. Primary antibody was in general applied as recommended by manufacturer. (E.g. WB for E-cadherin; 0.25µg antibody was diluted in 1ml of 1xTBS-T containing 4% dried milk). Membrane was placed on a piece of parafilm and the Ab-

solution was applied for 1h. Primary antibody incubation was followed by 5 washes in 10ml 1xTBS-T. Membranes were the incubated 1h at RT with 1µg of secondary antibody diluted in 10ml 1xTBS-T containing 4% dried milk. Membranes were subsequently washed 5 times in 10ml 1xTBS-T.

Blots were developed using ECL™ western blotting detection system and finally exposed to photographic paper (Film).

References

Andersen H*, Mejlvang J*, Mahmood S, Gromova I, Gromov P, Lukanidin E, Kriajevska M, Mellon JK, Tulchinsky E.; Immediate and delayed effects of E-cadherin inhibition on gene regulation and cell motility in human epidermoid carcinoma cells. **Mol Cell Biol** 2005 Vol 25: 9138-9150. (*Shared first-authorship)

Akhtar N, Hotchin NA.; RAC1 regulates adherens junctions through endocytosis of E-cadherin. **Mol Biol Cell.** 2001 Apr;12(4):847-62.

Barnes CJ, Vadlamudi RK, Mishra SK, Jacobson RH, Li F, Kumar R. ; Functional inactivation of a transcriptional corepressor by a signaling kinase. **Nat Struct Biol.** 2003 Aug;10(8):622-8.

Battle E., Sancho E., Franci C., Dominguez D., Monfar M., Baulida J., Garcia De Herreros A.; The transcription factor snail is a repressor of E-cadherin gene expression in epithelial tumour cells.;**Nat Cell Biol** 2000 Feb;2(2):84-9

Beavon I.R.G.; The E-cadherin-catenin complex in tumour metastasis: structure, function and regulation.;**European Journal of Cancer** 2000 36:1607-1620

Becker KF, Atkinson MJ, Reich U, Becker I, Nekarda H, Siewert JR, Hofler H.; E-cadherin gene mutations provide clues to diffuse type gastric carcinomas. **Cancer Res.** 1994 Jul 15;54(14):3845-52.

Behrens J.; Cadherins ad catenins: Role in signal transduction and tumor progression;
Cancer and Metastasis Reviews 1999 18:15-30

**Behrens J., Vakaet L., Friis R., Winterhager E., Van Roy F., Mareel M.M.,
Birchmeier W.**; Loss of epithelial differentiation and gain of invasiveness correlates with
tyrosine phosphorylation of the E-cadherin/beta-catenin complex in cells transformed with
a temperature-sensitive v-SRC gene; **J Cell Biol 1993** Feb;120(3):757-66

Bellovin DI, Bates RC, Muzikansky A, Rimm DL, Mercurio AM.; Altered localization
of p120 catenin during epithelial to mesenchymal transition of colon carcinoma is
prognostic for aggressive disease. **Cancer Res. 2005** Dec 1;65(23):10938-45.

Berger DP, Herbstritt L, Dengler WA, Marme D, Mertelsmann R, Fiebig HH.;
Vascular endothelial growth factor (VEGF) mRNA expression in human tumor models of
different histologies. **Ann Oncol. 1995** Oct;6(8):817-25.

**Berx G. Cleton-Jansen A-M, Nollet F., de Leeuw F.J., Van de Vijver M.J., Cornelisse
C. and Van Roy F.**; E-cadherin is a tumour/invasion suppressor gene mutated in human
lobular breast cancers; **The EMBO Journal 1995** Vol.14. No.24:6107-6115

**Berx G. Cleton-Jansen A-M, Strumane K., de Leeuw F.J., Nollet F., Van Roy F. and
Cornelisse C.**; E-cadherin is inactivated in a majority of invasive human lobular breast
cancers by truncation mutations throughout its extracellular domain; **Oncogene 1996**
13:1919-1925

Bhowmick NA, Zent R, Ghiassi M, McDonnell M, Moses HL.; Integrin beta 1 signaling is necessary for transforming growth factor-beta activation of p38MAPK and epithelial plasticity. **J Biol Chem.** 2001 Dec 14;276(50):46707-13.

Bindels S, Mestdagt M, Vandewalle C, Jacobs N, Volders L, Noel A, van Roy F, Berx G, Foidart JM, Gilles C.; Regulation of vimentin by SIP1 in human epithelial breast tumor cells. **Oncogene.** 2006 Aug 17;25(36):4975-85.

Bielenberg DR, Bucana CD, Sanchez R, Mulliken JB, Folkman J, Fidler IJ.; Progressive growth of infantile cutaneous hemangiomas is directly correlated with hyperplasia and angiogenesis of adjacent epidermis and inversely correlated with expression of the endogenous angiogenesis inhibitor, IFN-beta. **Int J Oncol.** 1999 Mar;14(3):401-8.

Blanco MJ, Moreno-Bueno G, Sarrio D, Locascio A, Cano A, Palacios J, Nieto MA.; Correlation of Snail expression with histological grade and lymph node status in breast carcinomas. **Oncogene.** 2002 May 9;21(20):3241-6.

Bolos V, Peinado H, Perez-Moreno MA, Fraga MF, Esteller M, Cano A. ;The transcription factor Slug represses E-cadherin expression and induces epithelial to mesenchymal transitions: a comparison with Snail and E47 repressors. **J Cell Sci.** 2003 Feb 1;116(Pt 3):499-511.

Boyd JM, Subramanian T, Schaeper U, La Regina M, Bayley S, Chinnadurai G.

A region in the C-terminus of adenovirus 2/5 E1a protein is required for association with a cellular phosphoprotein and important for the negative modulation of T24-ras mediated transformation, tumorigenesis and metastasis. **EMBO J.** 1993 Feb;12(2):469-78.

Boyer B., Vallés A.M. and Edme N.; Induction and Regulation of Epithelial-Mesenchymal transitions; **Biochemical Pharmacology** 2000 Vol.60:1091-1099

Byrne RR, Shariat SF, Brown R, Kattan MW, Morton RA JR, Wheeler TM, Lerner SP.; E-cadherin immunostaining of bladder transitional cell carcinoma, carcinoma in situ and lymph node metastases with long-term followup. **J Urol.** 2001 May;165(5):1473-9.

Cano A., Perez-Moreno M.A., Rodrigo I., Locascio A., Blanco M.J., del Barrio M.G., Portillo F., Nieto M.A.; The transcription factor snail controls epithelial-mesenchymal transitions by repressing E-cadherin expression; **Nat Cell Biol** 2000 Feb;2(2):76-83

Carver EA, Jiang R, Lan Y, Oram KF, Gridley T.; The mouse snail gene encodes a key regulator of the epithelial-mesenchymal transition. **Mol Cell Biol.** 2001 Dec;21(23):8184-8.

Clarke K., Smith K., Gullick W.J. and Harris A.L.; Mutant epidermal growth factor receptor enhances induction of vascular endothelial growth factor by hypoxia and insulin-like growth factor-1 via a PI3 kinase dependent pathway. **British Journal of Cancer** 2001 May 18;84(10):1322-9.

Comijn J., Berx G., Vermassen P., Verschueren K., van Grunsven L., Bruyneel E., Mareel M., Huylebroeck D., van Roy F.;The two-handed E box binding zinc finger

protein SIP1 downregulates E-cadherin and induces invasion.;**Mol Cell** 2001 Jun;7(6):1267-78

Conacci-Sorrell M., Zhurinsky J., Ben-Ze'ev A.;The cadherin-catenin adhesion system in signaling and cancer. **J Clin Invest.** 2002 Apr;109(8):987-91

Chitaev N.A. and Troyanovski S.M.; Adhesive But Not Lateral E-cadherin Complexes Require Calcium and Catenins for Their Formation; **Journal of Cell Biology** 1998 Vol.142 No.3:837-846

St. Croix B., Sheehan C., Rak J.W., Florenes V.A. Slingerland J.M., Kerbel R.S.; E-Cadherin-dependent growth suppression is mediated by the cyclin-dependent kinase inhibitor p27(KIP1). **Journal of Cell Biol.** 1998 Jul 27;142(2):557-71.

Chinnadurai G. CtBP, an unconventional transcriptional corepressor in development and oncogenesis. **Mol Cell.** 2002 Feb;9(2):213-24

Chen KT, Lin JD, Liou MJ, Weng HF, Chang CA, Chan EC. ;An aberrant autocrine activation of the platelet-derived growth factor alpha-receptor in follicular and papillary thyroid carcinoma cell lines. **Cancer Lett.** 2005 Aug 26

Come C, Magnino F, Bibeau F, De Santa Barbara P, Becker KF, Theillet C, Savagner P.; Snail and slug play distinct roles during breast carcinoma progression. **Clin Cancer Res.** 2006 Sep 15;12(18):5395-402.

Daniel J.M. and Reynolds A.B.; The catenins p120^{ctn} interacts with Kaiso, a novel BTB/POZ domain zinc finger transcription factor. **Mol. Cell. Biol.** **1999**, 19, 3614-3623

Daniel J.M., Spring C.M., Crawford H.C., Reynolds A.B., Baig A.; The p120(ctn)-binding partner Kaiso is a bi-modal DNA-binding protein that recognizes both a sequence-specific consensus and methylated CpG dinucleotides. **Nucleic Acids Res.** **2002** Jul 1;30(13):2911-9.

De Craene B, van Roy F, Berx G. ; Unraveling signalling cascades for the Snail family of transcription factors. **Cell Signal.** **2005** May;17(5):535-47.

Desmouliere A, Guyot C, Gabbiani G.; The stroma reaction myofibroblast: a key player in the control of tumor cell behavior. **Int J Dev Biol.** **2004**;48(5-6):509-17.

Dhomen N, Marais R.; New insight into BRAF mutations in cancer. **Curr Opin Genet Dev.** **2007** Feb;17(1):31-9.

Drees F, Pokutta S, Yamada S, Nelson WJ, Weis WI.; Alpha-catenin is a molecular switch that binds E-cadherin-beta-catenin and regulates actin-filament assembly. **Cell.** **2005** Dec 2;123(5):903-15.

Eger A, Stockinger A, Schaffhauser B, Beug H, Foisner R.; Epithelial mesenchymal transition by c-Fos estrogen receptor activation involves nuclear translocation of beta-catenin and upregulation of beta-catenin/lymphoid enhancer binding factor-1 transcriptional activity. **J Cell Biol.** **2000** Jan 10;148(1):173-88.

Eger A, Aigner K, Sonderegger S, Dampier B, Oehler S, Schreiber M, Berx G, Cano A, Beug H, Foisner R.; δ EF1 is a transcriptional repressor of E-cadherin and regulates epithelial plasticity in breast cancer cells. **Oncogene**. 2005 Mar 31;24(14):2375-85.

Elloul S, Elstrand MB, Nesland JM, Trope CG, Kvalheim G, Goldberg I, Reich R, Davidson B.; Snail, Slug, and Smad-interacting protein 1 as novel parameters of disease aggressiveness in metastatic ovarian and breast carcinoma. **Cancer**. 2005 Apr 15;103(8):1631-43.

Emuss V, Garnett M, Mason C, Marais R.; Mutations of C-RAF are rare in human cancer because C-RAF has a low basal kinase activity compared with B-RAF. **Cancer Res**. 2005 Nov 1;65(21):9719-26.

Fearon E.R., Dang C.V.; Cancer genetics: tumor suppressor meets oncogene. **Curr Biol**. 1999 Jan 28;9(2):R62-5. Review.

Friday BB and Adjei AA. ; K-ras as a target for cancer therapy. **Biochim Biophys Acta**. 2005 Sep 1

Fujita Y, Krause G, Scheffner M, Zechner D, Leddy HE, Behrens J, Sommer T, Birchmeier W.; Hakai, a c-Cbl-like protein, ubiquitinates and induces endocytosis of the E-cadherin complex. **Nat Cell Biol**. 2002 Mar;4(3):222-31.

Fukata M., Kuroda S., Nakagawa M., Kawajiri A., Itoh N., Shoji I., Matsuura Y., Yonehara S., Fujisawa H., Kikuchi A., Kaibuchi K.; Cdc42 and Rac1 regulate the interaction of IQGAP1 with beta-catenin. **J Biol Chem**, 1999. 274(37): p. 26044-50.

Fukata M., Kaibuchi K.; Rho-family GTPases in cadherin-mediated cell-cell adhesion.

Nat Rev Mol Cell Biol 2001 Dec;2(12):887-97

Gallier AJ, Schiemann WP.; Beta3 integrin and Src facilitate transforming growth factor-beta mediated induction of epithelial-mesenchymal transition in mammary epithelial cells. **Breast Cancer Res.** 2006;8(4):R42.

Gates J, Peifer M.; Can 1000 reviews be wrong? Actin, alpha-Catenin, and adherens junctions. **Cell.** 2005 Dec 2;123(5):769-72.

Giannini A.L., Vivanco M.M. and Kypta R.M.; α -catenin inhibits β -catenin signalling by preventing formation of a β -catenin**T-cell factor**DNA complex. **J Biol Chem** 2000 Vol 275, No 29:21883-21888

Giroldi L.A., Bringuier P.P., de Weijert M., Jansen C., van Bokhoven A., Schalken J.A.; Role of E boxes in the repression of E-cadherin expression. **Biochem Biophys Res Commun.** 1997 Dec 18;241(2):453-8.

Gottardi C.J., Wong E., Gumbiner B.M.; E-cadherin suppresses cellular transformation by inhibiting beta-catenin signaling in an adhesion-independent manner. **J Cell Biol.** 2001 May 28;153(5):1049-60.

Grady WM, Myeroff LL, Swinler SE, Rajput A, Thiagalingam S, Lutterbaugh JD, Neumann A, Brattain MG, Chang J, Kim SJ, Kinzler KW, Vogelstein B, Willson JK,

Markowitz S. ; Mutational inactivation of transforming growth factor beta receptor type II in microsatellite stable colon cancers. **Cancer Res.** 1999 Jan 15;59(2):320-4.

Grotegut S, von Schweinitz D, Christofori G, Lehembre F.; Hepatocyte growth factor induces cell scattering through MAPK/Egr-1-mediated upregulation of Snail. **EMBO J.** 2006 Aug 9;25(15):3534-45.

van Grunsven LA, Papin C, Avalosse B, Opdecamp K, Huylebroeck D, Smith JC, Bellefroid EJ.; XSIP1, a Xenopus zinc finger/homeodomain encoding gene highly expressed during early neural development. **Mech Dev.** 2000 Jun;94(1-2):189-93.

van Grunsven LA, Michiels C, Van de Putte T, Nelles L, Wuytens G, Verschueren K, Huylebroeck D. ; Interaction between Smad-interacting protein-1 and the corepressor C-terminal binding protein is dispensable for transcriptional repression of E-cadherin. **J Biol Chem.** 2003 Jul 11;278(28):26135-45.

Hajra K.M., Chen D.Y., Fearon E.R.;The SLUG zinc-finger protein represses E-cadherin in breast cancer.; **Cancer Res** 2002 Mar 15;62(6):1613-8

Hajra K.M., Fearon E.R.; Cadherin and catenin alterations in human cancer. **Genes Chromosomes Cancer** 2002 Jul;34(3):255-68

Hakimelahi S., Parker H.R., Gilchrist A.J., Barry M., Li Z., Bleackley R.C., Pasdar M.; Plakoglobin regulates the expression of the anti-apoptotic protein BCL-2. **J Biol Chem.** 2000 14;275(15):10905-11.

Hanahan D. and Weinberg R.A.; The Hallmarks of Cancer; **Cell 2000** Vol.100:57-70

Hay ED.; The mesenchymal cell, its role in the embryo, and the remarkable signaling mechanisms that create it. **Dev Dyn. 2005** Jul;233(3):706-20. Review.

Hayflick L. ; The illusion of cell immortality. **Br J Cancer. 2000** Oct;83(7):841-6. Review.

He T.C., Sparks A.B., Rago C., Hermeking H., Zawel L., da Costa L.T., Morin P.J., Vogelstein B., Kinzler K.W.; Identification of c-MYC as a target of the APC pathway. **Science 1998** Sep 4;281(5382):1509-12

Hennig G., Lowrick O., Birchmeier W., Behrens J.; Mechanisms identified in the transcriptional control of epithelial gene expression. ; **J Biol Chem 1996** Jan 5;271(1):595-602

Hennig G., Behrens J., Truss M., Frisch S., Reichmann E., Birchmeier W.; Progression of carcinoma cells is associated with alterations in chromatin structure and factor binding at the E-cadherin promoter in vivo.; **Oncogene. 1995** Aug 3;11(3):475-84.

Herrera RE, Makela TP, Weinberg RA.; TGF beta-induced growth inhibition in primary fibroblasts requires the retinoblastoma protein. **Mol Biol Cell. 1996** Sep;7(9):1335-42.

Horn HF, Vousden KH. Coping with stress: multiple ways to activate p53.

Oncogene. 2007 Feb 26;26(9):1306-16

Hunts JH, Shimizu N, Yamamoto T, Toyoshima K, Merlino GT, Xu YH, Pastan I.; Translocation chromosome 7 of A431 cells contains amplification and rearrangement of EGF receptor gene responsible for production of variant mRNA. **Somat Cell Mol Genet.** 1985 Sep;11(5):477-84.

Ikenouchi J, Matsuda M, Furuse M, Tsukita S.; Regulation of tight junctions during the epithelium-mesenchyme transition: direct repression of the gene expression of claudins/occludin by Snail. **J Cell Sci.** 2003 May 15;116(Pt 10):1959-67.

Irby R.B., Yeatman T.J.; Increased Src activity disrupts cadherin/catenin-mediated homotypic adhesion in human colon cancer and transformed rodent cells. **Cancer Res.** 2002 May 1;62(9):2669-74.

Ji. X., Woodard A.S., Rimm D.L. and Fearon E.R.; Transcriptional Defects Underlie Loss of E-cadherin in Breast cancer; **Cell Growth & Differentiation** 1997 Vol.8:773-778

Katsanis N, Fisher EM.; A novel C-terminal binding protein (CTBP2) is closely related to CTBP1, an adenovirus E1A-binding protein, and maps to human chromosome 21q21.3. **Genomics.** 1998 Jan 15;47(2):294-9.

Kanungo J., Pratt S.J., Marie H and Longmore G.D.; Ajuba, a Cytosolic LIM Protein, Shuttles into the Nucleus and Affects Embryonal Cell Proliferation and Fate Decisions; **Mol. Biol. Cell** 2000 Vol. 11, Issue 10, 3299-3313

Knudsen KE, Diehl JA, Haiman CA, Knudsen ES.; Cyclin D1: polymorphism, aberrant splicing and cancer risk. **Oncogene.** 2006 Mar 13;25(11):1620-8.

Koyama-Honda I, Ritchie K, Fujiwara T, Iino R, Murakoshi H, Kasai RS, Kusumi A.; Fluorescence imaging for monitoring the colocalization of two single molecules in living cells. **Biophys J.** 2005 Mar;88(3):2126-36.

Kumar V, Carlson JE, Ohgi KA, Edwards TA, Rose DW, Escalante CR, Rosenfeld MG, Aggarwal AK. ; Transcription corepressor CtBP is an NAD(+)-regulated dehydrogenase. **Mol Cell.** 2002 Oct;10(4):857-69.

Kuroda S, Fukata M, Nakagawa M, Fujii K, Nakamura T, Ookubo T, Izawa I, Nagase T, Nomura N, Tani H, Shoji I, Matsuura Y, Yonehara S, Kaibuchi K.; Role of IQGAP1, a target of the small GTPases Cdc42 and Rac1, in regulation of E-cadherin-mediated cell-cell adhesion. **Science.** 1998 Aug 7;281(5378):832-5.

Lanza F, Bi S, Castoldi G, Goldman JM.; Abnormal expression of N-CAM (CD56) adhesion molecule on myeloid and progenitor cells from chronic myeloid leukemia. **Leukemia.** 1993 Oct;7(10):1570-5.

Lee JM, Dedhar S, Kalluri R, Thompson EW.; The epithelial-mesenchymal transition: new insights in signaling, development, and disease. **J Cell Biol.** 2006 Mar 27;172(7):973-81.

Lewis J.E., Wahl J.K., Sass K.M., Jensen P.J., Johnson K.R., Wheelock M.J.; Cross-talk between adherens junctions and desmosomes depends on plakoglobin.; **J Cell Biol** 1997 24;136(4):919-34

Lin S, Wang W, Wilson GM, Yang X, Brewer G, Holbrook NJ, Gorospe M.; Down-regulation of cyclin D1 expression by prostaglandin A(2) is mediated by enhanced cyclin D1 mRNA turnover. **Mol Cell Biol.** 2000 Nov;20(21):7903-13.

Long J, Zuo D, Park M.; Pc2-mediated sumoylation of Smad-interacting protein 1 attenuates transcriptional repression of E-cadherin. **J Biol Chem.** 2005 Oct 21;280(42):35477-89.

Marie H., Pratt S.J., Betson M., Epple H., Kittler J.T., Meek L., Moss S.J., Troyanovsky S., Attwell D., Longmore D.A. and Braga V.M.M.; The LIM Protein Ajuba Is Recruited to Cadherin-dependent Cell Junctions through an Association with α -Catenin; **J Biol Chem** 2003 Jan 10;278(2):1220-8

Maeda M, Johnson KR, Wheelock MJ.; Cadherin switching: essential for behavioral but not morphological changes during an epithelium-to-mesenchyme transition. **J Cell Sci.** 2005 Mar 1;118(Pt 5):873-87.

Maruhashi M, Van De Putte T, Huylebroeck D, Kondoh H, Higashi Y. Involvement of SIP1 in positioning of somite boundaries in the mouse embryo. **Dev Dyn.** 2005 Oct;234(2):332-8.

Mejlvang J, Kriajevska M, Berditchevski F, Bronstein I, Lukanidin EM, Pringle JH, Mellon JK, Tulchinsky EM.; Characterization of E-cadherin-dependent and -independent events in a new model of c-Fos-mediated epithelial-mesenchymal transition. **Exp Cell Res.** 2007 Jan 15;313(2):380-93.

Miyakawa Y, Matsushime H.; Rapid downregulation of cyclin D1 mRNA and protein levels by ultraviolet irradiation in murine macrophage cells. **Biochem Biophys Res Commun.** 2001 Jun 1;284(1):71-6

Nagafuchi A, Ishihara S, Tsukita S.; The roles of catenins in the cadherin-mediated cell adhesion: functional analysis of E-cadherin-alpha catenin fusion molecules. **J Cell Biol.** 1994 Oct;127(1):235-45.

Nieto MA.; The early steps of neural crest development. **Mech Dev.** 2001 Jul;105(1-2):27-35.

Oka H., Shiozaki H, Kobayashi K., Inoue M., Tahara H., Kobayashi T., Takatsuka Y., Matsuyoshi N., Hirano S., Takeichi M and Mori T.; Expression of E-cadherin Cell Adhesion Molecules In Human Breast Cancer Tissues and Its Relationship to Metastasis; **Cancer Research** 1993 53:1696-1701

Ozturk N, Erdal E, Mumcuoglu M, Akcali KC, Yalcin O, Senturk S, Arslan-Ergul A, Gur B, Yulug I, Cetin-Atalay R, Yakicier C, Yagci T, Tez M, Ozturk M.; Reprogramming of replicative senescence in hepatocellular carcinoma-derived cells. **Proc Natl Acad Sci U S A.** 2006 Feb 14;103(7):2178-83.

Oyama T, Kanai Y, Ochiai A, Akimoto S, Oda T, Yanagihara K, Nagafuchi A, Tsukita S, Shibamoto S, Ito F, et al.; A truncated beta-catenin disrupts the interaction between E-cadherin and alpha-catenin: a cause of loss of intercellular adhesiveness in human cancer cell lines. **Cancer Res.** 1994 Dec 1;54(23):6282-7.

Pacquelet A, Rorth P.; Regulatory mechanisms required for DE-cadherin function in cell migration and other types of adhesion. **J Cell Biol.** 2005 Aug 29;170(5):803-12.

Park DJ, Nakamura H, Chumakov AM, Said JW, Miller CW, Chen DL, Koeffler HP.; Transactivational and DNA binding abilities of endogenous p53 in p53 mutant cell lines. **Oncogene.** 1994 Jul;9(7):1899-906.

Patrone G, Puppo F, Cusano R, Scaranari M, Ceccherini I, Puliti A, Ravazzolo R.; Nuclear run-on assay using biotin labeling, magnetic bead capture and analysis by fluorescence-based RT-PCR. **Biotechniques.** 2000 Nov;29(5):1012-4, 1016-7.

Peinado H, Portillo F, Cano A.; Transcriptional regulation of cadherins during development and carcinogenesis. **Int J Dev Biol.** 2004a;48(5-6):365-75.

Peinado H, Marin F, Cubillo E, Stark HJ, Fusenig N, Nieto MA, Cano A. Snail and E47 repressors of E-cadherin induce distinct invasive and angiogenic properties in vivo. **J Cell Sci.** 2004b Jun 1;117(Pt 13):2827-39.

Perl A.K., Dahl U., Wilgenbus P., Cremer H., Semb H., Christofori G.; Reduced expression of neural cell adhesion molecule induces metastatic dissemination of pancreatic beta tumor cells. **Nat Med.** 1999 Mar;5(3):286-91.

Perez-Moreno M.A., Locascio A., Rodrigo I., Dhondt G., Portillo F., Nieto M.A., Cano A.; A new role for E12/E47 in the repression of E-cadherin expression and epithelial-mesenchymal transitions.; **J Biol Chem** 2001 Jul 20;276(29):27424-31

Pertz O., Bozic D., Kock A.W., Fauser C., Brancaccio A. and Engel J.; A new crystal structure, Ca²⁺ dependence and mutational analysis reveal molecular details of E-cadherin homoassociation; **The EMBO Journal** 1999 Vol.18 No.7:1738-1747

Pokutta S., Drees F., Takai Y., Nelson W.J., Weis W.I.; Biochemical and structural definition of the 1-afadin- and actin-binding sites of alpha-catenin.; **J Biol Chem.** 2002 24;277(21):18868-74.

Van de Putte T, Maruhashi M, Francis A, Nelles L, Kondoh H, Huylebroeck D, Higashi Y. ;Mice lacking ZFH1B, the gene that codes for Smad-interacting protein-1, reveal a role for multiple neural crest cell defects in the etiology of Hirschsprung disease-mental retardation syndrome. **Am J Hum Genet.** 2003 Feb;72(2):465-70.

Vestweber D, Kemler R.; Identification of a putative cell adhesion domain of uvomorulin. **EMBO J.** 1985 Dec 16;4(13A):3393-8.

Postigo AA, Dean DC; Differential expression and function of members of the zfh-1 family of zinc finger/homeodomain repressors. **Proc Natl Acad Sci.** 2000 Jun 6;97(12):6391-6.

Postigo AA, Depp JL, Taylor JJ, Kroll KL. ; Regulation of Smad signaling through a differential recruitment of coactivators and corepressors by ZEB proteins. **EMBO J.** 2003 May 15;22(10):2453-62.

Postigo AA. ; Opposing functions of ZEB proteins in the regulation of the TGFbeta/BMP signaling pathway. **EMBO J.** 2003 May 15;22(10):2443-52.

Provost E. and Rimm D.L.; Controversies at the cytoplasmic face of the cadherin-based adhesion complex.; **Curr Opin Cell Biol.** 1999 11(5):567-72.

Qian X, Karpova T, Sheppard AM, McNally J, Lowy DR.; E-cadherin-mediated adhesion inhibits ligand-dependent activation of diverse receptor tyrosine kinases. **EMBO J.** 2004 Apr 21;23(8):1739-48.

Radisky DC, Kenny PA, Bissell MJ.; Fibrosis and cancer: Do myofibroblasts come also from epithelial cells via EMT? **J Cell Biochem.** 2007 Jan 8;

Ramsay AG, Marshall JF, Hart IR.; Integrin trafficking and its role in cancer metastasis. **Cancer Metastasis Rev.** 2007 Sep 6

Rao DS, Gui D, Koski ME, Popoviciu LM, Wang H, Reiter RE, Said JW.; An inverse relation between COX-2 and E-cadherin expression correlates with aggressive histologic features in prostate cancer. **Appl Immunohistochem Mol Morphol.** 2006 Dec;14(4):375-83.

Remacle JE, Kraft H, Lerchner W, Wuytens G, Collart C, Verschueren K, Smith JC, Huylebroeck D. ; New mode of DNA binding of multi-zinc finger transcription factors: δ EF1 family members bind with two hands to two target sites. **EMBO J.** 1999 Sep 15;18(18):5073-84.

Ren B, Yee KO, Lawler J, Khosravi-Far R.; Regulation of tumor angiogenesis by thrombospondin-1. **Biochim Biophys Acta.** 2006 Apr;1765(2):178-88.

Renaud-Young M. and Gallin W.J.; In the first extracellular domain of E-cadherin, heterophilic interactions, but not the conserved His-Ala-Val motif, are required for adhesion.; **J Biol Chem.** 2002 Oct 18;277(42):39609-16.

Rimm D.L., Koslov E.R., Kebraie P., Cianci C.D., Morrow J.S.; Alpha 1(E)-catenin is an actin-binding and -bundling protein mediating the attachment of F-actin to the membrane adhesion complex.; **Proc Natl Acad Sci** 1995 12;92(19):8813-7

Rosivatz E, Becker I, Specht K, Fricke E, Lubert B, Busch R, Hofler H, Becker KF.; Differential expression of the epithelial-mesenchymal transition regulators snail, SIP1, and twist in gastric cancer. **Am J Pathol.** 2002 Nov;161(5):1881-91.

Savagner P, Yamada KM, Thiery JP.; The zinc-finger protein slug causes desmosome dissociation, an initial and necessary step for growth factor-induced epithelial-mesenchymal transition. **J Cell Biol.** 1997 Jun 16;137(6):1403-19.

Savagner P.; Leaving the neighborhood: molecular mechanisms involved during epithelial-mesenchymal transition. **Bioessays.** 2001 Oct;23(10):912-23.

Sheng G, dos Reis M, Stern CD.; Churchill, a zinc finger transcriptional activator, regulates the transition between gastrulation and neurulation. **Cell.** 2003 Nov 26;115(5):603-13.

Shapiro L., Fannon A.M., Kwong P.D., Thompson A., Lehmann M.S., Grubel G., Legrand J-F., Als-Nielsen J., Colman D.R. and Hendrickson W.A.; Structural basis of cell-cell adhesion by cadherins; **Nature** 1995 Vol.374:327-374

Shay JW, Bacchetti S.; A survey of telomerase activity in human cancer. **Eur J Cancer.** 1997 Apr;33(5):787-91.

Shi Y, Sawada J, Sui G, Affar el B, Whetstine JR, Lan F, Ogawa H, Luke MP, Nakatani Y, Shi Y.; Coordinated histone modifications mediated by a CtBP co-repressor complex. **Nature.** 2003 Apr 17;422(6933):735-8.

Shtutman M., Zhurinsky J., Simcha I., Albanese C., D'Amico M., Pestell R., Ben-Ze'ev A.; The cyclin D1 gene is a target of the beta-catenin/LEF-1 pathway. **Proc Natl Acad Sci USA.** 1999 May 11;96(10):5522-7.

Shtutman M, Zhurinsky J., Oren M., Levina E., Ben-Ze'ev A.; PML is a target gene of beta-catenin and plakoglobin, and coactivates beta-catenin-mediated transcription. **Cancer Res.** 2002 Oct 15;62(20):5947-54.

Simcha I., Shtutman M., Salomon D., Zhurinsky J., Sadot E., Geiger B., Ben-Ze'ev A.; Differential nuclear translocation and transactivation potential of beta-catenin and plakoglobin. **J Cell Biol.** 1998 15;141(6):1433-48.

Schmidt CR, Gi YJ, Patel TA, Coffey RJ, Beauchamp RD, Pearson AS.; E-cadherin is regulated by the transcriptional repressor SLUG during Ras-mediated transformation of intestinal epithelial cells. **Surgery.** 2005 Aug;138(2):306-12.

Sporn MB.; The war on cancer. *Ann N Y Acad Sci.* 1997 Dec 29;833:137-46.

Steinberg M.S. and McNutt P.M.; Cadherins and their connections: adhesion junctions have broader functions; *Current Opinion in Cell Biology* 1999 11:554-560

Stoker M, Perryman M.; An epithelial scatter factor released by embryo fibroblasts. *J Cell Sci.* 1985 Aug;77:209-23.

Sugimachi K, Tanaka S, Kameyama T, Taguchi K, Aishima S, Shimada M, Sugimachi K, Tsuneyoshi M.; Transcriptional repressor snail and progression of human hepatocellular carcinoma. *Clin Cancer Res.* 2003 Jul;9(7):2657-64.

Sundqvist A, Bajak E, Kurup SD, Sollerbrant K, Svensson C.; Functional knockout of the corepressor CtBP by the second exon of adenovirus E1a relieves repression of transcription. *Exp Cell Res.* 2001 Aug 15;268(2):284-93.

Takeda H., Nagafuchi A., Yonemura S., Tsukita S., Behrens J., Birchmeier W., Tsukita S.; V-src kinase shifts the cadherin-based cell adhesion from the strong to the weak state and beta catenin is not required for the shift. ; *J Cell Biol* 1995 Dec;131(6 Pt 2):1839-47

Thiery J.P. Epithelial-Mesenchymal transitions in tumor progression.; *Nat Rev Cancer.* 2002 Jun;2(6):442-54.

Thiery JP.; Epithelial-mesenchymal transitions in development and pathologies. **Curr Opin Cell Biol.** 2003 Dec;15(6):740-6

Thio SS, Bonventre JV, Hsu SI. ; The CtBP2 co-repressor is regulated by NADH-dependent dimerization and possesses a novel N-terminal repression domain. **Nucleic Acids Res.** 2004 Mar 22;32(5):1836-47.

Todaro L, Christiansen S, Varela M, Campodonico P, Pallotta MG, Lastiri J, Sacerdote de Lustig E, Bal de Kier Joffe E, Puricelli L.; Alteration of serum and tumoral neural cell adhesion molecule (NCAM) isoforms in patients with brain tumors. **J Neurooncol.** 2007 Jun;83(2):135-44.

Turner FE, Broad S, Khanim FL, Jeanes A, Talma S, Hughes S, Tselepis C, Hotchin NA.; Slug regulates integrin expression and cell proliferation in human epidermal keratinocytes. **J Biol Chem.** 2006 Jul 28;281(30):21321-31.

Tylzanowski P, Verschueren K, Huylebroeck D, Luyten FP. ; Smad-interacting protein 1 is a repressor of liver/bone/kidney alkaline phosphatase transcription in bone morphogenetic protein-induced osteogenic differentiation of C2C12 cells. **J Biol Chem.** 2001 Oct 26;276(43):40001-7.

U.S. National Institutes of Health, 2007; according to the web site:

<http://www.cancer.gov/cancertopics/alphalist>

Vandewalle C, Comijn J, De Craene B, Vermassen P, Bruyneel E, Andersen H, Tulchinsky E, Van Roy F, Berx G.; SIP1/ZEB2 induces EMT by repressing genes of different epithelial cell-cell junctions. **Nucleic Acids Res.** 2005 Nov 24;33(20):6566-78.

Vasioukhin V., Bauer C., Degenstein L., Wise B., Fuchs E.; Hyperproliferation and defects in epithelial polarity upon conditional ablation of alpha-catenin in skin. **Cell.** 2001 Feb 23 ;104(4):605-17.

Vega S, Morales AV, Ocana OH, Valdes F, Fabregat I, Nieto MA. ; Snail blocks the cell cycle and confers resistance to cell death. **Genes Dev.** 2004 May 15;18(10):1131-43.

Verschuere K, Remacle JE, Collart C, Kraft H, Baker BS, Tylzanowski P, Nelles L, Wuytens G, Su MT, Bodmer R, Smith JC, Huylebroeck D. ; SIP1, a novel zinc finger/homeodomain repressor, interacts with Smad proteins and binds to 5'-CACCT sequences in candidate target genes. **J Biol Chem.** 1999 Jul 16;274(29):20489-98.

Vleminckx K., Vakaet L., Jr., Mareel M., Fiers W. and Van Roy F.; Genetic Manipulation of E-cadherin Expression by Epithelial Tumor Cells Reveals an Invasion Suppressor role; **Cell** 1991 Vol.66:107-119

Walker JL and Assoian RK,; Integrin-dependent signal transduction regulating cyclin D1 expression and G1 phase cell cycle progression. **Cancer Metastasis Rev** 2005 Vol 24: 383-393.

Walker JL, Fournier AK, Assoian RK.; Regulation of growth factor signalling and cell cycle progression by cell adhesion and adhesion-dependent changes in cellular tension.

Cytokine Growth Factor Rev 2005 Vol 16: 395-405.

Watabe-Uchida M., Uchida N., Imamura Y., Nagafuchi A., Fujimoto K., Uemura T.,

Vermeulen S., Van Roy F., Adamson E.D. and Takeichi M.; α -catenin-vinculin

Interaction Function to Organize the Apical Junction Complex in Epithelial Cells; **Journal of Cell Biology 1998** Vol.142 No.3:847-857

Weis WI, Nelson WJ.; Re-solving the cadherin-catenin-actin conundrum. **J Biol Chem.**

2006 Nov 24;281(47):35593-7.

Weinel R.J., Neumann K., Kisker O. and Rosendahl A.; Expression and potential role of

E-cadherin in Pancreatic Carcinoma; **International Journal of Pancreatology 1996**

Vol.19 No.1:25-30

Wijnhoven B.P.L., Dinjens W.N.M. and Pignatelli M.; E-cadherin-catenin cell-cell

adhesion complex and human cancer; **British Journal of Surgery 2000** 87:992-1005

Yamada S, Pokutta S, Drees F, Weis WI, Nelson WJ.; Deconstructing the cadherin-

catenin-actin complex. **Cell. 2005** Dec 2;123(5):889-901.

Yagi T. and Takeichi M.; Cadherin superfamily genes: function, genomic organization,

and neurologic diversity. **Genes & Development 2000**, 14:1169-1180

Yoshimoto A, Saigou Y, Higashi Y, Kondoh H.; Regulation of ocular lens development by Smad-interacting protein 1 involving Foxe3 activation. **Development**. 2005 Oct;132(20):4437-48.

Zavadil J, Bottinger EP.; TGF-beta and epithelial-to-mesenchymal transitions. **Oncogene**. 2005 Aug 29;24(37):5764-74.

Zhang Q, Piston DW, Goodman RH.; Regulation of corepressor function by nuclear NADH. **Science**. 2002 Mar 8;295(5561):1895-7.

Zohn I, Li Y, Skolnik E, Anderson K, Han J and Niswander L.; p38 and a p38-Interacting Protein Are Critical for Downregulation of E-Cadherin during Mouse Gastrulation. **Cell** 2006 Jun (125) 957-969

Appendix A

**Table representing genes regulated by SIP1 in A431.
These results were obtained by cDNA microarray
analysis carried out at the MicroArray Facility of the
Flanders Interuniversity, in collaboration with Geert
Berx University of Ghent, Belgium**

Genes down-regulated by SIP1 expression in A431

Gene	Protein	Fold down-regulation
<i>ABCE1</i>	ATP-binding cassette, sub-family E (OABP), member 1	1.9
<i>ABLIM1</i>	actin binding LIM protein 1	3.1
<i>ADAMTS5</i>	ADAM metalloproteinase with thrombospondin type 1 motif, 5 (aggrecanase-2)	3.5
<i>ADRB2</i>	adrenergic, beta-2-, receptor, surface	2.1
<i>AIM1L</i>	absent in melanoma 1-like	3.4
<i>ALDH1A3</i>	aldehyde dehydrogenase 1 family, member A3	2.8
<i>ANKRD5</i>	ankyrin repeat domain 5	2.1
<i>AP1M2</i>	adaptor-related protein complex 1, mu 2 subunit	4.3
<i>AQP3</i>	aquaporin 3	5.0
<i>ASNS</i>	asparagine synthetase	3.9
<i>ASS</i>	argininosuccinate synthetase	3.1
<i>ASS</i>	argininosuccinate synthetase	2.8
<i>B4GALT4</i>	UDP-Gal:betaGlcNAc beta 1,4- galactosyltransferase, polypeptide 4	2.0
<i>BENE</i>	BENE protein	2.5
<i>BM-009</i>	hypothetical protein BM-009	2.0
<i>BPAG1</i>	bullous pemphigoid antigen 1, 230/240kDa	2.1
<i>BRUNOL5</i>	bruno-like 5, RNA binding protein (Drosophila)	2.8
<i>C14orf136</i>	chromosome 14 open reading frame 136	2.4
<i>C20orf42</i>	chromosome 20 open reading frame 42	2.0
<i>C4.4A</i>	GPI-anchored metastasis-associated protein homolog	4.2
<i>C4A</i>	complement component 4A	2.7
<i>C6orf4</i>	chromosome 6 open reading frame 4	2.4
<i>CA2</i>	carbonic anhydrase II	4.1
<i>CAPG</i>	capping protein (actin filament), gelsolin-like	2.2
<i>CAV2</i>	caveolin 2	2.0
<i>CCND1</i>	cyclin D1 (PRAD1: parathyroid adenomatosis 1)	6.7
<i>CD24</i>	CD24 antigen (small cell lung carcinoma cluster 4 antigen)	3.5
<i>CDH1</i>	cadherin 1, type 1, E-cadherin (epithelial)	3.7
<i>CHC1</i>	chromosome condensation 1	2.3
<i>CHEK1</i>	CHK1 checkpoint homolog (S. pombe)	2.1

Genes down-regulated by SIP1 expression in A431

Gene	Protein	Fold down-regulation
<i>CHRD</i>	chordin	2.5
<i>CHST10</i>	carbohydrate sulfotransferase 10	6.6
<i>CKMT1</i>	creatine kinase, mitochondrial 1 (ubiquitous)	5.5
<i>CL25022</i>	hypothetical protein CL25022	2.3
<i>CLDN4</i>	claudin 4	6.4
<i>CNN2</i>	calponin 2	2.3
<i>COL17A1</i>	collagen, type XVII, alpha 1	9.0
<i>CRABP2</i>	cellular retinoic acid binding protein 2	3.9
<i>CTH</i>	cystathionase (cystathionine gamma-lyase)	3.3
<i>CTPS</i>	CTP synthase	1.9
<i>CTSH</i>	cathepsin H	3.5
<i>CYB5R1</i>	cytochrome b5 reductase 1 (B5R.1)	1.9
<i>CYCS</i>	cytochrome c, somatic	2.0
<i>DDX21</i>	DEAD (Asp-Glu-Ala-Asp) box polypeptide 21	2.1
<i>DEF6</i>	differentially expressed in FDCP 6 homolog (mouse)	2.5
<i>DEFCAP</i>	death effector filament-forming Ced-4-like apoptosis protein	2.1
<i>DHCR7</i>	7-dehydrocholesterol reductase	3.2
<i>DKFZP566F</i>	DKFZP566F2124 protein	2.4
<i>DKFZP566H</i>	DKFZP566H073 protein	1.9
<i>DPP3</i>	dipeptidylpeptidase 3	2.0
<i>DSG3</i>	desmoglein 3 (pemphigus vulgaris antigen)	7.3
<i>DSP</i>	desmoplakin	7.2
<i>E48</i>	lymphocyte antigen 6 complex, locus D	4.1
<i>EBP</i>	emopamil binding protein (sterol isomerase)	2.2
<i>ENTPD3</i>	ectonucleoside triphosphate diphosphohydrolase 3	2.2
<i>EPHA2</i>	EphA2	2.3
<i>EPPK1</i>	epiplakin 1	2.5
<i>EVA1</i>	epithelial V-like antigen 1	2.9
<i>FAM3C</i>	family with sequence similarity 3, member C	2.0
<i>FAM3C</i>	family with sequence similarity 3, member C	1.9

Genes down-regulated by SIP1 expression in A431

Gene	Protein	Fold down-regulation
<i>FGFR2</i>	fibroblast growth factor receptor 2	2.8
<i>FKBP4</i>	FK506 binding protein 4, 59kDa	2.1
<i>FLJ10261</i>	hypothetical protein FLJ10261	4.2
<i>FLJ10312</i>	hypothetical protein FLJ10312	1.9
<i>FLJ11036</i>	hypothetical protein FLJ11036	2.0
<i>FLJ20073</i>	hypothetical protein FLJ20073	1.8
<i>FLJ20315</i>	hypothetical protein FLJ20315	2.2
<i>FLJ20421</i>	hypothetical protein FLJ20421	2.5
<i>FLJ20421</i>	hypothetical protein FLJ20421	2.1
<i>FLJ20442</i>	hypothetical protein FLJ20442	1.8
<i>FLJ20986</i>	hypothetical protein FLJ20986	2.4
<i>FLJ23042</i>	hypothetical protein FLJ23042	2.2
<i>FLJ23309</i>	hypothetical protein FLJ23309	2.9
<i>FTHFSDC1</i>	formyltetrahydrofolate synthetase domain containing 1	2.5
<i>FXVD3</i>	FXVD domain containing ion transport regulator 3	9.5
<i>FXVD3</i>	FXVD domain containing ion transport regulator 3	8.4
<i>FXVD3</i>	FXVD domain containing ion transport regulator 3	3.1
<i>FYB</i>	FYN binding protein (FYB-120/130)	3.2
<i>GADD45A</i>	growth arrest and DNA-damage-inducible, alpha	2.7
<i>GALNT3</i>	UDP-N-acetyl-alpha-D-galactosamine:polypeptide N-acetylgalactosaminyltransferase 3	3.5
<i>GARS</i>	glycyl-tRNA synthetase	2.4
<i>GART</i>	phosphoribosylglycinamide formyltransferase, phosphoribosylglycinamide synthetase	2.0
<i>GDA</i>	guanine deaminase	2.0
<i>GJB5</i>	gap junction protein, beta 5 (connexin 31.1)	2.7
<i>GOT1</i>	glutamic-oxaloacetic transaminase 1, soluble (aspartate aminotransferase 1)	2.2
<i>GOT2</i>	glutamic-oxaloacetic transaminase 2, mitochondrial	1.9
<i>GPD2</i>	glycerol-3-phosphate dehydrogenase 2 (mitochondrial)	2.3
<i>GPP34R</i>	GPP34-related protein	2.2
<i>GPR26</i>	G protein-coupled receptor 26	2.7
<i>GPR87</i>	G protein-coupled receptor 87	4.7

Genes down-regulated by SIP1 expression in A431

Gene	Protein	Fold down-regulation
<i>GSTM4</i>	glutathione S-transferase M4	2.0
<i>HBP17</i>	heparin-binding growth factor binding protein	7.7
<i>HMGA1</i>	high mobility group AT-hook 1	2.3
<i>IARS</i>	isoleucine-tRNA synthetase	2.1
<i>ICA1</i>	islet cell autoantigen 1, 69kDa	1.9
<i>IER5</i>	immediate early response 5	2.1
<i>IFI30</i>	interferon, gamma-inducible protein 30	2.1
<i>IGSF3</i>	immunoglobulin superfamily, member 3	2.0
<i>IL8RB</i>	interleukin 8 receptor, beta	2.2
<i>ITGA6</i>	integrin, alpha 6	1.8
<i>ITGB6</i>	integrin, beta 6	4.3
<i>ITPKC</i>	inositol 1,4,5-trisphosphate 3-kinase C	1.9
<i>JUP</i>	junction plakoglobin	2.5
<i>K6HF</i>	cytokeratin type II	4.2
<i>KIAA0153</i>	KIAA0153 protein	2.2
<i>KIAA0379</i>	KIAA0379 protein	1.9
<i>KIAA0937</i>	KIAA0937 protein	2.7
<i>KIAA1203</i>	KIAA1203 protein	2.4
<i>KIAA1522</i>	KIAA1522 protein	2.6
<i>KIAA1554</i>	KIAA1554 protein	2.2
<i>KIAA1609</i>	KIAA1609 protein	2.4
<i>KIFC3</i>	kinesin family member C3	1.9
<i>KLF4</i>	Kruppel-like factor 4 (gut)	2.2
<i>KLF5</i>	Kruppel-like factor 5 (intestinal)	2.2
<i>KRT13</i>	keratin 13	11.8
<i>KRT14</i>	keratin 14 (epidermolysis bullosa simplex, Dowling-Meara, Koebner)	7.8
<i>KRT15</i>	keratin 15	13.5
<i>KRT16</i>	keratin 16 (focal non-epidermolytic palmoplantar keratoderma)	6.4
<i>KRT17</i>	keratin 17	7.2
<i>KRT18</i>	keratin 18	2.1

Genes down-regulated by SIP1 expression in A431

Gene	Protein	Fold down-regulation
<i>KRT19</i>	keratin 19	7.6
<i>KRT4</i>	keratin 4	10.5
<i>KRT5</i>	keratin 5 (epidermolysis bullosa simplex, Dowling-Meara/Kobner/Weber-Cockayne types)	8.2
<i>KRT6B</i>	keratin 6B	5.4
<i>KRT7</i>	keratin 7	4.8
<i>KRT8</i>	keratin 8	2.5
<i>KRTHB1</i>	keratin, hair, basic, 1	4.2
<i>LAD1</i>	ladinin 1	4.3
<i>LAMA3</i>	laminin, alpha 3	4.2
<i>LAMC2</i>	laminin, gamma 2	2.5
<i>LCP1</i>	lymphocyte cytosolic protein 1 (L-plastin)	4.0
<i>LDOC1</i>	leucine zipper, down-regulated in cancer 1	2.8
<i>Link-GEFII</i>	Link guanine nucleotide exchange factor II	3.1
<i>LOC116211</i>	hypothetical protein BC013113	2.3
<i>LOC130576</i>	hypothetical protein LOC130576	2.9
<i>LRP8</i>	low density lipoprotein receptor-related protein 8, apolipoprotein e receptor	2.0
<i>LTA4H</i>	leukotriene A4 hydrolase	1.9
<i>MAPK13</i>	mitogen-activated protein kinase 13	2.3
<i>MARS</i>	methionine-tRNA synthetase	2.9
<i>MCM4</i>	MCM4 minichromosome maintece deficient 4 (<i>S. cerevisiae</i>)	2.3
<i>MGC16207</i>	hypothetical protein MGC16207	3.2
<i>MGC34923</i>	hypothetical protein MGC34923	2.8
<i>MGC4309</i>	hypothetical protein MGC4309	2.9
<i>MGC5338</i>	hypothetical protein MGC5338	2.2
<i>MGST2</i>	microsomal glutathione S-transferase 2	1.9
<i>MLLT4</i>	myeloid/lymphoid or mixed-lineage leukemia (trithorax homolog, <i>Drosophila</i>)	2.1
<i>MN1</i>	meningioma (disrupted in balanced translocation) 1	3.4
<i>MUTYH</i>	mutY homolog (<i>E. coli</i>)	1.9
<i>MYC</i>	v-myc myelocytomatosis viral oncogene homolog (avian)	2.1
<i>NAKAP95</i>	neighbor of A-kinase anchoring protein 95	2.4

Genes down-regulated by SIP1 expression in A431

Gene	Protein	Fold down-regulation
<i>NALP2</i>	NACHT, LRR and PYD containing protein 2	2.3
<i>NET1</i>	neuroepithelial cell transforming gene 1	3.6
<i>NET-7</i>	transmembrane 4 superfamily member tetraspan NET-7	2.1
<i>NFE2</i>	nuclear factor (erythroid-derived 2), 45kDa	2.5
<i>NOLC1</i>	nucleolar and coiled-body phosphoprotein 1	2.7
<i>NUP50</i>	nucleoporin 50kDa	2.1
<i>P1P373C6</i>	hypothetical protein P1 p373c6	1.9
<i>PCDH1</i>	protocadherin 1 (cadherin-like 1)	2.9
<i>PCNA</i>	proliferating cell nuclear antigen	2.0
<i>PFKFB3</i>	6-phosphofructo-2-kinase/fructose-2,6-biphosphatase 3	1.8
<i>PHGDH</i>	phosphoglycerate dehydrogenase	1.9
<i>PI4K2B</i>	phosphatidylinositol 4-kinase type-II beta	2.4
<i>PIGPC1</i>	p53-induced protein PIGPC1	4.3
<i>PIM1</i>	pim-1 oncogene	2.2
<i>PLXNA2</i>	plexin A2	2.0
<i>POU3F4</i>	POU domain, class 3, transcription factor 4	3.1
<i>PRO2521</i>	hypothetical protein PRO2521	3.1
<i>PRSS8</i>	protease, serine, 8 (prostasin)	3.1
<i>PSAT1</i>	phosphoserine aminotransferase 1	4.0
<i>PSTPIP1</i>	proline-serine-threonine phosphatase interacting protein 1	1.9
<i>PTGS1</i>	prostaglandin-endoperoxide synthase 1	2.8
<i>PTPN11</i>	protein tyrosine phosphatase, non-receptor type 11 (Noo syndrome 1)	2.5
<i>PTPRU</i>	protein tyrosine phosphatase, receptor type, U	2.3
<i>RAB17</i>	RAB17, member RAS oncogene family	2.1
<i>RAB25</i>	RAB25, member RAS oncogene family	9.5
<i>RAI</i>	RelA-associated inhibitor	2.5
<i>RAI3</i>	retinoic acid induced 3	3.3
<i>RARSL</i>	arginyl-tRNA synthetase-like	1.8
<i>RIN2</i>	Ras and Rab interactor 2	2.0
<i>RRM2</i>	ribonucleotide reductase M2 polypeptide	2.1

Genes down-regulated by SIP1 expression in A431

Gene	Protein	Fold down-regulation
<i>RTP801</i>	HIF-1 responsive RTP801	2.6
<i>S100A14</i>	S100 calcium binding protein A14	5.8
<i>S100A2</i>	S100 calcium binding protein A2	4.4
<i>SC4MOL</i>	sterol-C4-methyl oxidase-like	2.1
<i>SCNN1A</i>	sodium channel, nonvoltage-gated 1 alpha	3.7
<i>SDC1</i>	syndecan 1	2.2
<i>SFN</i>	stratifin	3.9
<i>SIM2</i>	single-minded homolog 2 (Drosophila)	2.4
<i>SLC1A5</i>	solute carrier family 1 (neutral amino acid transporter), member 5	3.7
<i>SLC20A1</i>	solute carrier family 20 (phosphate transporter), member 1	1.9
<i>SLC35D1</i>	solute carrier family 35, member D1	2.4
<i>SLC38A1</i>	solute carrier family 38, member 1	2.5
<i>SLC3A2</i>	solute carrier family 3 (activators of dibasic and neutral amino acid transport)	5.0
<i>SLC7A11</i>	solute carrier family 7, (cationic amino acid transporter, y+ system) member 11	3.1
<i>SLC7A5</i>	solute carrier family 7 (cationic amino acid transporter, y+ system), member 5	6.3
<i>SLPI</i>	secretory leukocyte protease inhibitor (antileukoprotease)	1.9
<i>SNAI2</i>	snail homolog 2 (Drosophila)	2.1
<i>SORL1</i>	sortilin-related receptor, L(DLR class) A repeats-containing	2.1
<i>SPIB</i>	Spi-B transcription factor (Spi-1/PU.1 related)	2.8
<i>SPINT2</i>	serine protease inhibitor, Kunitz type, 2	2.9
<i>SPTBN1</i>	spectrin, beta, non-erythrocytic 1	2.4
<i>ST14</i>	suppression of tumorigenicity 14 (colon carcinoma, matriptase, epithin)	2.9
<i>SYPL</i>	synaptophysin-like protein	2.0
<i>TACSTD2</i>	tumor-associated calcium signal transducer 2	7.6
<i>TARS</i>	threonyl-tRNA synthetase	2.1
<i>TBL2</i>	transducin (beta)-like 2	1.8
<i>TDE2</i>	tumor differentially expressed protein 2	4.4
<i>THAP10</i>	THAP domain containing 10	3.9
<i>TNFAIP2</i>	tumor necrosis factor, alpha-induced protein 2	1.8
<i>TNFSF10</i>	tumor necrosis factor (ligand) superfamily, member 10	10.6

Genes down-regulated by SIP1 expression in A431

Gene	Protein	Fold down-regulation
<i>TP73L</i>	tumor protein p73-like	7.5
<i>TPD52</i>	tumor protein D52	2.0
<i>TPD52L1</i>	tumor protein D52-like 1	6.2
<i>TRIM29</i>	tripartite motif-containing 29	2.8
<i>UBN1</i>	ubiquitin 1	2.7
<i>UPP1</i>	uridine phosphorylase 1	1.9
<i>VAMP8</i>	vesicle-associated membrane protein 8 (endobrevin)	2.6
<i>VAV3</i>	vav 3 oncogene	2.6
<i>VEGF</i>	vascular endothelial growth factor	3.2
<i>WARS</i>	tryptophanyl-tRNA synthetase	2.0
<i>YARS</i>	tyrosyl-tRNA synthetase	2.5
<i>ZNF23</i>	zinc finger protein 23 (KOX 16)	2.0

Genes down-regulated by SIP1 expression in A431

Gene	Protein	Fold up-regulation
<i>ACADSB</i>	acyl-Coenzyme A dehydrogenase, short/branched chain	4.4
<i>ADAMTS1</i>	a disintegrin-like and metalloprotease (reprolysin type) with thrombospondin type 1 motif, 1	5.2
<i>AKR1C3</i>	aldo-keto reductase family 1, member C3 (3-alpha hydroxysteroid dehydrogenase, type II)	2.5
<i>ALDH1A1</i>	aldehyde dehydrogenase 1 family, member A1	4.3
<i>ANTXR1</i>	anthrax toxin receptor 1	2.8
<i>ANXA5</i>	annexin A5	2.8
<i>APOB</i>	apolipoprotein B (including Ag(x) antigen)	2.2
<i>B3GALT6</i>	UDP-Gal:betaGal beta 1,3-galactosyltransferase polypeptide 6	2.2
<i>C14orf132</i>	chromosome 14 open reading frame 132	2.7
<i>C1S</i>	complement component 1, s subcomponent	8.1
<i>C20orf100</i>	chromosome 20 open reading frame 100	2.4
<i>C20orf110</i>	chromosome 20 open reading frame 110	2.1
<i>C5orf5</i>	chromosome 5 open reading frame 5	2.4
<i>C9orf25</i>	chromosome 9 open reading frame 25	2.2
<i>CA1</i>	carbonic anhydrase I	2.0
<i>CAT</i>	catalase	2.0
<i>CBARA1</i>	calcium binding atopy-related autoantigen 1	1.9
<i>CBLB</i>	Cas-Br-M (murine) ecotropic retroviral transforming sequence b	2.6
<i>CCNDBP1</i>	cyclin D-type binding-protein 1	2.1
<i>CCNG2</i>	cyclin G2	2.0
<i>CDH2</i>	cadherin 2, type 1, N-cadherin (neuronal)	1.9
<i>CFL2</i>	cofilin 2 (muscle)	2.7
<i>CGI-49</i>	CGI-49 protein	3.0
<i>CLN2</i>	ceroid-lipofuscinosis, neuronal 2, late infantile (Jansky-Bielschowsky disease)	2.1
<i>COPZ2</i>	coatamer protein complex, subunit zeta 2	2.3
<i>CP</i>	ceruloplasmin (ferroxidase)	6.8
<i>CRI1</i>	CREBBP/EP300 inhibitory protein 1	1.9
<i>CRIP1</i>	cysteine-rich protein 1 (intestinal)	6.6
<i>CXX1</i>	CAAX box 1	2.3
<i>CYBRD1</i>	cytochrome b reductase 1	3.7

Genes down-regulated by SIP1 expression in A431

Gene	Protein	Fold up-regulation
<i>CYP1B1</i>	cytochrome P450, family 1, subfamily B, polypeptide 1	2.6
<i>DECR1</i>	2,4-dienoyl CoA reductase 1, mitochondrial	1.8
<i>DIO2</i>	deiodinase, iodothyronine, type II	3.1
<i>DKFZP586</i>	DKFZP586N0721 protein	2.1
<i>DKFZP761</i>	hypothetical protein DKFZp761F241	4.5
<i>DKK1</i>	dickkopf homolog 1 (<i>Xenopus laevis</i>)	8.4
<i>DPP4</i>	dipeptidylpeptidase 4 (CD26, adenosine deaminase complexing protein 2)	7.9
<i>EDIL3</i>	EGF-like repeats and discoidin I-like domains 3	4.2
<i>EMP3</i>	epithelial membrane protein 3	5.5
<i>EXT1</i>	exostoses (multiple) 1	1.9
<i>FADS1</i>	fatty acid desaturase 1	1.9
<i>FKBP8</i>	FK506 binding protein 8, 38kDa	1.8
<i>FLJ20287</i>	hypothetical protein FLJ20287	2.2
<i>FLJ25084</i>	hypothetical protein FLJ25084	2.3
<i>FLOT1</i>	flotillin 1	1.9
<i>FSTL1</i>	follistatin-like 1	4.0
<i>FSTL3</i>	follistatin-like 3 (secreted glycoprotein)	2.0
<i>FUT4</i>	fucosyltransferase 4 (alpha (1,3) fucosyltransferase, myeloid-specific)	3.1
<i>FZD4</i>	frizzled homolog 4 (<i>Drosophila</i>)	2.3
<i>GABARAP</i>	GABA(A) receptor-associated protein	2.4
<i>GABARAPL</i>	GABA(A) receptor-associated protein like 1	2.2
<i>GALNS</i>	galactosamine (N-acetyl)-6-sulfate sulfatase (Morquio syndrome, mucopolysaccharidosis type IVA)	1.9
<i>GBA</i>	glucosidase, beta; acid (includes glucosylceramidase)	1.8
<i>GNAS</i>	GNAS complex locus	2.2
<i>GRINA</i>	glutamate receptor, ionotropic, N-methyl D-aspartate-associated protein 1 (glutamate binding)	2.3
<i>GSN</i>	gelsolin (amyloidosis, Finnish type)	3.1
<i>GSTA4</i>	glutathione S-transferase A4	4.2
<i>GSTM3</i>	glutathione S-transferase M3 (brain)	2.7
<i>HATH6</i>	basic helix-loop-helix transcription factor 6	9.0
<i>HAVCR1</i>	hepatitis A virus cellular receptor 1	2.3

Genes down-regulated by SIP1 expression in A431

Gene	Protein	Fold up-regulation
<i>HBP1</i>	HMG-box transcription factor 1	2.1
<i>HPCAL1</i>	hippocalcin-like 1	2.8
<i>HRASLS3</i>	HRAS-like suppressor 3	2.1
<i>IER3</i>	immediate early response 3	2.6
<i>IFITM1</i>	interferon induced transmembrane protein 1 (9-27)	2.0
<i>IFITM2</i>	interferon induced transmembrane protein 2 (1-8D)	4.4
<i>IFITM3</i>	interferon induced transmembrane protein 3 (1-8U)	4.1
<i>IGFBP2</i>	insulin-like growth factor binding protein 2, 36kDa	1.8
<i>IL17RE</i>	interleukin 17 receptor E	2.4
<i>ING4</i>	inhibitor of growth family, member 4	2.0
<i>ITM2C</i>	integral membrane protein 2C	1.9
<i>KIAA0882</i>	KIAA0882 protein	1.9
<i>KIAA0962</i>	KIAA0962 protein	2.0
<i>KIAA1474</i>	teashirt 3	2.3
<i>KIAA1644</i>	KIAA1644 protein	6.2
<i>KYNU</i>	kynureninase (L-kynurenine hydrolase)	3.4
<i>LAMB2</i>	laminin, beta 2 (laminin S)	2.5
<i>LAMC1</i>	laminin, gamma 1 (formerly LAMB2)	2.8
<i>LEPRE1</i>	leucine proline-enriched proteoglycan (leprecan) 1	2.2
<i>LGALS1</i>	lectin, galactoside-binding, soluble, 1 (galectin 1)	12.4
<i>LMO7</i>	LIM domain only 7	1.9
<i>LOC221002</i>	CG4853 gene product	2.7
<i>LOC283120</i>	hypothetical protein LOC283120	7.1
<i>LOC51064</i>	glutathione S-transferase subunit 13 homolog	1.8
<i>LOC51149</i>	truncated calcium binding protein	1.9
<i>LOXL4</i>	lysyl oxidase-like 4	2.8
<i>LRRN3</i>	leucine rich repeat neuronal 3	2.7
<i>MAGED1</i>	melanoma antigen, family D, 1	3.3
<i>MAGED2</i>	melanoma antigen, family D, 2	3.2
<i>MAL</i>	mal, T-cell differentiation protein	3.2

Genes down-regulated by SIP1 expression in A431

Gene	Protein	Fold up-regulation
<i>MAP3K5</i>	mitogen-activated protein kinase kinase kinase 5	2.5
<i>MARCKS</i>	myristoylated alanine-rich protein kinase C substrate	1.9
<i>MBNL1</i>	muscleblind-like (Drosophila)	2.1
<i>MEF2C</i>	MADS box transcription enhancer factor 2, polypeptide C (myocyte enhancer factor 2C)	2.3
<i>MK-STYX</i>	map kinase phosphatase-like protein MK-STYX	1.9
<i>MLC1SA</i>	myosin light chain 1 slow a	1.8
<i>MPV17</i>	MpV17 transgene, murine homolog, glomerulosclerosis	2.3
<i>MRF2</i>	modulator recognition factor 2	3.2
<i>MSI2</i>	musashi homolog 2 (Drosophila)	2.6
<i>MVP</i>	major vault protein	2.1
<i>MYBPC2</i>	myosin binding protein C, fast type	7.6
<i>MYL6</i>	myosin, light polypeptide 6, alkali, smooth muscle and non-muscle	1.9
<i>NCOA7</i>	nuclear receptor coactivator 7	1.9
<i>NEU1</i>	sialidase 1 (lysosomal sialidase)	2.1
<i>NFKBIE</i>	nuclear factor of kappa light polypeptide gene enhancer in B-cells inhibitor, epsilon	2.0
<i>NGFRAP1</i>	nerve growth factor receptor (TNFRSF16) associated protein 1	2.3
<i>NPDC1</i>	neural proliferation, differentiation and control, 1	2.1
<i>NRP1</i>	neuropilin 1	2.0
<i>NT5E</i>	5'-nucleotidase, ecto (CD73)	3.4
<i>PAK1</i>	p21/Cdc42/Rac1-activated kinase 1 (STE20 homolog, yeast)	3.1
<i>PDCD4</i>	programmed cell death 4 (neoplastic transformation inhibitor)	2.0
<i>PDK2</i>	pyruvate dehydrogenase kinase, isoenzyme 2	2.2
<i>PHKA2</i>	phosphorylase kinase, alpha 2 (liver)	2.0
<i>PLCD3</i>	phospholipase C, delta 3	5.3
<i>PLEKHC1</i>	pleckstrin homology domain containing, family C (with FERM domain) member 1	4.1
<i>PNMA1</i>	paraneoplastic antigen MA1	2.1
<i>PPGB</i>	protective protein for beta-galactosidase (galactosialidosis)	1.8
<i>PRO1073</i>	PRO1073 protein	2.1
<i>PRSS11</i>	protease, serine, 11 (IGF binding)	15.4
<i>PTPRK</i>	protein tyrosine phosphatase, receptor type, K	2.4

Genes down-regulated by SIP1 expression in A431

Gene	Protein	Fold up-regulation
<i>PTRF</i>	polymerase I and transcript release factor	2.4
<i>PXMP3</i>	peroxisomal membrane protein 3, 35kDa (Zellweger syndrome)	2.2
<i>QSCN6</i>	quiescin Q6	14.6
<i>RAB31</i>	RAB31, member RAS oncogene family	1.9
<i>RABAC1</i>	Rab acceptor 1 (prenylated)	2.3
<i>RARRES1</i>	retinoic acid receptor responder (tazarotene induced) 1	15.0
<i>RFX4</i>	regulatory factor X, 4 (influences HLA class II expression)	2.6
<i>RNF28</i>	ring finger protein 28	1.8
<i>RNUT1</i>	RNA, U transporter 1	2.0
<i>RPS27L</i>	ribosomal protein S27-like	4.3
<i>S100A6</i>	S100 calcium binding protein A6 (calcyclin)	3.1
<i>SCARB2</i>	scavenger receptor class B, member 2	2.0
<i>SDCBP</i>	Syntenin	1.9
<i>SDCBP</i>	syndecan binding protein (syntenin)	1.9
<i>SERPINH1</i>	serine (or cysteine) proteinase inhibitor, clade H (heat shock protein 47), member 1, (collagen binding protein 1)	2.8
<i>SH3BGRL</i>	SH3 domain binding glutamic acid-rich protein like	2.4
<i>SLC12A8</i>	solute carrier family 12 (potassium/chloride transporters), member 8	3.6
<i>SNX15</i>	sorting nexin 15	2.0
<i>SPARC</i>	secreted protein, acidic, cysteine-rich (osteonectin)	8.8
<i>SPON2</i>	spondin 2, extracellular matrix protein	2.6
<i>SPUVE</i>	protease, serine, 23	2.9
<i>SULT1C1</i>	sulfotransferase family, cytosolic, 1C, member 1	2.2
<i>TENS1</i>	tensin-like SH2 domain-containing 1	2.2
<i>TGFBR2</i>	transforming growth factor, beta receptor II (70/80kDa)	2.8
<i>THBS1</i>	thrombospondin 1	2.5
<i>THRA</i>	thyroid hormone receptor, alpha (erythroblastic leukemia viral (v-erb-a) oncogene homolog, avian)	2.3
<i>TM4SF10</i>	transmembrane 4 superfamily member 10	4.4
<i>TMSB4X</i>	thymosin, beta 4, X-linked	2.4
<i>TPCN1</i>	two pore segment channel 1	1.8
<i>TPST1</i>	tyrosylprotein sulfotransferase 1	3.9

Genes down-regulated by SIP1 expression in A431

Gene	Protein	Fold up-regulation
<i>TXNRD1</i>	thioredoxin reductase 1	2.0
<i>TXNRD2</i>	thioredoxin reductase 2	2.4
<i>URB</i>	steroid sensitive gene 1	4.4
<i>VAT1</i>	vesicle amine transport protein 1 homolog (T californica)	3.0
<i>VEGFC</i>	vascular endothelial growth factor C	3.7
<i>VIM</i>	Vimentin	29.5
<i>VMP1</i>	likely ortholog of rat vacuole membrane protein 1	2.6

Appendix B

(Publication)

Andersen H*, Mejlvang J*, Mahmood S, Gromova I, Gromov P, Lukanidin E, Kriajevska M, Mellon JK, Tulchinsky E.; Immediate and delayed effects of E-cadherin inhibition on gene regulation and cell motility in human epidermoid carcinoma cells. **Mol Cell Biol 2005** Vol 25
(*Shared first-authorship)

Immediate and Delayed Effects of E-Cadherin Inhibition on Gene Regulation and Cell Motility in Human Epidermoid Carcinoma Cells

Henriette Andersen,^{2†} Jakob Mejlvang,^{1†} Shaukat Mahmood,² Irina Gromova,³ Pavel Gromov,³ Eugene Lukanidin,² Marina Kriajevska,¹ J. Kilian Mellon,¹ and Eugene Tulchinsky^{1*}

Department of Cancer Studies and Molecular Medicine, University of Leicester, Leicester LE1 9HN, United Kingdom¹;
Department of Molecular Cancer Biology, Danish Cancer Society, Strandboulevarden 49, Copenhagen 2100, Denmark²;
and Department of Proteomics in Cancer, Danish Cancer Society, Strandboulevarden 49, Copenhagen 2100, Denmark³

Received 1 March 2005/Returned for modification 8 April 2005/Accepted 21 July 2005

The invasion suppressor protein, E-cadherin, plays a central role in epithelial cell-cell adhesion. Loss of E-cadherin expression or function in various tumors of epithelial origin is associated with a more invasive phenotype. In this study, by expressing a dominant-negative mutant of E-cadherin (Ec1WVM) in A431 cells, we demonstrated that specific inhibition of E-cadherin-dependent cell-cell adhesion led to the genetic reprogramming of tumor cells. In particular, prolonged inhibition of cell-cell adhesion activated expression of vimentin and repressed cytokeratins, suggesting that the effects of Ec1WVM can be classified as epithelial-mesenchymal transition. Both short-term and prolonged expression of Ec1WVM resulted in morphological transformation and increased cell migration though to different extents. Short-term expression of Ec1WVM up-regulated two AP-1 family members, *c-jun* and *fra-1*, but was insufficient to induce complete mesenchymal transition. AP-1 activity induced by the short-term expression of Ec1WVM was required for transcriptional up-regulation of AP-1 family members and down-regulation of two other Ec1WVM-responsive genes, *S100A4* and *igfbp-3*. Using a dominant-negative mutant of c-Jun (TAM67) and RNA interference-mediated silencing of c-Jun and Fra-1, we demonstrated that AP-1 was required for cell motility stimulated by the expression of Ec1WVM. In contrast, Ec1WVM-mediated changes in cell morphology were AP-1-independent. Our data suggest that mesenchymal transition induced by prolonged functional inhibition of E-cadherin is a slow and gradual process. At the initial step of this process, Ec1WVM triggers a positive autoregulatory mechanism that increases AP-1 activity. Activated AP-1 in turn contributes to Ec1WVM-mediated effects on gene expression and tumor cell motility. These data provide novel insight into the tumor suppressor function of E-cadherin.

E-cadherin is an epithelial calcium-binding transmembrane glycoprotein that mediates formation of adherens junctions ensuring stable homophilic cell-cell adhesion. The extracellular domain of E-cadherin consists of five cadherin repeats involved in the formation of parallel E-cadherin dimers. N termini of parallel dimers interact with other parallel dimers exposed on the membrane of neighboring cells, forming complexes in *trans*, linking epithelial cells to each other (9, 64). The structural basis of the formation of *trans* dimers is the mutual incorporation of Trp² into a hydrophobic pocket of the interacting E-cadherin molecule (54). Cytoplasmic E-cadherin domains interact with either β - or γ -catenin, which in turn binds α -catenin, providing a link with the actin cytoskeleton and hence strengthening adhesion (9, 16). Disruption of E-cadherin-mediated intercellular adhesion is a hallmark of epithelial-mesenchymal transition (EMT), a phenomenon which occurs at certain stages of normal development and in the malignant progression of carcinoma (59, 60). Different molecular mechanisms including gene mutations (4, 26, 66), hyper-

methylation of the promoter (17), and transcriptional silencing by transcriptional repressors (Snail, Slug, ZEB-2/SIP1, ZEB-1, and E12/E47) (2, 8, 6, 14, 20, 46) contribute to the inactivation of E-cadherin linked with tumor progression. Reexpression of E-cadherin may induce morphological reversion and suppress cell growth and invasion suggesting an important function for E-cadherin in EMT (24, 56, 58, 67). The mechanism of tumor suppressor function of E-cadherin is not completely understood and may be linked with its role in signal transduction. Indeed, E-cadherin has been implicated not only in epithelial adhesion but also in the regulation of cell signaling. Being an important player in the Wnt signal transduction pathway, β -catenin links E-cadherin with cellular signaling networks (9, 16, 29, 47). In different systems, sequestration of β -catenin by the cytoplasmic domain of E-cadherin prevents its nuclear translocation and inhibits β -catenin/T-cell factor (TCF)-mediated transcriptional activity (42, 51). In a model of Fos protein-induced EMT, loss of E-cadherin activated β -catenin signaling in murine nontumorigenic Ep-1 cells (19). Inhibition of β -catenin signaling by E-cadherin may result in suppression of cell growth, providing a molecular basis for adhesion-independent tumor suppression function of E-cadherin (24, 57). A direct link between the functional status of E-cadherin and β -catenin signaling has been demonstrated in colon carcinoma cells SW480 harboring a mutant APC gene. In these cells, inhibition

* Corresponding author. Mailing address: Department of Cancer Studies and Molecular Medicine, University of Leicester, Hodgkin bldg., lab 302, Lancaster Rd., Leicester LE1 9HN, United Kingdom. Phone: 44 116 252 5584. Fax: 44 116 252 5616. E-mail: et32@le.ac.uk.

† H.A. and J.M. contributed equally to this work.

of adherens junctions by an anti-E-cadherin blocking antibody resulted in activation of β -catenin/TCF-dependent transcription with subsequent activation of the transcriptional repressor, Slug, and repression of E-cadherin gene transcription (15). However, in other in vitro models of EMT, loss of E-cadherin expression did not result in increased β -catenin/TCF transcriptional activity (14; J. Mejlvang et al., unpublished data). Moreover, β -catenin/TCF transcriptional activity does not correlate with E-cadherin status in breast, gastric, and pancreatic carcinoma cell lines (7, 61). It has been suggested that E-cadherin influences cell signaling through receptor tyrosine kinases (RTKs). E-cadherin and epidermal growth factor receptor (EGFR) colocalize to basolateral areas of epithelial cells and have been reported to form multicomponent complexes (28, 44). Formation of adhesive complexes leads to transient ligand-independent activation of EGFR and subsequent activation of mitogen-activated protein kinase (MAPK) (43), phosphatidylinositol 3-kinase (30, 43) signaling cascades, and Rac1 (5, 30). E-cadherin engagement may influence the activity of small GTPases via Src-dependent phosphorylation of RhoA-specific GTPase-activating protein p190RhoGAP (39). In dense epithelial cultures, E-cadherin also activates another RTK, EphA2, and inhibits cell proliferation (68). Recently, E-cadherin-mediated adhesion has been shown to repress ligand-induced activation of several RTKs including EGFR/Neu, insulin-like growth factor 1 receptor and c-Met in Madin-Darby canine kidney (MDCK) (48) but not in SW480 cell lines (15). However, although it is documented that E-cadherin affects cell signaling through RTKs, cytoskeletal reorganization, and β -catenin/TCF, there is a substantial lack of experimental work investigating the consequence of inhibition of E-cadherin-mediated adhesion for gene regulation.

In this report, we demonstrate that prolonged functional inactivation of E-cadherin by a dominant-negative E-cadherin mutant, Ec1WVM, is sufficient to induce full EMT in A431 cells. Short-term inactivation of E-cadherin has a lesser effect on the expression of target genes but is sufficient to activate the transcription factor AP-1. Activation of AP-1 by Ec1WVM appeared to be essential for some of its transcriptional effects. In addition, Ec1WVM regulates tumor cell motility in an AP-1-dependent manner.

MATERIALS AND METHODS

Cell lines and transfections. A431, a human vulvar epidermoid adenocarcinoma cell line, and all clones were cultured in Dulbecco's modified Eagle's medium supplemented with 10% fetal bovine serum. Doxycycline (DOX; 2 μ g/ml) was added for indicated time periods. For prolonged treatments, DOX-containing medium was changed every second day. All transfections of plasmid DNA were performed by electroporation with a single pulse of 250 V and 250 μ F by using the Gene Pulser Xcell electroporation system (Bio-Rad). To generate clones with stable expression of Ec1WVM, A431 cells were transfected with a pCMVEc1WVM plasmid (12) provided by S. Troyanovsky (Washington University Medical School, St. Louis, Mo.), and clones with altered (clones W1 to W6) and unchanged morphology (clones NT-1 and NT-2) were selected in the presence of 200 μ g/ml of G418. To generate A431 clones with inducible expression, we first transfected A431 cells with the pUHD-172.1 construct and obtained A431 clones expressing the TET-responsive transcriptional activator, rTA. Individual clones were analyzed by transfection with the pUHC13-3 construct encoding firefly luciferase. Luciferase activity was detected in cells growing in the presence or absence of DOX for 48 h, and a clone with minimal leakage was selected (clone A431-TET-on). In the second round of transfection, A431-TET-on cells were transfected with pBI-Ec1WVM, pBI-Ec1WVM-TAM67, or pUHD-c-Fos constructs along with pTK-Hyg vector (BD Bioscience Clontech).

Clones were selected in the presence of 60 μ g/ml hygromycin B, and the inducibility of Ec1WVM, TAM67-green fluorescent protein (GFP), and c-Fos was examined by Western blotting and immunofluorescence analysis.

Plasmids. To generate pBI-Ec1WVM, the Ec1WVM sequence was excised from pCMVEc1WVM and subcloned into multiple cloning site I of a bidirectional tetracycline (TET)-responsive vector pBI (BD Clontech). To construct a vector with simultaneous expression of Ec1WVM and a dominant-negative AP-1 mutant, a fragment coding for the TAM67-GFP fusion protein was excised from pGFP-TAMPuro (27) (provided by R. Hennigan, University of Cincinnati, Cincinnati, Ohio) and inserted into multiple cloning site II of pBI-Ec1WVM. To generate pUHD-c-Fos, c-Fos cDNA was cut out from pCMV-c-Fos and subcloned into pUHD-10-3.

Gene reporter assays. To determine β -catenin/TCF/lymphoid enhancer factor (LEF) transcriptional activity, 31D6 cells were transfected with 2 μ g of pTOPFLASH or pFOPFLASH reporter constructs. The efficiency of each transfection was monitored using 400 ng of cotransfected β -galactosidase expression vector, pCMV β -gal (Invitrogen). Cells were maintained with or without DOX for 48 h and lysed, and the luciferase activity was measured with a Lumat LB9501 tube luminometer (Berthold). The lysates obtained were also tested for β -galactosidase activity by using *o*-nitrophenyl- β -D-galactopyranoside (Sigma) as a chromogenic substrate. Results were expressed as a ratio of pTOPFLASH and pFOPFLASH reporter activities normalized to the activity of β -galactosidase in each experiment. To examine AP-1 activity, cells were transfected with an AP-1-dependent reporter pTREx5Luc containing five copies of an AP-1-binding element upstream of the minimal *c-fos* promoter (13). To demonstrate the specificity of AP-1 activation, we used a pRSVLuc reporter (13) that is largely AP-1-independent. Transfected cells were incubated for 2 days with or without DOX, and luciferase activity was measured and normalized to the β -galactosidase activity.

One-dimensional SDS electrophoresis and Western blotting. Proteins (10 or 20 μ g) were denatured, separated on precast 4 to 20% gradient sodium dodecyl sulfate (SDS)-polyacrylamide gels (Invitrogen), and then transferred to Immobilon-P membranes (Millipore) by the standard procedure. Following protein transfer, blots were incubated in blocking solution with primary antibody at a dilution of 1:1,000 (for anti-myc tag antibody, clone 9E10; Santa-Cruz Biotech), 1:2,000 (for anti-E-cadherin antibody; BD Biosciences), 1:400 (for anti-GFP antibody; BD Biosciences), or 1:500 (for anti-c-Fos, anti-Fra-1, and anti-c-Jun antibodies; Santa-Cruz Biotech). Immunoreactive proteins were detected using an enhanced chemiluminescence system (Amersham).

Metabolic labeling. Cells were grown to approximately 70% confluence in microtiter 24-well culture dishes and labeled overnight in Dulbecco's modified Eagle's medium lacking methionine and containing 1% dialyzed fetal calf serum and 1 mCi/ml [³⁵S]methionine. Following labeling, cells were gently washed twice with phosphate-buffered saline solution and harvested by solubilization in lysis buffer for two-dimensional polyacrylamide gel electrophoresis (2D PAGE).

2D PAGE and image analysis. After cells were washed, excess phosphate-buffered saline solution was removed from the wells. A total of 50 μ l of lysis buffer (40) was overlaid on cell monolayers, and the cells were lysed in solution by gentle pipetting. Samples were kept at -20° C until use. Whole protein lysates were subjected to isoelectrofocusing 2D PAGE as previously described (11). From 20 to 35 μ l of sample was applied to the first dimension. Proteins were visualized using autoradiography and/or phosphorimaging followed by a silver staining procedure compatible with mass spectrometry analysis (25). Image analysis was performed using PDQUEST 7.1 software (Bio-Rad). Detection of low-abundant protein spots on silver-stained gels was highly enhanced by the superimposition of the dry silver gel with the corresponding autoradiograph.

Protein identification by mass spectrometry. Protein spots of interest were excised from the dry silver-stained gels, followed by rehydration in water for 30 min at room temperature. Proteins were "in-gel" digested with bovine trypsin for 12 h as previously described (55). The reaction was stopped by adding trifluoroacetic acid up to 0.4%, followed by shaking for 20 min at room temperature to increase peptide recovery. Peptides were concentrated on microcolumns containing C₁₈-based 3M Empore plugs (49) and eluted with 50% acetonitrile-0.2% trifluoroacetic acid directly on the target and cocrystallized with cyano matrix (2 mg/ml cyano-4-hydroxycinnamic acid in 0.5% trifluoroacetic acid-acetonitrile, 1:2 [vol/vol]). The extraction procedure strongly increased the amount of peptides, thus allowing direct sequence analysis of low intensity peptides. Mass spectrometry was performed using a Reflex IV matrix-assisted laser desorption/ionization-time of flight (MALDI-TOF) mass spectrometer equipped with a Scout 384 ion source. All spectra were obtained in positive reflector mode with delayed extraction, using an accelerating voltage of 28 kV. Each spectrum represented an average of 100 to 200 laser shots, depending on the signal-to-noise ratio. The resulting mass spectra were internally calibrated by using the autodi-

gested tryptic mass values (805,417, 906,505, 1153,574, 1433,721, 2163,057, and 2273,160) visible in all spectra. Calibrated spectra were processed by the Xmass 5.1.1 and BioTools 2.1 software packages (Bruker Daltonik, GmbH). All spectra were analyzed manually as previously described (10).

Microarray hybridization. Hybridization of Atlas human cDNA expression arrays (Clontech) was performed basically as recommended by the manufacturer. Briefly, filters were prehybridized for 12 to 16 h at 68°C in 10 ml of ExpressHyb solution plus 100 µg/ml denatured sheared salmon sperm DNA. Radiolabeled probes were purified, heat denatured, and then added to 5- to 10-ml aliquots of hybridization buffer containing salmon sperm DNA. The final probe concentration was 5×10^6 to 10×10^6 cpm/hybridization. After extensive washing (three times with $2 \times$ SSC [$1 \times$ SSC is 0.15 M NaCl plus 0.015 M sodium citrate]–1% SDS and two to three times with $0.1 \times$ SSC–0.5% SDS, each for 30 min at 68°C), the membranes were subjected to phosphorimaging analysis, and differential signals were identified by AtlasImage software.

Northern blotting. For Northern blot analysis, total RNA was isolated by the guanidine isothiocyanate method and separated in 1.2% agarose gels. RNA blotting and hybridization were performed as previously described (50). Radioactive DNA probes were synthesized using a random-primed labeling kit (Amersham). For radioactive labeling, 200- to 300-bp cDNA fragments corresponding to coding parts of identified genes were generated by reverse transcriptase PCR.

RNA interference. Purified and annealed synthetic oligonucleotides were purchased from Ambion (Austin, TX). The target sequence for Fra-1 was validated previously (63). The target sequence for c-Jun was GAUCCUGAAACAGAGC AUG. A total of 2×10^6 cells were transfected with 2 µg of small interfering RNA (siRNA) by the nucleofection technique in buffer V (nucleofection protocol T-20). The nucleofector device and a nucleofection kit were obtained from Amaxa (Cologne, Germany) and used in accordance with the manufacturer's recommendations. At 30 h after transfection, cells were harvested, counted, and processed for cell motility assays or Western blotting.

Cell motility assays. For wound-healing assays, wounds were generated by 20-µl pipette tips in confluent cultures of cells growing in 6- or 24-well plates. Areas of wounds were marked and photographed at different time points using a digital camera attached to a phase-contrast microscope (Nikon TE 2000-S). Where indicated, cells were maintained in the presence of DOX for 48 h prior to the creation of wounds. A transwell migration assay was performed using 24-well transwell plates containing 8-µm-pore-size polycarbonate filters (Corning Costar Corp., Cambridge, MA). A total of 1×10^5 cells were added to the top chambers and incubated overnight. Adhered cells were allowed to migrate toward serum gradient used as a chemoattractant in the lower chamber for 4 h. Those cells that did not migrate through the pores in the membrane were removed by scraping the membrane with a cotton swab. Cells that migrated to the underside of transwell filters were fixed, stained with a Gurr rapid staining kit (BDH), and counted by bright-field microscopy at a magnification of $\times 200$ in four random fields using the ImageJ program.

RESULTS

Long-term expression of a dominant-negative E-cadherin mutant in A431 cells affects gene expression. Though the involvement of E-cadherin in cell signaling is documented, the effects of E-cadherin dominant-negative mutants on gene regulation have not been systematically studied. To examine whether the prolonged inhibition of cell-cell adhesion in epithelial cells influences gene expression, we generated clones of A431 human epidermoid carcinoma cells expressing a dominant-negative E-cadherin mutant, Ec1WVM. This mutant harbors a Trp²/Ala amino acid substitution in the first cadherin-like repeat, leading to an inability of the mutant protein to form *trans* dimers. The dominant effect of Ec1WVM on cell morphology has been described earlier (12). Ec1WVM contains a C-terminal six-myc tag epitope and a 17-amino-acid deletion in the cytosolic domain, eliminating the recognition by a commercial anti-E-cadherin antibody (clone C20820; BD Bioscience). These modifications allow differentiation between wild-type and mutant forms of E-cadherin in transfected cells. We selected six clones that exhibited altered fibroblastoid mor-

phology (clones W1 to W6) and two clones (NT-1 and NT-2) that were morphologically indistinguishable from the parental cells (Fig. 1A). As expected, W1 to W6 but not NT-1 and NT-2 clones expressed Ec1WVM (Fig. 1B). Expression levels of the endogenous E-cadherin was significantly lower in W1 to W6 clones than in NT1, NT2, or parental cells (Fig. 1B), consistent with its destabilization in cells expressing different dominant-negative E-cadherin mutants (12, 38, 65). To test whether the expression of Ec1WVM resulted in alteration in the cellular content of other proteins, we employed a proteomic approach based on 2D PAGE coupled with MALDI-TOF mass spectrometry. Cells were [³⁵S]methionine labeled, and total protein extracts from two clones expressing Ec1WVM (W2 and W3) and two control clones (NT-1 and NT-2) were subjected to 2D gel electrophoresis. Approximately 800 protein spots were detected on average in each gel. A total of 350 well-focused and relatively abundant proteins were matched and selected for quantitation. Steady-state levels of [³⁵S]methionine incorporation were estimated as a mean value for each protein spot in all sample pairs. The levels of actin as well as the total quantity of valid spots were used to normalize the amount of labeled proteins that entered the gels. Our results showed that the majority of the 350 quantitated proteins which represented essentially the most abundant components of the A431 proteome, showed no significant alterations in their levels in cells expressing the E-cadherin mutant compared with NT-1 and NT-2 clones. However, we identified 10 proteins (or 2.8% of the proteome) that were consistently deregulated by a factor of 2.0 and more. The identity of seven deregulated proteins was determined by MALDI-TOF mass spectrometry. The most striking up-regulation was observed for the mesenchymal marker vimentin (by a factor of 100) (Fig. 1C). As can also be seen from Table 1 and Fig. 1C, three keratins, namely, keratin 15 and two isoforms of keratin 13, were highly down-regulated in A431 cells expressing Ec1WVM.

As an independent approach to examine Ec1WVM-dependent gene expression and to test whether gene transcription was affected, we employed BD Atlas human general cDNA and human cancer cDNA expression arrays containing in combination approximately 900 spotted genes. To minimize the effects of clonal variations, cDNA from two Ec1WVM-positive (W1 and W3) and two control clones (NT-1 and NT-2) was applied. Using Atlas arrays, we have identified nine genes (or 1% of all spotted genes) differentially expressed in epithelial clones versus clones with compromised intercellular adhesion. Two genes (keratin 13 and vimentin) identified in 2D protein gels were present on Atlas membranes and demonstrated differential transcription in Ec1WVM-expressing versus control clones. Six of the genes identified by Atlas arrays exhibited enhanced expression in A431 clones with compromised adhesion, whereas transcription of three genes was inhibited. Validation of the results obtained from the analysis of the cDNA array was performed by Northern blotting (Fig. 2). The effects of Ec1WVM on gene expression varied from subtle activation of urokinase plasminogen activator (1.7-fold activation) to the initiation of de novo transcription of vimentin. The genes with altered expression (summarized in Table 1) play a role in epithelial-mesenchymal transition/tumor cell invasion (six genes), signal transduction (six genes), gene regulation (two genes), or metabolism (two genes). Of importance, activation

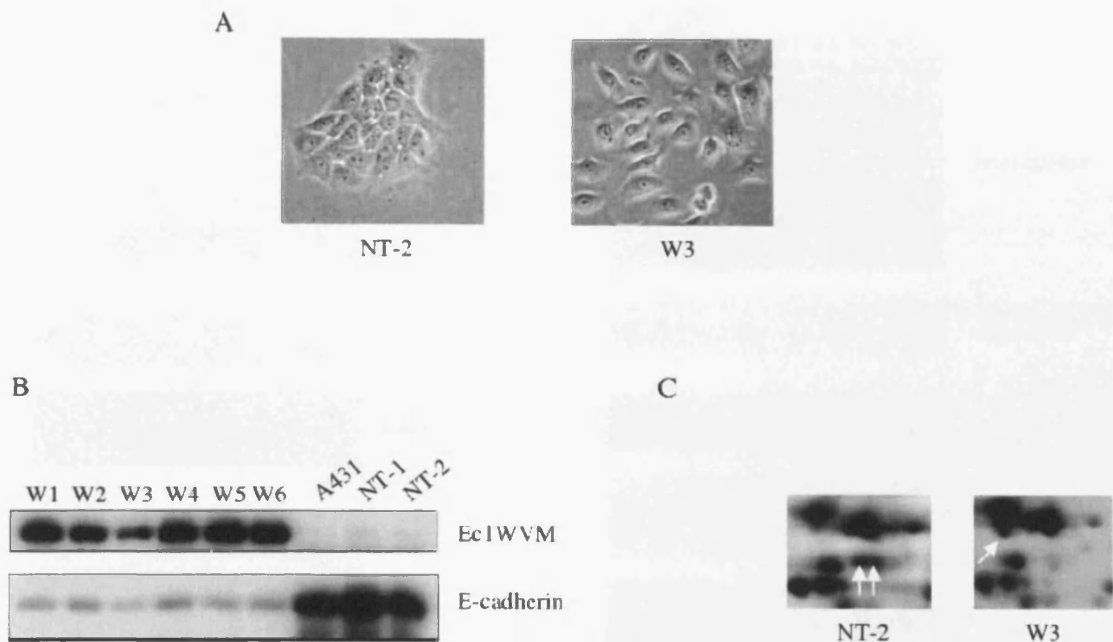


FIG. 1. Characterization of stable A431 clones expressing Ec1WVM. (A) Phase-contrast images of NT-2 and W3 clones. (B) Detection of wild-type E-cadherin and Ec1WVM in clones with altered (W1 to W6) and epithelial morphology (NT-1 and NT-2). A total of 20 μ g of proteins was analyzed by Western blotting with antibodies as indicated. (C) 2D gel (isoelectrofocusing) autoradiographs of [35 S]methionine-labeled proteins from NT-2 and W3 cells. Only fractions of 2D gel autoradiographs are shown. The positions of keratin 13, keratin 13 variant (NT-2 panel), and vimentin (W3 panel) are indicated by arrows.

TABLE 1. Genes and proteins up- or down-regulated in A431 clones expressing Ec1WVM: summary of cDNA array analysis and 2D PAGE combined with mass spectrometry data

Gene and function ^a	Effect of Ec1WVM ^b	Method of detection ^c
Epithelial mesenchymal transition/ tumor cell invasion		
Vimentin	+	Array and 2D
Cytokeratin 13	-	Array and 2D
Cytokeratin 15	-	2D
S100A4	-	Array
MMP-2	+	Array
uPA	+	Array
Signal transduction		
Neuregulins	+	Array
Small GTPase Ran	+	2D
Rho GDI	+	2D
DJ-1, a positive regulator of AR signaling	+	2D
IGFBP-3	-	Array
Ser/Thr protein phosphatase 2A	-	2D
Transcription factors		
Fra-1	+	Array
c-Jun	+	Array
Metabolism		
L-Lactate dehydrogenase	-	2D
Isocitrate dehydrogenase	-	2D

^a uPA, urokinase plasminogen activator; MMP-2, matrix metalloproteinase 2; IGFBP-3, insulin-like growth factor binding protein 3; AR, androgen receptor.

^b +, up-regulation; -, down-regulation.

^c 2D, 2D PAGE combined with mass spectrometry.

of vimentin and down-regulation of keratins indicate that Ec1WVM-mediated alterations in the gene expression pattern can be classified as EMT.

Effects of Ec1WVM on transcription of different genes require different duration of Ec1WVM expression. The observed effects on gene expression mediated by the E-cadherin mutant may either be direct or require prolonged inhibition of intercellular adhesion. To discriminate between these possibilities, we generated A431 clones with the DOX-regulated expression of Ec1WVM (clone 31D6; TET-on system). In cells treated with DOX, synthesis of Ec1WVM was induced as early as in 6 h, and alterations in cell morphology became evident at 24 h. At 48 h, Ec1WVM decreased the level of endogenous E-cadherin and induced full morphological transition of 31D6 cells, whose appearance became very similar to that of cells stably expressing Ec1WVM (Fig. 3A). 31D6 cells were maintained in the presence of DOX for different time periods or without DOX, and the expression of Ec1WVM-dependent genes was examined by Northern blot hybridization. Genes encoding components of intermediate filaments were not affected by Ec1WVM even after 16 days of induction (data not shown). Down-regulation of *igfbp-3* and *S100A4* genes occurred gradually, and after 16 days of incubation in the presence of DOX, expression of these genes reached levels comparable to those observed in stable clones (Fig. 3B). Conversely, *fra-1* and *c-jun* transcription was activated already after 48 h of stimulation by DOX, concomitant with morphological transformation of 31D6 cells.

Both genes immediately activated by Ec1WVM encode proteins, which belong to the AP-1 transcription factor family.

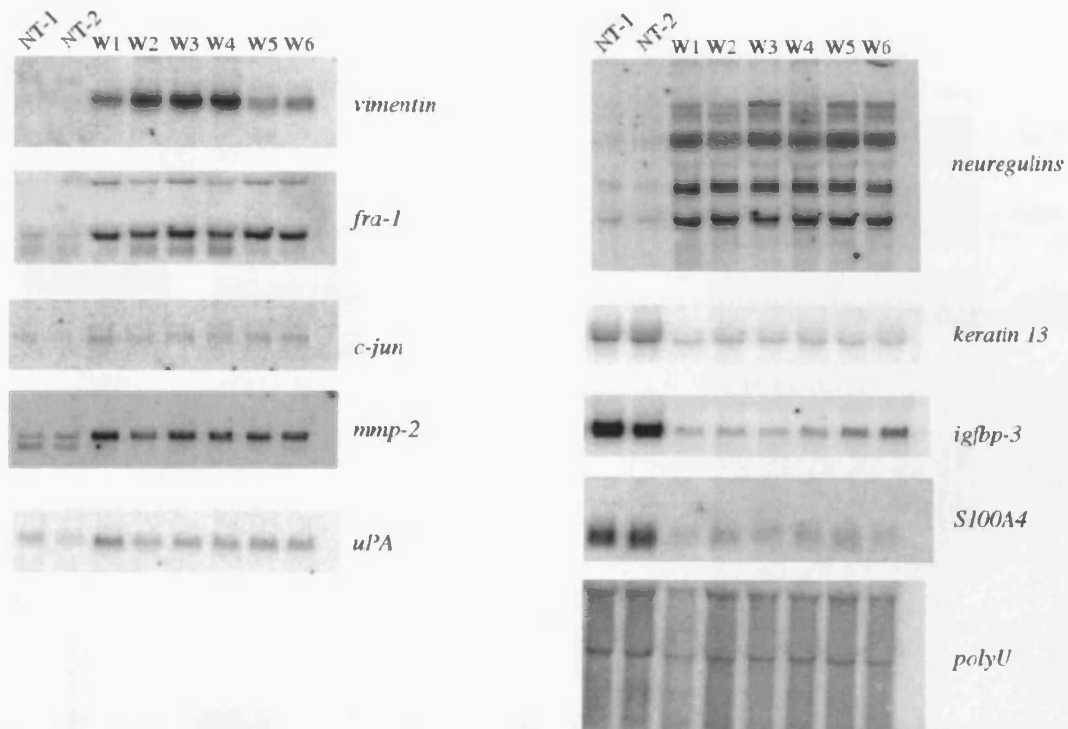


FIG. 2. Validation of Atlas cDNA microarray data. Transcription of genes identified in W1 to W6, NT-1, and NT-2 clones was analyzed by Northern blotting. Equal loading was verified by hybridization with the labeled *polyU* probe.

Consistent with their up-regulation by Ec1WVM in 31D6 cells, a reporter driven by a synthetic AP-1-dependent promoter (pTREx5Luc) was activated by DOX more than 4.5-fold. In contrast, DOX treatment did not influence transcriptional activity of a viral promoter located in the long terminal repeat of Rous sarcoma virus (Fig. 3C). Recently, Conacci-Sorrell et al. reported that functional inhibition of E-cadherin in SW480 cells resulted in nuclear translocation of β -catenin and activation of β -catenin-mediated transcription (15). As both *fra-1* and *c-jun* genes can be activated by β -catenin signaling (36), we examined whether this pathway was stimulated in 31D6 cells upon DOX treatment. However, a TOPFLASH/FOPFLASH reporter assay performed in DOX-treated or untreated 31D6 cells has demonstrated no effect of Ec1WVM on β -catenin/TCF-dependent transcription (Fig. 3D). Similarly, no activation of β -catenin signaling was observed in stable W2 and W3 clones (data not shown). Therefore, activation of AP-1 by Ec1WVM does not involve β -catenin signaling.

Prolonged and short-term (to a lesser extent) expression of Ec1WVM activates tumor cell migration. Prolonged and short-term expression of Ec1WVM in A431 cells resulted in loss of an epithelial pattern of cell growth and in cell dissociation (Fig. 1 and 3). Prolonged Ec1WVM expression down-regulated keratins and activated expression of vimentin (Fig. 2 and Table 1). Since cells undergoing EMT acquire a migratory phenotype, we hypothesized that Ec1WVM may affect cell motility and lead to increased cell migration into a wound. To test this, wounds were created in confluent cultures of NT-2, W2, and 31D6 cells and 31D6 cells pretreated with DOX for 48 h, and

closure of wounds was monitored after 8 and 17 h. As expected, cells expressing Ec1WVM displayed accelerated wound closure compared with NT-2 and 31D6 cells maintained in the absence of DOX (Fig. 4). Whereas migration of clones with epithelial morphology closed wounds by approximately 50% in 17 h, wounds disappeared in W2 cell cultures. DOX-treated 31D6 cells exhibited an intermediate motility, and in 17 h they migrated approximately 1.7-fold faster than untreated cells. The moderate activation of cell motility in DOX-treated 31D6 cells was statistically significant. On the other hand, DOX produced no effect on migration of stable W3 and NT-2 clones (data not shown).

Transcriptional effects of Ec1WVM require AP-1 activity. Transcription of two members of the AP-1 transcription factor family, *fra-1* and *c-jun*, was activated by Ec1WVM as early as 48 h upon DOX stimulation of 31D6 cells. Positive autoregulatory loops are known to activate *fra-1* and *c-jun* transcription via AP-1-binding elements located in the *fra-1* intronic enhancer and *c-jun* gene promoter (1, 3). To test whether AP-1 activity is necessary for Ec1WVM-mediated up-regulation of *fra-1* and *c-jun* transcription, we employed a bicistronic DOX-sensitive vector pBI to generate a clone in which both Ec1WVM and the AP-1 dominant-negative mutant TAM67 fused with the enhanced green fluorescent protein (TAM67-GFP) are simultaneously induced by DOX (Fig. 5A, clone G10). Simultaneous induction of both Ec1WVM and TAM67 mutant proteins in G10 cells resulted in cell dissociation. There were no clear differences in cell morphology between DOX-treated G10 and 31D6 cells (compare Fig. 3A with 5A). Ex-

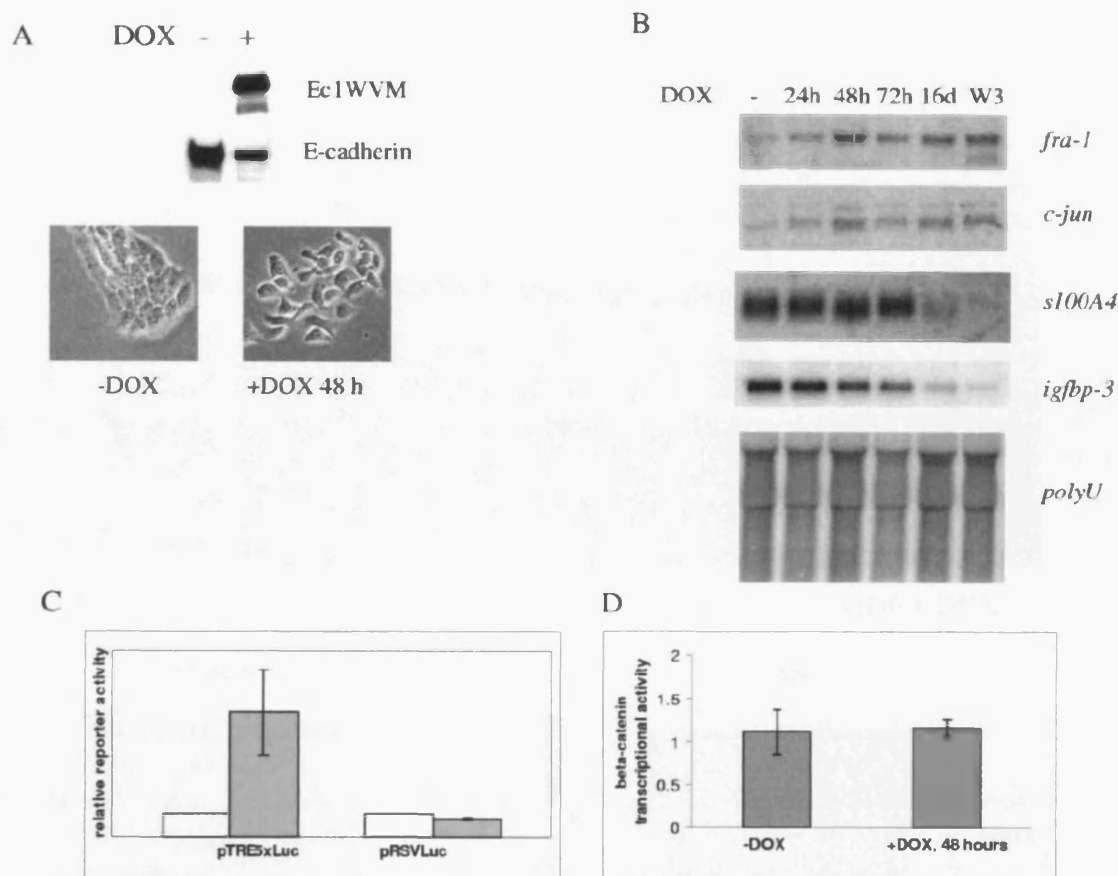


FIG. 3. Ec1WVM mutant induces rapid response in A431 cells. (A) Characterization of the 31D6 clone with DOX-regulated expression of Ec1WVM. Induction of Ec1WVM by DOX treatment for 48 h results in cell dissociation and morphological alterations. Immunoblot analysis of Ec1WVM and endogenous E-cadherin expression is shown in the upper part of the panel. 31D6 cells were maintained in the presence or absence of DOX for 48 h and analyzed with anti-myc and anti-E-cadherin antibodies. (B) Ec1WVM affects transcription of *fra-1*, *c-jun*, *S100A4*, and *igfbp-3* in 31D6 cells. Total RNA was extracted from 31D6 cells maintained without DOX or with DOX for the indicated periods of time. Gene expression was examined by Northern blotting using ^{32}P -labeled probes as indicated. The membrane was probed with labeled *polyU* probe to demonstrate equal loading. (C) Ec1WVM activates AP-1-driven transcription in 31D6 cells. 31D6 cells were transfected with the AP-1-dependent reporter pTRE5Luc or with pRSVLuc along with the control β -galactosidase-expressing vector pCMV β -gal and maintained in the presence (+) or absence (-) of DOX. At 48 h posttransfection, luciferase activity was measured and normalized to the β -galactosidase activity. The results (average and standard deviations) are expressed as the relative activation of luciferase in DOX-treated cells (gray bars) compared to that in untreated cells (white bars). (D) Ec1WVM does not influence TCF/LEF transcriptional activity. 31D6 cells were transfected with pTOPFLASH or pFOPFLASH reporters along with pCMV β -gal and maintained in the absence or presence of DOX for 48 h. Relative TCF/LEF transcriptional activity was defined as ratio of pTOPFLASH/pFOPFLASH luciferase activities normalized to the β -galactosidase level detected in each transfection. The results (means \pm standard deviations) of three independent experiments are shown.

pression of TAM67 not only suppressed AP-1 activation by Ec1WVM but also significantly inhibited the basal AP-1 activity detected in nonstimulated cells. In addition, TAM67 effectively blocked the stimulatory effect of Ec1WVM on *fra-1* and *c-jun* gene transcription (Fig. 5B), suggesting that AP-1 activity is necessary for transcriptional activation of both AP-1 family members induced by the dominant-negative mutant of E-cadherin. Similarly, in a striking difference with 31D6 cells expressing only Ec1WVM, *igfbp-3* and *S100A4* transcription was not affected or only insignificantly affected in G10 cells even after 16 days of culturing in the presence of DOX (compare Fig. 3B with 5B). Therefore, Ec1WVM affects expression of *S100A4* and *igfbp-3* also in AP-1-dependent manner.

Next, we aimed to examine whether stimulation of AP-1 is

sufficient for the transcriptional up-regulation of *fra-1* and *c-jun* genes in A431 cells. Since an AP-1 family member, c-Fos, was most efficient in inducing EMT in murine epithelial cells (19, 21) and has been shown to directly regulate *fra-1* expression (3, 37), we chose to generate a clone of A431 cells with inducible DOX-dependent expression of c-Fos (clone B4). Even though c-Fos strongly activated AP-1-regulated reporter in B4 cells, epithelial cell morphology was not affected (Fig. 5A). Treatment of B4 cells with DOX for 48 h was sufficient to activate transcription of *fra-1* but not *c-jun* (Fig. 5B). Given that TAM67 effectively blocked *c-jun* activation (Fig. 5B), we concluded that Ec1WVM-mediated activation of AP-1 was necessary but not sufficient to up-regulate *c-jun*. These data suggested that although both genes were activated by

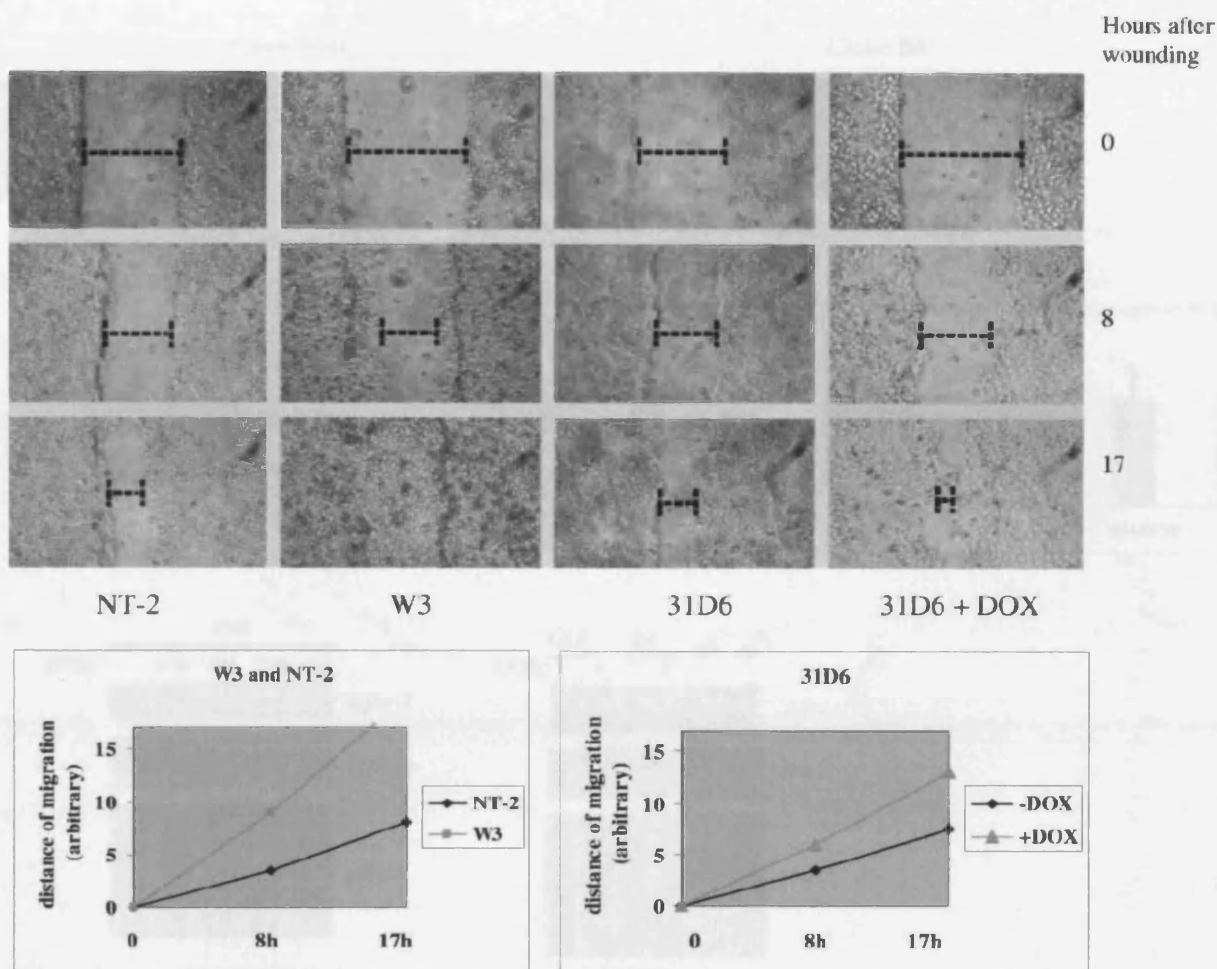


FIG. 4. Effect of Ec1WVM on tumor cell motility. Wounds were created in confluent cultures of NT-2, W3, and 31D6 cells cultured with (+) or without (-) DOX for 48 h prior the experiment. Wounds were marked and photographed after 0, 8, or 17 h. Experiments were repeated three times, and results of a typical experiment are shown. Wound closure at various time intervals was measured in arbitrary units and represented in graphs.

Ec1WVM in an AP-1-dependent manner, the exact mechanisms of transcriptional up-regulation of *fra-1* and *c-jun* were different.

AP-1 is critical for the activation of tumor cell motility by Ec1WVM. We aimed to evaluate whether the effect on tumor cell motility produced by Ec1WVM was AP-1 dependent. Migration into a wound of G10 or B4 cells either maintained without DOX or pretreated with DOX for 48 h was examined. As a positive control, we used a highly motile W3 cell line constitutively expressing Ec1WVM (Fig. 6). Expression of TAM67 not only counteracted the stimulatory effect of Ec1WVM on cell migration observed in 31D6 cells but also almost completely blocked cell motility (Fig. 6, clone G10). Moreover, activation of c-Fos in B4 cells was sufficient to stimulate cell migration into a wound (Fig. 6). Therefore, at early stages of EMT, Ec1WVM-mediated effects on tumor cell motility involve AP-1.

Next, we addressed the question whether the Ec1WVM-mediated activation of the two AP-1 family members Fra-1 and

c-Jun contributes to the enhanced cell motility at later stages of EMT. W3 cells are very motile in wound-healing (Fig. 4 and 6) and transwell migration (data not shown) assays. They express a high level of vimentin and low levels of cytokeratins 13 and 15 and, therefore, can be considered as an end-point of Ec1WVM-induced EMT. We employed RNA interference to suppress the elevated expression of c-Jun and Fra-1 in W3 cells. By transfecting c-Jun and Fra-1-specific siRNAs, we inhibited expression of c-Jun and Fra-1 to levels similar to the level observed in parental A431 cells (Fig. 7A). The effects of single and double knockdowns on cell migration were evaluated in wound-healing and transwell migration assays. Transfection of W3 cells with the scrambled siRNA produced insignificant (if any) effect on cell migration in both wound-healing (compare Fig. 4 and 6 with 7B) and transwell migration assays (data not shown). However, in both assays, W3 cells with reduced Fra-1 and c-Jun expression levels migrated more slowly than cells transfected with the control siRNA (Fig. 7B and C). Although Fra-1 knockdown was more efficient than suppres-

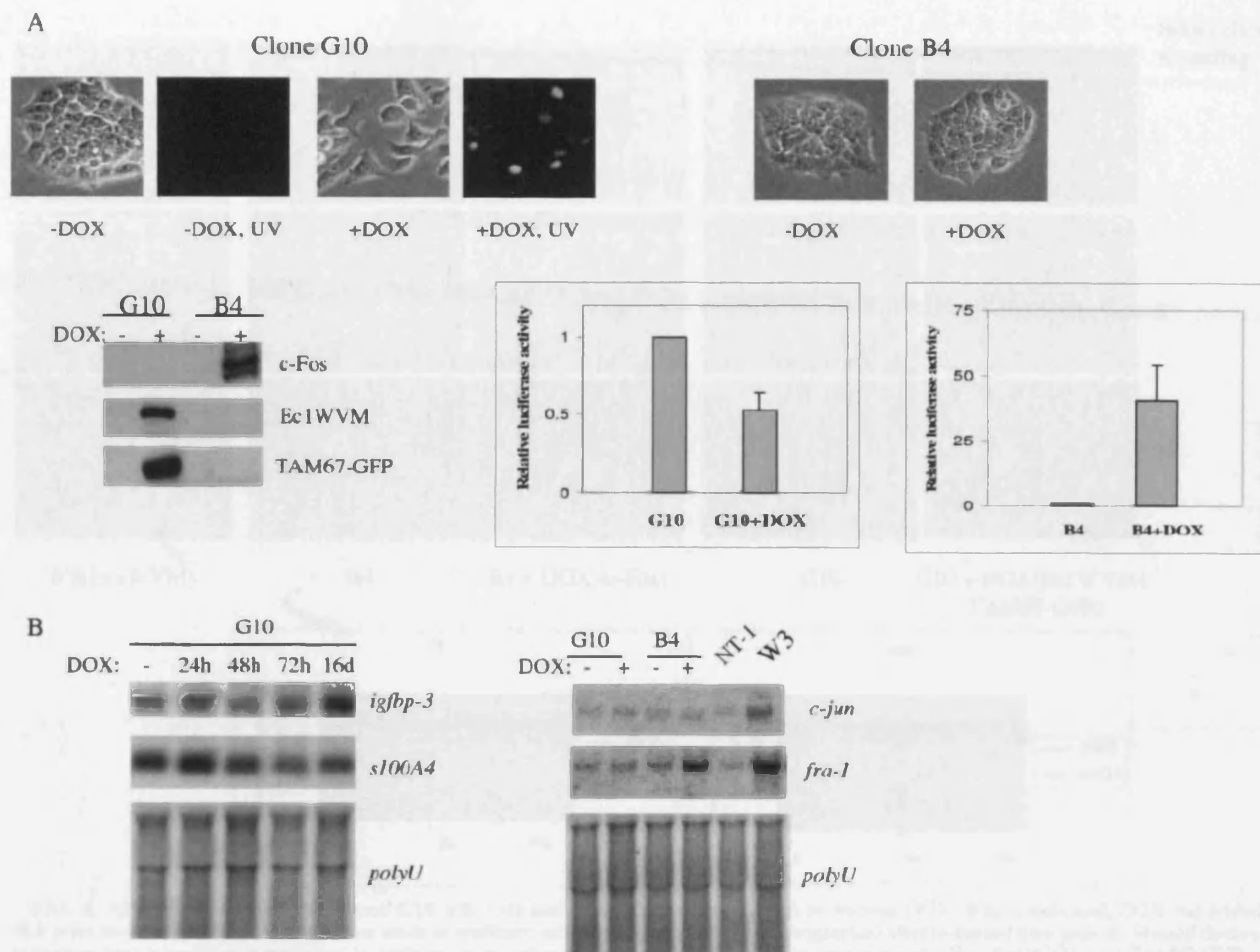


FIG. 5. AP-1 is involved in transcriptional effects of Ec1WVM. (A) Characterization of G10 and B4 clones. DOX induces morphological transformation of G10 but not B4 cells. Phase-contrast and fluorescence microscopy of cells cultured with or without DOX for 48 h is presented. Nuclear localization of TAM67-GFP in DOX-treated G10 cells is demonstrated. Expression of TAM67-GFP fusion protein, Ec1WVM, and c-Fos was examined in DOX-treated or untreated G10 and B4 cells by Western blotting with anti-c-Fos, anti-GFP, and anti-myc antibodies. The effect of DOX treatment on AP-1-dependent transcription in B4 and G10 cells is shown. Cells were transiently transfected with the AP-1-regulated reporter pTREx5Luc, and the activity was determined as described in the legend to Fig. 3. (B) Northern blot analysis of *S100A4*, *igfbp-3*, *c-jun*, and *fra-1* gene expression in G10 and B4 clones. G10 cells were cultured without DOX or with DOX treatment for indicated time periods (left). RNA was isolated, blotted, and hybridized to *S100A4* and *igfbp-3* probes. A Northern blot hybridization of RNA from G10 and B4 cells untreated or treated with DOX for 48 h is shown (right). RNA was hybridized to labeled probes as indicated. Hybridization to *polyU* confirms equal loading.

sion of c-Jun, both knockdowns produced similar effects on wound closure (Fig. 7B). In transwell assays, cells transfected with siRNA specific for c-Jun migrated even somewhat more slowly than cells with suppressed Fra-1 expression (Fig. 7C). Simultaneous knockdown of c-Jun and Fra-1 resulted in the most efficient inhibition of cell motility (Fig. 7B and C). Therefore, enhanced expression of Fra-1 and c-Jun was critically important to maintain enhanced motility of W3 cells.

Ec1WVM does not increase the level of phosphorylated EGFR in A431 cells. Recent work by Qian et al. has demonstrated that the ligand-dependent activation of EGFR and another RTK is negatively regulated by E-cadherin in an adhesion-dependent manner (48). As in a variety of cell types, activation of RTK ultimately results in activation of AP-1, and given that A431 cells express EGFR at very high levels, we hypothesized that

Ec1WVM activates AP-1 via EGFR. To test this hypothesis, we evaluated expression levels of phosphorylated EGFR in stable W2 and NT-2 clones and in 31D6 cells maintained in the absence or in the presence of DOX for 48 h. However, these experiments clearly demonstrated that Ec1WVM does not increase the level of phospho-EGFR in A431 cells (Fig. 8). Moreover, treatment of cells with EGF at different concentrations resulted in activation of EGFR independently of Ec1WVM expression. Thus, activation of AP-1 by Ec1WVM was EGFR independent.

DISCUSSION

EMT underlies dispersing cell lineages in embryonic development and contributes to progression of carcinoma during epithelial tumorigenesis (52, 59, 60). Although a number of in

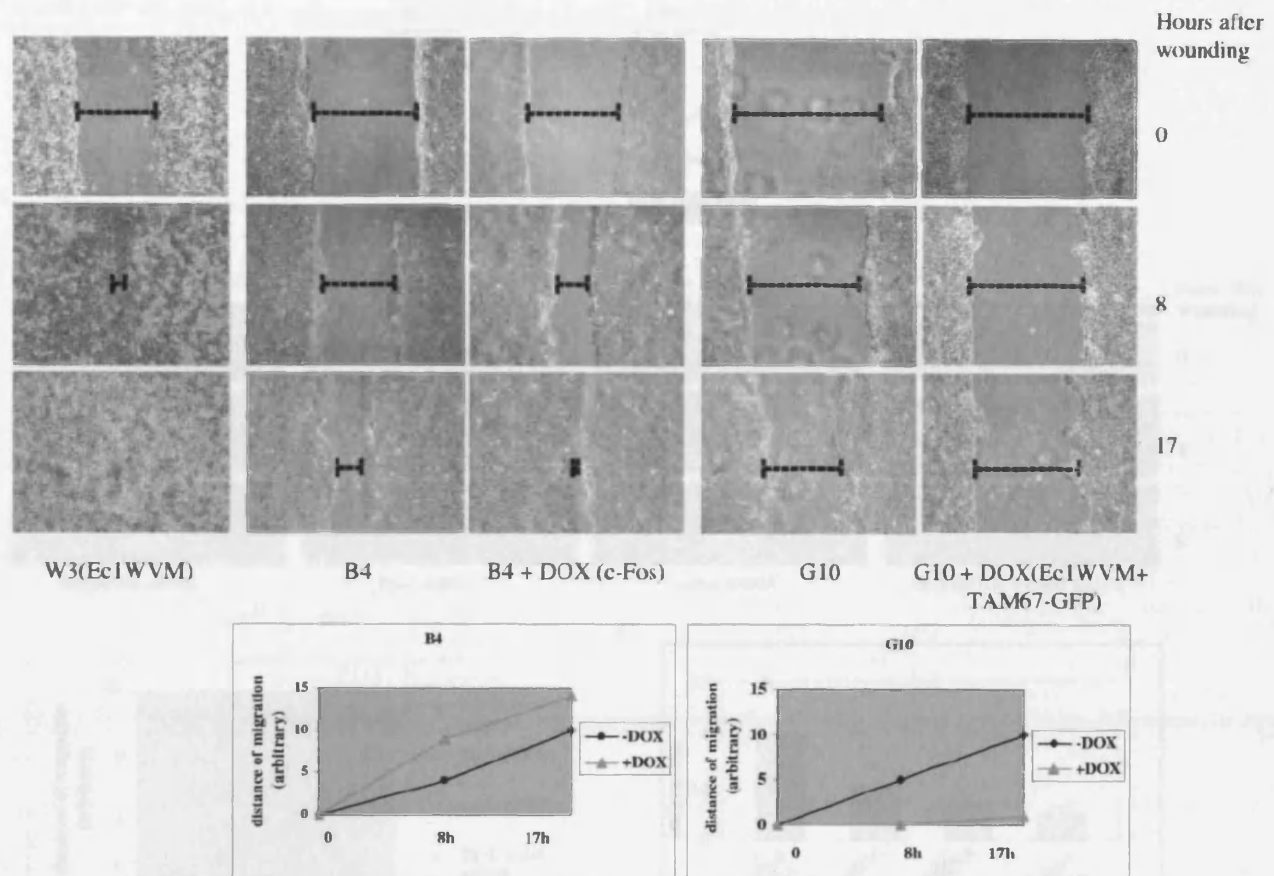


FIG. 6. AP-1 controls motility of B4 and G10 cells. G10 and B4 cells were cultured with or without DOX. Where indicated, DOX was added 48 h prior to the experiment. Wounds were made in confluent cell cultures, marked, and photographed after indicated time periods. Wound closure at various time intervals was measured in arbitrary units and represented in graphs. Ectopic expression of c-Fos, Ec1WVM, and TAM67-GFP is indicated in brackets.

in vitro models of EMT exist, there is no clear consensus on the definition of this phenomenon. In most studies, loss of epithelial polarity accompanied by an increase in cell motility, repression of the epithelial markers E-cadherin and cytokeratins, and activation of the mesenchymal marker vimentin is considered as EMT. In in vitro models of epithelial cancer, EMT can be initiated by various groups of signaling molecules. These include growth factors (EGF, hepatocyte growth factor, transforming growth factor β , or fibroblast growth factor 2) (34, 57, 59), transcription factors (c-Fos, c-Jun, Snail, Slug, ZEB-1, ZEB-2/SIP1, and E47) (2, 6, 8, 14, 19, 20, 21), small GTPases (Ras and Rac) (18, 33), or protein kinases, such as constitutively activated MEK (53). Here, we have demonstrated that prolonged inhibition of E-cadherin function is sufficient for induction of morphological conversion and stimulation of tumor cell motility. By two approaches, we found that stable expression of a dominant-negative E-cadherin mutant, Ec1WVM, alters gene expression pattern. Given that down-regulation of keratins 15 and 13 and activation of vimentin has been observed, we concluded that Ec1WVM induced a complete EMT in A431 cells. Our data show that several phases can be delineated in Ec1WVM-mediated EMT. Morphological

alterations, a moderate but statistically significant increase in cell motility, and activation of AP-1 occurred within 24 to 48 h. Immunoprecipitation experiments demonstrated that these effects were concomitant with the replacement of wild-type E-cadherin by a mutant in adhesive complexes (data not shown). The extended (3 to 16 days) expression of Ec1WVM resulted in down-regulation of *S100A4* and *igfbp-3*, which required AP-1 activity. The majority of changes in gene expression (including up-regulation of vimentin and repression of cytokeratins) were observed only in stable clones but not in 31D6 cells even after 16 days of cultivation in the presence of DOX. In addition, cells constitutively expressing Ec1WVM more rapidly migrated into wounds than DOX-treated 31D6 cells. We therefore conclude that completion of EMT requires prolonged (more than 16 days) inhibition of E-cadherin function.

Transcriptional up-regulation of *fra-1* and *c-jun* and functional activation of AP-1 are early events in Ec1WVM-mediated EMT. Stimulation of *fra-1* and *c-jun* transcription can be blocked by TAM67-GFP (Fig. 5B), suggesting that Ec1WVM activates a positive autoregulatory mechanism that keeps AP-1 activity elevated in cells with compromised cell-cell adhesion.

A431 cells, as other cell lines derived from epithelial cancers,

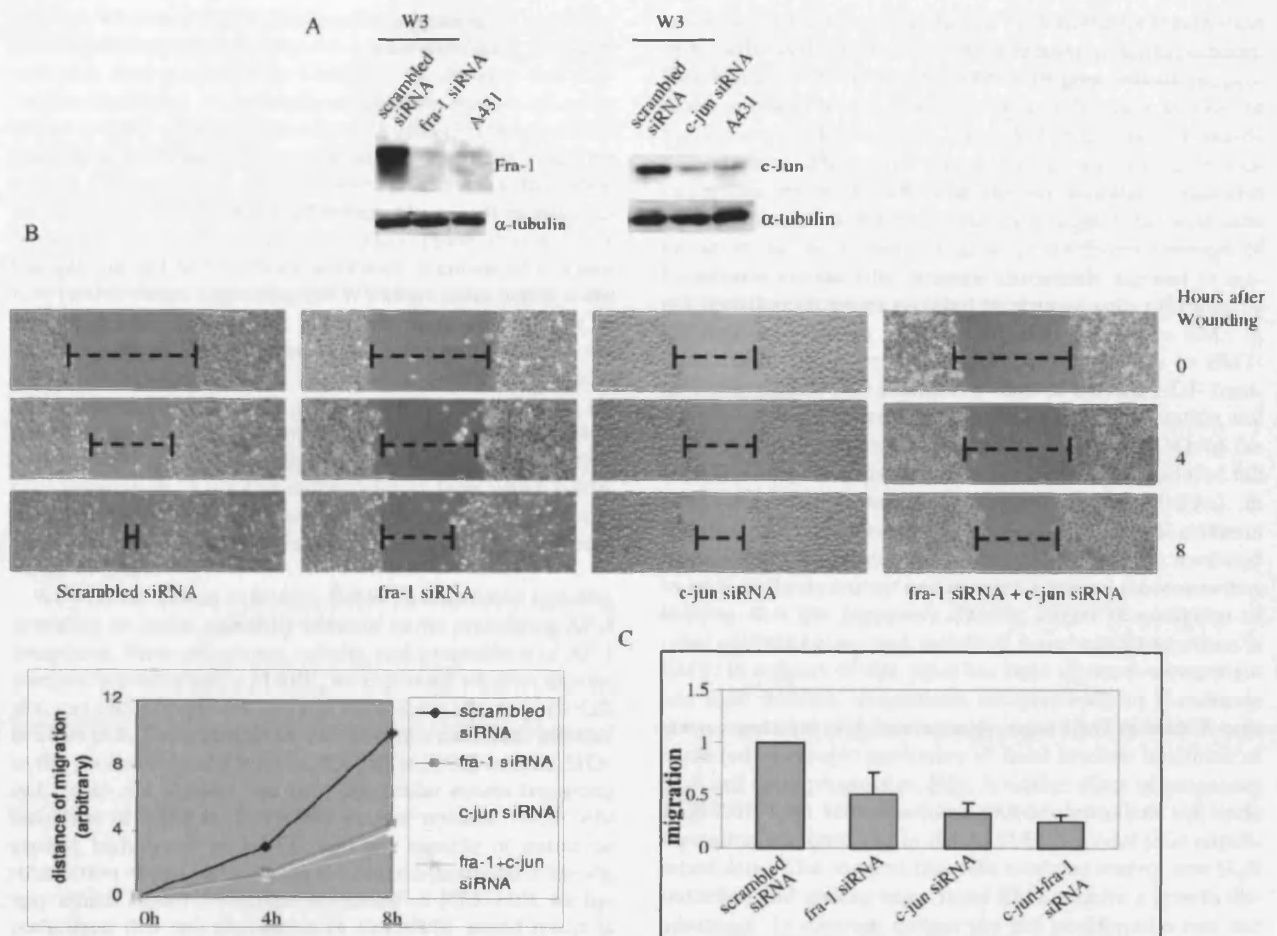


FIG. 7. AP-1 family members c-Jun and Fra-1 are essential for increased motility of W3 cells. (A) RNA interference-mediated inhibition of c-Jun and Fra-1 expression in W3 cells. Cells were transfected with siRNAs targeting c-Jun and Fra-1. Scrambled siRNA was used as a control. The extent of silencing was determined by Western blotting as indicated. (B) Knockdown of c-Jun or Fra-1 retards wound closure. W3 cells were transfected with scrambled siRNA or specific siRNA inhibiting c-Jun or Fra-1 expression. Cell migration was analyzed in wound-healing assays after indicated time intervals. (C) Cell migration was analyzed in transwell motility assay. Expression of c-Jun, Fra-1, or c-Jun and Fra-1 in combination was silenced by RNAi in W3 cells. A total of 10^5 cells were seeded onto 8 μ M polycarbonate transwell filters and allowed to migrate toward fetal calf serum gradient. Cells that migrated to the lower surface of the filter were stained and counted microscopically. Migration was normalized to that of W3 cells transfected with the control siRNA. Data are means \pm the standard deviations of triplicate experiments. The experiments were repeated three times with similar results.

migrate as cell aggregates, sheets, or clusters (collective migration). In this form of migration, aggregated cells move as a functional unit, in which subsets of active cells utilize actin-mediated ruffles and generate integrin-dependent traction.

Other cells included in an aggregate are passively dragged forward by means of intercellular adhesion (reviewed in reference 22). Given that induction of c-Fos in clone B4 does not affect epithelial morphology but is sufficient to accelerate cell

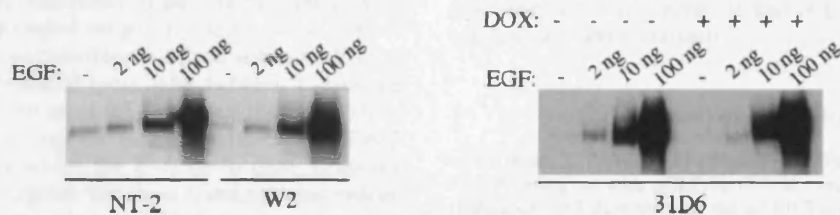


FIG. 8. Expression of Ec1WVM does not alter phosphorylation of EGFR. NT-2, W3, or 31D6 cells were serum depleted for 24 h and treated with indicated concentrations of EGF for 5 min. Expression of Ec1WVM in 31D6 cells was induced by adding DOX for 48 h. EGFR phosphorylation was detected in Western blotting using a phospho-specific antibody.

motility, we conclude that collective migration of epithelial cells is positively regulated by AP-1. This conclusion is consistent with data generated by Malliri et al. showing that prolonged expression of a dominant-negative mutant of c-Jun blocks motility of nonstimulated A431 cells (35). Loss of cell-cell adhesion during EMT results in a switch from collective toward different forms of more efficient individual migration patterns (22). TAM67-GFP effectively blocks cell motility activated by Ec1WVM at an early EMT phase (clone G10). Completion of EMT further contributes to enhanced cell motility (stable clones expressing Ec1WVM are more active in the wounding-healing assay than 31D6 cells pretreated with DOX for 48 h). By RNA interference we demonstrated that enhanced expression of c-Jun and Fra-1 is required for active migration of W3 cells, e.g., at later EMT stages. Taken together, these data clearly demonstrate that the role of AP-1 in cell motility is not restricted to the control of the epithelial type of cell migration. A positive autoregulatory loop, which is triggered by Ec1WVM and activates transcription of *fra-1* and *c-jun* genes, is essential for enhanced cell motility at different stages of EMT.

We were interested to identify Ec1WVM-mediated signaling providing an initial activating stimulus to the preexisting AP-1 complexes. Since abundance, activity, and composition of AP-1 complex is controlled by MAPK, we examined whether expression and phosphorylation levels of MAPK are affected by DOX in 31D6 cells. Even though we did observe a moderate increase in the phosphorylation level of MAPKs in DOX-treated 31D6 cells (data not shown), the exact molecular events triggering induction of AP-1 by Ec1WVM remain unclear. A431 cells express high levels of EGFR and are capable of autocrine stimulation of this receptor. As E-cadherin-mediated adhesion may inhibit ligand-dependent activation of RTK (48), we hypothesized that the application of Ec1WVM would result in activation of EGFR in the A431 cell system. However, Ec1WVM had no effect on phosphorylation of EGFR in DOX-stimulated 31D6 cells (Fig. 8), suggesting that RTK pathways are unlikely to be involved in the activation of AP-1 by Ec1WVM. Nor is β -catenin signaling, known to activate *fra-1* and *c-jun* gene transcription, involved in Ec1WVM-mediated activation of AP-1 (Fig. 3D). One of the hallmarks of EMT is the reorganization of the actin-based cytoskeleton, which reflects loss of epithelial polarity and a switch from cell-cell to cell-substratum interactions. Recently, we found that expression of Ec1WVM in c-Fos-transformed murine epithelioid carcinoma cells resulted in increased cell adhesion to the extracellular matrix components (J. Mejlvang et al., unpublished data). Therefore, we suggest that Ec1WVM may affect cell-substratum interactions also in the A431 cell system, stimulating integrin signaling and hence triggering the initial AP-1 activation. The documented reciprocity between the level of organization of adherens junctions and focal adhesions (31), as well as previously described cross talks between E-cadherin and specific integrin receptors (65), supports this hypothesis.

EMT-inducing transcription factors Snail, Slug, ZEB-2/SIP1, or E47 directly inhibit the E-cadherin gene promoter. Emerging evidence suggests that these transcriptional repressors act downstream of a variety of EMT-initiating signals to down-regulate E-cadherin gene transcription (15, 20, 23, 45). In addition to transcriptional repression, several other genetic

and epigenetic mechanisms may be responsible for inactivation of E-cadherin-dependent cell-cell adhesion in human cancers. E-cadherin function can be inhibited by gene mutations, promoter polymorphisms, promoter hypermethylation, and loss of the E-cadherin locus (4, 17, 26, 66). For instance, in poorly differentiated diffuse-type gastric cancer and lobular breast carcinoma, mutations affecting the extracellular E-cadherin domain have been observed. Our data suggest that structural mutations in the E-cadherin gene or consistent cleavage of E-cadherin extracellular domains chronically exposed to matrix metalloproteinases secreted by stromal cells (32) may be sufficient to trigger a process ultimately leading to EMT in tumor cells. Often, cells respond relatively rapidly to EMT-initiating signals. For example, 5 days of chronic EGF treatment is sufficient to induce morphological transformation and to down-regulate epithelial markers in A431 cells (34). In the same cell line, the transcription factor ZEB-2/SIP1 induced full EMT as rapidly as within 48 h (our unpublished data). In contrast, EMT induced by the dominant-negative E-cadherin mutant is a slow process. Different kinetics of EMTs mediated by an E-cadherin mutant and its transcriptional repressors may indicate that the repressors directly inhibit transcription of other epithelial genes and, therefore, have broader functions in EMT. In support of this, Snail has been shown to down-regulate tight junction components independently of E-cadherin down-regulation (41). Interestingly, rapid EMT of MDCK cells mediated by ectopic expression of Snail involves inhibition of G_1/S cell cycle progression (62). A similar effect of exogenous ZEB-2/SIP1 on retinoblastoma protein-dependent cell cycle regulation was observed in the A431/SIP1 model (our unpublished data). This suggests that cells retaining control over G_1/S transition and undergoing a rapid EMT acquire a growth disadvantage. In contrast, neither the cell proliferation rate nor cell cycle progression was affected in the EMT model reported here (data not shown). Therefore, it is plausible to speculate that SIP1 or Snail induces either transient EMT or stable EMT only in those cells in which control over G_1/S transition has been lost. Gradual EMT initiated by mutations of the components of E-cadherin complex or by cleavage of E-cadherin by proteases may be a prevalent mechanism of stable EMT in cancer cells, in which the control over G_1/S transition is not completely compromised (such as A431 or MDCK cells).

Prolonged inhibition of epithelial adhesion alters expression of several genes that are critical players in signal transduction pathways controlling tumor cell motility and invasive growth. The challenge is to further elucidate molecular mechanisms linking inhibition of epithelial cell adhesion with the alterations in cell signaling networks. This may lead to the design of novel methods uncoupling the loss of E-cadherin from tumor cell invasion and metastasis.

ACKNOWLEDGMENTS

We thank S. Troyanovsky (Washington University Medical School) who provided us with pCMVEc1WVM construct and R. Hennigan (University of Cincinnati) for the pGFP-TAMpuro vector.

We acknowledge financial support from the Prostate Research Campaign UK and the European Association of Urology (European Urology Scholarship Programme).

REFERENCES

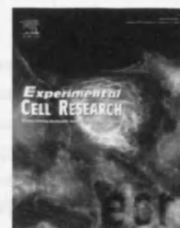
1. Angel, P., K. Hattori, T. Smeal, and M. Karin. 1988. The c-jun proto-oncogene is positively autoregulated by its product, jun/AP-1. *Cell* 55:875-885.
2. Battle, E., E. Sancho, C. Franci, D. Dominguez, M. Monfar, J. Baulida, A. De Herreros. 2000. The transcription factor snail is a repressor of E-cadherin gene expression in epithelial tumour cells. *Nat. Cell Biol.* 2:84-89.
3. Bergers, G., P. Graninger, S. Braselmann, C. Wrighton, and M. Busslinger. 1995. Transcriptional activation of the *fra-1* gene by AP-1 is mediated by regulatory sequences in the first intron. *Mol. Cell Biol.* 15:3748-3758.
4. Bexz, G., K. Becker, H. Hoffer, and F. van Roy. 1998. Mutations of the human E-cadherin (CDH1) gene. *Hum. Mutat.* 12:226-237.
5. Betson, M., E. Lozano, J. Zhang, and V. Braga. 2002. Rac activation upon cell-cell contact formation is dependent on signaling from the epidermal growth factor receptor. *J. Biol. Chem.* 277:36962-36969.
6. Bolos, V., H. Peinado, M. Perez-Moreno, M. Fraga, M. Esteller, and A. Cano. 2003. The transcription factor Slug represses E-cadherin expression and induces epithelial to mesenchymal transitions: a comparison with Snail and E47 repressors. *J. Cell Sci.* 116:499-511.
7. Caca, K., F. Kolligs, J. X. M. Hayes, J. Qian, A. Yahanda, D. Rimm, J. Costa, and E. Fearon. 1999. Beta- and gamma-catenin mutations, but not E-cadherin inactivation, underlie T-cell factor/lymphoid enhancer factor transcriptional deregulation in gastric and pancreatic cancer. *Cell Growth Differ.* 10:369-376.
8. Cano, A., M. A. Pérez-Moreno, I. Rodrigo, A. Locascio, M. J. Blanco, M. G. del Barrio, F. Portillo, and M. A. Nieto. 2000. The transcription factor Snail controls epithelial-mesenchymal transitions by repressing E-cadherin expression. *Nat. Cell Biol.* 2:76-83.
9. Cavallaro, U., and G. Christofori. 2004. Cell adhesion and signalling by cadherins and Ig-CAMs in cancer. *Nat. Rev. Cancer.* 4:118-132.
10. Celis, J. E., P. Gromov, T. Cabezon, J. Moreira, N. Ambartsumian, K. Sandelin, F. Rank, I. Gromova. 2004. Proteomic characterization of the interstitial fluid perfusing the breast tumor microenvironment: a novel resource for biomarker and therapeutic target discovery. *Mol. Cell Proteomics* 3:327-344.
11. Celis, J. E., S. Trentemølle, and P. Gromov. Gel-based proteomics: high resolution two-dimensional gel electrophoresis of proteins. Isoelectric focusing (IEF) and nonequilibrium pH gradient electrophoresis (NEPHGE). In J. E. Celis, N. Carter, T. Hunter, D. Shotton, K. Simons and J. V. Small (ed.), *Cell biology, a laboratory handbook*, vol. 4, 3rd ed., in press. Academic Press, San Diego, Calif.
12. Chitavev, N., S. Troyanovsky. 1998. Adhesive but not lateral E-cadherin complexes require calcium and catenins for their formation. *J. Cell Biol.* 142:837-846.
13. Cohn, M., L. Hjeltno, L.-C. Wu, P. Guldborg, E. Lukanidin, and E. Tulchinsky. 2001. Characterization of Sp1, AP-1, CBF and KRC binding sites and minisatellite DNA as functional elements of the metastasis-associated mts1/S100A4 gene intronic enhancer. *Nucleic Acids Res.* 29:3335-3346.
14. Comijn, J., G. Bexz, P. Vermassen, K. Verschuere, L. van Grunsven, E. Bruyneel, M. Mareel, D. Huylebroeck, and F. van Roy. 2001. The two-handed E box binding zinc finger protein SIP1 downregulates E-cadherin and induces invasion. *Mol. Cell* 7:1267-1278.
15. Conacci-Sorrell, M., I. Simcha, T. Ben-Yedida, J. Blechman, P. Savanger, and A. Ben-Ze'ev. 2003. Autoregulation of E-cadherin expression by cadherin-cadherin interactions: the roles of beta-catenin signalling, Slug and MAPK. *J. Cell Biol.* 163:847-857.
16. Conacci-Sorrell, M., J. Zhurinsky, and A. Ben-Ze'ev. 2002. The cadherin-catenin adhesion system in signalling and cancer. *J. Clin. Investig.* 109:987-991.
17. Di Croce, L., and P. Pelicci. 2003. Tumour-associated hypermethylation: silencing E-cadherin expression enhances invasion and metastasis. *Eur. J. Cancer.* 39:413-414.
18. Edme, N., J. Downward, J.-P. Thiery, and B. Boyer. 2002. Ras induces NBT-II epithelial cell scattering through the coordinate activities of Rac and MAPK pathways. *J. Cell Sci.* 115:2591-2601.
19. Eger, A., A. Stockinger, B. Schaffhauser, H. Beug, and R. Foisner. 2000. Epithelial mesenchymal transition by c-Fos estrogen receptor activation involves nuclear translocation of beta-catenin and upregulation of beta-catenin/lymphoid enhancer binding factor-1 transcriptional activity. *J. Cell Biol.* 148:173-188.
20. Eger, A., K. Aigner, S. Sonderegger, B. Dampier, S. Oehler, M. Schreiber, G. Bexz, A. Cano, H. Beug, and R. Foisner. 2005. DeltaEF1 is a transcriptional repressor of E-cadherin and regulates epithelial plasticity in breast cancer cells. *Oncogene* 24:2375-2385.
21. Flalka, I., H. Schwarz, E. Reichmann, M. Ott, M. Busslinger, H. Beug. 1996. The estrogen-dependent c-JunER protein causes a reversible loss of mammary epithelial cell polarity involving a destabilization of adherens junctions. *J. Cell Biol.* 132:1115-1132.
22. Friedl, P., and K. Wolf. 2003. Tumour-cell invasion and migration: diversity and escape mechanisms. *Nat. Rev. Cancer* 3:362-374.
23. Fujita, N., D. Jaye, M. Kajita, C. Geigerman, C. Moreno, and P. Wade. 2003. MTA3, a Mi-2/NuRD complex subunit, regulates an invasive growth pathway in breast cancer. *Cell* 113:207-219.
24. Gottardi, C., E. Wong, and B. Gumbiner. 2001. E-cadherin suppresses cellular transformation by inhibiting beta-catenin signalling in an adhesion-independent manner. *J. Cell Biol.* 153:1049-1060.
25. Gromova, I., and J. E. Celis. Protein detection in gels by silver staining: a procedure compatible with mass-spectrometry in cell biology. In J. E. Celis, N. Carter, T. Hunter, D. Shotton, K. Simons and J. V. Small (ed.), *Cell biology, a laboratory handbook*, vol. 4, 3rd ed., in press. Academic Press, San Diego, Calif.
26. Guilford, P., J. Hopkins, J. Harraway, M. McLeod, N. McLeod, P. Harawira, H. Taitte, R. Scoular, A. Miller, and A. Reeve. 1998. E-cadherin germline mutations in familial gastric cancer. *Nature* 392:402-405.
27. Hennigan, R., and P. Stambrook. 2001. Dominant negative c-jun inhibits activation of the cyclin D1 and cyclin E kinase complexes. *Mol. Biol. Cell* 12:2352-2363.
28. Hoschuetzky, H., H. Aberle, and R. Kemler. 1994. Beta-catenin mediates the interaction of the cadherin-catenin complex with epidermal growth factor receptor. *J. Cell Biol.* 127:1375-1380.
29. Huelsken, J., and W. Birchmeier. 2001. New aspects of Wnt signaling pathways in higher vertebrates. *Curr. Opin. Genet. Dev.* 11:547-553.
30. Kovacs, E. M., R. All, A. McCormack, and A. Yap. 2002. E-cadherin homophilic ligation directly signals through Rac and phosphatidylinositol 3-kinase to regulate adhesive contacts. *J. Biol. Chem.* 277:6708-6718.
31. Levenberg, S., B.-Z. Katz, K. Yamada, and B. Geiger. 1998. Long-range and selective autoregulation of cell-cell or cell-matrix adhesions by cadherin or integrin ligands. *J. Cell Sci.* 111:347-357.
32. Lochter, A., S. Galosy, J. Muschler, N. Freedman, Z. Werb, and M. Bissell. 1997. Matrix metalloproteinase stromelysin-1 triggers a cascade of molecular alterations that leads to stable epithelial-to-mesenchymal conversion and premalignant phenotype in mammary epithelial cells. *J. Cell Biol.* 139:1861-1872.
33. Lozano, E., M. Betson, and V. Braga. 2003. Tumor progression: small GTPases and loss of cell-cell adhesion. *Bioessays* 25:452-463.
34. Lu, Z., S. Ghosh, Z. Wang, and T. Hunter. 2003. Downregulation of caveolin-1 function by EGF leads to the loss of E-cadherin, increased transcriptional activity of beta-catenin, and enhanced tumor cell invasion. *Cancer Cell* 4:499-515.
35. Malliri, A., M. Symons, R. Hennigan, A. Hurlstone, R. Lamb, T. Wheeler, and B. Ozanne. 1998. The transcription factor AP-1 is required for EGF-induced activation of Rho-like GTPases, cytoskeletal rearrangements, motility, and in vitro invasion of A431 cells. *J. Cell Biol.* 143:1087-1099.
36. Mann, B., M. Gelos, A. Siedow, M. Hanski, A. Gratchev, M. Ilyas, W. Bodmer, M. Moyer, E. Riecken, H. Bühr, and C. Hanski. 1999. Target genes of beta-catenin-T cell-factor/lymphoid-enhancer-factor signaling in human colorectal carcinomas. *Proc. Natl. Acad. Sci. USA* 96:1603-1608.
37. Matsuo, K., J. Owens, M. Tonko, C. Elliott, T. Chambers, and E. Wagner. 2000. Fos1 is a transcriptional target of c-Fos during osteoclast differentiation. *Nat. Genet.* 24:184-187.
38. Nieman, M., J. B. Kim, K. R. Johnson, and M. J. Wheelock. 1999. Mechanism of extracellular domain-deleted dominant negative cadherins. *J. Cell Sci.* 112:1621-1632.
39. Noren, N., W. Arthur, and K. Burridge. 2003. Cadherin engagement inhibits RhoA via p190RhoGAP. *J. Biol. Chem.* 278:13615-13618.
40. O'Farrell, P. H. 1975. High resolution two-dimensional electrophoresis of proteins. *J. Biol. Chem.* 250:4007-4021.
41. Ohkubo, T., and M. Ozawa. 2004. The transcription factor Snail downregulates the tight junction components independently of E-cadherin downregulation. *J. Cell Sci.* 117:1675-1685.
42. Orsulic, S., O. Huber, H. Aberle, S. Arnold, and R. Kemler. 1999. E-cadherin binding prevents beta-catenin nuclear localisation and beta-catenin/LEF-1-mediated transactivation. *J. Cell Sci.* 112:1237-1245.
43. Pece, S., M. Chiariello, C. Murga, and J. Gutkind. 1999. Activation of the protein kinase Akt/PKB by the formation of E-cadherin-mediated cell-cell junctions. Evidence for the association of phosphatidylinositol 3-kinase with the E-cadherin adhesion complex. *J. Biol. Chem.* 274:19347-19351.
44. Pece, S., and J. Gutkind. 2000. Signaling from E-cadherins to the MAPK pathway by the recruitment and activation of epidermal growth factor receptors upon cell-cell contact formation. *J. Biol. Chem.* 275:41227-41233.
45. Peinado, H., M. Quintanilla, and A. Cano. 2003. Transforming growth factor beta-1 induces snail transcription factor in epithelial cell lines. *J. Biol. Chem.* 278:21113-21123.
46. Perez-Moreno, M. A., A. Locascio, I. Rodrigo, G. Dhondt, F. Portillo, M. A. Nieto, and A. Cano. 2001. A new role for E12/E47 in the repression of E-cadherin expression and epithelial-mesenchymal transitions. *J. Biol. Chem.* 276:27424-27431.
47. Polakis, P. 2000. Wnt signalling and cancer. *Genes Dev.* 14:1837-1851.
48. Qian, X., T. Karpova, A. Sheppard, J. McNally, and D. Lowy. 2004. E-cadherin-mediated adhesion inhibits ligand-dependent activation of diverse receptor tyrosine kinases. *EMBO J.* 21:1739-1784.
49. Rappalber, J., Y. Ishihama, and M. Mann. 2003. Stop and go extraction tips

- for matrix-assisted laser desorption/ionization, nanoelectrospray, and LC/MS sample pretreatment in proteomics. *Anal. Chem.* 75:663–670.
50. Sambrook, J., and D. W. Russell. 2001. *Molecular cloning: a laboratory manual*, 3rd ed. Cold Spring Harbor Laboratory Press, Cold Spring Harbor, N.Y.
 51. Sanson, B., P. White, and J.-P. Vincent. 1996. Uncoupling cadherin-based adhesion from wingless signalling in *Drosophila*. *Nature* 383:627–630.
 52. Savagner, P. 2001. Leaving the neighborhood: molecular mechanisms involved during epithelial-mesenchymal transition. *Bioessays* 23:912–923.
 53. Schramek, H., E. Felfel, E. Healy, and V. Pollack. 1997. Constitutively active mutant of the mitogen-activated protein kinase kinase MEK1 induces epithelial dedifferentiation and growth inhibition in Madin-Darby canine kidney-C7 cells. *J. Biol. Chem.* 272:11426–11433.
 54. Shapiro, L., A. M. Fannon, P. D. Kwong, A. Thompson, M. S. Lehmann, G. Grubel, J.-F. Legrand, J. Als-Nielsen, D. R. Colman, and W. A. Hendrickson. 1995. Structural basis of cell-cell adhesion by cadherins. *Nature* 374:327–337.
 55. Shevchenko, A., M. Wilm, O. Vorm, and M. Mann. 1996. Mass spectrometric sequencing of proteins silver-stained polyacrylamide gels. *Anal. Chem.* 68:850–858.
 56. St. Croix, B., C. Sheehan, J. Rak, V. Florenes, J. Slingerland, and R. Kerbel. 1998. E-cadherin-dependent growth suppression is mediated by the cyclin-dependent kinase inhibitor p27(KIP1). *J. Cell Biol.* 142:557–571.
 57. Stockinger, A., A. Eger, J. Wolf, H. Beug, and R. Foisner. 2001. E-cadherin regulates cell growth by modulating proliferation-dependent beta-catenin transcriptional activity. *J. Cell Biol.* 154:1185–1196.
 58. Takeichi, M. 1993. Cadherins in cancer: implications for invasion and metastasis. *Curr. Opin. Cell Biol.* 5:806–811.
 59. Thiery, J.-P. 2003. Epithelial-mesenchymal transitions in development and pathologies. *Curr. Opin. Cell Biol.* 15:740–746.
 60. Thiery, J.-P., and D. Chopin. 1999. Epithelial cell plasticity in development and tumor progression. *Cancer Metastasis Rev.* 18:31–42.
 61. van de Wetering, M., N. Barker, I. Harkes, M. van der Heyden, N. Dijk, A. Hollestelle, J. Kljijn, H. Clevers, and M. Schutte. 2001. Mutant E-cadherin breast cancer cells do not display constitutive Wnt signaling. *Cancer Res.* 61:278–284.
 62. Vega, S., A. Morales, O. Ocaña, F. Valdés, I. Fabregat, and M. A. Nieto. 2004. Snail blocks the cell cycle and confers resistance to cell death. *Genes Dev.* 118:1131–1143.
 63. Vial, E., E. Sahai, and C. J. Marshall. 2003. ERK-MAPK signaling coordinately regulates activity of Rac1 and RhoA for tumor cell motility. *Cancer Cell* 4:67–79.
 64. Vleminckx, K., and R. Kemler. 1999. Cadherins and tissue formation: integrating adhesion and signalling. *Bioessays* 21:211–220.
 65. von Schlippe, M., J. Marshall, P. Perry, M. Stone, A. J. Zhu, and I. R. Hart. 2000. Functional interaction between E-cadherin and av-containing integrins in carcinoma cells. *J. Cell Sci.* 113:425–437.
 66. Wang, H.-D., J. Ren, and L. Zhang. 2004. CDH1 germline mutation in hereditary gastric carcinoma. *World J. Gastroenterol.* 10:3088–3093.
 67. Wong, A., and B. Gumbiner. 2003. Adhesion-independent mechanism for suppression of tumor cell invasion by E-cadherin. *J. Cell Biol.* 161:1191–1203.
 68. Zantek, N., M. Azimi, M. Fedor-Chalken, B. Wang, R. Brackenbury, and M. Kinch. 1999. E-cadherin regulates the function of the EphA2 receptor tyrosine kinase. *Cell Growth Differ.* 10:629–638.

Appendix C

(Publication)

Mejlvang J, Kriajevska M, Berditchevski F, Bronstein I, Lukanidin EM, Pringle JH, Mellon JK, Tulchinsky EM.; Characterization of E-cadherin-dependent and -independent events in a new model of c-Fos-mediated epithelial-mesenchymal transition. **Exp Cell Res.** 2007 ;313(2):380-93

available at www.sciencedirect.com
www.elsevier.com/locate/yexcr

Research Article

Characterization of E-cadherin-dependent and -independent events in a new model of c-Fos-mediated epithelial–mesenchymal transition

Jakob Mejlvang^{a,b}, Marina Kriajevska^a, Fedor Berditchevski^c, Igor Bronstein^d, Eugene M. Lukanidin^b, J. Howard Pringle^e, J. Kilian Mellon^a, Eugene M. Tulchinsky^{a,*}

^aDepartment of Cancer Studies and Molecular Medicine, University of Leicester, Hodgkin Bldg., Lancaster Rd, LE1 9HN, Leicester, UK

^bDepartment of Molecular Cancer Biology, Danish Cancer Society, Copenhagen, Denmark

^cCancer Research UK Institute for Cancer Studies, University of Birmingham, Birmingham, UK

^dMedical Research Council National Institute for Medical Research, The Ridgeway, Mill Hill, London, UK

^eDepartment of Cancer Studies and Molecular Medicine, Robert Kirkpatrick Clinical Sciences Bldg., Leicester, UK

ARTICLE INFORMATION

Article Chronology:

Received 2 June 2006

Revised version received

13 October 2006

Accepted 19 October 2006

Available online 26 October 2006

Keywords:

Epithelial–mesenchymal transition

c-Fos

E-cadherin

Cell adhesion

DNA methylation

ABSTRACT

Fos proteins have been implicated in control of tumorigenesis-related genetic programs including invasion, angiogenesis, cell proliferation and apoptosis. In this study, we demonstrate that c-Fos is able to induce mesenchymal transition in murine tumorigenic epithelial cell lines. Expression of c-Fos in MT1TC1 cells led to prominent alterations in cell morphology, increased expression of mesenchymal markers, vimentin and S100A4, DNA methylation-dependent down-regulation of E-cadherin and abrogation of cell–cell adhesion. In addition, c-Fos induced a strong β -catenin-independent proliferative response in MT1TC1 cells and stimulated cell motility, invasion and adhesion to different extracellular matrix proteins. To explore whether loss of E-cadherin plays a role in c-Fos-mediated mesenchymal transition, we expressed wild-type E-cadherin and two different E-cadherin mutants in MT1TC1/c-fos cells. Expression of wild-type E-cadherin restored epithelioid morphology and enhanced cellular levels of catenins. However, exogenous E-cadherin did not influence expression of c-Fos-dependent genes, only partly suppressed growth of MT1TC1/c-fos cells and produced no effect on c-Fos-stimulated cell motility and invasion in matrigel. On the other hand, re-expression of E-cadherin specifically negated c-Fos-induced adhesion to collagen type I, but not to laminin or fibronectin. Of interest, mutant E-cadherin which lacks the ability to form functional adhesive complexes had an opposite, potentiating effect on cell adhesion to collagen I. These data suggest that cell adhesion to collagen I is regulated by the functional state of E-cadherin. Overall, our data demonstrate that, with the exception of adhesion to collagen I, c-Fos is dominant over E-cadherin in relation to the aspects of mesenchymal transition assayed in this study.

© 2006 Elsevier Inc. All rights reserved.

* Corresponding author. Fax: +44 252 116 2525616.

E-mail address: et32@le.ac.uk (E.M. Tulchinsky).

Introduction

AP-1 transcription factors (Jun/Jun homodimers and Fos/Jun heterodimers) are activated on transcriptional and post-translational levels in response to a multitude of extracellular stimuli. Activated AP-1 binds TREs (TPA-responsive elements) located in enhancers of target genes to up-regulate transcription by recruiting transcriptional co-activators CBP/p300 or JAB1 [1]. AP-1 has been implicated in most fundamental biological processes including cell proliferation [2,3], differentiation [4–6], apoptosis [7–9] and tumorigenesis [9,10]. The prototypical member of the Fos protein family, the transcription factor c-Fos efficiently transforms rodent fibroblasts *in vitro* [11,12], induces formation of osteosarcomas in transgenic animals [13,14] and is required for Src- and Ras-induced oncogenic transformation [10]. The transforming ability of c-Fos and the fact that its expression is tightly linked to mitogenic stimulation by growth factors suggest a role for c-Fos in the control of cell growth [3]. Although c-fos knockout mice are growth retarded, c-fos^{-/-} fibroblasts proliferate normally, likely due to the fact that other Fos family members (FosB, Fra-1 or Fra-2) compensate for the lack of c-Fos [15,16]. The particular function of Fos proteins in tumor cells is context-specific, and the expression of v-Fos in primary or immortalized human fibroblasts does not alter cell proliferation [17], whereas in epithelial hepatocytes, c-Fos-estrogen receptor (Fos-ER) chimera inhibits cell growth [8]. Clearly, the function of c-Fos in tumorigenesis is not restricted to cell cycle control. Since c-Fos, v-Fos and Fra-1 proteins activate the expression of genes implicated in invasion and angiogenesis and influence cell motility [18–23], a role for Fos proteins at later stages of epithelial tumorigenesis has been proposed. The essential role of c-Fos in progression from non-invasive papilloma to malignant tumors has been directly shown in the multistep skin carcinogenesis model using c-fos null mice [24]. Relevant to these data, Fos-ER induces epithelial-mesenchymal transition (EMT) in mouse non-tumorigenic Ep-1 cells [25].

EMT is a regulated phenotypic modulation of epithelial cells, which results in the generation of invasive, motile cell phenotypes. EMT occurs in embryogenesis during gastrulation and neural crest cell migration and at the later stages of epithelial tumorigenesis leading to the formation of metastatic tumors [26]. A hallmark of EMT is the dissociation of adherens junctions, the homophilic E-cadherin-mediated epithelial cell-cell adhesion contacts. Loss of E-cadherin function during embryonic development and tumor progression is believed to have implications for cellular signaling networks [27,28]. Disappearance of E-cadherin may affect signaling by influencing activity of Rho proteins [29], via modulation of receptor tyrosine kinases (EGFR, ErbB2, IGFR or EPHA2) function [30–32] or by activating the β -catenin pathway [33–35]. β -catenin interacts with the C-terminal domain of E-cadherin and links the E-cadherin complexes to the actin cytoskeleton providing stable cell adhesion. A small pool of free β -catenin may interact with TCF/LEF transcription factors and activate transcription by providing a transactivation domain [36]. β -catenin signaling contributes to tumorigenesis by transcriptional activation of genes regulating cell cycle progression and tumor cell invasion. The signaling pool of β -

catenin may be sequestered by E-cadherin leading to the inhibition of β -catenin signaling. In the last 5 years, progress has been made in understanding mechanisms responsible for the silencing of E-cadherin in tumor progression. Transcriptional repressors belonging to three protein families, Snail/Slug, ZEB-1(DeltaEF1)/ZEB-2(SIP1) and E12/E47 have been shown to directly interact with *e-cadherin* promoter DNA and actively repress transcription. Other mechanisms of functional inhibition of E-cadherin include gene mutations [37–39] and hypermethylation of a CpG island near the *e-cadherin* transcription start site [40,41]. Loss of E-cadherin expression or mutations in the gene are associated with several forms of epithelial cancer [42], and an invasion suppressor role for E-cadherin has been demonstrated in a transgenic mouse model [43]. The EMT of Ep-1 cells induced by the activation of Fos-ER was accompanied by changes in gene expression program involving down-regulation of E-cadherin and up-regulation of mesenchymal markers and several extracellular matrix-degrading proteases [25]. Loss of E-cadherin resulted in nuclear re-localization of β -catenin and β -catenin/LEF-dependent transcription [44]. Activation of this pathway was shown to be essential for the proliferation and survival of Ep-1 cells undergoing Fos-ER-mediated EMT [34].

Thus, the considerable amount of experimental data suggests a regulatory role for c-Fos at later stages of epithelial tumorigenesis. In addition, deregulation of c-Fos expression has been reported in several forms of human cancer (for references, see [45]). However, c-Fos function in established carcinoma cell cultures has not been studied. In this study, we show that epithelioid mouse mammary adenocarcinoma cells undergo EMT in response to c-Fos. Morphological transition of these cells was concomitant with the down-regulation of E-cadherin. We address the mechanisms of E-cadherin down-regulation and its involvement in c-Fos-mediated EMT in carcinoma cells.

Materials and methods

Plasmids

A retroviral vector containing c-Fos (pMVC-fos) has been described earlier [21]. To generate E-cadherin-expressing vectors, myc-tagged wild-type or mutant E-cadherin cDNA [46] was subcloned in pIRESpuro2 expression vector conferring puromycin resistance.

Retroviral infection

Infection of mouse epithelioid carcinoma cells with a pMVC-fos virus or with the empty vector, pMV-7, has been described previously [21]. Briefly, GP+E packaging cell line [47] was employed to produce replication-defective retroviruses. Virus-containing supernatant was used to infect MT1TC1, VMR-Liv or RAC10P cells using 4 μ g/ml polybrene. Infected cell populations were selected for 10 days in the presence of 400 μ g/ml G418.

Cell lines and transfections

Mouse mammary epithelioid adenocarcinoma cell lines MT1TC1 [48], VMR-Liv [49] and Rac10P [50], cells infected

with retroviral vectors, all clones expressing E-cadherin and human embryonic kidney (HEK)-293 cells were cultured in DMEM containing 10% fetal bovine serum. In some experiments, cells were treated with 5-Aza-dC at a concentration of 5 μ M. To generate E-cadherin expressing clones, MT1TC1/pMVC-fos subclone, A11 (2×10^6 cells in 100 μ l of phosphate-buffered saline) was transfected by electroporation with a single pulse of 250 V and 250 μ Fd by using the Gene Pulser Xcell electroporation system (Bio-Rad). Transfected cells were seeded on 96 well plates with subsequent selection of clones in the presence of puromycin at a concentration of 0.5 μ g/ml.

Reporter gene assays

To determine TCF/LEF transcriptional activity, cells were transfected as described above with 2 μ g pTOPFLASH or pFOPFLASH luciferase reporter constructs. The efficiency of each transfection was monitored using 400 ng cotransfected β -galactosidase expression vector, pCMV β -gal (Invitrogen). In some experiments, 1 μ g of expression vector for truncated β -catenin, pCGN Δ β -cat [51] was added. At 2 days post-transfection, cells were lysed and the luciferase activity was measured with a tube luminometer (Berthold). The lysates obtained were also tested for β -galactosidase activity by using o-nitrophenyl- β -D-galactopyranoside (Sigma) as a chromogenic substrate. Results were expressed as a ratio of pTOPFLASH and pFOPFLASH reporter activities normalized to the activity of β -galactosidase in each experiment. E-cadherin promoter activity was analyzed in similar manner using 2 μ g of luciferase reporter constructs containing either wild-type E-cadherin promoter, or E-cadherin promoter with mutated E2 boxes [52].

Western blotting

Total protein concentrations were measured using the BCA protein assay kit (Pierce). Denatured protein samples were resolved in gradient polyacrylamide gels. Proteins were transferred to Immobilon-P membranes (Millipore) by standard procedures and incubated in blocking solution with primary antibodies for 1 h at room temperature. Primary antibodies were purchased from Santa Cruz (Myc epitope 9E10, Fra-1), BD Transduction labs (E-cadherin, β -catenin, α -catenin, p120 catenin), NeoMarkers (MMP-2), Oncogene Research Products (c-Fos) and Sigma (α -tubulin). An antibody to the α 2 integrin subunit was purchased from Chemicon; anti-integrin β 1 subunit antibody was from BD Bioscience Pharmingen. Antibody to integrin α 1 was provided by Dr Danker and anti- α 11 antibody was a gift of Dr Gullberg.

Northern blotting

For Northern blot analysis, total RNA was extracted with TRIzol reagent (Invitrogen) and separated in 1.2% agarose gels. RNA blotting and hybridization were performed as described [53]. Radioactive DNA probes were synthesized using random-primed labeling kit (Amersham). For radioactive labeling, 200–300 bp cDNA fragments corresponding to coding parts of genes were generated by RT PCR.

Hybridization of cDNA expression array

To identify genes differentially expressed in clones expressing wild-type E-cadherin or Ec1WVM mutant, the Atlas Human cancer 1.2 cDNA Expression Array was used (Clontech Laboratories, Inc.). Total RNA was isolated from A11, Ec1-1, Ec1-2, Ec1WVM-2 and Ec1WVM-3 clones treated with RNase-free DNase (Ambion), labeled and then hybridized with arrays according to manufacturer's protocols. The filters were exposed to PhosphorImager screens at room temperature for 72 h and scans were quantified using AtlasImage Software (BD Clontech) allowing a global background correction.

Immunofluorescent staining

For immunofluorescent staining, cells were grown for 2–3 days in 10-well glass microscope slides (VWR). Cells were washed and fixed in acetone/methanol (1:1) solution for 3 min on ice. After rinsing, the slides were incubated with primary antibodies for 1 h at room temperature, rinsed and incubated in Alexa 488-conjugated rabbit anti-mouse IgG (Pierce) for 1 h. Cells were examined and photographed using Nikon TE 2000-S inverted microscope.

Biological methods

For cell growth analysis, MTT assay was used. MTT reagent (3-[4,5-dimethylthiazol-2-yl]-2,5-diphenyltetrazolium bromide) was purchased from Sigma. 96-well plates were seeded with 500, 1000 or 1500 cells per well, and cell growth was assayed everyday by MTT conversion according to manufacturer's recommendations. The absorbance was measured on a plate reader (Dynex Technologies) at a test wavelength of 570 nm. To avoid potential artifacts generated as a result of differences in MTT conversion between different cell lines and errors in cell counting, the absorbance at each time point was normalized to the absorbance measured at 48 h taken as 1.

For cell adhesion assays, 96 well tissue culture plates were coated with 20 μ g/ml human laminin, 50 μ g/ml human fibronectin or 200 μ g/ml rat collagen type I (all from BD Biosciences) by overnight adsorption at 4°C. Plates were blocked in 1% bovine serum albumin in serum free media for 1 h at 37°C. For the assay, cells were grown for 72–96 h to form dense cultures with established intercellular contacts and detached from plastic by incubation with the nonenzymatic cell dissociation buffer (Invitrogen). 10^5 cells in 100 μ l suspension were applied per well. To control the amount of cells, 100 μ l of cell suspension in DMEM containing 10% fetal bovine serum (FBS) was seeded in three wells and incubated for 3 h. Plates were incubated for 40 min (laminin, fibronectin) or 1.5 h and 3 h (collagen I) rinsed three times with serum-free medium and the extent of adhesion was determined after fixation and staining of adherent cells with 0.1% crystal violet in 20% ethanol and absorbance measurements at 570 nm using a microplate assay reader (Dynex Technologies). A blank value corresponding to BSA-coated wells was subtracted. Adhesion to substrates was normalized to the total amount of cells determined in assays performed in the presence of 10% fetal bovine serum.

To monitor cell motility, the directed migration assay was performed using uncoated 24-well transwell plates with 8 μm pores (BD Biosciences). 5×10^4 cells were seeded in culture inserts. Adhered cells were allowed to migrate toward gradient of serum used as a chemoattractant in the lower chamber for 3 h. Non-motile cells on the top of the filter were removed using a cotton swab. Cells traversing the membrane were fixed, stained with a Gurr rapid staining kit (BDH) and counted by bright-field microscopy at a magnification of $\times 200$ in four random fields using the ImageJ program.

To analyze cell invasion, the inverse invasion assay was performed as described [23]. In brief, 6×10^4 cells were seeded on the underside of the polycarbonate filter of a Transwell chamber containing 100 μl of matrigel basement membrane matrix (Becton Dickinson) diluted 1:1. Cells were allowed to adhere for 3 h and washed by DMEM. Transwell chambers were placed in wells, filled with 1 ml of DMEM with or without DOX. In 3 days, cells were fixed in methanol and stained for 1 h in propidium iodide solution (10 $\mu\text{g/ml}$). Optical sections were scanned at 10 μM intervals using the confocal microscope Zeiss 510.

Quantitative real-time PCR analysis

RNA was isolated using TRIzol reagent (Invitrogen). cDNA synthesis was carried out using random hexamers and Superscript II (Invitrogen). PCR was performed using SYBR Green PCR Master Mix in the PRISM 7700 Sequence Detection System (Applied Biosystems). Primers were designed to cross exon–exon boundaries (Supplementary Table 1) and used at a concentration of 900 nM. Each sample was run in triplicate. The C_T (threshold cycle when fluorescence intensity exceeds 10 times the SD of the baseline fluorescence) values for the target amplicon and endogenous control (β -actin) were determined for each sample. Quantification was performed using the comparative C_T method ($\Delta\Delta C_T$).

Methylation specific PCR (MSP)

Genomic DNA was isolated by standard methods and treated with sodium bisulfite as previously described [54]. Methylated (M) and unmethylated (U) primers for E-cadherin promoter were designed using MethPrimer program [55] as indicated in Supplementary Fig. 1. PCR products were run on 3% agarose gels and visualized after ethidium bromide staining.

Statistics

Statistical analysis was performed with Student's *t* test using GraphPad Prism Software. Differences were considered to be statistically significant at $P < 0.05$.

Results

Prolonged expression of c-Fos induces EMT in mouse epithelial tumor cell lines

The ability of c-Fos to induce EMT in carcinoma cells retaining epithelial features has not been studied. To address this issue, we selected three murine tumorigenic epithelial cell lines.

VMR-Liv, Rac10P and MT1TC1. Cell lines were infected with a retroviral vector, pMVc-fos, or with an empty vector, pMV-7, and cells harboring viral sequences were selected in the presence of G418. Gross morphological alterations occurred in all cell lines infected with pMVc-fos. The cells lost epithelial appearance, became elongated and spindle shaped resembling the morphology of mesenchymal cells. In all three cell lines, breakdown of epithelial morphology was accompanied by a significant inhibition of *e-cadherin* gene transcription. On the other hand, cells infected with the control virus retained the parental epithelial cell phenotype (Fig. 1A). These observations indicate that prolonged c-Fos expression in mouse epithelial tumor cell lines results in alterations resembling EMT. Since among three cell lines analyzed, MT1TC1 cells exhibited most stable polarized epithelial phenotype that was entirely altered by c-Fos expression, these cells were chosen for further experiments. We analyzed the effect of c-Fos on the expression of α - and β -catenins, which in conjunction with E-cadherin are essential components of adherens junctions. In MT1TC1c-fos cells, protein expression of α - and β -catenins was strongly reduced. However, whereas c-Fos inhibited *e-cadherin* transcription, the level of α - and β -catenins mRNA was not affected (Fig. 1B). These data suggest that the formation of the E-cadherin-catenin complexes may prevent catenins from proteolytic degradation in cytoplasm and that the introduction of exogenous E-cadherin may stabilize catenins and restore epithelial adhesion in MT1TC1/c-fos cells. Up-regulation of two mesenchymal markers vimentin and S100A4 (see Fig. 3) demonstrates completeness of c-Fos-mediated EMT in MT1TC1 cells.

Exogenous wild-type and mutant E-cadherin expression in MT1TC1 cells

To assess the role of E-cadherin loss in c-Fos-mediated EMT, we aimed to express wild-type E-cadherin (Ec1) and two E-cadherin mutants (Ec1 $\Delta\beta$ and Ec1WVM) [46] in MT1TC1/c-fos cells (Fig. 2A). Ec1 $\Delta\beta$ lacks a β -catenin-binding domain, whereas Ec1WVM harbors a Trp²Val³/AlaGly substitution preventing formation of adhesive E-cadherin complexes and producing a strong dominant-negative effect on cell–cell adhesion [46]. All E-cadherin derivatives contained a C-terminal 6xmyc tag epitope and a 17 amino acid deletion in the cytosolic domain eliminating the recognition by a commercial anti-E-cadherin antibody (BD Bioscience, clone C20820). These modifications allowed us to differentiate between endogenous and exogenous forms of E-cadherin in transfected cells. To minimize cloning artifacts, we obtained sub-clones of MT1TC1/c-fos cells that appeared to be morphologically identical and expressed similar levels of c-Fos (data not shown). One of the sub-clones, A11, has been used to generate transfected cell lines for each construct. All clones including A11 parental cell line contained equal quantities of c-Fos indicating that the differences between E-cadherin-expressing clones are not due to the different c-Fos levels (Fig. 2B). As expected, immunoprecipitation of E-cadherin/catenin complexes with 9E10 antibody followed by Western blotting demonstrated that E-cadherin is associated with α - and β -catenins in Ec1 and Ec1WVM but not in Ec1 $\Delta\beta$ clones (data not shown). Accordingly, ectopic expression of Ec1 and Ec1WVM.

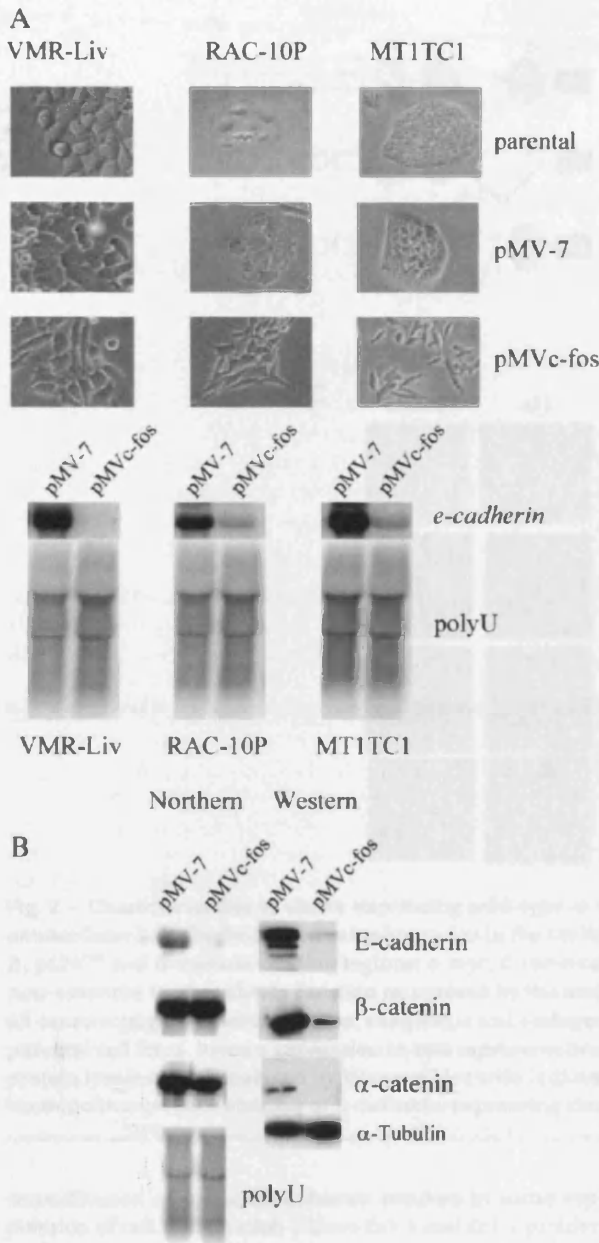


Fig. 1 – c-Fos induces EMT in mouse epithelioid adenocarcinoma cell lines. (A) Phase contrast microscopy of parental cells, cells infected with the c-Fos-expressing retrovirus (pMVc-fos) or with the empty vector (pMV-7). Transcription of the *e-cadherin* gene in cells infected with pMV-7 or with pMVc-fos was analyzed by Northern blot. The blots were re-hybridized with polyU probe. **(B)** Northern and Western blot analysis of E-cadherin and catenins in MT1TC1/pMV-7 and MT1TC1/c-fos cells.

but not Ec1Δβ restored protein levels of α- and β-catenins providing evidence that the down-regulation of catenins in MT1TC1/c-fos cells was indeed due to transcriptional repression of the *e-cadherin* gene. Contrary to α- and β-catenins, the

average p120^{ctn} expression level was higher in Ec1Δβ than in Ec1 clones. The enhanced stabilization of p120^{ctn} by an E-cadherin mutant with the deleted β-catenin-binding domain may indicate the negative effect of β-catenin on E-cadherin/p120^{ctn} interaction. Cells transfected with Ec1WVM and Ec1Δβ retained a fibroblastoid phenotype similar to the parental A11 cells. On the contrary, Ec1-expressing cells, although retaining elongated cell shape, exhibited more epithelial morphology with extended cell-cell contact regions. However, re-introduction of wild-type E-cadherin was insufficient to fully restore MT1TC1 polarized cobblestone-type cell phenotype (Fig. 2C). MT1TC1 and Ec1 cells similarly displayed epithelial staining pattern for E-cadherin, and β-catenin. Although E-cadherin mutants were delivered to the cell surface, we observed more cytoplasmic staining for Ec1WVM and Ec1Δβ than for Ec1 protein. In Ec1WVM clones, catenins were localized to the cell surface and cytoplasm (Fig. 2C).

E-cadherin does not suppress the effect of c-Fos on gene expression

There are gross alterations in the gene expression program in the course of EMT. We assayed the expression of direct c-Fos transcriptional targets in parental cell lines and in E-cadherin-expressing clones. Expression of AP-1 immediate targets Fra-1 [12,56], S100A4 [57] and MMP-2 [58] was significantly higher in A11 than in MT1TC1 cells (Fig. 3). However, in all E-cadherin-expressing cell lines, the expression of these genes was not suppressed. Similarly, up-regulation of a mesenchymal marker, vimentin and down-regulation of endogenous E-cadherin was not affected by exogenous E-cadherin or by either of the mutants (Fig. 3). To examine whether reconstitution of epithelial adhesion in Ec1 clones may suppress the effects of c-Fos on the expression of any other genes, we compared the transcription of 1176 cancer-related genes in Ec1-1, Ec1-2, Ec1WVM-2, Ec1WVM-3 and A11 cells (Atlas Mouse Cancer 1.2 Array, Clontech). However, apart from several clonal variations, no difference in gene expression in these cell lines was observed. Therefore, at least for the majority of the genes, E-cadherin does not suppress the effect of c-Fos on gene expression in A11 cells.

c-Fos activates cell proliferation, cell motility and invasion to a greater extent independently of E-cadherin and β-catenin signaling

As c-Fos is widely recognized as a regulator of cell proliferation and apoptosis, we employed the MTT assay to test, whether cell growth was affected in A11 cells and E-cadherin-expressing subclones. Firstly, to exclude potential artifacts generated as a result of subcloning of MT1TC1/c-fos cells, proliferation curves of A11 cells and two other MT1TC1/c-fos subclones were compared using the MTT assay. These three cell lines were found to proliferate with similar rates (data not shown). Expression of c-Fos resulted in activation of growth rate (doubling time of A11 and MT1TC1 cells differed by 25–30%; compare growth curves for MT1TC1 and A11 cell lines in Fig. 4A). Since E-cadherin has been implicated in cell growth control, we tested whether down-regulation of E-cadherin contributed to the effect of c-Fos on cell proliferation. The

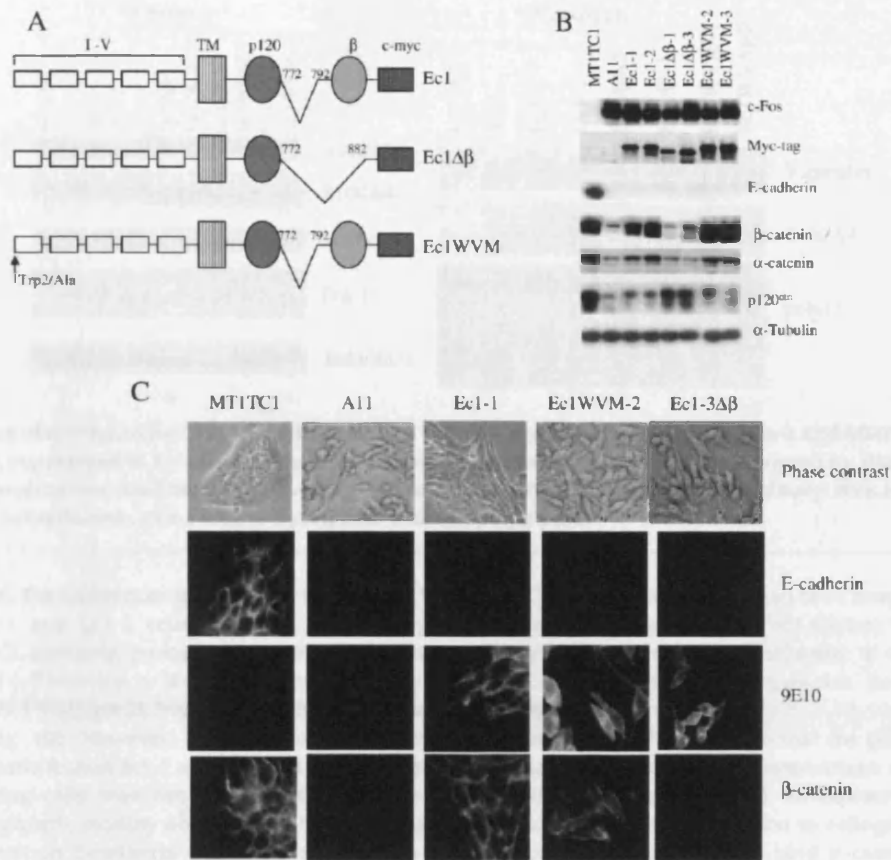


Fig. 2 – Characterization of clones expressing wild-type or mutant E-cadherin. (A) Schematic diagram of constructs. I–V, extracellular E-cadherin-like domains (mutation in the Ec1WVM construct is indicated); TM, transmembrane domain; p120 and β , p120^{ex} and β -catenin-binding regions; c-myc, C-terminal myc-tag. Deletions are indicated. Note that an epitope non-essential for E-cadherin function recognized by the antibody (C20820, BD, Transduction Laboratories) has been deleted in all constructs. (B) Detection of c-Fos, exogenous and endogenous E-cadherin and catenins in E-cadherin expressing clones and parental cell lines. Protein expression in two representative clones for each E-cadherin construct is shown. Equal amounts of protein lysates were analyzed by Western blot with indicated antibodies. (C) Phase contrast microscopy and indirect immunofluorescence staining of E-cadherin-expressing clones and parental cell lines.

reconstitution of epithelial adhesion resulted in some suppression of cell proliferation (clones Ec1-1 and Ec1-2 proliferated somewhat slower than clones expressing E-cadherin mutants or A11 cells). However, the strong effect of c-Fos on cell proliferation in MT1TC1 cells cannot be solely attributed to loss of E-cadherin. Of note, E-cadherin mutants defective in intercellular adhesion produced no effect on cell growth independently of their ability to bind and stabilize β -catenin (Fig. 4A). These data argue against the involvement of β -catenin pathway in the proliferative response of MT1TC1 cells induced by c-Fos expression. Indeed, the TOPFLASH/FOPFLASH reporter assay demonstrated very low TCF-dependent transcriptional activity in MT1TC1 or A11 cells (Fig. 4B) when compared with the data obtained in human colorectal cancer cell lines in which this pathway is constitutively active (100–150-fold difference between TOPFLASH and FOPFLASH activities [59]). Moreover, no activation of TCF-dependent transcription was observed in MT1TC1 or A11 cells transfected with the Δ CGN Δ - β -catenin vector expressing a stabilized

form of β -catenin which lacks the 57 N-terminal amino acids and stimulates TCF-driven transcription more efficiently than wild-type β -catenin. As a positive control, we used HEK-293 cell line in which Δ N- β -catenin induced 27-fold activation of TCF-driven transcription (Fig. 4B). These data suggest that MT1TC1 cells were not competent to transduce β -catenin signals even in artificial conditions of transient transfection, when β -catenin was expressed in non-physiological levels. Therefore, c-Fos-induced EMT of MT1TC1 cells did not involve β -catenin signaling.

As EMT generates more motile and invasive cell variants, we analyzed migratory capabilities of cells using three different approaches, wound-healing, transwell migration assay and 3D Matrigel invasion assay. Whereas MT1TC1, A11 cells and all clones equally displayed very slow wound closure (data not shown), directed transwell motility assay revealed significant activation of cell motility as a result of c-Fos-mediated EMT. A11 cells migrated through the pores of transwell filters 10-fold more efficiently than MT1TC1 cells.

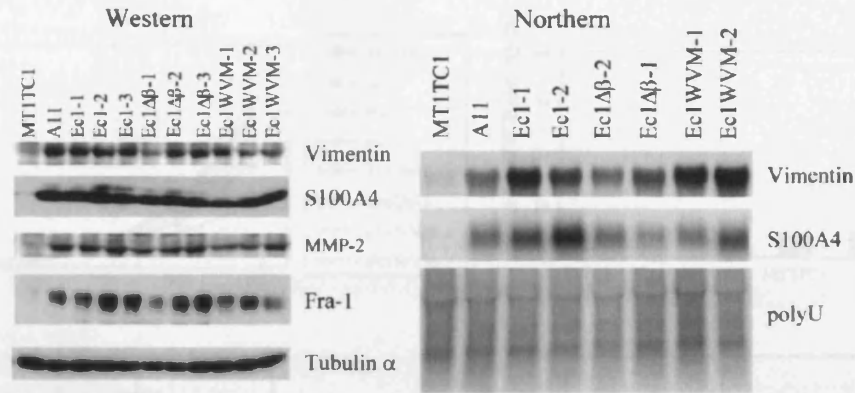


Fig. 3 – Expression of mesenchymal markers (vimentin and S100A4) and c-Fos direct targets (Fra-1 and MMP-2) is enhanced in A11 cells, but not suppressed in E-cadherin-expressing clones. Expression of proteins was analyzed by Western blot as indicated. Equal loading was confirmed by re-probing the membrane with an anti- α -tubulin antibody. RNA level was assessed by Northern blot hybridization. Filter was re-hybridized with the polyU probe.

On the other hand, the differences in migration between A11 and Ec1-1 or A11 and Ec1-2 cells were not statistically significant (Fig. 4C). Similarly, prolonged expression of c-Fos strongly activated cell invasion in 3D matrigel invasion assay. A11 cells penetrated matrigel 22.5-fold more efficiently than MT1TC1 cells (Fig. 4D). However, the inhibitory effect of exogenous E-cadherin (clones Ec1-1 and Ec1-2) on the invasion of c-Fos-expressing cells was not significant. Therefore, activation of cell growth, motility and invasion by c-Fos was largely independent on E-cadherin down-regulation and β -catenin signaling (Fig. 4).

c-Fos activates cell-ECM adhesion. The role of E-cadherin

Given that there is an evidence of cross-talk between integrins and E-cadherin [60–64], we aimed to examine whether c-Fos-induced EMT involved changes in cell-matrix interactions and whether these changes were dependent on loss of E-cadherin. To test the functional status of extracellular matrix receptors in E-cadherin-expressing clones and parental cell lines, we measured cell adhesion to fibronectin, laminin or type I collagen. c-Fos-mediated EMT increased adhesion to fibronectin (2.5-fold), laminin (4.8-fold) and collagen (5.3-fold) (Figs. 5A and B). Re-expression of wild-type or mutant E-cadherin in A11 cells produced no or only minimal effect on cell adhesion to laminin or fibronectin. On the contrary, wild-type E-cadherin but not mutants completely reverted the stimulatory effect of c-Fos on cell adhesion to collagen I (Fig. 5B, left panel). Moreover, whereas the Ec1Δ β mutant had statistically insignificant effect on the adhesion to collagen I, Ec1WVM protein defective in the formation of adhesive dimers, strongly stimulated adhesion by 4.3- (clone Ec1WVM-2) or 3.8-fold (clone Ec1WVM-3) (Fig. 5B, right panel). In addition, Ec1WVM-2, to a lesser extent Ec1Δ β -1 and A11 cells, but not MT1TC1 or Ec1-1 cells, were able to proliferate on collagen I-coated plates confirming different abilities of different clones to interact with this substrate (Fig. 5B). Canonical integrin receptors, α 2 β 1, α 1 β 1 and α 11 β 1 mediate cell adhesion to collagen I. By immunoblotting analysis with anti- β 1 and anti- α 11 antibodies, we found that all transfectants express these subunits

(Fig. 5C). On the other hand, no α 1 or α 2 integrin subunits were detectable in the lysates (data not shown). Thus, the effect of wild-type E-cadherin on cell adhesion to collagen I was not due to alterations in the expression levels of collagen I receptor.

Overall, these data indicate that the general activation of cell-matrix interaction is a determinant of c-Fos-mediated EMT of MT1TC1 cells (Fig. 5). Re-expression of E-cadherin specifically influenced adhesion to collagen I depending on the ability of E-cadherin to bind β -catenin and to form functional adhesive dimers.

Transcriptional repression of the E-cadherin gene by c-Fos involves hypermethylation of the E-cadherin promoter

After having analyzed the role of the down-regulation of E-cadherin in c-Fos-mediated EMT in MT1TC1 cells, we intended to identify mechanisms of *e-cadherin* transcriptional repression by c-Fos. Transcriptional repressors of Snail/Slug and ZEB-1(DeltaEF1)/ZEB-2(SIP1) families mediate TGF- β and EGF-induced repression of the *e-cadherin* gene [65–68]. As activation of AP-1 is involved in TGF- β and EGF-induced signal transduction pathways, we suggested that SIP1, Snail and Slug proteins might also act in the c-Fos-induced EMT pathway and inhibit *e-cadherin* transcription. Consistent with this suggestion, the transcription of three out of four analyzed E-cadherin repressors, Snail, ZEB1(DeltaEF1) and ZEB2(SIP1) was up-regulated in A11 cells by 6.2-, 24- and 3.2-fold, respectively (Fig. 6A). The fourth repressor, Slug, was expressed at very low levels in MT1TC1 and A11 cells, and the amplification of *slug* cDNA was detected only in 30th–32nd amplification cycle of real-time PCR. Snail, ZEB1(DeltaEF1) and ZEB2(SIP1) proteins repress *e-cadherin* transcription via direct interaction with the conserved E2-boxes located in the *e-cadherin* promoter. To test whether the enhanced expression of Snail, ZEB1(DeltaEF1) and ZEB2(SIP1) contributed to the transcriptional silencing of E-cadherin in A11 cells, we compared activities of the wild-type E-cadherin promoter and E-cadherin promoter with mutated E2 boxes [52] in MT1TC1 and A11 cells. Mutating E2 boxes activated E-

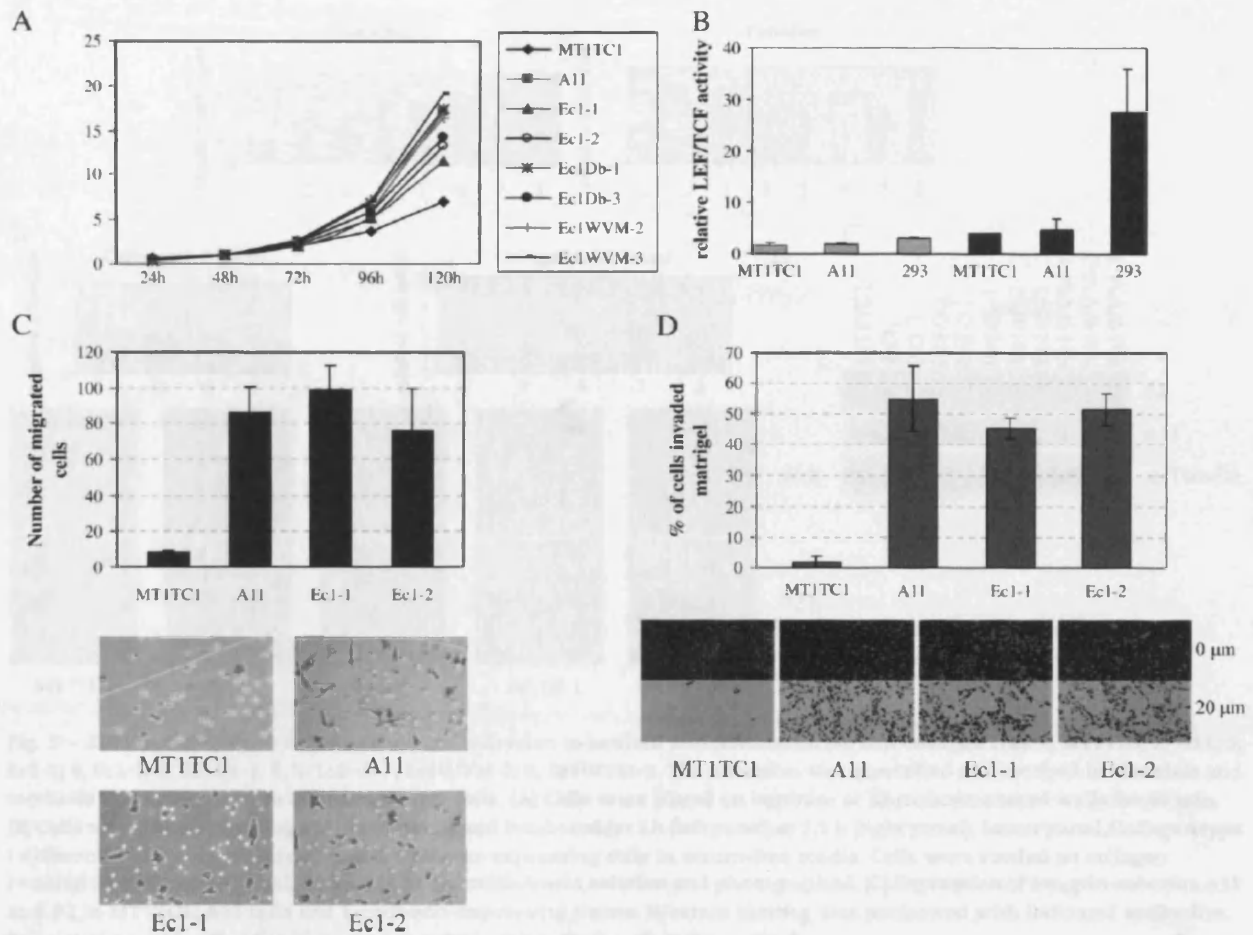


Fig. 4 – Effects of *c-Fos* and E-cadherin on cell growth, TCF/LEF reporter activity, cell motility and invasion. (A) Proliferation of MT1TC1, A11 parental cells and clones expressing either wild-type or mutant E-cadherin was analyzed by MTT assay. The assay was performed as described in Materials and methods. The relative proliferation rate was expressed as fold difference between the absorbance assessed at 24, 72, 96 and 120 h time points and the absorbance measured after 48 h taken for 1. (B) Analysis of TCF/LEF reporter activity in MT1TC1, A11 or HEK 293 cells. Cells were transfected with pTOPFLASH or pPOPFLASH reporters. Relative TCF/LEF transcriptional activity was defined as ratio of pTOPFLASH/pPOPFLASH luciferase activities normalized to the β -galactosidase level detected in each transfection. The results (means \pm SD) of three independent experiments are shown. Black bars, TCF/LEF transcriptional activity measured in cells cotransfected with the 1 μ g of Δ N- β -catenin-expressing vector pCGN Δ N β -cat. Light bars, TCF/LEF transcriptional activity in the absence of pCGN Δ N β -cat. (C) Migration of MT1TC1, A11, Ec1-1 or Ec1-2 cells was analyzed in directed Transwell motility assay. Bar graphs summarize the results of three independent experiments (mean \pm SD). Representative photographs show migrated cells. (D) Inverted 3D matrigel invasion assay. Example of confocal microscope sections of propidium iodide-stained cells used to quantitate the invasion assay. Upper panels show cells on the underside of the filter. Lower panels are representative microscopic images of sections at the distance of 20 μ m from the filter and show cells which invaded into matrigel. Cells were quantified in four microscopic fields and bars show percentage of cells invading the matrigel (mean \pm SD). The experiment was repeated twice with similar results.

cadherin promoter in MT1TC1 and A11 cells by factor of 1.3 (1.3 ± 0.3) and 1.9 (1.9 ± 0.45), respectively (Fig. 6B). Small impact of E2 boxes on E-cadherin promoter activity suggested that the full repression of *e-cadherin* in A11 cells was largely independent of Snail, ZEB1(DeltaEF1) or ZEB2(SIP1). Additionally, RNAi-mediated depletion of these transcription factors did not restore E-cadherin mRNA or protein levels in A11 cells confirming this suggestion (data not shown). As aberrant methylation of the CpG island in the E-cadherin

promoter has been reported in a variety of cancers, we hypothesized that hypermethylation of *e-cadherin* promoter DNA mediated transcriptional silencing of the gene in A11 cells. DNA was isolated from MT1TC1, A11 cells and from A11 cells maintained in the presence of an inhibitor of the DNA methylation, 5-Aza-dC. DNA was treated with sodium bisulfite and amplified with primer pairs specific for methylated and unmethylated *e-cadherin* alleles (methylation-specific PCR). Whereas only unmethylated *e-cadherin*

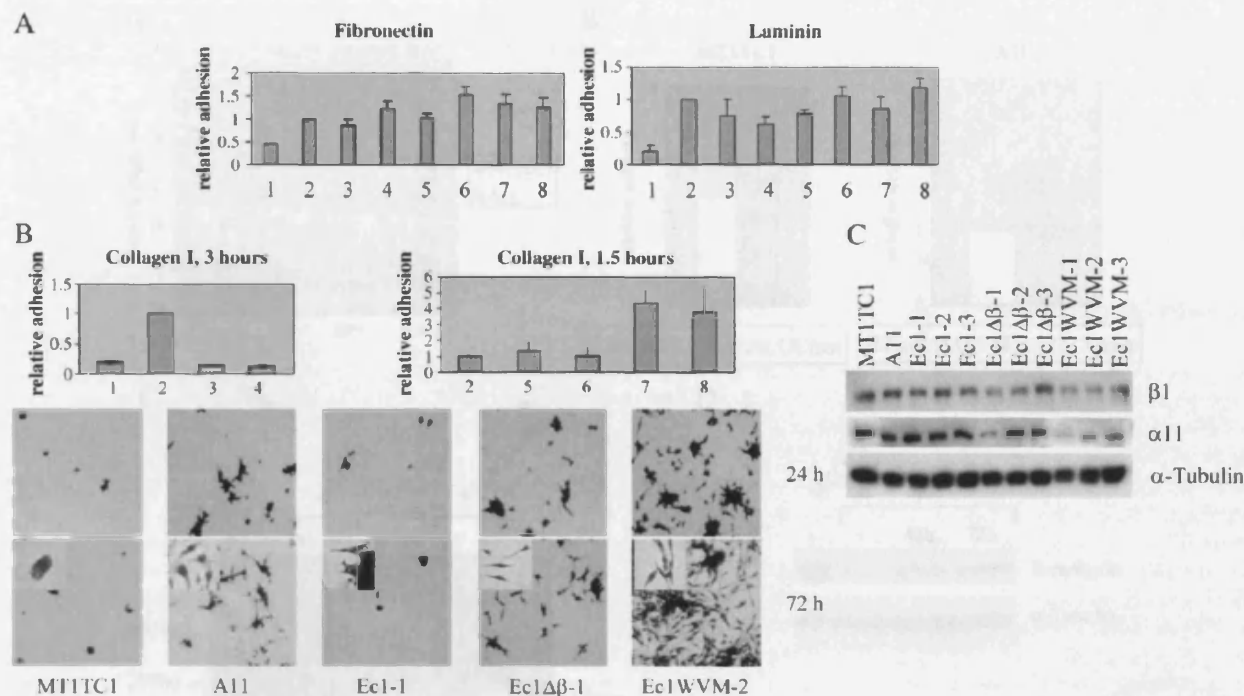


Fig. 5 - Effects of c-Fos and E-cadherin on cell adhesion to laminin and fibronectin (A) and collagen I (B). 1, MT1TC1; 2, A11; 3, Ec1-1; 4, Ec1-2; 5, Ec1Δβ-1; 6, Ec1Δβ-3; 7, Ec1WVM-2; 8, Ec1WVM-3. The adhesion was quantified as described in Materials and Methods and normalized to adhesion of A11 cells. (A) Cells were plated on laminin- or fibronectin-coated wells for 40 min. (B) Cells were plated on collagen I coated wells and incubated for 3 h (left panel) or 1.5 h (right panel). Lower panel, Collagen type I differently supports proliferation of E-cadherin-expressing cells in serum-free media. Cells were seeded on collagen I-coated 24-well plates, fixed, stained in hematoxylin/eosin solution and photographed. (C) Expression of integrin subunits α11 and β1 in MT1TC1, A11 cells and E-cadherin-expressing clones. Western blotting was performed with indicated antibodies. To control equal loading the blot was re-probed with an anti-α-Tubulin antibody.

alleles were present in MT1TC1 cells, in A11 cells, we detected the 5-Aza-dC-sensitive hypermethylation of the *e-cadherin* promoter DNA (Fig. 6C). Furthermore, treatment of A11 cells by 5-Aza-dC for 48 or 72 h resulted in the reactivation of E-cadherin expression (Fig. 6D). These data demonstrate the involvement of DNA methylation in c-Fos-mediated inhibition of E-cadherin expression in MT1TC1 cells.

Discussion

c-Fos induces EMT in mouse epithelioid carcinoma cells

Oncogenic properties of Fos proteins have been mainly studied in immortalized or primary fibroblasts. Considerably less is known regarding the function of c-Fos in carcinoma cell lines. Prolonged expression of the Fos-ER chimera induced EMT in murine non-tumorigenic epithelial cells Ep-1 [25]. In contrast to the immortalized murine epithelial cells, morphology of fully transformed human epidermal cells A431 was not altered by c-Fos [7]. It is worth noting that the effects of c-Fos and Fos-ER cannot be directly collated, because the transforming potential and transactivating properties are significantly

elevated in Fos-ER fusion protein compared with wild-type c-Fos [69]. In this study, we show that c-Fos can induce EMT in three tumorigenic mouse mammary carcinoma cell lines that retain the epithelial phenotype (Fig. 1). Therefore, the responsiveness of transformed murine mammary epithelial cells to c-Fos seems to be their general feature.

Fos family members have been proposed to be master regulators of motility and invasion in rodent fibroblasts [17,19]. Here, we show that cell migration and invasion into Matrigel were strongly activated also in epithelial cells as a result of c-Fos-mediated EMT. This observation indicates that the c-Fos protein is a conserved component of a genetic pathway underlying cell-invasive behavior in different lineages.

In fibroblasts, Fos proteins are indispensable for growth factor-induced cell cycle progression, since neutralizing antibodies raised to Fos proteins inhibit cell growth [2]. In MT1TC1 cells, c-Fos markedly activated cell proliferation (Fig. 4A). It has been reported that Fos-ER-mediated mesenchymal conversion of non-tumorigenic epithelial cells involved up-regulation of β-catenin/TCF transcriptional activity which was essential for proliferation [34,44]. However, our results indicate that MT1TC1 or MT1TC1/c-fos cells are not competent for transducing β-catenin/TCF signals and therefore the effect

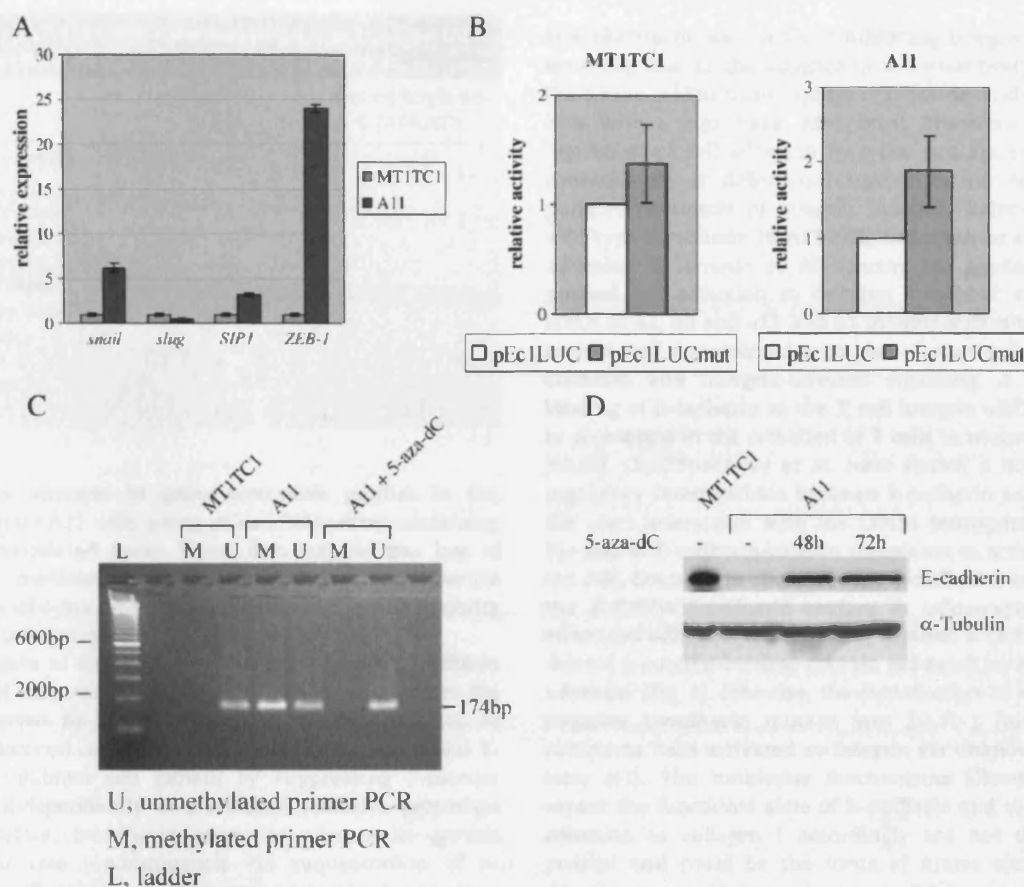


Fig. 6 – Promoter DNA methylation is implicated in the silencing of the *e-cadherin* gene in A11 cells. (A) Transcriptional repressors of the *e-cadherin* gene are up-regulated in A11 cells. Transcription of *snail*, *slug*, *ZEB1(DeltaEF1)* and *ZEB2(SIP1)* in MT1TC1 or A11 cells was analyzed by real-time quantitative PCR using primer sets given in the Supplementary Table 1. Amplification was performed in triplicate. Data are presented as the mean \pm SD. (B) E2 boxes in the *e-cadherin* promoter only minimally contribute to the transcriptional repression of the *e-cadherin* gene in A11 cells. MT1TC1 or A11 cells were transiently transfected with the wild-type E-cadherin promoter reporter (pEc1LUC) or with a similar construct containing mutated E2 boxes (pEc1LUCmut). pCMV β -gal was used in each experiment to monitor transfection efficiency. The normalized luciferase activity of the pEc1LUCmut reporter was expressed as fold difference relative to the normalized activity of pEc1LUC taken as 1. Results represent the mean \pm SD of four independent experiments. (C) E-cadherin promoter sequences are methylated in A11, but not in MT1TC1 cells. DNA samples from MT1TC1, A11 or A11 cells maintained in the presence of 5 μ M 5-Aza-dC for 4 days were treated with sodium bisulfite and PCR-amplified with primer pairs specific for unmethylated (U) and methylated (M) *e-cadherin* alleles designed as indicated in Supplementary Fig. 1. (D) 5-Aza-dC re-activates E-cadherin expression in A11 cells. Proteins were extracted from cells maintained in the absence or presence of 5 μ M 5-Aza-dC. A total of 5 μ g (MT1TC1) or 10 μ g (A11) of proteins was analyzed by Western blotting with antibodies as indicated. Expression of E-cadherin was analyzed by a Western blot. Equal loading was confirmed using an anti- α -tubulin antibody.

of c-Fos on the proliferation of MT1TC1 cells does not require β -catenin signaling (Fig. 4B). These observations are in line with the idea that the minor fraction of cytoplasmic β -catenin is modified at adherens junctions and this modification is essential for the generation of an active β -catenin signaling pool [35,70]. If so, by inducing loss of epithelial adhesion c-Fos would rather inhibit than stimulate β -catenin/TCF transcriptional activity. The absence of a link between loss of E-cadherin and β -catenin signaling is consistent with the observation that β -catenin/TCF transcriptional activity does not correlate with the E-cadherin status in different carcinoma cell lines [71,72].

Role of E-cadherin in c-Fos-mediated EMT

We aimed to examine contribution of E-cadherin loss to c-Fos-mediated EMT in MT1TC1 cells with intrinsic inability to transduce β -catenin signals. Re-expression of either wild-type or mutant E-cadherin was not able to reverse c-Fos-mediated EMT as evaluated by majority of criteria (summarized in Table 1). Even though re-introduction of wild-type E-cadherin restored protein levels of catenins and to some extent reversed cell morphology towards an epithelial phenotype, the expression of vimentin, S100A4, Fra-1 or MMP-2 was not affected. Similarly, we were not able to

Table 1 – Cell features altered during c-Fos-induced EMT and their dependence on E-cadherin expression

	Effect of c-Fos	Dependence on E-cadherin
Expression of EMT markers	+	-
Cell proliferation	+	±
Cell motility/invasion	+	-
Wound-healing assay	-	-
Transwell assay	+	-
3D matrigel invasion	+	-
Cell adhesion	+	-
Laminin	+	-
Fibronectin	+	-
Collagen I	+	+

detect any changes in gene expression profiles in Ec1 clones versus A11 cells using Atlas cDNA array containing 1178 cancer-related genes. These data suggest that loss of E-cadherin-mediated epithelial adhesion does not influence the effects of c-Fos on the transcription of the vast majority of Fos-responsive genes.

Expression of the wild-type but not mutant E-cadherin resulted in only minor inhibition of cell growth, not to the level observed in MT1TC1 cells (Fig. 4A). In contrast, in SW480 colorectal cells expressing mutant APC, exogenous E-cadherin inhibited cell growth by suppressing β -catenin signaling independently of E-cadherin adhesive properties [35]. Therefore, E-cadherin seems to execute its growth suppressor role predominantly via sequestration of β -catenin in cells which are dependent on β -catenin signaling. Growth stimulation induced by c-Fos in MT1TC1 is β -catenin-independent and to a large extent independent of E-cadherin loss as well. Partial suppression of c-Fos-mediated activation of cell proliferation by wild-type but not mutant E-cadherin may occur via inhibition of signaling pathways initiated by RTKs. This hypothesis is in line with the recent observation that only E-cadherin molecules retaining adhesive activity inhibit ligand-dependent activation of EGFR and IGF-1R [32].

The effects of exogenous E-cadherin on motility and invasion of c-Fos-expressing cells were statistically not significant (Figs. 4C and D). Wong and Gumbiner studied biological features of breast and prostate cancer cell lines and demonstrated the importance of β -catenin/E-cadherin interactions for E-cadherin-mediated suppression of cell invasion via Matrigel [59]. Data suggest that the invasion suppressive role of E-cadherin is cell line-dependent. In particular, c-Fos is dominant over E-cadherin in relation to the control of tumor cell invasion.

c-Fos induces cell adhesion in an E-cadherin-dependent or -independent manner

The effect of c-Fos on cell-matrix adhesion in epithelial cells has not been studied before. In this paper, we show that prolonged c-Fos expression results in increased adhesion to collagen I, laminin and fibronectin without increasing cellular level of β 1 integrin subunit. Interestingly, Fra-1 has been shown to reduce cell adhesion to collagen I, laminin

and fibronectin also without inhibiting integrin β 1 expression [23]. Due to the absence of a transactivation domain, Fra-1 may inhibit transcription of c-Fos-dependent genes in cells with a high basal AP-1 level. Therefore, differential regulation of cell adhesion by c-Fos and Fra-1 might be a consequence of differential transcriptional regulation of putative regulators of integrin function. Reintroduction of wild-type E-cadherin in A11 cells had a minor effect on cell adhesion to laminin or fibronectin, but significantly suppressed cell adhesion to collagen I without affecting the levels of α 1, α 2 and α 11 and β 1 integrin subunits. There are several well documented examples of cross-talk between E-cadherin and integrin-directed signaling. A heterotypic binding of E-cadherin to the T cell integrin α E β 7 is thought to play a role in the retention of T cells in mucosal epithelia [60,62]. Chattopadhyay et al. have shown a novel level of regulatory interrelations between E-cadherin and integrins: the α 3 β 1 interaction with the CD151 tetraspanin regulates the link of E-cadherin/catenin complexes to actin cytoskeleton [64]. Contrary to the wild-type E-cadherin, expression of the Ec1WVM E-cadherin mutant in c-Fos-expressing cells enhanced adhesion to collagen I, whereas E-cadherin with a deleted β -catenin-binding domain produced no effect on cell adhesion (Fig. 5). Likewise, the introduction of a dominant-negative E-cadherin mutant into ZR-75-1 human breast carcinoma cells activated α v integrin via unknown mechanisms [61]. The molecular mechanisms allowing cells to sensor the functional state of E-cadherin and to change cell adhesion to collagen I accordingly are not clear at the present and could be the focus of future studies. As all clones express α 11, but not α 1 and α 2 integrin subunits, the cross-talk exists either between α 11 β 1- and E-cadherin-dependent adhesion complexes, or alternatively, another probably non-conventional collagen I receptor is affected by E-cadherin. Interestingly, the direct physical interaction between collagen I receptor α 2 β 1- and E-cadherin [63] has been reported. One can suggest that if there is a direct interaction also between α 11 and E-cadherin, this complex can affect adhesion by recruiting novel adaptors (such as catenins) to focal adhesions.

Repression of E-cadherin by c-Fos involves epigenetic mechanisms

Slug, Snail and ZEB2(SIP1) act in EMT-inducing pathways downstream of EGF and TGF- β [65–67], the growth factors which activate c-Fos in numerous cell systems. Another ZEB family member, ZEB1(DeltaEF1), has been shown to directly mediate transcriptional repression of E-cadherin by Fos-ER in Ep-1 cells [73]. Therefore, it was plausible to suggest that a member of Snail or ZEB transcription factor families mediates E-cadherin repression in A11 cells in response to c-Fos. However, although three out of four transcriptional repressors analyzed were indeed up-regulated in A11 cells, their contribution to the E-cadherin gene regulation was minimal (Fig. 6 and data not shown). In contrast, the examination of the methylation status of the *e-cadherin* promoter and experiments with 5-Aza-dC indicated that E-cadherin repression in A11 cells was based on DNA methylation. To our knowledge, these data are the first example of epigenetic silencing of a

gene in an *in vitro* EMT model. The molecular mechanism of c-Fos-mediated *de novo* methylation of *e-cadherin* promoter sequences remains to be studied in future work.

Acknowledgments

We thank Dr. Troyanovsky (Washington University Medical School, USA) who kindly provided us with Ec1, Ec1WVM and Ec1D β cDNAs. We thank Dr. Cano (Instituto de Investigaciones Biomédicas, Spain) for reporter plasmids containing wild-type and mutant E-cadherin promoter, Dr. Ben Ze'ev and Dr. Zhurinsky (The Weizmann Institute of Science, Israel) for pCGNAN β -cat plasmid, Dr. Danker (Centre for Biochemistry and Biophysics, Germany) for anti- α 1 antibody and Dr. Gullberg (Uppsala University, Sweden) for anti- α 11 antibody. We acknowledge the financial support from the Prostate Research Campaign UK and European Urological Association.

Appendix A. Supplementary data

Supplementary data associated with this article can be found, in the online version, at doi:10.1016/j.yexcr.2006.10.017.

REFERENCES

- [1] M. Karin, L.-Z. Liu, E. Zandi, AP-1 function and regulation, *Curr. Opin. Cell Biol.* 9 (1997) 240–246.
- [2] K. Kovary, R. Bravo, The Jun and Fos protein families are both required for cell cycle progression in fibroblasts, *Mol. Cell Biol.* 11 (1991) 4466–4472.
- [3] E. Shaulian, M. Karin, AP-1 in cell proliferation and survival, *Oncogene* 20 (2001) 2390–2400.
- [4] N. Basset-Séguin, P. Demoly, J. Moles, A. Tesnières, C. Gauthier-Rouvière, S. Richard, J. Blanchard, J. Guilhou, Comparative analysis of cellular and tissular expression of *c-fos* in human keratinocytes: evidence of its role in cell differentiation, *Oncogene* 9 (1994) 765–771.
- [5] S. Rutberg, E. Saez, A. Glick, A. Dlugosz, B. Spiegelman, S. Yuspa, Differentiation of mouse keratinocytes is accompanied by PKC-dependent changes in AP-1 proteins, *Oncogene* 13 (1996) 167–176.
- [6] E. Wagner, Functions of AP1 (Fos/Jun) in bone development, *Ann. Rheum. Dis.* 61 (Suppl. 2) (2002) 40–42.
- [7] V. Mils, J. Piette, C. Barette, J. Veyrone, A. Tesniere, C. Escot, J. Guilhou, N. Basset-Séguin, The proto-oncogene *c-fos* increases the sensitivity of keratinocytes to apoptosis, *Oncogene* 13 (1997) 1555–1561.
- [8] M. Mikula, J. Gotzmann, A. Fisher, M. Wolschek, C. Thallinger, R. Schulte-Hermann, H. Beug, W. Mikulits, The proto-oncoprotein c-Fos negatively regulates hepatocellular tumorigenesis, *Oncogene* 22 (2003) 6725–6738.
- [9] R. Eferl, E. Wagner, AP-1: a double-edged sword in tumorigenesis, *Nat. Rev., Cancer* 3 (2003) 859–868.
- [10] W. Jochum, E. Passegue, E. Wagner, AP-1 in mouse development and tumorigenesis, *Oncogene* 20 (2001) 2401–2412.
- [11] R. Wisdom, I. Verma, Transformation by Fos proteins requires a C-terminal transactivation domain, *Mol. Cell Biol.* 13 (1993) 7429–7438.
- [12] G. Bergers, P. Graninger, S. Braselmann, C. Wrighton, M. Busslinger, Transcriptional activation of the *fra-1* gene by AP-1 is mediated by regulatory sequences in the first intron, *Mol. Cell Biol.* 15 (1995) 3748–3758.
- [13] Z.Q. Wang, A. Grigoriadis, U. Mohle-Steinlein, E. Wagner, A novel target cell for *c-fos*-induced oncogenesis: development of chondrogenic tumours in embryonic stem cell chimeras, *EMBO J.* 10 (1991) 2437–2450.
- [14] A. Grigoriadis, K. Schellander, Z.Q. Wang, E. Wagner, Osteoblasts are target cells for transformation in *c-fos* transgenic mice, *J. Cell Biol.* 122 (1993) 685–701.
- [15] S. Brusselbach, U. Mohle-Steinlein, Z. Wang, M. Schreiber, F. Lucibello, R. Muller, E. Wagner, Cell proliferation and cell cycle progression are not impaired in fibroblasts and ES cells lacking c-Fos, *Oncogene* 10 (1995) 79–86.
- [16] J. Brown, E. Nigh, R. Lee, H. Ye, M. Thompson, F. Saudou, R. Pestell, M. Greenberg, Fos family members induce cell cycle entry by activating cyclin D1, *Mol. Cell Biol.* 18 (1998) 5609–5619.
- [17] L. Scott, J. Vass, E. Parkinson, D. Gillespie, J. Winnie, B. Ozanne, Invasion of normal human fibroblasts induced by v-Fos is independent of proliferation, immortalization, and the tumor suppressors p16INK4a and p53, *Mol. Cell Biol.* 24 (2004) 1540–1559.
- [18] O. Kustikova, D. Kramerov, M. Grigorian, V. Berezin, E. Bock, E. Lukanidin, E. Tulchinsky, Fra-1 induces morphological transformation and increases *in vitro* invasiveness and motility of epithelioid adenocarcinoma cells, *Mol. Cell Biol.* 18 (1998) 7095–7105.
- [19] B. Ozanne, L. McGarry, H. Spence, I. Johnston, J. Winnie, L. Meagher, G. Stapleton, Transcriptional regulation of cell invasion: AP-1 regulation of a multigenic invasion programme, *Eur. J. Cancer* 36 (2000) 1640–1648.
- [20] L. Marconcini, S. Marchio, L. Morbidelli, E. Cartocci, A. Albin, M. Ziche, F. Bussolino, S. Oliviero, *c-fos*-induced growth factor/vascular endothelial growth factor D induces angiogenesis *in vivo* and *in vitro*, *Proc. Natl. Acad. Sci. U. S. A.* 96 (1999) 9671–9676.
- [21] H. Andersen, S. Mahmood, V. Tkach, M. Cohn, O. Kustikova, M. Grigorian, V. Berezin, E. Bock, E. Lukanidin, E. Tulchinsky, The ability of Fos family members to produce phenotypic changes in epithelioid cells is not directly linked to their transactivation potentials, *Oncogene* 21 (2002) 4843–4848.
- [22] V. Tkach, E. Tulchinsky, E. Lukanidin, C. Vinson, E. Bock, V. Berezin, Role of the Fos family members, c-Fos, Fra-1 and Fra-2, in the regulation of cell motility, *Oncogene* 22 (2003) 5045–5054.
- [23] E. Vial, E. Sahai, C. Marshall, ERK-MAPK signalling co-ordinately regulates activity of Rac1 and RhoA for tumour cell motility, *Cancer Cell* 4 (2003) 67–79.
- [24] E. Saez, S. Rutberg, E. Meller, H. Oppenheim, J. Smoluk, S. Yuspa, B. Spiegelman, *c-fos* is required for malignant progression of skin tumors, *Cell* 82 (1995) 721–732.
- [25] E. Reichmann, H. Schwarz, E. Deiner, I. Leitner, M. Eilers, J. Berger, M. Busslinger, H. Beug, Activation of an inducible c-FosER fusion protein causes loss of epithelial polarity and triggers epithelial-fibroblastoid cell conversion, *Cell* 71 (1992) 1103–1116.
- [26] P. Savagner, Leaving the neighborhood: molecular mechanisms involved during epithelial-mesenchymal transition, *BioEssays* 23 (2001) 912–923.
- [27] K. Vlemminckx, R. Kemler, Cadherins and tissue formation: integrating adhesion and signalling, *BioEssays* 21 (1999) 211–220.
- [28] U. Cavallaro, G. Christofori, Cell adhesion and signalling by cadherins and Ig-CAMs in cancer, *Nat. Rev., Cancer* 4 (2004) 118–132.
- [29] N. Noren, W. Arthur, K. Burridge, Cadherin engagement

- inhibits RhoA via p190RhoGAP, *J. Biol. Chem.* 278 (2003) 13615-13618.
- [30] B. St Croix, C. Sheehan, J. Rak, V. Florenes, J. Slingerland, R. Kerbel, E-Cadherin-dependent growth suppression is mediated by the cyclin-dependent kinase inhibitor p27 (KIP1), *J. Cell Biol.* 142 (1998) 557-571.
- [31] N. Zantek, M. Azimi, M. Fedor-Chaiken, B. Wang, R. Brackenbury, M. Kinch, E-cadherin regulates the function of the EphA2 receptor tyrosine kinase, *Cell Growth Differ* 10 (1999) 629-638.
- [32] X. Qian, T. Karpova, A. Sheppard, J. McNally, D. Lowy, E-cadherin-mediated adhesion inhibits ligand-dependent activation of diverse receptor tyrosine kinases, *EMBO J.* 21 (2004) 1739-1784.
- [33] S. Orsulic, O. Huber, H. Aberle, S. Arnold, R. Kemler, E-cadherin binding prevents β -catenin nuclear localisation and β -catenin/LEF-1-mediated transactivation, *J. Cell Sci.* 112 (1999) 1237-1245.
- [34] A. Stockinger, A. Eger, J. Wolf, H. Beug, R. Foisner, E-cadherin regulates cell growth by modulating proliferation-dependent beta-catenin transcriptional activity, *J. Cell Biol.* 154 (2001) 1185-1196.
- [35] C. Gottardi, E. Wong, B. Gumbiner, E-cadherin suppresses cellular transformation by inhibiting β -catenin signalling in an adhesion-independent manner, *J. Cell Biol.* 153 (2001) 1049-1060.
- [36] P. Polakis, Wnt signalling and cancer, *Genes Dev.* 14 (2000) 1837-1851.
- [37] G. Berx, K. Becker, H. Hofler, F. van Roy, Mutations of the human E-cadherin (CDH1) gene, *Hum. Mutat.* 12 (1998) 226-237.
- [38] P. Guilford, J. Hopkins, J. Harraway, M. McLeod, N. McLeod, P. Harawira, H. Taite, R. Scouler, A. Miller, A. Reeve, E-cadherin germline mutations in familial gastric cancer, *Nature* 392 (1998) 402-405.
- [39] H.D. Wang, J. Ren, L. Zhang, CDH1 germline mutation in hereditary gastric carcinoma, *World J. Gastroenterol.* 10 (2004) 3088-3093.
- [40] L. Di Croce, P. Pelicci, Tumour-associated hypermethylation: silencing E-cadherin expression enhances invasion and metastasis, *Eur. J. Cancer* 39 (2003) 413-414.
- [41] S. Hirohashi, Y. Kanai, Cell adhesion system and human cancer morphogenesis, *Cancer Sci.* 94 (2003) 575-581.
- [42] F. Nollet, G. Berx, F. van Roy, The role of the E-cadherin/catenin adhesion complex in the development and progression of cancer, *Mol. Cell Biol. Res. Commun.* 2 (1999) 77-85.
- [43] A. Peri, P. Wilgenbus, U. Dahl, H. Semb, G. Christofori, A causal role for E-cadherin in the transition from adenoma to carcinoma, *Nature* 392 (1998) 190-193.
- [44] A. Eger, A. Stockinger, B. Schaffhauser, H. Beug, R. Foisner, Epithelial mesenchymal transition by c-Fos estrogen receptor activation involves nuclear translocation of beta-catenin and upregulation of beta-catenin/lymphoid enhancer binding factor-1 transcriptional activity, *J. Cell Biol.* 148 (2000) 173-188.
- [45] P. Ferrara, E. Andermarcher, G. Bossis, C. Acquaviva, F. Brockly, I. Jariel-Encontre, M. Piechaczyk, The structural determinants responsible for c-Fos protein proteasomal degradation differ according to the conditions of expression, *Oncogene* 22 (2003) 1461-1474.
- [46] N. Chitaev, S. Troyanovsky, Adhesive but not lateral E-cadherin complexes require calcium and catenins for their formation, *J. Cell Biol.* 142 (1998) 837-846.
- [47] D. Markowitz, S. Goff, A. Bank, A safe packaging line for gene transfer: separating viral genes on two different plasmids, *J. Virol.* 62 (1988) 1120-1124.
- [48] S. Barnett, S. Eccles, Studies of mammary carcinoma metastasis in a mouse model system: I Derivation and characterization of cells with different metastatic properties during tumor progression in vivo, *Clin. Exp. Metastasis* 2 (1984) 15-36.
- [49] V. Senin, A. Ivanov, A. Afanasjeva, A. Buntsevich, New organospecific metastatic transplanted tumors of mice and their use for studying laser effect on dissemination, *Vestnik USSR Acad. Med. Sci.* 5 (1984) 85-91.
- [50] A. Sonnenberg, H. Daams, J. Calafat, J. Hilgers, *In vitro* differentiation and progression of mouse mammary tumor cells, *Cancer Res.* 46 (1984) 5913-5922.
- [51] I. Simcha, M. Shtutman, D. Salomon, J. Zhurinsky, E. Sadot, B. Geiger, A. Ben-Ze'ev, Differential nuclear translocation and transactivation potential of beta-catenin and plakoglobin, *J. Cell Biol.* 141 (1998) 1433-1448.
- [52] V. Bolos, H. Peinado, M. Perez-Moreno, M. Fraga, M. Esteller, A. Cano, The transcription factor Slug represses E-cadherin expression and induces epithelial to mesenchymal transitions: a comparison with Snail and E47 repressors, *J. Cell Sci.* 116 (2003) 499-511.
- [53] J. Sambrook, D. Russell, *Molecular Cloning. A Laboratory Manual*, CSHL Press, Cold Spring Harbor, NY, 2001.
- [54] J. Herman, J. Graff, S. Myohanen, B. Nelkin, S. Baylin, Methylation-specific PCR: a novel PCR assay for methylation status of CpG islands, *Proc. Natl. Acad. Sci. U. S. A.* 93 (1996) 9821-9826.
- [55] L. Li, R. Dahiya, MethPrimer: designing primers for methylation PCRs, *Bioinformatics* 18 (2002) 1427-1431.
- [56] K. Matsuo, J. Owens, M. Tonko, C. Elliott, T. Chambers, E. Wagner, Fos1 is a transcriptional target of c-Fos during osteoclast differentiation, *Nat. Genet.* 24 (2000) 184-187.
- [57] M. Cohn, I. Hjelmsø, L.-C. Wu, P. Guldberg, E. Lukanidin, E. Tulchinsky, Characterization of Sp1, AP-1, CBF and KRC binding sites and minisatellite DNA as functional elements of the metastasis-associated mts1/S100A4 gene intronic enhancer, *Nucleic Acids Res.* 29 (2001) 3335-3346.
- [58] M. Bergman, S. Cheng, N. Honbo, L. Piacentini, J. Karliner, D. Lovett, A functional activating protein 1 (AP-1) site regulates matrix metalloproteinase 2 (MMP-2) transcription by cardiac cells through interactions with JunB-Fra1 and JunB-FosB heterodimers, *Biochem. J.* 369 (2003) 485-496.
- [59] A. Wong, B. Gumbiner, Adhesion-independent mechanism for suppression of tumor cell invasion by E-cadherin, *J. Cell Biol.* 161 (2003) 1191-1203.
- [60] K. Cepek, S. Shaw, C. Parker, G. Russell, J. Morrow, D. Rimm, M. Brenner, Adhesion between epithelial cells and T lymphocytes mediated by E-cadherin and the alpha E beta 7 integrin, *Nature* 372 (1994) 190-193.
- [61] M. von Schlippe, J. Marshall, P. Perry, M. Stone, A. Zhu, I. Hart, Functional interaction between E-cadherin and av-containing integrins in carcinoma cells, *J. Cell Sci.* 113 (2000) 425-437.
- [62] E. Corps, C. Carter, P. Karecla, T. Ahrens, P. Evans, P. Kilshaw, Recognition of E-cadherin by integrin alpha(E)beta(7): requirement for cadherin dimerization and implications for cadherin and integrin function, *J. Biol. Chem.* 276 (2001) 30862-30870.
- [63] J. Whittard, S. Craig, A. Mould, A. Koch, O. Pertz, J. Engel, M. Humphries, E-cadherin is a ligand for integrin alpha2beta1, *Matrix Biol.* 21 (2002) 525-532.
- [64] N. Chattopadhyay, Z. Wang, L. Ashman, S. Brady-Kalnay, J. Kreidberg, $\alpha 3 \beta 1$ integrin-CD151, a component of the cadherin-catenin complex, regulates PTP μ expression and cell-cell adhesion, *J. Cell Biol.* 163 (2003) 1351-1362.
- [65] Z. Lu, S. Ghosh, Z. Wang, T. Hunter, Downregulation of caveolin-1 function by EGF leads to the loss of E-cadherin, increased transcriptional activity of beta-catenin, and enhanced tumor cell invasion, *Cancer Cell* 4 (2003) 415-499.

- [66] H. Peinado, M. Quintanilla, A. Cano, Transforming growth factor β -1 induces snail transcription factor in epithelial cell lines, *J. Biol. Chem.* 278 (2003) 21113–21123.
- [67] J. Comijn, G. Berx, P. Vermassen, K. Verschueren, L. van Grunsven, E. Bruyneel, M. Mareel, D. Huylebroeck, F. van Roy, The two-handed E-box binding zinc finger protein SIP1 downregulates E-cadherin and induces invasion, *Mol. Cell* 7 (2001) 1267–1278.
- [68] B. De Craene, F. van Roy, G. Berx, Unraveling signalling cascades for the Snail family of transcription factors, *Cell. Signal.* 17 (2005) 535–547.
- [69] M. Schuermann, G. Hennig, R. Muller, Transcriptional activation and transformation by chimaeric Fos-estrogen receptor proteins: altered properties as a consequence of gene fusion, *Oncogene* 10 (1993) 2781–2790.
- [70] J. Klingelhofer, R. Troyanovsky, O. Laur, S. Troyanovsky, Exchange of catenins in cadherin–catenin complex, *Oncogene* 228 (2003) 1181–1188.
- [71] K. Caca, F. Kolligs, J. Hayes, J. Qian, A. Yahanda, D. Rimm, J. Costa, E. Fearon, Beta- and gamma-catenin mutations, but not E-cadherin inactivation, underlie T-cell factor/lymphoid enhancer factor transcriptional deregulation in gastric and pancreatic cancer, *Cell Growth Differ.* 10 (1999) 369–376.
- [72] M. van de Wetering, N. Barker, I. Harkes, M. van der Heyden, N. Dijk, A. Hollestelle, J. Klijn, H. Clevers, M. Schutte, Mutant E-cadherin breast cancer cells do not display constitutive Wnt signalling, *Cancer Res.* 61 (2001) 278–284.
- [73] A. Eger, K. Aigner, S. Sonderegger, B. Dampier, S. Oehler, M. Schreiber, G. Berx, A. Cano, H. Beug, R. Foisner, DeltaEF1 is a transcriptional repressor of E-cadherin and regulates epithelial plasticity in breast cancer cells, *Oncogene* 24 (2005) 2375–2385.

Appendix D

(Publication)
(PROOF VERSION)

Mejlvang J, Kriaievska M, Vandewalle C, Chernova T, Sayan AE, Berx G, Mellon JK, Tulchinsky E.; Direct Repression of Cyclin D1 by SIP1 Attenuates Cell Cycle Progression in Cells Undergoing an Epithelial Mesenchymal Transition. *Mol Biol Cell.* 2007 Sep 12

Direct Repression of Cyclin D1 by SIP1 Attenuates Cell Cycle Progression in Cells Undergoing an Epithelial Mesenchymal Transition^D

Jakob Mejlvang,* Marina Kriaievska,* Cindy Vandewalle,[†] Tatyana Chernova,[‡] A. Emre Sayan,* Geert Berx,[†] J. Kilian Mellon,* and Eugene Tulchinsky*

*Department of Cancer Studies and Molecular Medicine and [†]Medical Research Council Toxicology Unit, University of Leicester, Leicester LE1 9HN, United Kingdom; and [‡]Unit of Molecular and Cellular Oncology, Department for Molecular Biomedical Research, Flanders Institute for Biotechnology-Ghent University, BE-9052 Gent, Belgium

Submitted May 3, 2007; Revised August 27, 2007; Accepted September 4, 2007
Monitoring Editor: Ben Margolis

Zinc finger transcription factors of the Snail/Slug and ZEB-1/SIP1 families control epithelial-mesenchymal transitions in development in cancer. Here, we studied SIP1-regulated mesenchymal conversion of epidermoid A431 cells. We found that concomitant with inducing invasive phenotype, SIP1 inhibited expression of cyclin D1 and induced hypophosphorylation of the Rb tumor suppressor protein. Repression of cyclin D1 was caused by direct binding of SIP1 to three sequence elements in the cyclin D1 gene promoter. By expressing exogenous cyclin D1 in A431/SIP1 cells and using RNA interference, we demonstrated that the repression of cyclin D1 gene by SIP1 was necessary and sufficient for Rb hypophosphorylation and accumulation of cells in G1 phase. A431 cells expressing SIP1 along with exogenous cyclin D1 were highly invasive, indicating that SIP1-regulated invasion is independent of attenuation of G1/S progression. However, in another epithelial-mesenchymal transition model, gradual mesenchymal conversion of A431 cells induced by a dominant negative mutant of E-cadherin produced no effect on the cell cycle. We suggest that impaired G1/S phase progression is a general feature of cells that have undergone EMT induced by transcription factors of the Snail/Slug and ZEB-1/SIP1 families.

INTRODUCTION

An important event in the development of malignant epithelial tumors is epithelial-mesenchymal transition (EMT), a process of generation of motile and invasive mesenchymal cells from polarized epithelia. Because EMT plays a fundamental role at certain stages of normal development (gastrulation, neural crest migration, somitogenesis), it has been suggested that some elements of embryonic transdifferentiation programs are exploited by cells of growing carcinoma (Thiery, 2003). Cells undergoing EMT are characterized by massive alterations in gene expression patterns. They acquire expression of mesenchymal but lose epithelial markers. A central event in EMT is loss of epithelial cadherin (E-cadherin), a surface receptor that plays an essential role in the formation of adherens junctions and that is often mutated or lost in cancer cells (Thiery and Chopin, 1999; Thiery, 2003).

In recent years, several direct transcriptional repressors of E-cadherin (Snail, Slug, ZEB-1, SIP1, and E47) have been identified (Batlle *et al.*, 2000; Cano *et al.*, 2000; Comijn *et al.*, 2001; Perez-Moreno *et al.*, 2001; Bolos *et al.*, 2003; Eger *et al.*,

2005). These proteins act downstream in EMT-inducing signal transduction pathways activated by TGF β , FGF, and EGF growth factors, integrin engagement, and hypoxia (Imai *et al.*, 2003; De Craene *et al.*, 2005a; Krishnamachary *et al.*, 2006; Imamichi *et al.*, 2007). ZEB-1/SIP1 and Snail/Slug family members directly interact with the response elements in the proximal *e-cadherin* gene promoter and actively repress transcription recruiting transcriptional corepressors such as CtBP or mSinA (Furusawa *et al.*, 1999; Shy *et al.*, 2003; Peinado *et al.*, 2004). More recently, direct repression of other epithelial genes by Snail and SIP1 has been reported (De Craene *et al.*, 2005b; Vandewalle *et al.*, 2005; Moreno-Bueno *et al.*, 2006). In addition, Snail/Slug and ZEB-1/SIP1 proteins mediate up-regulation of genes implicated in cell invasion and motility (e.g., vimentin, members of the matrix metalloproteinase (MMP) family of proteases, fibronectin).

The mechanisms of transcriptional activation is less clear; in some cases, indirect activation of genes implicated in EMT by Snail and SIP1 takes place (Jorda *et al.*, 2005; Taki *et al.*, 2006). In contrast to Snail and Slug, ZEB-1, and SIP1 proteins interact with transcriptional coactivators pCAF and p300 (Postigo *et al.*, 2003; van Grunsven *et al.*, 2006). This biochemical difference may indicate that Snail and SIP1 family members activate expression of mesenchymal markers via fundamentally different mechanisms. In vivo studies demonstrated that Snail/Slug and ZEB-1/SIP1 proteins have different functions in embryonic development and are involved in the control of distinct EMT programs. Snail regulates gastrulation, and *snail*^{-/-} mutant embryos exhibit severe defects in EMT required for generation of the mesoderm cell layer

This article was published online ahead of print in *MBC in Press* (<http://www.molbiolcell.org/cgi/doi/10.1091/mbc.E07-05-0406>) on September 12, 2007.

^DThe online version of this article contains supplemental material at *MBC Online* (<http://www.molbiolcell.org>).

Address correspondence to: Eugene Tulchinsky (et32@le.ac.uk).

(Carver *et al.*, 2001). On the other hand, experiments with *snai2*-deficient mice (Jiang *et al.*, 1998) and generation of conditional *snai1*^{-/-} knockout embryos demonstrated that neither Snail nor Slug is required for the delamination and migration of neural crest cells (Murray and Gridley, 2006). In contrast, homozygous mutant embryos lacking *zfh1b*, the gene encoding SIP1, display early arrest in cranial neural crest migration (van de Putte *et al.*, 2003).

In a number of clinical studies, transcription of genes encoding Snail/Slug and ZEB-1/SIP1 proteins has been detected in breast (Blanco *et al.*, 2002; Elloul *et al.*, 2005), ovarian (Elloul *et al.*, 2005), gastric (Rosivatz *et al.*, 2002), and hepatocellular (Sugimachi *et al.*, 2003) carcinoma cells, and Snail immunoreactivity significantly correlated with breast cancer metastasis (Zhou *et al.*, 2004). Activation of Snail, Slug, E47, ZEB1, and SIP1 is an important, but not the only instrument that is utilized by cancer cells to acquire motile characteristics. Inactivation of *e-cadherin* by gene mutations (Berx *et al.*, 1998; Guilford *et al.*, 1998) or consistent cleavage of the E-cadherin extracellular domain chronically exposed to matrix metalloproteinases secreted by stromal cells may be sufficient to trigger a process ultimately leading to EMT in tumor cells (Lochter *et al.*, 1997). Recently, we explored a model of functional inhibition of E-cadherin in squamous carcinoma cells A431 by a dominant negative E-cadherin mutant (Andersen *et al.*, 2005). Expression of this mutant triggered a program of gradual EMT, which eventually resulted in activation of vimentin and increased cell motility.

In nonpathological conditions, EMT represents the profound de-differentiation program that must be incompatible with cell proliferation (Burstyn-Cohen and Kalchauer, 2002). Indeed, in 8.5 dpc mouse embryos, cells expressing Snail are characterized by decreased incorporation of bromodeoxyuridine (BrdU; Vega *et al.*, 2004). In Madin-Darby canine kidney (MDCK) cells and in primary keratinocytes, Snail family members induce cell cycle arrest in G1 phase and hypophosphorylation of the Rb protein (Vega *et al.*, 2004; Turner *et al.*, 2006). Complex cell cycle-regulating networks are dependent on cell-cell adhesion, integrin signaling, cell spreading, and actomyosin contractility (Walker *et al.*, 2005). Therefore, there are many potential molecular schemes by which EMT may affect cell proliferation in embryonic development and cancer. However, in cancer cells, the interrelationship between cell growth and EMT can be circumvented by the defects in the molecular pathways controlling the cell cycle. In this study, we analyze cell cycle progression in two EMT models based on conditional expression of either SIP1 or a dominant negative E-cadherin mutant Ec1WVM in the same cell line. We show that SIP1, but not Ec1WVM, induces accumulation of cells in the G1 phase of cell cycle. This effect is largely mediated by the direct transcriptional repression of the cyclin D1 gene by SIP1.

MATERIALS AND METHODS

Plasmids

Vectors expressing myc-tagged wild-type SIP1 (pUHDmyc-SIP1) and myc-tagged SIP1 with the mutated C-terminal Zn finger (pTREmyc-SIP1ZFmut) have been described (Comijn *et al.*, 2001; van Grunsven *et al.*, 2003). To generate a doxycycline (DOX)-regulated cyclin D1 expression vector (pBicycD1), the cyclin D1 coding sequence was amplified and cloned into pBI vector (BD Bioscience, Clontech, Palo Alto, CA). To analyze cyclin D1 promoter activity, we generated two luciferase reporter vectors, pwtCCND1LUC and pmutCCND1LUC. To generate pwtCCND1LUC, a fragment of the cyclin D1 5'-flanking sequence (-1025 to +18) was cloned into pGL3 basic vector (Promega Biotech, Madison, WI). To create pmutCCND1LUC, three Z-boxes with coordinates -1014 to -1010; -857 to -853, and -300 to -290 were mutated by introducing a single nucleotide substitution (5'-AGGTG replaced by 5'-AGATG) using conventional PCR-based methods.

Cell Lines and Transfections

To generate A431 clones with the inducible expression of wild-type or mutant SIP1 (Tet-On system), we used a clone of A431 cells expressing Tet-responsive transcriptional activator rtTA (Andersen *et al.*, 2005). Cells were transfected either with the pUHDmyc-SIP1 or pTREmyc-SIP1ZFmut along with the pTK-Hyg vector (BD Bioscience Clontech). Selection of stable clones was carried out in the presence of 60 µg/ml hygromycin B. Clones with concurrent DOX-regulated expression of SIP1 and cyclin D1 were obtained by cotransfecting A431/SIP1 cells with pBicycD1 and pPuro (BD Bioscience Clontech; conveys resistance to puromycin), followed by the selection of puromycin-resistant cells in the presence of 0.5 µg/ml puromycin. Transfections of plasmid DNA were performed by electroporation with a single pulse of 250 V and 250 µF by using the Gene Pulser Xcell electroporation system (Bio-Rad Laboratories, Hercules, CA). Established cell lines were cultured in DMEM supplemented with 10% fetal bovine serum with or without DOX (2 µg/ml).

Immunofluorescence

For immunofluorescent staining, cells were grown for 2 d in 10-well glass microscope slides (VWR International, Fontenay-sous-Bois, France). Cells were washed and fixed in acetone/methanol (1:1) solution for 3 min on ice. After rinsing, the slides were incubated with primary antibodies for 1 h at room temperature, rinsed, and incubated with Alexa 488-conjugated rabbit anti-mouse IgG (Pierce, Rockford, IL) for 1 h. The anti-vinculin antibody was from BD Biosciences, Transduction Laboratories. Cells were examined and photographed using a confocal inverted microscope (Axiovert 200M; Zeiss, Oberkochen, Germany). To monitor BrdU incorporation, cells were pulse-labeled with BrdU for 40 min and stained with DAPI and an anti-BrdU antibody (Roche, Mannheim, Germany) according to the protocols supplied with the Detection kit I (Roche). Proportion of BrdU-positive cells was quantified in several microscopic fields and are presented as mean ± SD.

Western Blotting

Proteins (10 or 20 µg) were denatured, separated on 6% or precast 4–20% gradient SDS-polyacrylamide gels (Invitrogen), and then transferred to Immobilon-P membranes (Millipore, Bedford, MA) by the standard procedure. After protein transfer, blots were incubated in blocking solution with primary antibody at a dilution of 1:1000 (for anti-myc tag antibody, clone 9E10; Santa Cruz Biotechnology, Santa Cruz, CA) and 1:500 (for anti-cyclin D1, anti-p21, anti-p16, anti-p27, and anti-Rb antibodies; Santa Cruz Biotechnology). Immunoreactive proteins were detected using an enhanced chemiluminescence system (Amersham Pharmacia Biotech, Piscataway, NJ).

cDNA Microarray Analysis

Construction of 20K microarrays, probe labeling, hybridization, and scanning were carried out at the MicroArray Facility of the Flanders Interuniversity Institute for Biotechnology. Changes in spot intensities >1.8 or <0.55 were regarded as significant in this system.

RNA Interference

Purified and annealed synthetic oligonucleotides specific for cyclin D1 or control small interfering RNA (siRNA) were purchased from Ambion (Austin, TX). Target sequence for cyclin D1 was validated previously by the company. Cells ($n = 2 \times 10^5$) were transfected with 0.2 nmol of siRNA by nucleofection technique in buffer V (nucleofection protocol T-20). The nucleofector device and a nucleofection kit were obtained from Amaxa (Köln, Germany) and used in accordance with the manufacturer's recommendations. At 48 h after transfection, cells were harvested, counted, and processed for fluorescence-activated cell sorting (FACS) analysis or Western blotting.

Determination of Cyclin D1 mRNA Stability

Cells were maintained in the presence or absence of DOX for 48 h. Then, actinomycin D (ActD) was added at the concentration of 5 µg/ml for various time periods. Total RNA was isolated, and transcription of *cyclin D1*, *GAPDH*, and *fosl1* was analyzed by RT-PCR or quantitative real time PCR.

FACS Analysis

A431/SIP1 and A431/SIP1/cyclin D1 cells or cells nucleofected with siRNA were grown in the presence or absence of DOX for 48 h, harvested, fixed in 70% ethanol, treated with RNase (1 mg/ml), and stained with propidium iodide (PI; 50 µg/ml). The cellular DNA content was evaluated using FACS flow cytometer.

Three-dimensional Matrigel Invasion Assay

Invasion was analyzed in inverse invasion assay as previously described (McGarry *et al.*, 2004) with minor modifications. A431/SIP1 and A431/SIP1/cyclin D1 cells were maintained with or without DOX for 48 h. Cells ($n = 6 \times 10^4$) were seeded on the underside of the polycarbonate filter of a Transwell chamber containing 100 µl of matrigel basement membrane matrix (Becton

Dickinson, Oxford, United Kingdom) diluted 1:1. Cells were allowed to adhere for 3 h and washed by DMEM. Transwell chambers were placed in wells filled with 1 ml of DMEM with or without DOX. In 3 d, cells were fixed in methanol and stained for 1 h in PI solution (10 µg/ml). Optical sections were scanned at 10-µm intervals using the confocal microscope Zeiss Axiovert 200M. To perform statistical analysis of the invasive potential of A431/SIP1 and A431/SIP1/cyclD1 cells, the amount of cells entering matrigel and remaining at the filter was calculated in 12 optical fields. The values were expressed as a percentage of cells that penetrated matrigel.

Cell Adhesion and Transwell Migration Assays

Cell adhesion assay was carried out essentially as previously described (Mejlvang *et al.*, 2007). Ninety-six-well tissue culture plates were coated with 50 µg/ml human fibronectin or 50 µg/ml rat collagen type I (all from BD Biosciences). Cells were allowed to adhere for 15 min. In some experiments, a blocking antibody A1B2 known to prevent adhesion to both substrates (Brockbank *et al.*, 2005) has been mixed with the cells for 10 min before the assay.

A directed transwell migration assay was performed using 24-well transwell plates containing 8-µm pore-size polycarbonate filters (Corning Costar, Cambridge, MA). Cells (n = 10⁴) were cultured with or without DOX for 48 h, seeded in culture inserts, and maintained overnight. Adhered cells were allowed to migrate toward gradient of serum used as a chemoattractant in the lower chamber for 2 h. Cells that migrated to the underside of transwell filters were fixed, stained with a Gurr rapid staining kit (BDH, Dagenham, United Kingdom), and counted by bright-field microscopy at a magnification of ×200 in four random fields using the ImageJ program.

Nuclear Run-On Assay

Nuclear run-on assay was based on the incorporation of biotin-16-UTP in nascent transcripts according to Patrone *et al.* (2000). Briefly, cells were maintained with or without DOX for 48 h. Cells were harvested and consequently resuspended in buffer I (10 mM Tris-Cl, pH 7.4, 3 mM MgCl₂, 10 mM NaCl, 150 mM sucrose, 0.5% NP40) or buffer II (10 mM Tris-Cl, pH 7.4, 3 mM MgCl₂, 10 mM NaCl, 150 mM sucrose) and centrifuged at 500 × g for 10 min. Nuclei were then resuspended in buffer III (40% glycerol, 50 mM Tris-HCl, pH 8.5, 5 mM MgCl₂, 0.1 mM EDTA) and quickly frozen.

To perform nuclear run-on reactions, 2 × 10⁶ nuclei were incubated in a reaction buffer (4 mM of each NTP, 200 mM KCl, 20 mM Tris-Cl, pH 8.0, 5 mM MgCl₂, 4 mM dithiothreitol, 200 mM sucrose) for 30 min at 29°C and stopped by adding RNase-free DNase I. In some reactions (negative controls), 0.5 mM UTP instead of biotin-16-UTP was used. Total RNA was isolated by TRIzol extraction, and biotinylated RNA was purified using agarose-conjugated streptavidin beads. Beads were washed two times with 15% formamide and five times with 2× SSC. Isolated biotinylated RNA was used for RT-PCR.

Real-time Quantitative PCR

RNA was isolated using TRIzol reagent (Invitrogen). cDNA synthesis was carried out using random hexamers and Superscript II (Invitrogen). PCR was performed using SYBR Green PCR Master Mix in the PRISM 7700 Sequence Detection System (Applied Biosystems, Foster City, CA). Primers were de-

signed to cross exon-exon boundaries and used at the concentration 900 nM. Each sample was run in triplicate. The C_T (threshold cycle when fluorescence intensity exceeds 10 times the SD of the baseline fluorescence) values for the target amplicon and endogenous control (28S) were determined for each sample. Quantification was performed using the comparative C_T method (ΔΔC_T).

Luciferase Reporter Assay

To determine transcriptional activity of cyclin D1 reporters, A431/SIP1 cells were transfected with 1 µg reporter constructs. The efficiency of each transfection was monitored using 400 ng cotransfected β-galactosidase expression vector, pCMVβ-gal (BD Biosciences). Cells were maintained with DOX for 48 h and lysed, and the luciferase activity was measured with a Lumat LB9501 tube luminometer (Berthold Detection Systems, Pforzheim, Germany). The luciferase activity was normalized to the activity of β-galactosidase determined using o-nitrophenyl-β-D-galactopyranoside (Sigma, Poole, Dorset, United Kingdom) as a chromogenic substrate.

Chromatin Immunoprecipitation Assay

A431/SIP1 cells were cultured for 24 h in the presence or absence of DOX. Cross-linking, immunoprecipitation, and DNA purification were performed using chromatin immunoprecipitation (ChIP)-IT kit (Active Motif, Carlsbad, CA) according to the manufacturer's protocol. Immunoprecipitated DNA was analyzed by real-time quantitative PCR.

Statistics

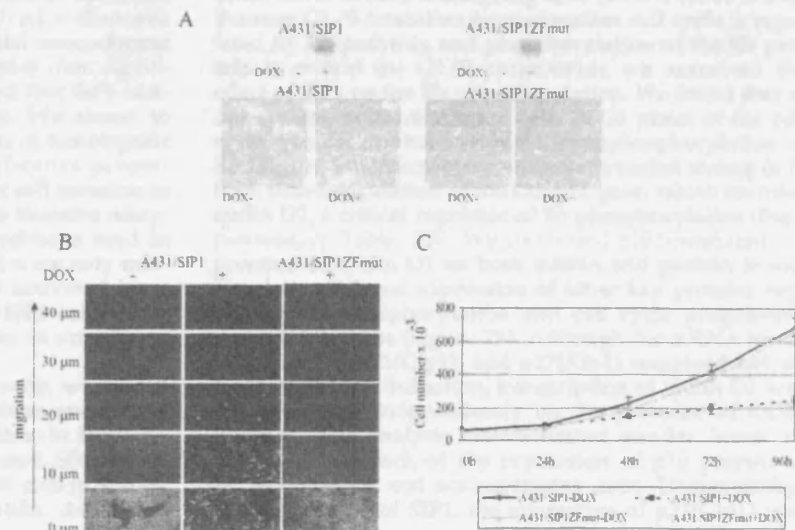
Results are expressed as the mean ± SD. Student's t test was used to evaluate the differences between groups.

RESULTS

SIP1-mediated EMT in A431 Cells: Switch from a Proliferative to an Invasive State

To study the physiological effects of SIP1 in carcinoma cells, we generated clones of the squamous carcinoma cell line A431 with the DOX-regulated expression of 6xMyc-tagged SIP1 (clone A431/SIP1). Treatment with DOX resulted in rapid accumulation of SIP1 in 95–98% of nuclei of A431/SIP1 cells, leading to cell scattering and dramatic morphological conversion from an epithelial cell state to a fibroblast-like phenotype. On the other hand, A431 cells expressing 6xMyc-tagged SIP1 with the mutated C-terminal Zn-finger retained entirely polarized epithelial morphology (Figure 1A). Expression of wild-type SIP1 promoted cytoplasmic redistribution of the adherens junctions and tight junction proteins (data not shown). The staining of DOX-treated cells

Figure 1. SIP1 induces cell invasion and inhibits cell growth. (A) Characterization of DOX-regulated A431 clones expressing SIP1 or SIP1ZFmut. Phase-contrast images of DOX-inducible A431 cell clones expressing myc-tagged SIP1 or SIP1ZFmut. Western blots show the expression of wild-type or mutant SIP1 in cells maintained with or without DOX for 48 h. (B) Inverse invasion assay of DOX-treated or untreated A431/SIP1 and A431/SIP1ZFmut cells. Confocal microscope sections of PI-stained cells were used to analyze the invasion assay. The row corresponding to 0 µm shows cells on the underside of the filter. Other sections show cells invaded into matrigel at different distances as indicated. The experiment was repeated four times, and results of a typical experiment are shown. (C) SIP1 inhibits cell growth. A431/SIP1 or A431/SIP1ZFmut cells were cultured with and without DOX, and cell number was counted at different time points as indicated. Experiments were repeated three times with similar results. Data shown are mean ± SDs of triplicate experiments.



J. Mejlvang et al.

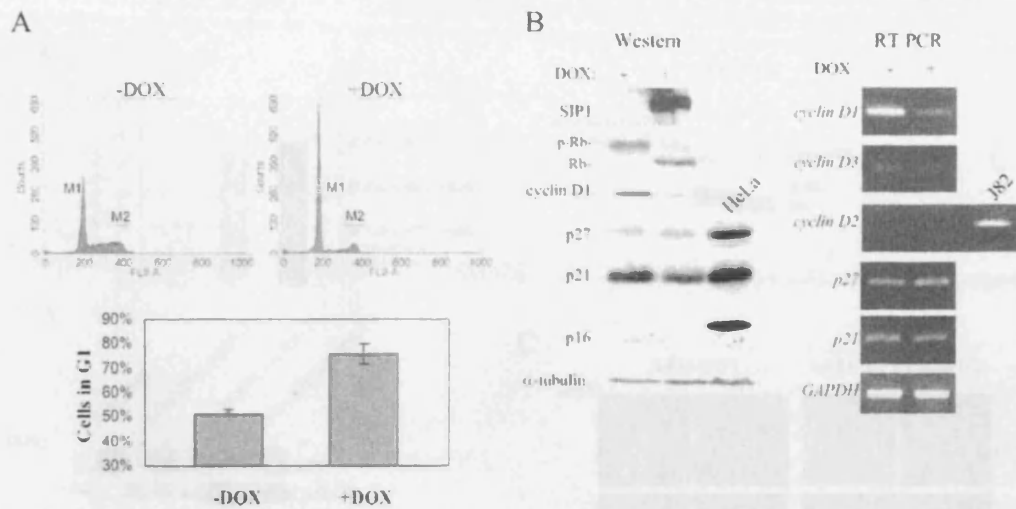


Figure 2. SIP1 negatively regulates G1/S transition. (A) FACS analysis of A431/SIP1 cells maintained in the absence or presence of DOX for 48 h. The diagram shows mean \pm SDs of triplicate experiments. $p < 0.0001$ (*t* test). (B) Expression of molecules regulating G1/S transition in A431/SIP1 cells. Cells were cultured with or without DOX for 48 h, and the expression of indicated genes was analyzed by Western blotting or RT-PCR. Note the appearance of the hypophosphorylated form of Rb in DOX-treated cells.

with phalloidin or an anti-vinculin antibody indicated that SIP1-inhibited cell-cell adhesion, but promoted formation of focal adhesions and disappearance of F-actin from intercellular borders (Supplementary Figure S1A). In addition, SIP1-activated cell adhesion to collagen and fibronectin (Supplementary Figure S1B). We used a cDNA microarray technique to obtain a global view on the number of genes regulated by SIP1 in A431 cells. Forty-eight hours of SIP1 induction led to prominent changes in gene expression profiles. We found that out of 20,000 genes analyzed, SIP1 repressed 281 genes by a factor of 0.55 or less and activated 204 genes by a factor of 1.8 or more (corresponds to the ~2.4% of human genome; Supplementary Tables S1A and S1B).

RT-PCR analysis of the selected genes demonstrated the reliability of the microarray hybridization (Supplementary Figure S2). Transcription of all genes tested was not affected in cells expressing SIP1 with the inactivated C-terminal Zn-finger domain. The largest cluster in a group of genes down-regulated by SIP1 contained markers of epithelial differentiation (components of epithelial microfilaments and junctional proteins). Given that essential mesenchymal genes (vimentin, fibronectin, and N-cadherin) were significantly up-regulated by SIP1, we concluded that SIP1 activated a program of EMT in A431 cells. We aimed to examine how the mesenchymal conversion of tumorigenic cells influenced their invasive and proliferative properties. We examined effects of SIP1 on tumor cell invasion in an inverse three-dimensional (3D) *in vitro* invasion assay. As we expected, in the experimental conditions used in this study, cells maintained without DOX were only minimally invasive. SIP1 induction strongly activated invasion, and in the presence of DOX A431/SIP1 cells penetrated matrigel at the distance of more than 40 μ m (Figure 1B).

To analyze the effects of SIP1 on cell growth, we seeded equal amounts of cells on six-well culture plates, maintained them with and without DOX, and counted them in 24, 48, 72, and 96 h. Already after 24 h of DOX-treatment, SIP1 significantly decreased the doubling time of A431 cells ($p < 0.05$; Figure 1C). Consistent with this observation, A431/SIP1

cells incubated with DOX for 48 h incorporated 3.2-fold less BrdU than cells maintained in the absence of DOX (see Figure 3C). As expected, expression of SIP1 with the mutated C-terminal Zinc-finger domain produced no effect on cell proliferation or matrigel invasion (Figure 1, B and C). Taken together, these data demonstrated that SIP1-induced EMT program encompasses a global genetic reprogramming and switch from a proliferative to an invasive type of cell behavior.

Transition into S Phase of the Cell Cycle Is Inhibited by SIP1

Having demonstrated inhibition of cell growth by SIP1, we analyzed the effect of SIP1 on cell cycle distribution. FACS analysis of A431/SIP1 cell cultures maintained with or without DOX for 48 h showed that SIP1 increased proportion of cells in G1 phase (Figure 2A). Percent of cells passing through S phase, G2, and mitosis was two times lower in cells undergoing EMT (24 ± 4 vs. $49 \pm 3\%$). Because G1/S transition in mammalian cell cycle is regulated by Rb pathway and phosphorylation of the Rb protein is critical for G1/S progression, we examined the effect of SIP1 on the Rb phosphorylation. We found that in our system, accumulation of cells in G1 phase of the cell cycle was concomitant with the hypophosphorylation of Rb (Figure 2B). Microarray analysis revealed strong (6.7-fold) down-regulation of the *CCND1* gene, which encodes cyclin D1, a critical regulator of Rb phosphorylation (Supplementary Table S1B). We confirmed SIP1-mediated repression of cyclin D1 on both mRNA and protein levels. Next, we analyzed expression of other key proteins regulating Rb phosphorylation and cell cycle progression through G1 phase (Figure 2B). Although the mRNA levels of cyclin D3, p21(Cip1), and p27(Kip1) remained not altered upon SIP1 induction, transcription of cyclin D2 was not detectable independently on the presence of DOX. Western blot analysis demonstrated similar levels of p27(Kip1) and lack of the expression of p16 protein in SIP1-expressing and nonexpressing cells. Unexpectedly, in the presence of SIP1, the expression of p21(Cip1) was

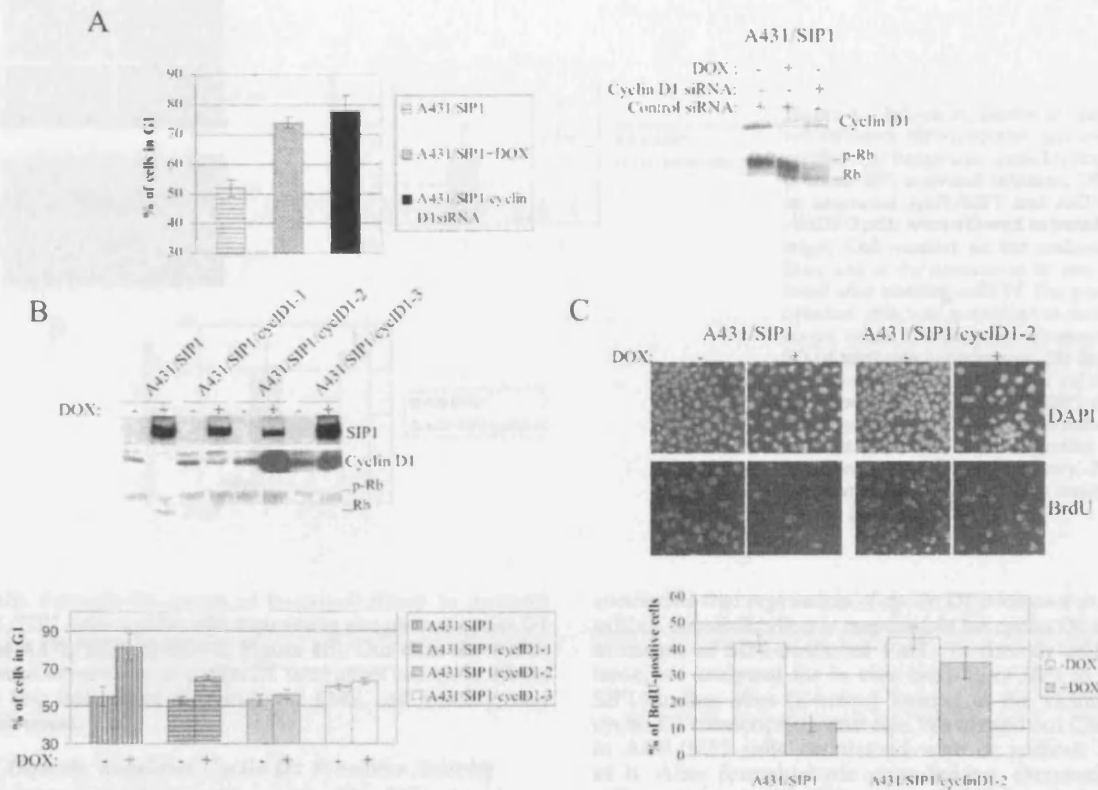


Figure 3. SIP-1 attenuates cell cycle progression via cyclin D1 down-regulation. (A) RNAi-mediated repression of cyclin D1 leads to accumulation of A431/SIP1 cells in G1 phase of the cell cycle. FACS analysis of cell cycle distribution of A431/SIP1 cells, in which cyclin D1 expression was reduced either by SIP1 or by RNAi. Control cells were cultured with or without DOX for 48 h. Results are mean \pm SD of three experiments. Right panel, Western blot analysis of cyclin D1 and Rb expression in A431/SIP1 cells transfected with the negative control siRNA or cyclin D1-specific siRNA. 20 μ g of total proteins was loaded in each lane. (B) Exogenous cyclin D1 counteracts the effect of SIP1 on Rb phosphorylation and cell cycle distribution. Clones with simultaneous DOX-regulated expression of SIP1 and cyclin D1 were generated and the phosphorylation of Rb was analyzed by Western blotting. Bottom, cells were cultured in the presence or absence of DOX for 48 h, and cell cycle distribution was monitored by FACS. (C) DOX-induced A431/SIP1 and A431/SIP1/cyclinD1-2 cells differently incorporate BrdU after 40-min pulse labeling. After the labeling, BrdU incorporation was detected by fluorescence microscopy with the monoclonal anti-BrdU antibody. Total cell number was identified by blue fluorescence (DAPI DNA staining). Proportion of BrdU-positive cells was quantified in six microscopic fields and presented as mean \pm SD. The experiment was repeated twice with similar results.

reduced on protein level, although mRNA level was not affected (Figure 2B).

Cyclin D1 Down-Regulation Is Necessary and Sufficient for SIP1-induced Changes in Cell Cycle Distribution

Cyclin D1 down-regulation correlated with Rb hypophosphorylation and accumulation of the cells in G1 phase of the cell cycle. To analyze whether SIP1 affects cell cycle distribution via cyclin D1, we used two approaches. First, we inhibited endogenous cyclin D1 level in A431/SIP1 cells by RNA interference (RNAi). The reduction in cyclin D1 levels in A431/SIP1 cells caused by siRNA resulted in the accumulation of cells in G1 and Rb hypophosphorylation, resembling the effect of SIP1 (Figure 3A). In parallel experiments, we generated clones of A431/SIP1 cells with simultaneous DOX-regulated expression of SIP1 and cyclin D1 (Figure 3B, clones 1-3). Although in the absence of DOX, all clones retained epithelial phenotype, DOX treatment induced morphological transformation and cell scattering, which was identical to the effect produced by SIP1 in parental A431/SIP1 cells (data not shown). In clone 1, activation of exogenous cyclin D1 resulted in partial suppression of the effect of

SIP1 on total cyclin D1 level. In DOX-treated cells of clone 1, Rb hypophosphorylation was partly suppressed, and the proportion of cells retained in G1 dropped from 82 to 62%. In clones 2 and 3, DOX treatment led to the very high cyclin D1 expression significantly exceeding cyclin D1 levels in DOX-untreated A431/SIP1 cells. In these clones, overexpression of cyclin D1 completely blocked Rb hypophosphorylation and abandoned the effect of SIP1 on cell cycle distribution (Figure 3B). Moreover, enforced expression of cyclin D1 bypassed the effect of SIP1 on the level of BrdU incorporation (Figure 3C). Taken together, these data indicate that repression of cyclin D1 is indispensable for the effects of SIP1 on cell cycle distribution.

Ectopic Expression Cyclin D1 Does Not Interfere with the Motile Behavior of SIP1-expressing Cells

Using 3D matrigel invasion assay, we found that cells simultaneously expressing SIP1 and cyclin D1 were at least as invasive as cells expressing SIP1 only (Figure 4A). In addition, we analyzed migratory capabilities of A431/SIP1 cells expressing or nonexpressing exogenous cyclin D1 using a transwell motility assay. SIP1 strongly activated migration

J. Mejlvang et al.

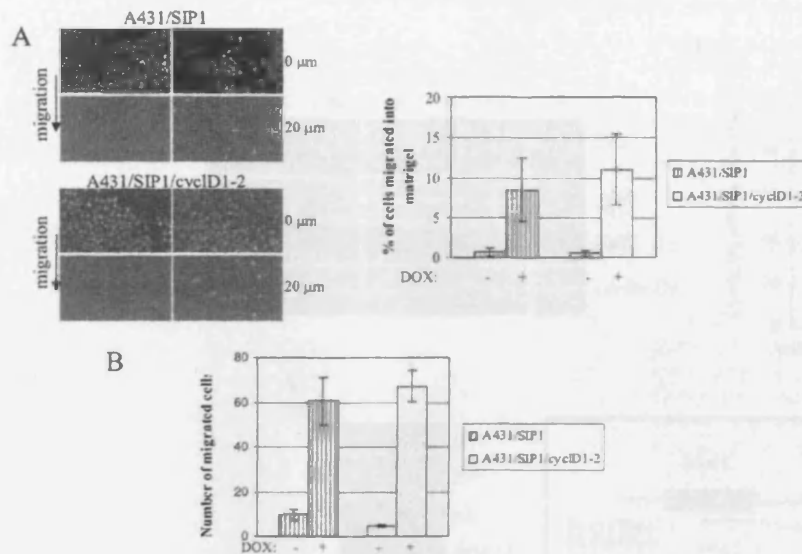


Figure 4. Ectopic expression of cyclin D1 does not influence SIP1-mediated cell invasion and motility. (A) Exogenous cyclin D1 does not compromise SIP1-activated invasion. DOX-treated or untreated A431/SIP1 and A431/SIP1/cyclinD1-2 cells were allowed to invade into matrigel. Cell number on the underside of the filter and at the distance of 20 μm was quantified after staining with PI. The percentage of invaded cells was quantified in twelve microscopic fields. The diagram represents mean \pm SD of triplicate experiments. (B) Enforced expression of cyclin D1 does not influence SIP1-activated cell motility. A431/SIP1 and A431/SIP1/cyclinD1-2 cells were maintained with or without DOX for 48 h. Migration was analyzed in transwell motility assay. Bar graphs summarize the results of three separate experiments (mean \pm SD).

of cells through the pores of transwell filters in parental A431/SIP1 cells and in cells expressing exogenous cyclin D1 (clone A431/SIP1/cyclD1-2, Figure 4B). Our data show that enforced expression of cyclin D1 uncouples cell cycle effects from key features of SIP1-induced EMT, cell motility, and invasiveness.

SIP1 Directly Regulates Cyclin D1 Promoter Activity

There are two levels controlling cyclin D1 mRNA abundance in mammalian cells. Signaling networks, which coordinate G1/S transition, regulate activity of the cyclin D1 promoter. In addition, regulation of the cyclin D1 mRNA turnover plays an important role in the control of cyclin D1 function (Lin et al., 2000). To explore the possibility that SIP1 activates degradation of cyclin D1 mRNA, A431/SIP1 cells were treated with DOX for 48 h or left untreated and then incubated with ActD for different time periods. In control experiments, the concurrent treatment of cells with ActD and DOX for 8 h prevented SIP1 transcription and therefore proved the efficacy of ActD (Figure 5A, right panel). The application of ActD for 4 or 8 h revealed that cyclin D1 mRNA was very stable in DOX-treated and untreated A431/SIP1 cells compared with the stability of *fosl1* or *SIP1* mRNA (Figure 5A). To quantify the effects of SIP1 on cyclin D1 mRNA stability more accurately, we applied real-time PCR. The difference in the effects of 4 h ActD treatment on cyclin D1 mRNA stability in cells maintained with or without DOX was not statistically significant ($p = 0.3695$; $n = 5$; Figure 5B). To examine whether SIP1 regulates the transcription rate of cyclin D1, we carried out nuclear run-on assay with nuclei prepared from DOX-treated or untreated cells. Biotin-labeled UTP was incorporated into nascent transcripts, and after the transcriptional reaction was completed, newly synthesized RNA was affinity-purified and subjected to RT-PCR analysis.

With three primer sets (a scheme in Figure 5C), we demonstrated that SIP1 drastically inhibited the transcription rate of the cyclin D1 gene. In contrast, transcription of a SIP1-up-regulated gene, *prss11* was much more efficient in nuclei isolated from DOX-treated cells. In all control reactions, in which nonlabeled UTP was used, no PCR product was detected (data not shown). From these experiments, we

concluded that repression of cyclin D1 promoter rather than mRNA destabilization is responsible for cyclin D1 inhibition in course of SIP1-mediated EMT. To directly address this issue, we analyzed the in vivo binding of SIP1 to potential SIP1-binding sites (Z-boxes) located in the vicinity of the cyclin D1 transcription start site. We carried out ChIP assays in A431/SIP1 cells maintained with or without DOX for 24 h. After formaldehyde cross-linking, chromatin physically associated with SIP1 was pulled-down, and cyclin D1 promoter fragments enriched in SIP1-containing chromatin fraction were identified by quantitative PCR. As negative control a preimmune serum was used. Data indicated that three Z-boxes with coordinates -1014 to -1010 (Z-box 1); -857 to -853 (Z-box 2); and -300 to -290 (Z-box 3) are occupied by SIP1 in DOX-stimulated cells. In contrast, neither sequences upstream of Z-box 1 (Figure 6A), nor sequences containing Z-boxes 4 and 5 located at the first exon/intron boundary (+390 to +409) (data not shown) were detected in association with SIP1. Next, we aimed to test whether the physical binding of SIP1 to Z boxes 1-3 resulted in the repression of cyclin D1 promoter activity. Two luciferase reporters were generated. A wild-type reporter (*pwtCCND1LUC*) contained the -1025 to +18 cyclin D1 promoter sequence cloned upstream of the firefly luciferase gene. The second reporter (*pmutCCND1LUC*) had the same structure but with Z-boxes 1-3 inactivated by a single nucleotide substitution converting 5'-AGGTG to 5'-AGATG. This substitution has been previously shown to block binding of SIP1 to DNA (Remacke et al., 1999). Transient transfection experiments demonstrated that the mutation of Z-boxes 1-3 markedly activated reporter activity in SIP1-expressing cells (Figure 6B). Taken together with the results of ChIP analysis, these data indicate that SIP1 represses cyclin D1 transcriptional activity via direct interaction with Z-boxes 1-3 in the cyclin D1 promoter.

An E-Cadherin Dominant Negative Mutant Induces EMT But Does Not Influence Cell Cycle Progression in A431 Cells

EMT programs encompass deep reorganization of the cytoskeleton and modulation of cell adhesion. Significant body of evidence implicates integrins, cadherins and cytoskeletal

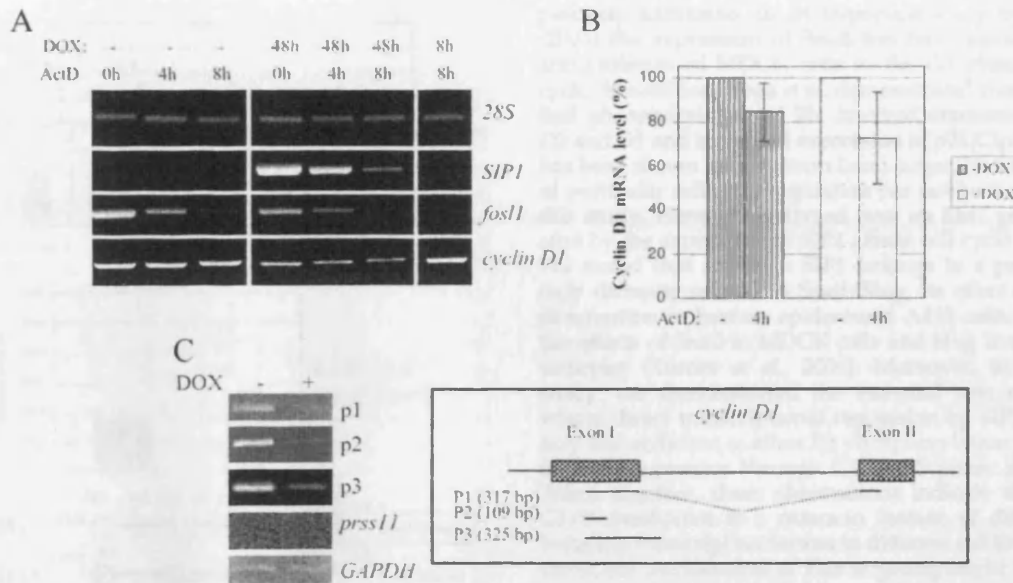


Figure 5. SIP1 regulates cyclin D1 promoter activity rather than the stability of cyclin D1 mRNA. (A) A431/SIP1 cells were maintained with or without DOX for 48 h. ActD was added for 4 or 8 h and expression of cyclin D1, SIP1, and *fosl1* was analyzed by RT-PCR. 28S rRNA was used as an ActD-insensitive control. Right panel, DOX and ActD were added simultaneously, and transcription of cyclin D1, SIP1, *fosl1*, and 28S rRNA was analyzed by RT-PCR 8 h later. (B) Quantification of cyclin D1 mRNA levels in A431/SIP1 cells maintained with or without DOX using real time PCR. Cells were treated with ActDC for 4 h, and amplification was performed in triplicate. Data are presented as the mean \pm SD. (C) Nuclei were isolated from A431/SIP1 cells maintained with or without DOX for 48 h and subjected to nuclear run-on assay. Isolation of nuclei, conditions of the reaction, and purification of biotinylated uridine-containing transcripts are described in *Materials and Methods*. Isolated transcripts corresponding to GAPDH, *prss11*, and cyclin D1 genes were amplified by RT-PCR and analyzed in an agarose gel. The scheme depicts fragments of the cyclin D1 mRNA detected by RT-PCR. Results are representative of two independent experiments.

tensions in the control of cell cycle (Walker and Assoian, 2005; Walker *et al.*, 2005). However, given that the effect of SIP1 on cyclin D1 expression was direct, cell cycle regulation might be not affected in course of EMT programs, which do not involve SIP1. To test this, we used a recently generated model of EMT based on the expression of a dominant negative E-cadherin mutant (Ec1WVM) in A431 cells (Andersen *et al.*, 2005). This mutant harbors a Trp²/Ala amino acid substitution in the first cadherin-like repeat, leading to an inability of the mutant protein to form *trans*-dimers. Forty-eight hours of Ec1WVM expression induced cell scattering and activated cell invasiveness (Figure 7A). Prolonged expression of Ec1WVM resulted in activation of vimentin, down-regulation of cytokeratins, and further increase in cell motility (Andersen *et al.*, 2005). However, neither long-term (data not shown), nor short-term Ec1WVM expression (Figure 7B) inhibited G1/S phase transition in A431 cells. In agreement with these data, we observed no effects on Rb phosphorylation or cyclin D1 expression in cells undergoing EMT in response to Ec1WVM (Figure 7B). These data indicate that in different EMT models, the G1/S transition depends on the nature of EMT-inducing signals.

DISCUSSION

Direct repression of *e-cadherin* transcription by Snail/Slug and ZEB-1/SIP1 proteins demonstrated in several epithelial cell lines is highly relevant to EMT and epithelial tumorigenesis. However, the functions of Snail/Slug and ZEB-1/SIP1 are not restricted to the repression of the *e-cadherin* gene. A number of genes encoding components of different epithelial intercellular adhesive complexes are directly or

indirectly repressed by Snail, Slug, ZEB-1, or SIP1 (Ohkubo and Ozawa, 2004; De Craene *et al.*, 2005b; Vandewalle *et al.*, 2005; Moreno-Bueno *et al.*, 2006; Aigner *et al.*, 2008; Supplementary Table SIB and this article). Moreover, expression of exogenous E-cadherin in MDCK/Snail or DLD/Snail cells was unable to restore epithelial differentiation or to inhibit Snail-induced invasion (Ohkubo and Ozawa, 2004; De Craene *et al.*, 2005b). Similarly, we found that ectopic expression of E-cadherin in A431/SIP1 cells did not revert EMT initiated by SIP1 induction (data not shown). These data suggest that Snail/Slug and ZEB-1/SIP1 proteins do not act through transcriptional repression of *e-cadherin*, but rather orchestrate EMT programs via independent and coordinated repression of multiple genes controlling epithelial features and by activation of mesenchymal genes.

In addition to the activation of canonical well-described EMT-related processes (cell dissociation, cell motility and invasiveness, global changes in gene expression pattern), SIP1 significantly stimulated adhesion of A431 cells to fibronectin and collagen I (Supplementary Figure S1B). In contrast, Slug inhibited adhesion of human epidermal keratinocytes to fibronectin and laminin-5 as a result of transcriptional repression of genes coding for $\alpha3$, $\beta1$, and $\beta4$ integrin subunits (Turner *et al.*, 2006). In A431 cells, transcription of these genes was not affected by SIP1 (data not shown), and the mechanism by which SIP1 activated cell-matrix adhesion remains unclear. However, results reported by Turner *et al.* and our data represent a rare example of a cell feature oppositely regulated by different Snail/Slug and ZEB-1/SIP1 proteins in two cell lines of common (epidermal) origin.

J. Mejlvang *et al.*

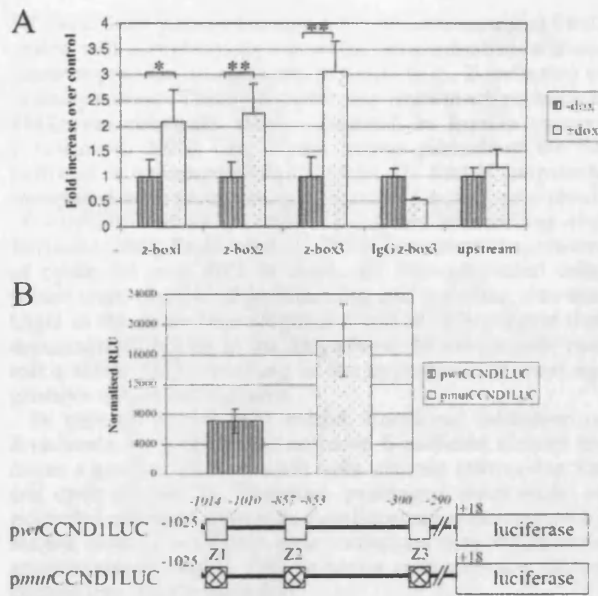


Figure 6. SIP1 directly regulates transcription of the cyclin D1 gene. (A) SIP1 interacts with three Z-box sequences in the cyclin D1 promoter in vivo. ChIP analysis of cyclin D1 promoter sequences in DOX-treated or untreated cells with the 9E10 antibody. As control an irrelevant antibody was used. Enrichment of SIP1-bound sequences was quantified by real-time PCR. Mean \pm SD are shown. $n = 9$; * $p < 0.01$; ** $p < 0.001$ (*t* test). (B) Luciferase reporter constructs *pwfCCND1LUC* and *pmutCCND1LUC* were transfected into A431/SIP1 cells. Cells were cultured in the presence of DOX for 48 h. Assays were carried out in triplicate, and four independent experiments were performed; a representative result is shown (mean \pm SD, $n = 3$). $p < 0.05$ (*t* test).

Snail/Slug and ZEB-1/SIP1 family members control distinct EMT programs that are implicated in many aspects of embryonic development, gastrulation, somitogenesis, and neural crest migration. It is therefore plausible to speculate that cancer cells recapitulate some elements of concealed embryonic differentiation programs to acquire metastatic capabilities. Given that normal differentiating cells do not proliferate, the intriguing question arises as to whether the EMT programs affect cell proliferation in cancer as well. However, to our knowledge, this issue has not been scrupulously addressed.

In an important study by Vega *et al.* (2004) the expression of Snail has been shown to induce accumulation of MDCK cells in the G1 phase of the cell cycle. In addition, Vega *et al.* demonstrated that Snail inhibited phosphorylation of Rb, lowered expression of cyclins D2 and D1 and increased expression of p21(Cip1). Cyclin D2 has been shown to be a direct Snail target. However, the role of particular cell cycle regulators has not been addressed in this study. Here, we analyzed how an EMT program initiated by the expression of SIP1 affects cell cycle progression. We found that although SIP1 belongs to a protein family only distantly related to Snail/Slug, its effect on cell cycle distribution in human epidermoid A431 cells is similar to the effects of Snail in MDCK cells and Slug in normal keratinocytes (Turner *et al.*, 2006). Moreover, in the present study, we demonstrated the essential role of cyclin D1 whose direct transcriptional repression by SIP1 is necessary and sufficient to affect Rb phosphorylation status and to inhibit progression through G1 into S phase in A431 cells. Taken together, these observations indicate that targeting G1/S checkpoint is a common feature of different EMT-inducing transcription factors in different cell lines, although the actual mechanisms of this targeting might be different.

Immunohistochemical data on the expression of Snail/Slug and especially ZEB-1/SIP1 family members in tumor tissue are limited. A proportion of ZEB1-positive tumors has been identified by immunohistochemical analysis of aggressive endometrial and non-small lung cancer specimens (Dohadwala *et al.*, 2006; Spoelstra *et al.*, 2006). In oral squamous cell carcinoma, SIP1 was detected in 27% of tumor specimens. SIP1 expression correlated with lack of E-cadherin immunoreactivity and low disease-specific survival (Maeda *et al.*, 2005). Similarly, Zhou *et al.* (2004) described extended E-cadherin-negative and Snail-positive areas in breast cancer surgical specimens, and this pattern significantly correlated with cancer metastasis. In another study, only a limited number of single Snail-positive cells has been detected at the periphery of tumor tissue in cervical squamous carcinoma and colon adenocarcinoma (Franci *et al.*, 2006). Studies on EMT of MDCK cells (Vega *et al.*, 2004) and data presented here suggest that cells maintaining control over G1/S transition and undergoing a rapid EMT in response to Snail or SIP1 acquire a growth disadvantage. Therefore, the functional status of the Rb pathway may determine the configuration of EMT programs utilized by cells of growing tumors. In carcinoma cells maintaining partial control over G1/S restriction point, members of the

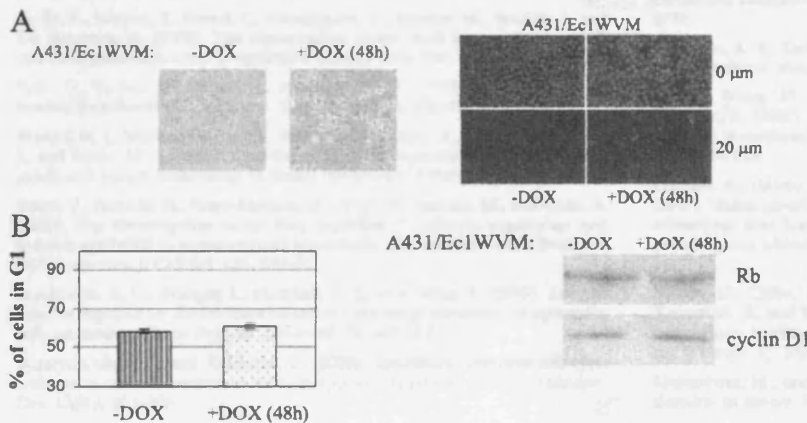


Figure 7. E-cadherin dominant negative mutant (Ec1WVM) induces invasion without affecting cell cycle. (A) DOX-activated expression of myc-tagged Ec1WVM in A431 cells (clone 31D6) induces cell scattering and invasion. Phase-contrast images of 31D6 cells treated with DOX for 48 h or left untreated. Right panel, results of a typical matrigel invasion assay of 31D6 cells. (B) FACS analysis of 31D6 cells cultured in the absence or presence of DOX for 48 h. Results are means \pm SD of three experiments. Bottom, Western blot analysis of cyclin D1 and Rb expression levels in DOX-treated (48 h) and untreated A431/Ec1WVM cells.

SIP1 and Snail protein families may induce a transient EMT, which will contribute to metastatic dissemination without stable repression of epithelial markers (e.g., E-cadherin) in primary tumors. This hypothesis may explain why complete EMTs are relatively rarely observed in human cancers (Christofori, 2006). One of the events perturbing the Rb pathway is overexpression of cyclin D1 that is frequently associated with carcinomas in humans (in part, as a result of amplification of the cyclin D1 gene; Malumbres and Barbacid, 2001; Knudsen *et al.*, 2006). Concurrent expression of cyclin D1 and SIP1 in A431 cell line-generated cells, which were capable of proliferating and invading into matrigel at the same time (Figures 3 and 4). We suggest that accumulated defects in the Rb pathway *in vivo* would permit a stable EMT, resulting in the appearance of most aggressive tumor cell variants.

In contrast to the SIP1 model, functional inhibition of E-cadherin by a dominant negative E-cadherin mutant induces a gradual EMT in A431 cells without attenuating the cell cycle (Figure 7). Therefore, prolonged inactivation of epithelial adhesion by matrix metalloproteinases secreted by stroma cells or *e-cadherin* gene mutations may represent a mechanism of a stable EMT in tumor cells retaining partial control over G1/S transition.

In conclusion, we have demonstrated that cyclin D1 is a new direct transcriptional target of SIP1. Taken together with previously published results (Vega *et al.*, 2004; Turner *et al.*, 2006), our data suggest that attenuated G1/S phase cell cycle transition is a common feature of EMT programs induced by Snail/Slug and ZEB-1/SIP1 proteins.

ACKNOWLEDGMENTS

We thank Jiri Lukas (Danish Cancer Society, Copenhagen) for his valuable comments on the manuscript. We thank Kristin Verschuere (University of Leuven, Belgium) for pTREmyc-SIP1Zfmut plasmid. We acknowledge the support from the Department of Cancer Studies and Molecular Medicine (University of Leicester, United Kingdom) and European Urology Fellowship Programme. C.V. was supported by the Fund for Scientific Research, Flanders (FWO) and the "Centrum voor Gewelzelen," Ghent. G.B. is a postdoctoral fellow with the FWO. The research by C.V. and G.B. has been supported by the Association for International Cancer Research (AICR-United Kingdom), FWO-Flanders and Interuniversitaire Attractiepolen (Belgian Government).

REFERENCES

Aigner, K. *et al.* (2008). The transcription factor ZEB1 (δ EF1) promotes tumour cell dedifferentiation by repressing master regulators of epithelial polarity. *Oncogene* (*in press*). doi: 10.1038/sj.onc.1210508.

Andersen, H., Mejlvang, J., Mahmood, S., Gromova, I., Gromov, P., Lukonidin, E., Krijavacka, M., Mellon, J. K., and Tulchinsky, E. (2005). Immediate and delayed effects of E-cadherin inhibition on gene regulation and cell motility in human epidermoid carcinoma cells. *Mol. Cell. Biol.* 25, 9138–9150.

Battle, E., Sancho, E., Franci, C., Dominguez, D., Monfar, M., Baulida, J., and De Herreros, A. (2000). The transcription factor snail is a repressor of E-cadherin gene expression in epithelial tumour cells. *Nat. Cell. Biol.* 2, 84–89.

Berx, G., Becker, K., Hoffer, H., and van Roy, F. (1998). Mutations of the human E-cadherin (CDH1) gene. *Hum. Mutat.* 12, 226–237.

Blanco, M. J., Moreno-Bueno, G., Sarrío, D., Locascio, A., Cano, A., Palacios, J., and Nieto, M. A. (2002). Correlation of Snail expression with histological grade and lymph node status in breast carcinomas. *Oncogene* 21, 3241–3246.

Bolos, V., Peinado, H., Perez-Moreno, M., Fraga, M., Esteller, M., and Cano, A. (2003). The transcription factor Slug represses E-cadherin expression and induces epithelial to mesenchymal transitions: a comparison with Snail and E47 repressors. *J. Cell Sci.* 116, 499–511.

Brockbank, E. C., Bridges, J., Marshall, C. J., and Sahai, E. (2005). Integrin beta1 is required for the invasive behaviour but not proliferation of squamous cell carcinoma cells *in vivo*. *Br. J. Cancer.* 92, 102–112.

Burstein-Cohen, T., and Kalchauer, C. (2002). Association between cell cycle and neural crest delamination through specific regulation of G1/S transition. *Dev. Cell* 3, 383–395.

Cano, A., Pérez-Moreno, M., Rodrigo, I., Locascio, A., Blanco, M., del Barrio, M., Portillo, F., and Nieto, M. A. (2000). The transcription factor Snail controls epithelial-mesenchymal transitions by repressing E-cadherin expression. *Nat. Cell. Biol.* 2, 76–83.

Carver, E., Jiang, R., Lan, Y., Oram, K., and Gridley, T. (2001). The mouse snail gene encodes a key regulator of the epithelial-mesenchymal transition. *Mol. Cell. Biol.* 21, 8184–8188.

Christofori, G. (2006). New signals from the invasive front. *Nature* 441, 444–450.

Comijn, J., Berx, G., Vermassen, P., Verschuere, K., van Grunven, L., Bruyneel, E., Mareel, M., Huylebrouck, D., and van Roy, F. (2001). The two-handed E box binding zinc finger protein SIP1 downregulates E-cadherin and induces invasion. *Mol. Cell* 7, 1267–1278.

De Craene, B., van Roy, F., and Berx, G. (2005a). Unravelling the signalling cascades for the Snail family of transcription factors. *Cell Signal.* 17, 535–547.

De Craene, B., Gilbert, B., Stove, C., Bruyneel, E., van Roy, F., and Berx, G. (2005b). The transcription factor snail induces tumour cell invasion through modulation of the epithelial cell differentiation program. *Cancer Res.* 65, 6237–6244.

Dohadwala, M. *et al.* (2006). Cyclooxygenase-2-dependent regulation of E-cadherin: prostaglandin E2 induces transcriptional repressors ZEB1 and snail in non-small cell lung cancer. *Cancer Res.* 66, 5338–5345.

Eger, A., Aigner, K., Sonderegger, S., Dampier, B., Oehler, S., Schreiber, M., Berx, G., Cano, A., Beug, H., and Foisner, R. (2005). DeltaEF1 is a transcriptional repressor of E-cadherin and regulates epithelial plasticity in breast cancer cells. *Oncogene* 24, 2375–2385.

Elloul, S., Elstrand, M., Nesland, J., Trope, C., Kvalheim, G., Goldberg, I., Reich, R., and Davidson, B. (2005). Snail, Slug, and Smad-interacting protein 1 as novel parameters of disease aggressiveness in metastatic ovarian and breast carcinoma. *Cancer* 103, 1631–1643.

Franci, C. *et al.* (2006). Expression of Snail protein in tumor-stroma interface. *Oncogene* 25, 5134–5144.

Furusawa, T., Moribe, H., Kondoh, H., and Higashi, Y. (1999). Identification of CtBP1 and CtBP2 as corepressors of zinc finger-homeodomain factor δ EF1. *Mol. Cell. Biol.* 19, 8581–8590.

Guilford, P., Hopkins, J., Harraway, J., McLeod, M., McLeod, N., Harawira, P., Taite, H., Scouler, R., Miller, A., and Reeve, A. (1998). E-cadherin germline mutations in familial gastric cancer. *Nature* 392, 402–405.

Imamichi, Y., Korig, A., Gress, T., and Menke, A. (2007). Collagen type I-induced Smad-interacting protein 1 expression downregulates E-cadherin expression in pancreatic cancer. *Oncogene* 26, 2381–2385.

Imai, T., Horiuchi, A., Wang, C., Oka, K., Ohira, S., Nikaido, T., and Konishi, I. (2003). Hypoxia attenuates the expression of E-cadherin via upregulation of SNAIL in ovarian carcinoma cells. *Am. J. Pathol.* 163, 1437–1447.

Jiang, R., Lan, Y., Norton, C., Sundberg, J., and Gridley, T. (1998). The Slug gene is not essential for mesoderm or neural crest development in mice. *Dev. Biol.* 198, 277–285.

Jorda, M., Olmeda, D., Vinyals, A., Valero, E., Cubillo, E., Llorens, A., Cano, A., and Fabra, A. (2005). Upregulation of MMP-9 in MDCK epithelial cell line in response to expression of the Snail transcription factor. *J. Cell Sci.* 118, 3371–3385.

Krishnamachary, B., Zagzag, D., Nagashawa, H., Rainey, K., Okuyama, H., Beek, J., and Semenza, G. (2006). Hypoxia-inducible factor-1-dependent repression of E-cadherin in von Hippel-Lindau tumor suppressor-null renal cell carcinoma mediated by TCF3, ZFH1A, and ZFH1B. *Cancer Res.* 66, 2725–2731.

Knudsen, K. E., Diehl, J., Haiman, C., and Knudsen, E. S. (2006). Cyclin D1, polymorphism, aberrant splicing and cancer risk. *Oncogene* 25, 1620–1628.

Lin, S., Wang, W., Wilson, G., Yang, X., Brewer, G., Holbrook, N., and Gorospe, N. (2000). Down-regulation of cyclin D1 expression by prostaglandin A2 is mediated by enhanced cyclin D1 mRNA turnover. *Mol. Cell. Biol.* 20, 7903–7913.

Lochter, A., Galoczy, S., Muschler, J., Freedman, N., Werb, Z., and Bissel, M. (1997). Matrix metalloproteinase stromelysin-1 triggers a cascade of molecular alterations that leads to stable epithelial-to-mesenchymal conversion and premalignant phenotype in mammary epithelial cells. *J. Cell Biol.* 139, 1861–1872.

Maeda, G., Chiba, T., Okazaki, M., Setoh, T., Taya, Y., Aoba, T., Kato, K., Kawashiri, S., and Imai, K. (2005). Expression of SIP1 in oral squamous cell carcinomas: implications for E-cadherin expression and tumour progression. *Int. J. Oncol.* 27, 1535–1541.

Malumbres, M., and Barbacid, M. (2001). To cycle or not to cycle: a critical decision in cancer. *Nat. Rev. Cancer* 1, 222–231.

J. Meijvang *et al.*

- McGarry, L., Wirnie, J., and Ozarne, B. W. (2004). Invasion of v-Fos(FBR)-transformed cells is dependent upon histone deacetylase activity and suppression of histone deacetylase regulated genes. *Oncogene* 23, 5284–5292.
- Meijvang, J., Krijavakva, M., Berditschevski, F., Bronstein, I., Lukanidin, E. M., Pringle, J. H., Mellon, J. K., and Tulchinsky, E. M. (2007). Characterization of E-cadherin-dependent and -independent events in a new model of c-Fos-mediated epithelial-mesenchymal transition. *Exp. Cell Res.* 313, 380–393.
- Moreno-Bueno, G. *et al.* (2006). Genetic profiling of epithelial cells expressing e-cadherin repressors reveals a distinct role for snail, slug, and e47 factors in epithelial-mesenchymal transition. *Cancer Res.* 66, 9543–9556.
- Murray, S., and Gridley, T. (2006). Snail family genes are required for left-right asymmetry determination, but not neural crest formation, in mice. *Proc. Natl. Acad. Sci. USA* 103, 10300–10304.
- Ohkubo, T., and Ozawa, M. (2004). The transcription factor Snail downregulates the tight junction components independently of E-cadherin downregulation. *J. Cell Sci.* 117, 1675–1685.
- Patrone, G., Puppo, F., Cusano, R., Scaranari, M., Ceccherini, I., Puliti, A., and Ravazzolo, R. (2000). Nuclear run-on assay using biotin labeling, magnetic bead capture and analysis by fluorescence-based RT-PCR. *BioTechniques* 29, 1012–1017.
- Peinado, H., Ballestar, E., Esteller, M., and Cano, A. (2004). Snail mediates E-cadherin repression by the recruitment of the Sin3A/histone deacetylase 1 (HDAC1)/HDAC2 complex. *Mol. Cell Biol.* 24, 306–319.
- Perez-Moreno, M. A., Locascio, A., Rodrigo, L., Dhondt, G., Portillo, F., Nieto, M. A., and Cano, A. (2001). A new role for E12/E47 in the repression of E-cadherin expression and epithelial-mesenchymal transitions. *J. Biol. Chem.* 276, 27424–27431.
- Postigo, A., Depp, J., Taylor, J., and Kroll, K. L. (2003). Regulation of Smad signaling through a differential recruitment of coactivators and corepressors by ZEB proteins. *EMBO J.* 22, 2453–2462.
- Remacle, J., Kraft, H., Lerchner, W., Wuytens, G., Collart, C., Verschuere, K., Smith, J., and Huybrebroeck, D. (1999). New mode of DNA binding of multi-zinc finger transcription factors: deltaEF1 family members bind with two hands to two target sites. *EMBO J.* 15, 5073–5084.
- Rosivatz, E., Becker, I., Specht, K., Fricke, E., Lubert, B., Busch, R., Hoffler, H., and Becker, K. F. (2002). Differential expression of the epithelial-mesenchymal transition regulators snail, SIP1 and twist in gastric cancer. *Am. J. Pathol.* 161, 1881–1891.
- Shy, Y., Sawada, J., Sui, G., el-Afif, B., Whetstone, J., Lan, F., Ogawa, H., Luke, M., Nakatani, Y., and Shi, Y. (2003). Coordinated histone modifications mediated by a CtBP co-repressor complex. *Nature* 422, 735–738.
- Spoelstra, N., Manning, N., Higashi, Y., Darling, D., Singh, M., Shroyer, K., Broadbent, R., Horwitz, K., and Richer, J. K. (2006). The transcription factor ZEB1 is aberrantly expressed in aggressive uterine cancers. *Cancer Res.* 66, 3893–3902.
- Sugimachi, K., Tanaka, S., Kameyama, T., Taguchi, K., Aishima, S., Shimada, M., Sugimachi, K., and Tsuneyoshi, M. (2003). Transcriptional repressor snail and progression of human hepatocellular carcinoma. *Clin. Cancer Res.* 9, 2657–2664.
- Taki, M., Verschuere, K., Yokoyama, K., Nagayama, M., and Kamata, N. (2006). Involvement of Ets-1 transcription factor in inducing matrix metalloproteinase-2 expression by epithelial mesenchymal transition in squamous carcinoma cells. *Int. J. Oncol.* 28, 487–496.
- Thiery, J. P. (2003). Epithelial-mesenchymal transitions in development and pathologies. *Curr. Opin. Cell Biol.* 15, 740–746.
- Thiery, J. P., and Chopin, D. (1999). Epithelial cell plasticity in development and tumor progression. *Cancer Metastasis Rev.* 18, 31–42.
- Turner, F., Broad, S., Khanim, F., Jeanes, A., Talma, S., Hughes, S., Tselepis, C., and Hotchin, N. (2006). Slug regulates integrin expression and cell proliferation in human epidermal keratinocytes. *J. Biol. Chem.* 281, 21321–21331.
- van de Putte, T., Maruhaashi, M., Francis, A., Nelles, L., Kondoh, H., Huybrebroeck, D., and Higashi, Y. (2003). Mice lacking Zfx1b, the gene that codes for Smad-Interacting Protein-1, reveal a role for multiple neural crest defects in the etiology of hirschsprung disease—mental retardation syndrome. *Am. J. Hum. Genet.* 72, 465–470.
- van Grunsven, L. A., Michiels, C., van de Putte, T., Nelles, L., Wuytens, G., Verschuere, K., and Huybrebroeck, D. (2003). Interaction between Smad-interacting protein-1 and the corepressor C-terminal binding protein is dispensable for transcriptional repression of E-cadherin. *J. Biol. Chem.* 278, 26135–26145.
- van Grunsven, L. A., Taelman, V., Michiels, C., Opdecamp, K., Huybrebroeck, D., and Bellefroid, E. J. (2006). δ EF1 and SIP1 are differentially expressed and have overlapping activities during *Xenopus* embryogenesis. *Dev. Dyn.* 235, 1491–1500.
- Vandewalle, C., Cozijn, J., Craene, B., Vermassen, P., Bruyneel, E., Andersen, H., Tulchinsky, E., van Roy, F., and Bex, G. (2005). SIP1/ZEB2 induces EMT by repressing genes of different epithelial cell-cell junctions. *Nucleic Acids Res.* 33, 6566–6578.
- Vega, S., Morales, A., Ocana, O., Valdes, F., Farnegat, L., and Nieto, M. A. (2004). Snail blocks the cell cycle and confers resistance to cell death. *Genes Dev.* 18, 1131–1143.
- Walker, J. L., and Assoian, R. K. (2005). Integrin-dependent signal transduction regulating cyclin D1 expression and G1 phase cell cycle progression. *Cancer Metastasis Rev.* 24, 383–393.
- Walker, J. L., Fournier, A. K., and Assoian, R. K. (2005). Regulation of growth factor signalling and cell cycle progression by cell adhesion and adhesion-dependent changes in cellular tension. *Cytokine Growth Factor Rev.* 16, 395–405.
- Zhou, B. P., Deng, J., Xia, W., Xu, J., Yan, M., Li, Y. M., Gunduz, M., and Hung, M. C. (2004). Dual regulation of Snail by GSK-3 β -mediated phosphorylation in control of epithelial-mesenchymal transition. *Nat. Cell Biol.* 6, 931–940.